Environmental Laboratory

US Army Corps of Engineers®
Engineer Research and
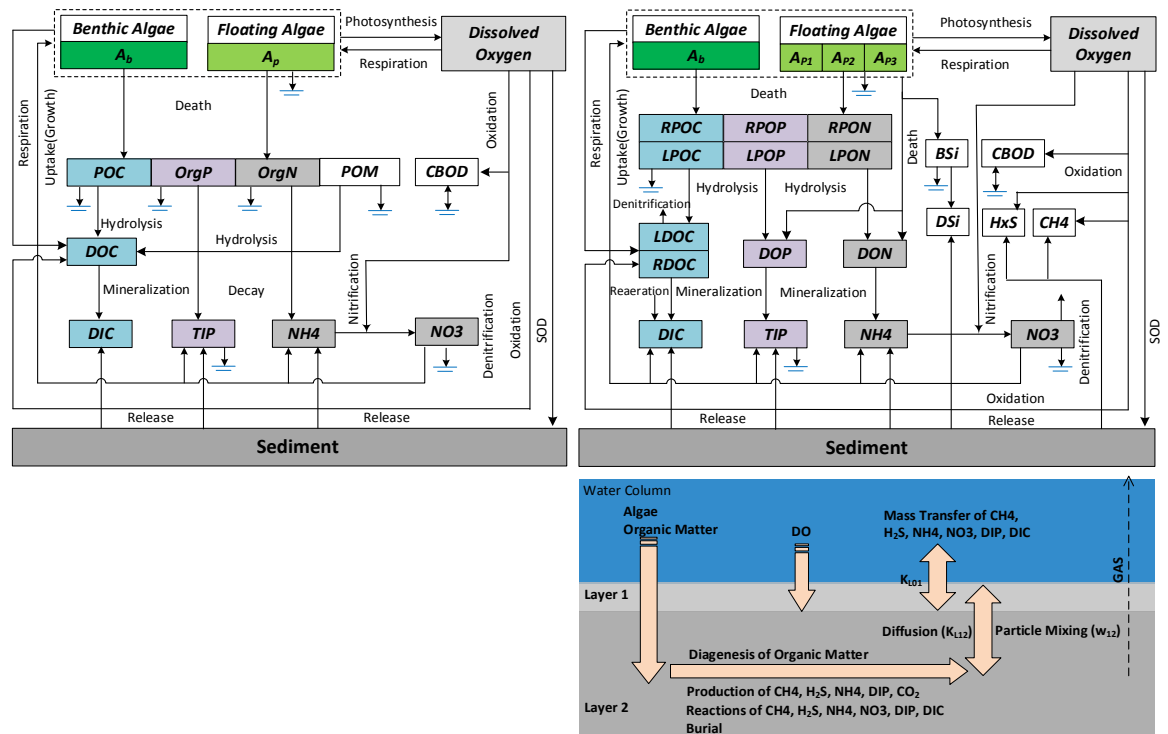Development Center

Ecosystem Management and Restoration Research Program (EMRRP)

Aquatic Nutrient Simulation Modules (NSMs) Developed for Hydrologic and Hydraulic Models

Zhonglong Zhang and Billy E. Johnson   February 2016

The U.S. Army Engineer Research and Development Center (ERDC) solves the nation's toughest engineering and environmental challenges. ERDC develops innovative solutions in civil and military engineering, geospatial sciences, water resources, and environmental sciences for the Army, the Department of Defense, civilian agencies, and our nation's public good. Find out more at www.erdc.usace.army.mil.

To search for other technical reports published by ERDC, visit the ERDC online library at http://acwc.sdp.sirsi.net/client/default.

Aquatic Nutrient Simulation Modules (NSMs) Developed for Hydrologic and Hydraulic Models

Zhonglong Zhang and Billy E. Johnson

Environmental Laboratory
U.S. Army Engineer Research and Development Center
3909 Halls Ferry Road
Vicksburg, MS 39180-6199

Final report

Prepared for   U.S. Army Corps of Engineers
Washington, DC   20314-1000

Abstract

This report offers details regarding the theory and mathematical
formulations used within the newly developed nutrient simulation modules
(NSMs) and its supporting water quality modules. The NSMs model the
aquatic ecosystem by computing the changing concentrations of water
quality constituents in a unit volume of water. The NSMs includes two
kinetics: NSMI, NSMII. The levels of NSMs are determined by the number
of interacting state variables involved in water quality simulation and the
degree of their interactions. NSMI models algae and benthic algae biomass,
simple nitrogen and phosphorus cycles, organic carbon, carbonaceous
biochemical oxygen demand, dissolved oxygen and pathogen using 16 state
variables. Water quality state variables may be individually activated or
deactivated. Using 24 state variables, NSMII models multiple algal groups,
benthic algae, nitrogen, phosphorus, and carbon cycles, carbonaceous
biochemical oxygen demand, dissolved oxygen, and pathogen. Additionally,
an optional benthic sediment diagenesis module was developed for coupling
with NSMII's water column kinetics. Sediment–water fluxes of dissolved
oxygen and nutrients are internally computed in the sediment diagenesis
module. The NSMs and its supporting water quality modules are written in
Fortran for Windows and are packaged as "plug in" dynamic linked
libraries. Each module must be coupled with hydrologic or hydraulic models
to perform water quality analysis.

Contents

Figures and Tables

Figures

Tables

Preface

This study was conducted as part of the U.S. Army Corps of Engineers (USACE) Ecosystem Management and Restoration Research Program (EMRRP). The study reported herein builds on a previous work unit funded by the USACE System-Wide Water Resources Program (SWWRP). Glenn Rhett was Program Manager of the EMRRP, and Dr. Alfred Confrancesco was the Technical Director.

This report was prepared by Dr. Zhonglong Zhang of LimnoTech, which was under contract to the U.S. Army Engineer Research and Development Center (ERDC), and Dr. Billy Johnson of the Water Quality and Contaminant Modeling Branch (WQCMB), Environmental Processes and Engineering Division (EPED), ERDC Environmental Laboratory (EL). Preparation of the report was under the general supervision of Dr. Dorothy Tillman, Chief, WQCMB; Warren Lorentz, Chief, EPED; and Dr. Beth Fleming, Director, ERDC-EL.

Additionally, Dr. Mark Dortch of the WQCMB and Dr. James Martin of Mississippi State University reviewed the report and provided helpful perspectives. Mark Jensen of Hydrologic Engineering Center (HEC) provided a guideline for the code development.

At the time of publication, COL Bryan S. Green, was Commander of ERDC, and Dr. Jeffery P. Holland was the Director.

Unit Conversion Factors

Multiply	By	To Obtain
degrees Fahrenheit (°F)	(F-32)/1.8	degrees Celsius (°C)
day (d)	86400	second (s)
inches (in)	25.4	millimeters (mm)
feet (ft)	0.3048	meters (m)
square feet (ft^2)	0.092903	square meters (m^2)
cubic feet (ft^3)	0.028317	cubic meters (m^3)
liter (L)	0.001	cubic meters (m^3)
pounds (mass) (lb)	453.59	grams (g)
pounds (mass) (lb)	0.45359	kilograms (kg)
pounds (mass) per cubic foot (lb/ft^3)	16.01846	kilograms per cubic meter (kg/m^3)
pounds (mass) per square foot (lb/ft^2)	4.882428	kilograms per square meter (kg/m^2)
pounds per square inch (psi)	6.8948	kilopascals (kPa)
atmosphere (atm)	1.01325×10^5	pascals (Pa)
millibar (mb)	10^2	pascals (Pa)
gallons (U.S. liquid) (gal)	3.7854	liters (L)
gallons (U.S. liquid) (gal)	3.785412 E-03	cubic meters (m^3)
parts per million (ppm)	1.0	milligrams per liter (mg/L)
calorie (cal)	4.184	joule (J)
langley (ly)	1.0	calorie per square centimeters (cal/cm^2)
langley (ly)	4184	joules per square meters (J/m^2)
langley/day (ly/d)	0.484	watt square meters (W/m^2)

Acronyms and Abbreviations

1-D	One Dimensional
2-D	Two Dimensional
ADH	Adaptive Hydraulics
AFDM	Ash-Free Dry Mass
BOD	Biological Oxygen Demand
BSi	Particulate Biogenic Silica
C	Carbon
CBOD	Carbonaceous Biological Oxygen Demand
CBOD5	5 day Carbonaceous Biological Oxygen Demand
CBODU	Ultimate Carbonaceous Biological Oxygen Demand
CFU	Colony Forming Unit
Chla	Chlorophyll-a
CH4	Methane
CO_2	Carbon Dioxide
D	Dry-weight
DIC	Dissolved Inorganic Carbon
DIN	Dissolved Inorganic Nitrogen
DIP	Dissolved Inorganic Phosphorus
DLL	Dynamic Linked Library
DO	Dissolved Oxygen
DOC	Dissolved Organic Carbon
DON	Dissolved Organic Nitrogen
DOP	Dissolved Organic Phosphorus
DSi	Dissolved Silica
EL	Environmental Laboratory
EMRRP	Ecosystem Management and Restoration Research Program

EPED	Environmental Processes and Engineering Division
eq	Equivalent
ERDC	U.S. Army Engineer Research and Development Center
FRP	Filterable Reactive Phosphorus
GSSHA	Gridded Surface Subsurface Hydrologic Analysis
GUI	Graphical User Interface
H_2S	Dissolved Hydrogen Sulfide
H&H	Hydrologic and Hydraulic
HEC	Hydrologic Engineering Center
HEC-HMS	Hydrologic Engineering Center-Hydrologic Modeling System
HEC-RAS	Hydrologic Engineering Center-River Analysis System
HEC-ResSim	Hydrologic Engineering Center-Reservoir System Simulation
ICM	CE-QUAL-ICM
LDOC	Labile Dissolved Organic Carbon
LPOC	Labile Particulate Organic Carbon
LPON	Labile Particulate Organic Nitrogen
LPOP	Labile Particulate Organic Phosphorous
ly	Langly
N	Nitrogen
NBOD	Nitrogenous Biochemical Oxygen Demand
NH4	Ammonium
NO3	Nitrate
NSM	Nutrient Simulation Module
NTU	Nephelometric Turbidity Units
NSMI	Nutrient Simulation Module I
NSMII	Nutrient Simulation Module II
NSMII-SedFlux	NSMII Benthic Sediment Diagenesis Module
NWS	National Weather Service

O$_2$	Oxygen
OrgN	Organic Nitrogen
OrgP	Organic Phosphorus
P	Phosphorus
PAR	Photosynthetically Active Radiation
POC	Particulate Organic Carbon
POM	Particulate Organic Matter
QUAL2E	Enhanced Stream Water Quality Model
PX	Pathogen
RIV1	CE-QUAL-RIV1
RDOC	Refractory Dissolved Organic Carbon
RPOC	Refractory Particulate Organic Carbon
RPON	Refractory Particulate Organic Nitrogen
RPOP	Refractory Particulate Organic Phosphorus
Si	Silica
SOD	Sediment Oxygen Demand
SO$_4$	Sulfate
TEMP	Water Temperature Simulation Module
TN	Total Nitrogen
TP	Total Phosphorous
TIC	Total Inorganic Carbon
TIP	Total Inorganic Phosphorous
TKN	Total Kjeldahl Nitrogen
TOC	Total Organic Carbon
TON	Total Organic Nitrogen
TOP	Total Organic Phosphorus
TSS	Total Suspended Solids

USACE	U.S. Army Corps of Engineers
W2	CE-QUAL-W2
WASP	Water Quality Analysis Simulation Program
WQCMB	Water Quality and Contaminant Modeling Branch

1   Introduction

1.1   Background

The U.S. Army Corps of Engineers (USACE) has a major responsibility for the regulation of the Nation's streams, rivers, and waterways. This often requires developing water quality models to resolve issues and concerns with regard to the environment and ecosystems. Hydrologic and hydraulic (H&H) models, which are state-of-the-art tools, have been developed and maintained by USACE. Examples of these include: HEC-RAS (Hydrologic Engineering Center-River Analysis System), HEC-HMS (Hydrologic Engineering Center-Hydrologic Modeling System), GSSHA (Gridded Surface Subsurface Hydrologic Analysis), and ADH (Adaptive Hydraulics). The further enhancement of these models to support water quality analysis and ecosystem management is needed. As a result of this need, a research work unit, "Development of Nutrient Simulation Modules," was initiated in the USACE System-Wide Water Resources Program (SWWRP). The roots of the research extend back to 2004. The goal from inception for this research has been to create "plug in" water quality modules as dynamic linked libraries (DLLs) for a variety of H&H models and to facilitate performing a system-wide water resources assessment.

The nutrient simulation module, developed under the SWWRP, includes three components for computing the water quality kinetics for the soil, overland flow, and aquatic systems. The USACE Ecosystem Management and Restoration Research Program (EMRRP) sponsored subsequent extension and enhancement of this aquatic nutrient simulation module. The aquatic nutrient simulation modules (called NSMs henceforth) described in this report were specifically developed by the Environmental Laboratory of U.S. Army Engineer Research and Development Center (ERDC) for the HEC-RAS model with the potential of being applicable to other H&H models.

1.2   "Plug In" Water quality Modules

A mathematical model is used to trace the concentration of each of the water quality constituents as it is advected either vertically or horizontally, as it diffuses (by molecular or turbulent transport) from regions of high concentrations to regions of low concentrations, and as it undergoes

chemical or biological reactions. Transport and fate of water quality constituents in aquatic systems are influenced by two major categories of processes: physical and biochemical.

Water quality kinetics refers to all of the biochemical reactions and transformations of the constituents. Because of the wide range of water quality issues, a variety of constituents may be included as state variables (Thomann and Mueller 1987, Chapra 1997). As such, many models with water quality capability have been developed. These models have included water quality kinetics as either separate modules or as an internal part of the hydrodynamic models. Coupled H&H and water quality models are a key tool for analyzing and predicting the water quality of receiving water. The NSMs were developed to address a wide range of one-dimensional (1-D) and two-dimensional (2-D) riverine water quality problems. The basic philosophy in developing the NSMs has been to use as much existing water quality kinetics as possible. However, appropriate levels of water quality kinetics for the NSM may not exist for some issues. In these cases, new components or algorithms were derived from recent research findings and open source literature. The following water quality models have been reviewed to formulate appropriate algorithms in NSMs: QUAL2E (Brown and Barnwell 1987), QUAL2K (Chapra et al. 2008), WASP (Wool et al. 2006), CE-QUAL-RIV1 (EL 1995a), CE-QUAL-W2 (Cole and Wells 2008), CE-QUAL-ICM (Cerco and Cole 1993, Cerco et al. 2004). These water quality models are well established in practice.

The principal attributes of the NSM include the following:

- The NSM solves internal source and sink equations for each water quality cell and for each constituent or state variable. The NSM is packaged as two "plug in" water quality modules (NSMI and NSMII). Each module must be integrated into H&H models when performing water quality analysis.
- NSMI uses 16 state variables to model algae, simple nitrogen and phosphorus cycles, the carbon cycle, carbonaceous biochemical oxygen demand, dissolved oxygen, and pathogen in the water column. Water quality state variables may be individually activated or deactivated.
- NSMII uses 24 state variables to model multiple algae, nitrogen, phosphorus, and carbon cycles and carbonaceous biochemical oxygen demand, dissolved oxygen, and pathogen. NSMII has the capability of dynamically computing the sediment oxygen demand and transfer of constituents between the water column and the benthic sediments through a sediment diagenesis module.

- The algorithms and mathematical formulations within newly developed NSMs have been tested and verified with a variety of examples, and compared against other water quality models.
- The modularity of NSM computer codes provides the flexibility for future enhancement, including the ability to add additional state variables and processes.
- The NSMs have been integrated into HEC-RAS with a pre- and post-processer designed to setup the model, perform the runs, and to present and analyze the results.

In this report, internal source and sink terms or kinetic equations in water quality modules are written as derivatives of concentration with respect to time. Units consistent with the Système Internationale (SI) are used. SI base units and their accepted symbols in this report are meter (m) for length, milligram (mg) for mass, Kelvin (K) or degree Celsius (°C) for temperature, Watts (W) for heat flux, and day (d) for time. Concentration is expressed in milligram per liter (mg L^{-1}).

1.3 Report Outline

In this report, techniques and algorithms included in NSMs and its supporting water quality modules are detailed. This report consists of seven chapters and five appendices, all of which are listed below.

- Chapter 1 introduces the background and topic of water quality kinetics.
- Chapter 2 briefly describes the water temperature simulation module (TEMP).
- Chapter 3 describes the processes and mathematical equations in NSMI.
- Chapter 4 describes the processes and mathematical equations in NSMII.
- Chapter 5 describes the benthic sediment diagenesis module.
- Chapter 6 presents a framework for integrating water quality modules into HEC-RAS.
- Chapter 7 presents summary and conclusions.
- Appendix A summarizes mathematical symbols used in the TEMP.
- Appendix B summarizes mathematical symbols used in NSMI.
- Appendix C summarizes mathematical symbols used in NSMII.
- Appendix D summarizes mathematical symbols used in the sediment diagenesis module.

2   Water Temperature Simulation Module (TEMP)

Water temperature is one of the most important physical characteristics of aquatic systems. In addition to its own effects, temperature influences all biological and chemical reactions in water quality models. Virtually all kinetic rates are temperature dependent. Therefore, water temperature is a required input parameter to make corrections for kinetic rates in NSMs. This chapter briefly describes the water temperature simulation module (TEMP). The TEMP includes two kinetics and utilizes equations of conservation of energy to compute water temperatures from a full energy balance or simplified energy balance. These equations express energy as the rate of energy flow, or flux, in units of Joules per second (J s^{-1}) or Watts (W). Temperature is expressed in degrees Celsius (°C), or in Kelvin (K). The two scales are offset by 273.16 K. That is, 0 °C is equivalent to 273.16 K.

2.1   Full Energy Balance

The full energy balance accounts for heat inputs and outputs from the forcing functions and for the heat exchange at the water surface and at the sediment–water interface. The main sources of heat exchange at the water surface are short-wave solar radiation, long-wave atmospheric radiation, conduction of heat from the atmosphere to the water, and direct heat inputs. The main sinks of heat exchange are long-wave radiation emitted by the water, evaporation, and conduction from the water to the atmosphere. The schematic of sources and sinks of heat at the air- and sediment-water interfaces is shown in Figure 1.

Figure 1. Sources and sinks of water column's heat energy (after Deas and Lowney 2000).
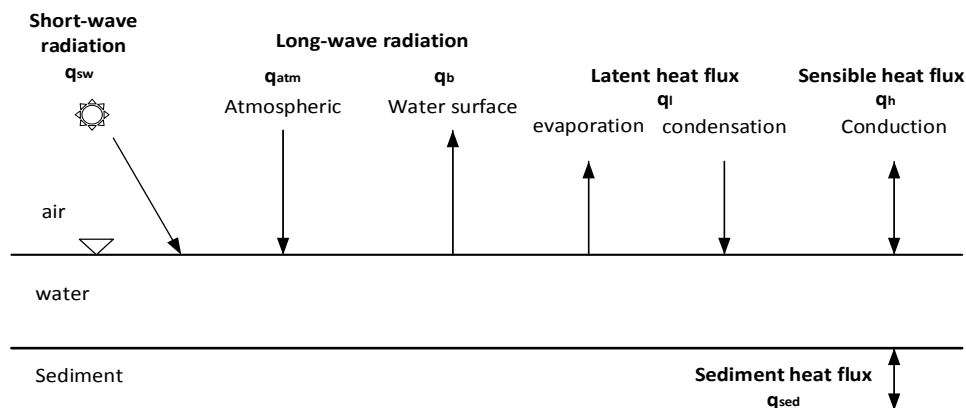
Units of heat flux (W m⁻²) are used to describe heat exchange at the air-water and sediment-water interfaces. The sign convention used herein is positive (+) for heat entering the water's surface, and negative (-) for heat leaving the water's surface. Net heat flux (q_{net}) for the water column is typically computed as

$$q_{net} = q_{sw} + q_{atm} - q_b + q_h - q_l + q_{sed},\qquad(2.1)$$

where

$$
\begin{aligned}
q_{sw} &= \text{short-wave solar radiation flux (W m}^{-2}\text{),}\\
q_{atm} &= \text{atmospheric (downwelling) long-wave radiation flux (W m}^{-2}\text{),}\\
q_b &= \text{back (upwelling) long-wave radiation flux (W m}^{-2}\text{),}\\
q_h &= \text{sensible heat flux (W m}^{-2}\text{),}\\
q_l &= \text{latent heat flux (W m}^{-2}\text{),}\\
q_{sed} &= \text{sediment–water heat flux (W m}^{-2}\text{).}
\end{aligned}
$$

Water temperature is computed based on the laws of conservation of energy. Heat and temperature are related by the specific heat of water. The change in water temperature due to a change in net heat flux (q_{net}) is described by the following equation

$$\rho_w C_{pw}\frac{\partial T_w}{\partial t} = \frac{A_s}{V} q_{net},\qquad(2.2)$$

where

$$
\begin{aligned}
T_w &= \text{water temperature (°C),}\\
t &= \text{time (s),}\\
\rho_w &= \text{density of water (kg m}^{-3}\text{),}\\
C_{pw} &= \text{specific heat capacity of water (J kg}^{-1}\,°\text{C}^{-1}\text{),}\\
V &= \text{volume of the water column (m}^3\text{),}\\
A_s &= \text{surface area of the water column cell (m}^2\text{),}\\
q_{net} &= \text{net heat flux at (W m}^{-2}\text{).}
\end{aligned}
$$

The density of water is dependent on the dissolved salt content as well as the temperature of the water. Density of seawater differs slightly from that of pure water; its freezing point as well as its maximum density point is lowered by dissolved salt. Water has its maximum density of 1 g cm⁻³ at 4°C. When the temperature changes from either greater or less than 4°C,

the density of water will become less than 1 g cm⁻³. The density of fresh water can be computed as a function of temperature with the following equation

$$\rho_w = 999.973 \left[1.0 - \frac{(T_w - 3.9863)^2 (T_w + 288.9414)}{508929.2(T_w + 68.12963)} \right], \quad (2.3)$$

Each term of heat fluxes in equation 2.1 can be computed from user-specified meteorological data and is briefly discussed below. Detailed discussion of equations and mechanisms can be found from Water Resources Engineers Inc. (1967), Brown and Barnwell (1987), and Deas and Lowney (2000). Much of this section was adopted from HEC (2010a) to match the kinetic implementations in original water temperature model.

2.1.1 Short-wave solar radiation

The short-wave solar radiation flux, q_{sw}, which reaches the surface of the earth, can be measured directly with a pyrheliometer. Some U.S. National Weather Service (NWS) stations record solar radiation. If observed data is not available, the q_{sw} can computed as from user-specified information of the cloudiness, site elevation, site location, air temperature, vapor pressure, and the dust coefficient

$$q_{sw} = q_o a_t (1 - R_s)(1 - 0.65 C_L{}^2), \quad (2.4)$$

where

q_0 = extraterrestrial radiation (W m⁻²),
α_t = atmospheric attenuation,
R_s = reflection coefficient,
C_L = percent of sky covered by clouds.

The extraterrestrial radiation is expressed as

$$q_o = \frac{Q_o}{r^2}(\sin \emptyset \sin \delta + \cos \emptyset \cos \delta \, cosh_r), \quad (2.5)$$

where

Q_0 = solar constant (= 1360 W m⁻²),
r = normalized radius of the earth's orbit (unitless),

ϕ = latitude of the site (rad),
δ = solar declination (rad),
h_r = solar hour angle (rad).

Atmospheric attenuation, α_t, is the fraction of radiation reaching the water surface after reduction by scattering and absorption. The reflection coefficient, R_s, can be computed as a function of the solar altitude. Cloud cover may affect the reflection coefficient. Solar declination is comprised by the angle through which a given hemisphere is tilted towards the Sun. It is a function of the day of year. Various methods have been published to estimate these parameters (Water Resources Engineers Inc. 1967, Brown and Barnwell 1987). Solar radiation is always positive in sign during the day, zero during nighttime hours.

2.1.2 Long-wave atmospheric radiation

Longwave radiation is specified as one of two types: downwelling radiation (q_{atm}) is emitted by the atmosphere, upwelling radiation (q_b) is emitted by the water surface. Downwelling radiation emitted by the earth's atmosphere toward the water's surface is positive in sign, and is a strong function of air temperature. The amount of atmospheric long-wave radiation is affected by clouds and particles in the atmosphere. Long-wave atmospheric radiation flux, q_{atm}, is typically computed using an empirical equation

$$q_{atm} = 0.937 \cdot 10^{-5}(1 + 0.17C_L^2)\sigma T_{ak}^6, \tag{2.6}$$

where

σ = Stefan-Boltzman constant (W m^{-2} K^{-4}),
T_{ak} = air temperature (K).

The net flux of solar radiation and atmospheric long-wave radiation is independent of the water temperature and is a function of known or observable meteorological conditions.

2.1.3 Back long-wave radiation

Upwelling radiation emitted by the water's surface is negative in sign, and represents a loss of heat from the water. The back (upwelling) long-wave radiation flux, q_b, is a strong function of water temperature. It is typically computed using the Stefan-Boltzman Fourth Power Radiation Law

$$q_b = 0.97\sigma T_{wK}^4, \tag{2.7}$$

where

T_{wk} = water temperature (K).

2.1.4 Latent heat flux

Energy associated with a phase change is termed latent heat. A gain (or loss) of energy occurs because of a change in phase such as condensation or evaporation. The magnitude of latent heat flux is a function of water temperature and atmospheric conditions including vapor pressure and atmospheric turbulence. The latent heat flux, q_l, is proportional to the difference between the saturated vapor pressure at the surface water temperature and the actual vapor pressure at the air temperature

$$q_\ell = \frac{0.622}{P} L \rho_w (e_s - e_a) f(u_w), \tag{2.8}$$

where

P = atmospheric pressure (mb),
L = latent heat of vaporization (J kg^{-1}), which is a function of water temperature,
e_s = saturated vapor pressure at water temperature (mb), which is a function of water temperature,
e_a = vapor pressure of overlying air (mb),
u_w = wind speed measured at a fixed height above the water surface (m s^{-1}),
$f(u_w)$ = wind function.

The saturation vapor pressure is the highest pressure of water vapor that can exist in equilibrium within a plane, free water surface at a given temperature. It can be computed using an empirical equation

$$e_s = 6984.505294 + T_{wk}\left(-188.903931 + T_{wk}\left(\begin{matrix}2.133357675 \\ +T_{wk}\left(\begin{matrix}-1.28858097\times10^{-2} \\ +T_{wk}\left(\begin{matrix}4.393587233\cdot10^{-5} \\ +T_{wk}\left(\begin{matrix}-8.023923082\cdot10^{-8} \\ +T_{wk}\cdot6.136820929\cdot10^{-11}\end{matrix}\right)\end{matrix}\right)\end{matrix}\right)\end{matrix}\right)\right) \qquad (2.9)$$

Vapor pressure is an expression of the moisture content of air, and is not a function of air temperature. Actual vapor pressure may be measured directly, or computed from wet bulb or dew point temperature (T_d). The difference e_s - e_a may be shown to be proportional to the difference T_w - T_d (Edinger et al. 1974). When $T_w > T_d$, water evaporates and q_l is positive (loss of heat from water), conversely, if $T_w < T_d$, water condenses on the surface and q_l is negative heat gain).

2.1.5 Sensible heat flux

Sensible heat describes the flux of heat through molecular or turbulent transfer between the air and water surface. The amount of heat gained or lost through sensible heat depends on the gradient of temperature in the vertical direction. The sensible heat flux, q_h, is typically computed using the following equation

$$q_h = \left(\frac{K_h}{K_w}\right) C_p \rho_w (T_a - T_w) f(u_w), \qquad (2.10)$$

where

$\quad\quad C_p$ = specific heat capacity of air at constant pressure (J kg^{-1} C^{-1}),
$\quad\quad T_a$ = air temperature (°C),
$\quad K_h/K_w$ = diffusivity ratio (unitless).

The direction of heat transfer depends on which of the two temperatures is higher. q_h is positive (a net gain from the water) when the air temperature is greater than the water temperature and is negative when $T_w > T_a$. The diffusivity ratio (K_h/K_w) is a parameter that allows the user to partition flux between latent and sensible heat. The diffusivity ratio is generally set to unity but the model allows it to range between 0.5 and 1.5. A range of 0.9 to 1.1 is recommended.

The wind function varies slightly for sensible and latent heat; however, the same wind function may be used for most water temperature applications. The wind speed function attempts to characterize the turbulent exchange characteristic between the water surface and the overlying air mass. The wind speed function is typically an empirical expression that is adjustable using the *a*, *b*, and *c* coefficients.

$$f(u_w) = f(R_i)(a + b \cdot u_w^c),$$ (2.11)

where

a = user-defined coefficient on the order of 10^{-6} (mb^{-1} m s^{-1}),
b = user-defined coefficient on the order of 10^{-6} (mb^{-1} m s^{-1}),
c = user-defined coefficient on the order of one,
$f(R_i)$ = function of Richardson number.

The coefficient '*a*' represents vertical convection occurring even when wind speed is zero, and is typically small, generally becoming significant only for artificially heated waters. In general, the coefficient '*b*' increases with increasing turbulence, and decreases with a stable atmosphere, and can vary by more than 50% (Fischer et al. 1979). The wind speed is measured at a 2 m height. The following equation converts wind speed from any measurement height to 2 m

$$u_{w2} = \frac{\ln(z/z_0)}{\ln(2/z_0)} u_w,$$ (2.12)

where

u_{w2} = wind speed measured at 2 m height (m s^{-1}),
z = station height (m),
z_0 = wind roughness height (m).

Typical values of z_0 include 0.001 m for wind speed < 2.3 m s^{-1}, 0.015 m for wind speed > 2.3 m s^{-1}, and range from 0.00015 to 0.01 m (Cole and Wells 2008).

f(R$_i$) is a function of air temperature, water temperature, and wind speed, varying from .03 under very stable conditions to 12.3 under unstable conditions. Without the Richardson number (R_i) included in the wind

function, the function tends to underestimate mixing processes under unstable atmospheric conditions and thus under predicts the surface fluxes. The converse is also true. The function tends to overpredict the surface fluxes under stable conditions. The R_i is a measure of atmospheric stability and can be computed as

$$R_i = -\frac{g(\rho_{air} - \rho_{sat}) \cdot 2}{\rho_{air} u_w^2},$$ (2.13)

where

$$
\begin{aligned}
Ri &= \text{Richardson number,} \\
g &= \text{acceleration of gravity } (= 9.806 \text{ m s}^{-2}), \\
\rho_{air} &= \text{density of moist air (at air temperature) (kg m}^{-3}), \\
\rho_{sat} &= \text{density of saturated air (at water temperature) (kg m}^{-3}).
\end{aligned}
$$

The R_i is positive for stable atmospheric conditions, negative for unstable, and near zero for neutral conditions. $f(R_i)$ is estimated from R_i using the following relationships

For an unstable atmosphere ($\rho_{air} > \rho_{sat}$),

$$f(R_i) = 12.3, \text{ Ri} \le -1,$$ (2.14a)

$$f(R_i) = (1 - 22Ri)^{+0.8}, -1 < \text{Ri} \le -0.01.$$ (2.14b)

For a neutral atmosphere,

$$f(R_i) = 1, -0.01 < \text{Ri} < +0.01.$$ (2.14c)

For a stable atmosphere ($\rho_{air} < \rho_{sat}$),

$$f(R_i) = (1 - 34Ri)^{-0.8} \; 0.01 \le \text{Ri} < 2,$$ (2.14d)

$$f(R_i) = 0.03, \text{ Ri} \ge 2.$$ (2.14e)

At least one full meteorological data set must be provided when applying the above full energy balance temperature simulation module. As a minimum, a time series of the following information at the meteorological station is required, e.g. short-wave solar radiation, atmospheric pressure,

air temperature, humidity, wind speed, and cloud cover. Because of large fluctuations in air temperature and solar radiation, hourly meteorological data are typically required.

2.1.6 Sediment–water heat flux and sediment temperature

Sediment heat exchange with water is generally small when compared to surface heat exchange and this exchange has often been neglected in modeling water temperature. However, heat exchange between benthic sediments and the water column is significant for shallow water. Therefore, sediment heat exchange is included in the full energy temperature simulation module. Sediment temperature is modeled from the sediment-water interface down to a user-defined depth. The only source or sink of sediment temperature included in the temperature simulation module is the exchange with the water column. The heat balance for the sediment layer can be written as

$$\rho_s C_{ps} \frac{dT_{sed}}{dt} = -\frac{q_{sed}}{h_2}. \tag{2.15}$$

The sediment–water heat flux (q_{net}) in equation 2.15 is expressed as

$$q_{sed} = \rho_s C_{ps} \frac{\alpha_s}{0.5 h_2} \left(T_{sed} - T_w \right), \tag{2.16}$$

where

T_{sed} = sediment temperature (°C),
h_2 = active sediment layer thickness (m),
α_s = sediment thermal diffusivity (m² s⁻¹),
ρ_s = density of sediments (kg m⁻³),
C_{ps} = specific heat capacity of sediments (J kg⁻¹ °C⁻¹).

Equation 2.15 states that the time change of heat storage within a well-mixed sediment layer is equal to the heat exchange between the sediment and the overlying water. Sediment–water heat flux, q_{sed}, is a function of water temperature, sediment temperature, heat storage capacity of sediment material, and thermal diffusivity of sediment material.

Thermal conductivity, α_s, is a measure of the ability of the bed sediment to conduct heat. α_s is not a simple constant for a particular bed. It varies in

both depth and time, depending upon sediment porosity and moisture content. Chapra et al. (2008) provided values for α_s with a range of 0.002–0.012 cm² s⁻¹ or a recommended value of 0.005 cm² s⁻¹. Chapra et al. (2008) also provided values of the product $\rho_s \cdot c_{ps}$ for various types of bed materials (Table 1).

Table 1. Thermal properties of various sediment materials (Chapra et al. 2008).

Material	Conductivity cal s⁻¹ cm⁻¹ °C⁻¹	Diffusivity cm² s⁻¹	ρ g cm³	C_p cal (g °C)⁻¹	$P \cdot C_p$ cal (cm³ °C)⁻¹
Sediment samples					
Mud flat[a]	0.0044	0.0048			0.906
Sand[a]	0.006	0.0079			0.757
Mud sand[a]	0.0043	0.0051			0.844
Mud[a]	0.0041	0.0045			0.903
Wet sand[b]	0.004	0.007			0.57
Sand 23% saturation with water[c]	0.0044	0.0126			0.345
Wet peat[b]	0.0009	0.0012			0.717
Rock[d]	0.0042	0.0118			0.357
Loam 75% saturation with water[c]	0.0043	0.006			0.709
Lake, gelatinous sediment[e]	0.0011	0.002			0.55
Concrete[e]	0.0037	0.008			0.46
Average of sediment samples	0.0037	0.0064			0.647
Component materials					
Water	0.0014	0.0014	1.00	0.999	1.000
Clay	0.0031	0.0098	1.49	0.210	0.310
Soil (dry)	0.0026	0.0037	1.50	0.465	0.700
Sand	0.0014	0.0047	1.52	0.190	0.290
Soil (wet)	0.0043	0.0045	1.81	0.525	0.950
Granite	0.0069	0.0127	2.70	0.202	0.540
Average of sediment samples	0.0033	0.0061	1.67	0.432	0.632

[a] Andrews and Rodvey (1980).

[b] Geiger (1965).

[c] Nakshabandi and Kohnke (1965).

[d] Chow et al. (1988 and Carslaw and Jaeger (1959).

[e] Hutchinson (1957), Jobson (1977), Likens and Johnson (1969).

The following default values are set within the full energy balance temperature simulation: $\rho_s = 1.6$ g cm^{-3} and $C_{ps} = 0.4$ cal g^{-1} °C^{-1}, which correspond to a product ($\rho_s \cdot c_{ps}$) of 0.64 cal cm^{-3} °C^{-1}. The thickness of the benthic sediment layer is set by default to 10 cm to capture the effect of the benthic sediments on the diel heat budget for the water.

2.2 Simplified Energy Balance

Unfortunately, the above temperature simulation module with all the sources and sinks of heat exchange requires measurements from a number of variables and coefficients that are not always readily available. Following Edinger et al. (1974), the simplified energy balance is computed based on an approximate heat balance derived by dew point temperature, short-wave solar radiation, and wind speed parameters. This approach simplifies the mathematical relationships of a complete energy balance and requires less input data. It assumes an equilibrium temperature, T_{eq}, will be reached under steady-state meteorological conditions. The net heat input, $K_T(T_{eq} - T_w)$, is assumed to be proportional to the difference of the actual temperature, T_w, and the equilibrium temperature, T_{eq}. Under a simplified energy balance, the change in water temperature due to a change in net heat flux is described by (Thomann and Mueller 1987)

$$\rho_w C_{pw} \frac{\partial T_w}{\partial t} = \frac{A_s}{V} K_T \left(T_{eq} - T_w \right),$$ (2.17)

where

$\quad K_T$ = overall heat exchange coefficient (W m^{-2} °C^{-1}),
$\quad T_{eq}$ = equilibrium temperature (°C).

The overall heat exchange coefficient, K_T, is computed from empirical relationships, which include wind speed, dew point temperature, and water temperature (Edinger et al. 1974)

$$K_T = 4.5 + 0.05 T_w + \beta \cdot f(u_w) + 0.47 f(u_w).$$ (2.18)

The wind function and β are expressed as

$$f(u_w) = 9.2 + 0.46 u_{w7}^2,$$ (2.19)

$$\beta = 0.35 + 0.015\frac{T_d + T_w}{2} + 0.0012\left(\frac{T_d + T_w}{2}\right)^2 , \qquad (2.20)$$

where

u_{w7} = wind speed measured at 7 m height (m s^{-1}).

The wind speed at 7 m can be computed from user-specifed wind speed at 2 m. Equilibrium temperature is an important concept used in water temperature modeling. Equilibrium temperature is attained when all meteorological conditions remain constant with respect to both space and time, and the water is allowed to reach a steady temperature in response to such static meteorological conditions. The equilibrium temperature, T_{eq}, can be computed from an empirical relationship involving the overall heat exchange coefficient, K_T, the dew point temperature, T_d, and the short-wave solar radiation, q_{sw}

$$T_{eq} = T_d + \frac{q_{sw}}{K_T} . \qquad (2.21)$$

The dewpoint temperature is the temperature the air needs to be cooled to make the air saturated. The actual vapor pressure of the air is the saturation vapor pressure at the dewpoint temperature. The drier the air, the larger the difference between the air temperature and dewpoint temperature. The minimum data requirements at a meteorological station necessary to apply the simplified energy balance temperature simulation module include: (1) dew point, (2) wind speed, and (3) short-wave solar radiation.

2.3 Temperature dependent coefficient correction

Reaction coefficients and rates are often measured at 20°C in the laboratory. These rates are required to be corrected using local water temperature. Most of temperature dependent water quality rates included in NSMs are corrected based on a modified Arrhenius Equation:

$$k(T) = k(20)\theta^{T_w - 20} , \qquad (2.22)$$

where

$k(T)$ = kinetic rate at local temperature (d^{-1}),

$k(20)$ = measured kinetic rate at 20°C (d⁻¹),

θ = temperature correction coefficient.

The coefficient θ usually ranges between 1.01 and 1.10. The user specified reaction rates at 20°C are then corrected by the above function to determine rates corresponding to local water temperature (Figure 2).

Figure 2. Relationship of coefficient and water temperature defined in Arrhenius Equation.
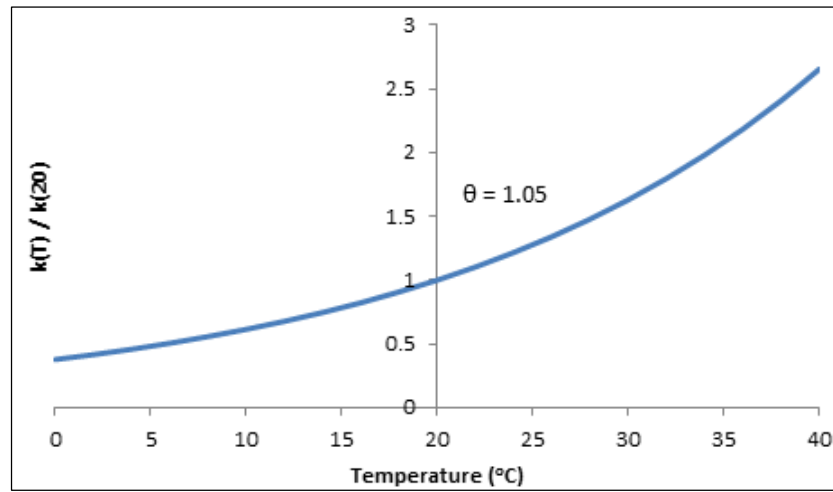
3   Nutrient Simulation Module I (NSMI)

3.1   Overview

The NSMI was designed to conduct an aquatic eutrophication simulation with simplified processes and minimum state variables. The algorithms that are incorporated into NSMI were derived, in part, from QUAL2E (Brown and Barnwell 1987), QUAL2K (Chapra et al. 2008), WASP (Wool et al. 2006), and CE-QUAL-RIV1 (EL 1995a). Both QUAL2E and QUAL2K are 1-D steady-state, in-stream water quality models. QUAL2E can model up to 15 constitutes, mainly including conservative mineral, algae, ammonia, nitrite, nitrate, organic nitrogen, phosphate, organic phosphorus, carbonaceous biological oxygen demand (CBOD), dissolved oxygen (DO), and coliform. QUAL2K is an updated version of QUAL2E with a Microsoft Excel graphical user interface (GUI). Constituents modeled in QUAL2K include ammonia, nitrate, organic nitrogen, organic and inorganic phosphorous, CBOD speciation, DO, algae, pH, and pathogen. QUAL2K explicitly simulates attached bottom algae and sediment–water interactions. Sediment–water fluxes of DO and nutrients are internally computed rather than being prescribed. The Water Quality Analysis Simulation Program (WASP) is a general dynamic mass-balance framework for modeling nutrient and contaminant transport and fate in surface waters. WASP can be applied in one, two, or three dimensions and includes standard eutrophication, advanced eutrophication, simple toxicant, and mercury kinetics. The standard eutrophication module predicts nutrients, phytoplankton, periphyton, CBOD, and DO dynamics. CE-QUAL-RIV1 (RIV1) is a 1-D riverine hydrodynamic and water quality model. RIV1 modeled water quality constituents include temperature, DO, CBOD, organic nitrogen, ammonia, nitrate, organic phosphorus, orthophosphate, coliform bacteria, dissolved iron, and dissolved manganese. The effects of algae and macrophytes on water quality constituents are modeled in RIV1. The NSMI shares some algorithms and formulations with these models.

Figure 3 provides an overview of the NSMI representation of water quality state variables and major processes involved in the water column. The nitrogen cycle is composed of three state variables: organic nitrogen, ammonium, and nitrate. The phosphorus cycle consists of organic phosphorus and inorganic phosphorus. The carbon cycle consists of particulate and dissolved organic carbon and dissolved inorganic carbon. CBOD, pathogen, and alkalinity are also modeled in NSMI. The NSMI does

not model benthic sediment processes but takes account of only sediment oxygen demand (SOD) and sediment release of inorganic nutrients.

Figure 3. Water quality state variables and major processes modeled in NSMI.
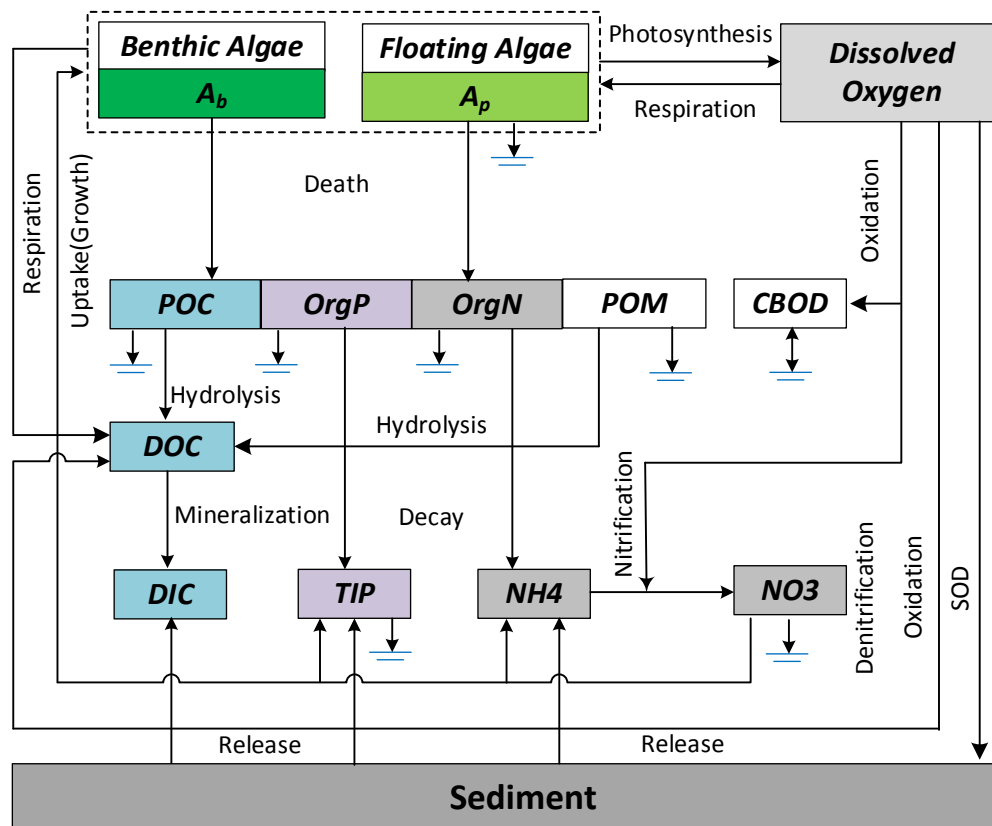
NSMI models up to 16 state variables. Table 2 lists the NSMI's state variables and the symbols. Chla, D, C, N, P and O_2 under the units refer to chlorophyll-a, dry weight, carbon, nitrogen, phosphorus, and oxygen, respectively. The colony forming unit (CFU) is a measure of viable bacterial numbers. The NSMI allows the user to selectively turn on and off each state variable, providing increased flexibility in its application. All state variables must be specified as "On" or "Off." When "On," the NSMI computes all internal source and sink terms associated with that state variable for every time step. When "Off," no calculations are conducted for the state variable. When a state variable is bypassed, the user does not need to provide any input parameters, boundary concentrations, or initial conditions.

Table 2. Water quality state variables modeled in NSMI.

Variable	Definition	Units	Option
A_p	Algae (Phytoplankton)	µg-Chla L^{-1}	On/Off
A_b	Benthic algae	g-D m^{-2}	On/Off
$OrgN$	Organic nitrogen	mg-N L^{-1}	On/Off
$NH4$	Ammonium	mg-N L^{-1}	On/Off
$NO3$	Nitrate	mg-N L^{-1}	On/Off
$OrgP$	Organic phosphorous	mg-P L^{-1}	On/Off
TIP	Total inorganic phosphorous	mg-P L^{-1}	On/Off
POC	Particulate organic carbon	mg-C L^{-1}	On/Off
DOC	Dissolved organic carbon	mg-C L^{-1}	On/Off
DIC	Dissolved inorganic carbon	mol L^{-1}	On/Off
POM	Particulate organic matter	mg-D L^{-1}	On/Off
POM_2	Sediment particulate organic matter	mg-D L^{-1}	On/Off
$CBOD_i$	Carbonaceous biochemical oxygen demand	mg-O$_2$ L^{-1}	0-10
DO	Dissolved oxygen	mg-O$_2$ L^{-1}	On/Off
PX	Pathogen	cfu (100 mL)$^{-1}$	On/Off
Alk	Alkalinity	mg-CaCO$_3$ L^{-1}	On/Off

3.2   Stoichiometric ratios

The stoichiometric relationships between algal processes and those resulting in the production or consumption of other state variables, such as carbon, nitrogen, and phosphorus are required in water quality models. In most water quality modeling studies, the Redfield ratio (Redfield 1958) is used due to a lack of site-specific data. The stoichiometric weights of carbon (C), nitrogen (N), and phosphorus (P) to g mass units for algal dry weight (D) are defined as

$$100 \text{ g-D} : 40 \text{ g-C} : 7.2 \text{ g-N} : 1 \text{ g-P}.$$

The above Redfield ratio shows that carbon comprises approximately 40 percent of the dry weight of aquatic plant. Chlorophyll-a is more commonly measured in aquatic systems as an estimate of algal biomass. The algal biomass is expressed in units of µg-Chla L^{-1} or mg-Chla m^{-3}. With this information, the stoichiometric ratio relation can be extended as

$$100 \text{ g-D} : 40 \text{ g-C} : 7.2 \text{ g-N} : 1.0 \text{ g-P} : (0.4 \sim 1.0) \text{ g-Chla}.$$

Chlorophyll-a exhibits a wide range of values, depending on the nutrient status of the algae (Harris 1986). Waters with less light would tend to have algae containing a higher chlorophyll-a content. The ratio (C:Chla) of algal carbon to a chlorophyll-a is typically between about 50 and 100.

Nitrogen, phosphorus, carbon, and dry weight biomass can be converted to chlorophyll-a or any of the other units by using the stoichiometric ratios. These ratios are internally computed in NSMI and listed in Table 3.

Table 3. Stoichiometric ratios internally computed in NSMI.

Symbol	Definition	Unit	Formulation[a]
r_{na}	algal N : Chla ratio	mg-N µg-Chla^{-1}	$r_{na} = AW_n / AW_a$
r_{pa}	algal P : Chla ratio	mg-P µg-Chla^{-1}	$r_{pa} = AW_p / AW_a$
r_{ca}	algal C : Chla ratio	mg-C µg-Chla^{-1}	$r_{ca} = AW_c / AW_a$
r_{da}	algal D : Chla ratio	mg-D µg-Chla^{-1}	$r_{da} = AW_d / AW_a$
r_{cd}	algal C : D ratio	mg-C mg-D^{-1}	$r_{cd} = AW_c / AW_d$
r_{oc}	O$_2$: C for carbon oxidation	mg-O$_2$ mg-C^{-1}	$r_{oc} = 32/12$
r_{on}	O$_2$: N ratio for nitrification	mg-O$_2$ mg-N^{-1}	$r_{on} = 2 \cdot 32/14$
r_{nb}	benthic algae N : D ratio	mg-N mg-D^{-1}	$r_{nb} = BW_n / BW_d$
r_{pb}	benthic algae P : D ratio	mg-P mg-D^{-1}	$r_{pb} = BW_p / BW_d$
r_{cb}	benthic algae C : D ratio	mg-C mg-D^{-1}	$r_{cb} = BW_c / BW_d$
r_{ab}	benthic Chla : D ratio	µg-Chla mg-D^{-1}	$r_{ab} = BW_a / BW_d$

[a] The symbols are defined in Table 6.

Stoichiometric ratios associated with oxygen are also listed in Table 3. The stoichiometric ratios for oxygen generation and consumption are derived based upon a typical chemical reaction for the plant photosynthesis and respiration (Chapra 1997). The oxidation of carbon organic matter consumes oxygen at a molar ratio of 1:1, equivalent to a ratio of 32/12 g-O$_2$ to 1 g-C. Algal photosynthesis produces oxygen at a molar ratio of 1:1, equivalent to a ratio of 32/12 g-O$_2$ to 1 g-C. The nitrification consumes oxygen at a molar ratio of 2:1, equivalent to a ratio of 2 · 32/14 g-O$_2$ to 1 g-N.

3.3   Algae

Aquatic plants serve as focal points in the nutrient cycles. The growth and proliferation of aquatic plants result in water quality degradation, or eutrophication. Phytoplankton concentrations also provide one estimate of

the eutrophication potential for the aquatic environment and an indication of a potential problem. Aquatic plants include two very broad categories: (1) those that move freely with water and (2) those that remain fixed or attached to the bottom. Both categories are commonly included as state variables in water quality models because they affect DO and nutrient cycles in aquatic environments, and because excessive algae populations are an environmental concern. The first category includes the microscopic phytoplankton and free-floating water weeds or certain types of plants. Both NSMI and NSMII refer to this category simply as algae. Two general approaches have been used to model floating algae in water quality models (Bowie et al. 1985):

- Aggregating all algae into a single constituent
- Aggregating the algae into a few dominant functional groups (for example, green algae, blue greens, diatoms, etc.)

NSMI uses the first approach, and NSMII uses the second approach. Algal biomass in aquatic environments can be estimated in three ways:

1. Quantifying chlorophyll-*a*
2. Measuring carbon biomass as ash-free dry mass
3. Measuring the particulate organic carbon

The chlorophyll-*a* procedure measures photosynthetic pigment common to all types of algae. The second and third approaches measure the carbon in a filtered water sample. Both NSMI and NSMII model the change in algal biomass expressed as mg-Chla L^{-1} for phytoplankton but as g-D m^{-2} for benthic algae. Because benthic algae can collect inorganic sediments, it is important to measure it as ash-free dry mass.

3.3.1 Algae kinetics

Algal source is photosynthesis or growth; and the sinks include respiration, mortality, and settling. Photosynthesis is the process by which algae uses sunlight to convert carbon dioxide (CO_2) into a food source and releases oxygen as a by-product. Respiration is the opposite of photosynthesis, indicating the products of photosynthesis become reactants in respiration and vice-versa. Because it requires light, photosynthesis occurs only during daylight hours. Respiration, on the other hand, occurs 24 hours a day. Algal mortality produces organic matter that eventually decays and further uses DO. Algal respiration and decomposition contribute to high oxygen

demands. The rates of growth, production, respiration, and mortality are derived from the change of the algae biomass over a time step. The internal source (+) and sink (-) equation for algal biomass can be written as

$$\frac{dA_p}{dt} = \mu_p A_p \qquad \text{Algal growth,} \qquad (3.1a)$$

$$-k_{rp}(T) \cdot A_p \qquad \text{Algal respiration,}$$

$$-k_{dp}(T) \cdot A_p \qquad \text{Algal mortality,}$$

$$-\frac{v_{sa}}{h} A_p \qquad \text{Algal settling,}$$

where

A_p = algae (µg-Chla L^{-1}),
μ_p = algal growth rate (d^{-1}),
$k_{rp}(T)$ = algal respiration rate (d^{-1}),
$k_{dp}(T)$ = algal mortality rate (d^{-1}),
v_{sa} = algal settling velocity (m d^{-1}).

Above modeled algae can be converted to dry weight biomass by

$$A_{pd} = r_{da} A_p, \qquad (3.1b)$$

where

r_{da} = algal D : Chla ratio (mg-D µg-Chla^{-1}),
A_{pd} = algae (dry weight) (mg-D L^{-1}).

3.3.2 Algal growth rate

The growth rate of algae depends on three principal components: temperature, light, and nutrients (ammonium and nitrate and inorganic phosphorus). Like many water quality models, limiting the effects of temperature, light, and nutrients can be used to correct the maximum growth rate. Three alternative (sets of) formulations are available for calculating the algal growth rate in NSMI: (1) multiplicative; (2) limiting nutrient; and (3) harmonic mean.

Multiplicative option:

This option multiplies the growth limiting factors for light, nitrogen, and phosphorus together to determine their net effect on the local algal growth rate. Each of these factors is independent; and under optimal conditions, each limiting factor has a value of one. If not optimal, it is given a fractional value. This option has its biological basis in the multiplicative effects of the enzymatic processes involved in photosynthesis. The algal growth rate is expressed as

$$\mu_p = \mu_{mxp}(T)FL \cdot FN \cdot FP\,, \tag{3.2}$$

where

$$
\begin{aligned}
\mu_{mxp}(T) &= \text{maximum algal growth rate (d}^{-1}\text{),} \\
FL &= \text{light limiting factor for algal growth (0–1.0),} \\
FN &= \text{N limiting factor for algal growth (0–1.0),} \\
FP &= \text{P limiting factor for algal growth (0–1.0).}
\end{aligned}
$$

Nutrient limiting option:

This option computes the local algal growth rate as limited by light and either nitrogen or phosphorus. The nutrient and light effects are multiplicative, but the nutrient effects are alternative with the smaller limitation factor. This approach mimics Liebig's law of the minimum. The algal growth rate is expressed as

$$\mu_p = \mu_{mxp}(T)FL \cdot \min\left(FN, FP\right). \tag{3.3}$$

Harmonic mean option:

The harmonic mean is mathematically analogous to the total resistance of two resistors in parallel and is a compromise between the previous two options. The algal growth rate is controlled by a multiplicative relation between light and nutrients while the nutrient limitation is represented by a harmonic mean. The algal growth rate is expressed as

$$\mu_p = \mu_{mxp}(T)FL\frac{2}{1/FN + 1/FP}. \tag{3.4}$$

3.3.2.1   *Light limitation*

Light is important as the controlling factor for photosynthesis and algal growth. The term *light* is used loosely here to refer to photosynthetically active radiation (PAR) in the waveband 400 to 700 nm. The light limiting factor for algal growth is computed based on PAR intensity by using the following three alternative sets of formulations: Half-saturation function (Baly 1935), Smith's function (Smith 1936), or Steele's function (Steele 1962). QUAL2E and QUAL2K models use these same formulations. All mathematical relationships show an increase in photosynthesis rate with increasing light intensity up to a maximum or saturation value (Figure 4).

Figure 4. Three functions used for computing algal growth light limiting factor (Chpara et al. 2008).
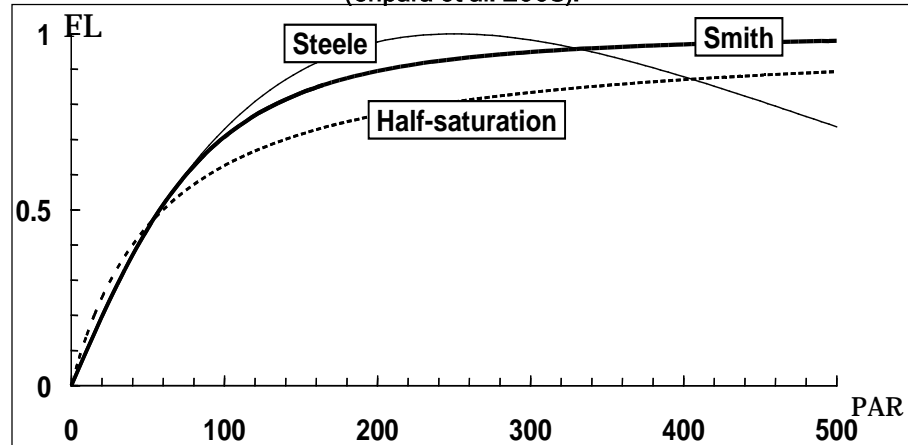
Half-saturation function:

$$FL_z = \frac{I_z}{K_L + I_z},$$
(3.5)

Smith's function:

$$FL_z = \frac{I_z}{\left(K_L^2 + I_z^2\right)^{0.5}},$$
(3.6)

Steele's function:

$$FL_z = \frac{I_z}{K_L}\exp\left(1 - \frac{I_z}{K_L}\right),$$
(3.7)

where

FL_z = light limiting factor for algal growth at depth z,

I_z = PAR intensity at a depth z below the water surface (W m^{-2}), which is radiation with a wavelength between 400 and 700 nm,

K_L = light limiting constant for the algal growth (W m^{-2}).

Photosynthesis occurs throughout the depth of the water column. Light attenuation is simulated as an exponential decrease of light intensity with depth according to the Beer-Lambert law

$$I_z = I_0 \exp(-\lambda \cdot z), \qquad (3.8)$$

where

I_0 = surface light intensity (W m^{-2}),

λ = light attenuation coefficient (m^{-1}),

z = depth from the water surface (m).

The surface light intensity (I_0) is a portion of the visible spectrum and thus is often assumed as a fixed fraction of the short-wave solar radiation used in heat budget computations. Incident short-wave solar radiation is often measured directly at meteorological stations; and can be computed from the site location, time of year, and cloud cover in the temperature simulation module. The magnitude of the visible range is roughly half the computed or observed short-wave solar radiation (Chapra et al. 2008).

$$I_0 = 0.47 \cdot q_{sw}, \qquad (3.9)$$

where

q_{sw} = incident short-wave solar radiation (W m^{-2}).

The light limiting factor is vertically averaged over depth. Substituting equation 3.8 into equations 3.5, 3.6, and 3.7, respectively, and integrating the equations over the depth of flow yields the following depth-averaged light limiting factors.

Half-saturation function:

$$FL = \frac{1}{\lambda \cdot h} \ln\left(\frac{K_L + I_0}{K_L + I_0 \cdot e^{-\lambda \cdot h}}\right),$$
(3.10)

Smith's function:

$$FL = \frac{1}{\lambda \cdot h} \ln\left(\frac{\frac{I_0}{K_L} + \sqrt{1 + \left(\frac{I_0}{K_L}\right)^2}}{\frac{I_0}{K_L} e^{-\lambda \cdot h} + \sqrt{1 + \left(\frac{I_0}{K_L} e^{-\lambda \cdot h}\right)^2}}\right),$$
(3.11)

Steele's function:

$$FL = \frac{2.718}{\lambda \cdot h}\left[e^{-\left(\frac{I_0}{K_L}\right)e^{-\lambda h}} - e^{-\left(\frac{I_0}{K_L}\right)}\right],$$
(3.12)

The relative merits of these light functions are discussed by various authors (Platt et al. 1981, Field and Effler 1982). The use of Smith's function is preferable over the half-saturation function if photoinhibition effects are considered as unimportant.

3.3.2.2   Nutrient limitation

Algae require nutrients such as ammonia, nitrate, and phosphate at various levels depending on the species. The nutrient limitation factor is determined by the concentration of carbon, nitrogen and phosphorus. Carbon is usually available in excess and so carbon limitation is not included in NSMI. Algae are capable of taking up and storing sufficient nutrients to sustain them. However, if the timing of algal blooms is not critical, intracellular storage of nutrients can be ignored within the model, constant stoichiometry is assumed, and the model is much simpler (Park and Clough 2010). Therefore, nutrient limitation by external concentrations is used in NSMI as in many other models. The nutrient limitation on algal growth is determined by the single most limiting nutrient where algal growth follows half-saturation function kinetics with respect to the important nutrients. The half-saturation function is widely used to compute nutrient limitation and primary productivity in water bodies. This function relates aquatic plants and algae growth rates with

available dissolved nutrients. The half-saturation function is evaluated in NSMI for both inorganic nitrogen and phosphorous, and the minimum value is chosen to correct the algal growth rate. Algae are assumed to use both ammonium and nitrate as sources of nitrogen. The limiting factor for the effect of nitrogen on algal growth rate is expressed as

$$FN = \frac{NH4 + NO3}{K_{sN} + (NH4 + NO3)}.$$ (3.13)

Similarly, the limiting factor for the effect of phosphorus on algal growth rate is expressed as

$$FP = \frac{DIP}{K_{sP} + DIP},$$ (3.14)

where

$NH4$ = ammonium (mg-N L^{-1}),
$NO3$ = nitrate (mg-N L^{-1}),
DIP = dissolved inorganic phosphorous (mg-P L^{-1}),
K_{sN} = half-saturation N limiting constant for algal growth (mg-N L^{-1}),
K_{sP} = half-saturation P limiting constant for algal growth (mg-P L^{-1}).

3.3.3 Light attenuation coefficient

Light attenuation is the loss of light intensity with depth as a result of scattering or absorption by substances within the water column and the water itself. The amount of light available to algae and benthic algae depends on both water depth and the rate of light attenuation. The light attenuation (also called extinction) rate describes the decrease in light intensity with depth in the water column, which is computed as the sum of several partial attenuation coefficients reliant on the concentrations of solids particles in suspension and their optical attributes. It includes the baseline attenuation rate for water, self shading of plants, attenuation due to suspended sediment and particulate organic matter, and algae. Baseline attenuation represents attenuation from color and other factors not taken into account by suspended solids and algae. The effect of organic matter on the light attenuation is considered based on water column POC. The light attenuation coefficient is given as (Chapra et al. 2008)

$$\lambda = \lambda_0 + \lambda_s \sum m_n + \lambda_m POM + \lambda_1 A_p + \lambda_2 \left(A_p \right)^{2/3},\qquad(3.15)$$

where

λ_0 = background light attenuation (m^{-1}),
λ_s = light attenuation by inorganic suspended solids (L $mg^{-1}\,m^{-1}$),
λ_m = light attenuation by organic matter (L $mg^{-1}\,m^{-1}$),
λ_1 = linear light attenuation by algae (m^{-1} (µg-Chla $L^{-1})^{-1}$),
λ_2 = nonlinear light attenuation by algae (m^{-1} (µg-Chla $L^{-1})^{-2/3}$),
POM = particulate organic matter (mg-D L^{-1}),
m_n = inorganic suspended solid "n" (mg L^{-1}).

The m_n does not include organic material in the above equation. Concentration of suspended solids can be computed from the inorganic solids module (sand-silt-clay).If the suspended solids have been incremented in value to include organic as well as inorganic materials suspended in the water column, then the default values of λ_s and λ_m need to be adjusted. The percentages of organic and inorganic material in water-quality samples can be determined using different methods (APHA 1992).

3.3.4 Solids partitioning of inorganic phosphorous

Sorption can be important in controlling both the transport and fate of inorganic phosphorus in aquatic systems. Sorption reactions are usually fast relative to other environmental processes, and therefore an equilibrium partitioning is assumed within the model. Under equilibrium partitioning, the distribution of the inorganic phosphorus between suspended solids and water can be adequately described through a linear sorption isotherm. The particulate and dissolved fractions of inorganic phosphorus are internally computed as

$$f_{dp} = \frac{1}{1 + 10^{-6} \sum k_{po4n} m_n} = 1 - f_{pp},\qquad(3.16)$$

where

f_{dp} = dissolved fraction of inorganic P (0–1.0),
f_{pp} = particulate fraction of inorganic P (0–1.0),
k_{dpo4n} = partition coefficient of inorganic P for soild "n" (L kg^{-1}).

The partitioning distribution coefficient (k_{dpo4}) is defined as the ratio of inorganic phosphorous concentration adsorbed onto solids (mass chemical per mass solids) to concentration of inorganic phosphorous dissolved in water (mass chemical per volume of water). It is displayed in units of L kg^{-1}. A wide range of partition coefficients for phosphate is found in literature.

3.4 Benthic Algae

Benthic algae are those that live on or in association with substrata (Stevenson 1996). The substrata can be natural or artificial. Benthic algal cover is a food source for invertebrates which graze on the plant material and in turn the invertebrates are food sources for fish in aquatic environments (Finlay et al. 2002). Most benthic algae in freshwater habitat are blue-green algae (Cyanophyta), green algae (Chlorophyta), diatoms (Bacillariophyta) or red algae (Rhodophyta) (Stevenson 1996). The term *periphyton* is sometimes used in reference to benthic algae and sometimes in reference to the entire attached community of microorganism, including algae, bacteria, fungi, and protozoa. To avoid confusion, *benthic algae* is used to designate the algal community attached to the bottom in NSMI and NSMII.

Benthic algae affect water quality in various ways, and their impact must often be considered to properly evaluate aquatic water quality conditions. Benthic algae growth involves the uptake of inorganic nutrients, the production of DO, and the effects of alkalinity. Mortality produces organic matter. Modeling benthic algae differ from algae in a number of fundamental ways:

- Benthic algae do not move with the water current
- Benthic algae typically dwell on or near the bottom. Therefore, they are not impacted by the average light in the water column but the light reaching the bottom (substrate)
- Benthic algae are limited by substrate available for growth. There is typically a maximum density for attached plants.

3.4.1 Benthic algae kinetics

NSMI has a state variable representing benthic algae. Benthic algae biomass is usually measured as AFDM or photosynthetic-pigment content (for example, chlorophyll-*a*). Benthic algae are modeled in terms of density per unit bottom area (g-D/m^2). The change of benthic algae biomass with respect to time is described using the following mass balance equation

$$\frac{dA_b}{dt} = \mu_b A_b \qquad\qquad \text{Benthic algae growth,} \qquad\qquad (3.17)$$

$$-k_{rb}(T) \cdot A_b \qquad\qquad \text{Benthic algae respiration,}$$

$$-k_{db}(T) \cdot A_b \qquad\qquad \text{Benthic algae mortality,}$$

where

A_b = benthic algae biomass (g-D m^{-2}),
μ_{lb} = growth rate for benthic algae (d^{-1}),
$\kappa_{rb}(T)$ = benthic algae base respiration rate (d^{-1}),
$k_{db}(T)$ = benthic algae mortality rate (d^{-1}).

Benthic algal biomass is converted into chlorophyll-*a* by the following equation

$$Chlb = r_{ab} A_b, \qquad\qquad (3.18)$$

where

r_{ab} = benthic Chla : D ratio (µg- Chla mg-D^{-1}),
$Chlb$ = benthic Chla (mg-Chla m^{-2}).

The conversion factor is based on the average ratio of chlorophyll *a* to AFDM. Production, respiration, and mortality for benthic algae largely follow the formulations for phytoplankton as discussed above.

3.4.2 Benthic algal growth rate

Productivity of benthic algae is a function of light intensity, temperature, and nutrient concentrations. The benthic algae growth rate depends on the availability of certain limiting resources, including light, nutrients (N and P), and bottom area density (space). These effects are simulated as limiting factors that attenuate the maximum growth rate. Two alternative (sets of) formulations are included for calculating the benthic algae growth rate: 1) multiplicative option and 2) nutrient limiting option. These formulations are similar to those for algae except for the effect of space limitation on benthic algal growth.

Multiplicative option:

$$\mu_b = \mu_{mxb}(T)\left(FL_b\right)\left(FN_b\right)\left(FP_b\right)\left(FS_b\right),\qquad(3.19)$$

where

$\mu_{mxb}(T)$ = maximum benthic algae growth rate (d^{-1}),
FL_b = light limiting factor for benthic algae growth (0–1.0),
FN_b = N limiting factor for benthic algae growth (0–1.0),
FP_b = P limiting factor for benthic algae growth (0–1.0),
FS_b = bottom space density limiting factor for benthic algae growth (0–1.0).

Nutrient limiting option:

$$\mu_b = \mu_{mxb}FL_b \cdot \min\left(FN_b, FP_b\right) \cdot FS_b.\qquad(3.20)$$

Temperature limitation factor is computed using Arrhenius Equation. Light limitation is represented using three optional functions. Nutrient limitation is dependent upon the concentrations of nitrogen and phosphorous in aquatic systems.

3.4.2.1 Light effect

The effect of light on the benthic algae rate is simulated as for algae. The difference is that for benthic algae, the light intensity used is the light intensity at the mean channel depth rather than the depth integrated value. The light limitation factor for benthic algae growth is determined by the amount of PAR reaching the channel bottom. Three alternative (sets of) formulations are included: half-saturation, Smith's, and Steele's function.

Half-saturation function:

$$FL_b = \frac{I_0 \cdot e^{-\lambda \cdot h}}{K_{Lb} + I_0 \cdot e^{-\lambda \cdot h}},\qquad(3.21)$$

Smith's function:

$$FL_b = \frac{I_0 \cdot e^{-\lambda \cdot h}}{\sqrt{K_{Lb}^2 + \left(I_0 \cdot e^{-\lambda \cdot h}\right)^2}},\qquad(3.22)$$

Steele's function:

$$FL_b = \frac{I_0 \cdot e^{-\lambda \cdot h}}{K_{Lb}} e^{\left(1 - \frac{I_0 \cdot e^{-\lambda \cdot h}}{K_{Lb}}\right)},$$ (3.23)

where

K_{Lb} = light limiting constant for benthic algae growth (W m^{-2}).

3.4.2.2   Nutrient effect

Nitrogen and phosphorus limiting factors for benthic algae growth are c computed as for algal growth (equations 3.13 and 3.14), with the exception that the user may supply different half-saturation nitrogen and phosphorous constants for benthic algae

$$FN_b = \frac{NH4 + NO3}{K_{sNb} + (NH4 + NO3)},$$ (3.24)

$$FP_b = \frac{DIP}{K_{sPb} + DIP},$$ (3.25)

where

K_{sNb} = half-saturation N limiting constant for benthic algae growth, (mg-N L^{-1}),

K_{sPb} = half-saturation P limiting constant for benthic algae growth (mg-P L^{-1}).

3.4.2.3   Bottom density effect

Benthic algae growth has an additional limitation based on available substrate, which includes the littoral bottom and the available bottom area. Attached algae typically exhibit lateral heterogeneity with higher densities at shallower depths. A half-saturation function is used to attenuate the growth rate of benthic algae as their density on the bottom increases

$$FS_b = 1 - \frac{A_b}{K_{Sb} + A_b},$$ (3.26)

where

K_{Sb} = half-saturation density constant for benthic algae growth (g-D m^{-2}).

3.5 Nitrogen Species

A simplified nitrogen cycle is modeled in NSMI. The nitrogen cycle simulates the transformations of organic nitrogen (OrgN), ammonium (NH4), nitrite (NO2) and nitrate (NO3). In aerobic water, there is a stepwise transformation from OrgN to NH4, to NO2), and finally to NO3. Both algae and benthic algae are linked to the nitrogen cycle via the processes of growth, respiration, and death, as shown in Figure 3. Both take up and release nutrients. As they die, hydrolytic bacteria quickly recycle nutrients into their respective pools at specified ratios and rates.

3.5.1 Organic nitrogen

Nitrogen kinetics however, requires some representation of the organic nitrogen as this generally makes up a significant part of the pollution load. The particulate and aqueous fractions of organic nitrogen (OrgN) are lumped together as one state variable in NSMI. Organic nitrogen in the water column is produced by both algae and benthic algae, and lost due to decay and settling. The production of organic nitrogen by algal death is computed using a stoichiometric coefficient representing the fraction of nitrogen content. Thus, internal source (+) and sink (-) equation for water column OrgN can be written as

$$\frac{dOrgN}{dt} = k_{dp}(T) \cdot r_{na} \cdot A_p \qquad \text{Algal mortality (A}_p\text{-->OrgN)}, \qquad (3.27)$$

$$- k_{on}(T) \cdot OrgN \qquad \text{Organic N decay (OrgN-->NH4)},$$

$$- \frac{v_{son}}{h} OrgN \qquad \text{Organic N settling (OrgN-->Bed)},$$

$$+ \frac{1}{h} k_{db}(T) \cdot r_{nb} A_b F_w F_b \qquad \text{Benthic algae mortality (A}_b\text{-->OrgN)},$$

where

$OrgN$ = organic nitrogen (mg-N L^{-1}),

r_{na} = algal N : Chla ratio (mg-N µg-Chla^{-1}),

$k_{on(T)}$ = decay rate of organic N into NH4 (d^{-1}),

v_{son} = organic N settling velocity (m d^{-1}),

r_{nb} = benthic algae N :D ratio (mg-N mg-D^{-1}),

F_w = fraction of benthic algae mortality into the water column (0–1.0),

F_b = fraction of bottom area available for benthic algae growth (0–1.0).

Because organic nitrogen is a byproduct of algae, computed organic nitrogen needs to be corrected for algal composition and compared to total organic nitrogen (TON) measurements. Measured TON includes organic nitrogen and the amount of nitrogen incorporated in algal biomass. Algal organic nitrogen is added to OrgN for comparison with measured TON.

3.5.2 Ammonium

The decay of organic nitrogen represents a source term for water column NH4. NH4 in the water column is assimilated by algae and benthic algae and is converted to nitrate as a result of nitrification. The nitrification process consumes oxygen. Algal uptake rate is based on the fraction of NH4 available as compared to NO3. Sediment releases of NH4 can be specified. The internal source (+) and sink (-) equation for water column NH4 can be written as

$$\frac{dNH4}{dt} = k_{on}(T) \cdot OrgN \qquad \text{Organic N decay (OrgN-->NH4),} \qquad (3.28)$$

$$- k_{nit}(T) \cdot NH4 \qquad \text{NH4 nitrification (NH4-->NO3),}$$

$$+ k_{rp}(T) \cdot r_{na} A_p \qquad \text{Algal respiration (A$_p$-->NH4),}$$

$$- F_1 \mu_p r_{na} A_p \qquad \text{Algal uptake (NH4-->A$_p$),}$$

$$+ k_{rb}(T) \cdot r_{nb} A_b \qquad \text{Benthic algae respiration (A$_b$-->NH4),}$$

$$- \frac{1}{h} F_2 \mu_b r_{nb} A_b F_b \qquad \text{Benthic algae uptake (NH4-->A$_b$),}$$

$$+ \frac{r_{nh4}}{h} \qquad \text{Sediment release (Bed<-->NH4),}$$

where

$k_{nit\ (T)}$ = nitrification rate of NH4 to NO3 (d^{-1}),
r_{nh4} = sediment release rate of NH4 (g-N m^{-2} d^{-1}),
F_1 = preference fraction of algal N uptake from NH4 (0–1.0),
F_2 = preference fraction of benthic algae N uptake from NH4 (0–1.0).

For physiological reasons, the preferred form for algal uptake is NH4. Preference fractions of algae and benthic algae uptake from water column NH4 are computed as

$$F_1 = \frac{P_N \cdot NH4}{P_N \cdot NH4 + (1 - P_N) NO3},$$ (3.29)

$$F_2 = \frac{P_{Nb} NH4}{P_{Nb} NH4 + (1 - P_{Nb}) NO3},$$ (3.30)

where

P_N = NH4 preference factor for algal growth,
P_{Nb} = NH4 preference factor for benthic algae growth.

The process of nitrification is carried out following a two-step process. During nitrification, NH4 is oxidized into NO2 first, then NO3. The equations for nitrification are summarized below.

$$NH_4 + \frac{3}{2}O_2 \rightarrow NO_2^- + 2H^+, \quad NO_2^- + \frac{1}{2}O_2 \rightarrow NO_3^-.$$
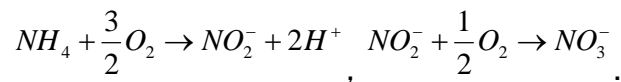
The oxygen consumed by the above nitrification can be computed as $r_{on} = 2\ 32/14 = 4.57$ g-O$_2$ g-N^{-1}. The nitrification rate reduces at low levels of DO, which can be corrected by applying the inhibition correction factor (Brown and Barnwell 1987)

$$k_{nit} = k_{nit}\left(1 - e^{-K_{NR} \cdot DO}\right),$$ (3.31)

where

K_{NR} = oxygen inhibition factor for nitrification (0.6 − 0.7) (mg-O$_2$ L^{-1}).

3.5.3 Nitrate

In NSMs, nitrite is lumped into nitrate as it exists in much smaller quantities. Nitrite and nitrate is simply referred to as nitrate (NO3) for short. Water column NO3 is formed by nitrification and removed by denitrification. Nitrate is used during photosynthesis. Denitrifying bacteria are known to flourish on the anaerobic surface layer of the sediment (Kusuda et al. 1994). Pauer and Auer (2000) claimed that denitrification is generally a sediment-based phenomena rather than one existing in the water column. However, denitrification can also occur in the water column where there is NO3 but little available oxygen (Di Toro 2001). Optimum conditions for denitrification are a high NO3, enough degradable organic material, a low DO, and a high temperature. Denitrification is limited by the availability of NO3 and is inhibited by DO. Following the convention of other water quality models in representing denitrification, NSMI also models water column denitrification. The internal source (+) and sink (-) equation for water column NO3 can be written as

$$\frac{dNO3}{dt} = k_{nit}(T) \cdot NH4 \qquad \text{NH4 nitrification (NH4-->NO3),} \qquad (3.32)$$

$$-\left(1 - \frac{DO}{K_{sOxdn} + DO}\right) k_{dnit}(T) \cdot NO3 \qquad \text{NO3 denitrification (NO3-->Loss),}$$

$$-\left(1 - F_1\right)\mu_p r_{na} A_p \qquad \text{Algal uptake (NO3-->A\textsubscript{p}),}$$

$$-\frac{1}{h}\left(1 - F_2\right)\mu_b r_{nb} A_b F_b \qquad \text{Benthic algae uptake from NO3 (NO3-->A\textsubscript{b}),}$$

$$-\frac{v_{no3}}{h} NO3 \qquad \text{Sediment denitrification (NO3<-->Bed),}$$

where

$k_{dnit}(T)$ = denitrification rate (d^{-1}),
K_{sOxdn} = half-saturation oxygen inhibition constant for denitrification ($mg\text{-}O_2\ L^{-1}$),
v_{no3} = sediment denitrification velocity ($m\ d^{-1}$).

3.5.4 Derived variables

Derived variables related to nitrogen species are computed as

$$DIN = NH4 + NO3,\qquad(3.33a)$$

$$TON = OrgN + r_{na} \cdot A_p,\qquad(3.33b)$$

$$TKN = NH4 + TON,\qquad(3.33c)$$

$$TN = NO3 + TKN,\qquad(3.33d)$$

where

DIN = dissolved inorganic nitrogen (mg-N L^{-1}),
TON = total organic nitrogen (mg-N L^{-1}),
TKN = total Kjeldahl nitrogen (mg-N L^{-1}),
TN = total nitrogen (mg-N L^{-1}).

3.6 Phosphorus Species

The phosphorus cycle is simpler than the nitrogen cycle. Total organic phosphorus, dissolved and particulate inorganic phosphorus are modeled in NSMI. A reaction specific to the phosphorus cycle is the adsorption and desorption of inorganic phosphorus. Inorganic phosphorus can be present in a dissolved form and adsorbed to suspended sediment particles (House et al. 1995). In waterways, the majority of phosphorus is in particulate form. Some of this phosphorus can readily become available through mineralization or desorption. However, most of the suspended solids attached to phosphorus remain unavailable. Because of the association of phosphorus with solids, its concentration often varies temporally in parallel with concentrations of suspended solids (Ekholm et al. 2000). Both algae and benthic algae are linked to the phosphorus cycle via the processes of growth, respiration, and death, as shown in Figure 3.

3.6.1 Organic phosphorus

NSMI includes organic phosphorus (OrgP) as a single state variable. Organic phosphorus in the water column is produced by both algae and benthic algae, and is lost due to mineralization and settling. The production of organic phosphorus by algal death is computed using a

stoichiometric coefficient representing the fraction of phosphorus content. The internal source (+) and sink (-) equation for water column OrgP can be written as

$$\frac{dOrgP}{dt} = k_{dp}(T) \cdot r_{pa} A_p \qquad \text{Algal mortality (A}_p\text{-->OrgP),} \qquad (3.34)$$

$$- k_{op}(T) \cdot OrgP \qquad \text{Organic P decay (OrgP-->DIP),}$$

$$- \frac{v_{sop}}{h} OrgP \qquad \text{Organic P settling (OrgP-->Bed),}$$

$$+ \frac{1}{h} k_{db}(T) \cdot r_{pb} A_b F_w F_b \qquad \text{Benthic algae mortality (A}_b\text{-->OrgP),}$$

where

$$
\begin{aligned}
OrgP &= \text{organic phosphorous (mg-P L}^{-1}\text{),} \\
r_{pa} &= \text{algal P : Chla ratio (mg-P μg-Chla}^{-1}\text{),} \\
k_{op}(T) &= \text{decay rate of organic P into DIP (d}^{-1}\text{),} \\
v_{sop} &= \text{organic P settling velocity (m d}^{-1}\text{),} \\
r_{pb} &= \text{benthic algae P : D ratio (mg-P mg-D).}
\end{aligned}
$$

Computed organic phosphorus also needs to be corrected for algal composition in order to compare with total organic phosphorus (TOP) measurements. Measured TOP includes organic phosphorus and the amount of phosphorus incorporated in algal biomass. Algal organic phosphorus is added to OrgP for comparison with measured TOP.

3.6.2 Total inorganic phosphorus

Inorganic phosphorous serves as one of the primary nutrients for aquatic plants. Phosphorus is often in short supply in an aquatic ecosystem and limits plant and algal growth (Correll 1998, Carpenter et al. 1998). Orthophosphate is the major form of biologically available phosphorus found in water. It is usually present as a combination of mono hydrogen phosphate (HPO_4^{2-}) and dehydrogen phosphate ($H_2PO_4^-$), depending on pH, but for simplicity it is also referred as phosphate (PO_4). In water quality reporting, inorganic phosphorous is usually referred to as dissolved inorganic phosphorus (DIP) or by the technical term filterable reactive

phosphorus (FRP). Inorganic phosphorus is generally strongly adsorbed to sediment particles and organic matter, which make the phosphorus unavailable as a nutrient (Tate et al. 1995). Sorption of inorganic phosphorus occurs in particular to the iron (III) oxyhydroxides in sediment particles. Other adsorbing components are aluminum hydroxides and silicates, manganese oxides, and organic matter. Sorption of inorganic phosphorous on suspended solids is modeled in NSMI. At equilibrium, the distribution of inorganic phosphorus between solids and water can be described by a linear equilibrium partitioning isotherm. Rather than modeling two different compartments, NSMI includes the total inorganic phosphorous (TIP) as a single state variable.

Inorganic phosphorous in the water column is lost due to uptake during algal growth and solids settling and gained due to sediment release and the decay of organic phosphorus. The released phosphorus may significantly increase the biologically available pool of phosphorous in water. The internal source (+) and sink (-) equation for water column TIP can be written as

$$\frac{dTIP}{dt} = k_{op}(T) \cdot OrgP \qquad \text{Organic P decay (OrgP-->DIP)}, \qquad (3.35)$$

$$-\frac{v_{sp}}{h} f_{pp} TIP \qquad \text{TIP net settling (TIP-->Bed)},$$

$$+ k_{rp}(T) \cdot r_{pa} A_p \qquad \text{Algal respiration (A}_p\text{-->DIP)},$$

$$- \mu_p r_{pa} A_p \qquad \text{Algal uptake (DIP-->A}_p\text{)},$$

$$+ k_{rb}(T) \cdot r_{pb} A_b \qquad \text{Benthic algae respiration (A}_b\text{-->DIP)},$$

$$- r_{pb} \mu_b \frac{A_b}{h} F_b \qquad \text{Benthic algae uptake (DIP-->A}_b\text{)},$$

$$+ \frac{r_{po4}}{h} \qquad \text{Sediment release (Bed<-->DIP)},$$

where

TIP = total inorganic phosphorus (mg-P L^{-1}),
v_{sp} = settling velocity of suspended sediments (m d^{-1}),
r_{po4} = sediment release rate of DIP (g-P m^{-2} d^{-1}).

3.6.3 Derived variables

The derived variables related to phosphorus species are computed as

$$DIP = f_{dp}TIP, \qquad (3.36a)$$

$$TOP = OrgP + r_{pa}.A_p, \qquad (3.36b)$$

$$TP = TIP + TOP, \qquad (3.36c)$$

where

TOP = total organic phosphorus (mg-P L^{-1}),
TP = total phosphorus (mg-P L^{-1}).

3.7 Particulate Organic Matter

Detritus or particulate organic matter (POM) represents fine organic materials suspended in the water column but capable of settling to the bottom. POM composition is usually similar to that of phytoplankton and it serves as a food source for zooplankton and fish. The POM is subjected to different processes within aquatic environment. POM increases due to plant death and is lost via dissolution and settling. POM also serves as a surrogate variable in NSMI, implicitly simulating particulate organic carbon if this state variable is turned off. However, carbon, nitrogen, and phosphorus in detritus are considered as separate state variables in NSMI. The internal source (+) and sink (-) equation for water column POM can be written as

$$\frac{dPOM}{dt} = k_{dp}(T) \cdot r_{da} A_p \qquad \text{Algal mortality (A}_p\text{-->POM)}, \qquad (3.37)$$

$$- k_{pom}(T) \cdot POM \qquad \text{POM dissolution},$$

$$- \frac{v_{som}}{h} POM \qquad \text{POM settling (POM-->Bed)},$$

$$+ \frac{1}{h} k_{db}(T) \cdot A_b F_b F_w \qquad \text{Benthic algal mortality (A}_b\text{-->POM)},$$

where

$k_{pom}(T)$ = POM dissolution rate (d^{-1}),
   v_{som} = POM settling velocity (m d^{-1}).

When water column POM settles to the bottom sediment, it is converted to organic sediment. The benthic sediment POM becomes a critical variable for contaminant modeling, therefore it is included in NSMI. Sediment POM consists of organic material and benthic organisms. Sediment POM is derived solely from settling of algae and POM from the water column. The rate change of sediment POM is determined by the following mass balance equation

$$h_2 \frac{dPOM_2}{dt} = v_{som}POM + v_{sa}r_{da}A_p \quad \text{POM deposition,} \tag{3.38}$$

$$+ k_{db}(T) \cdot A_b F_b (1 - F_w) \qquad \text{Benthic algal mortality (}A_b\text{-->}POM_2\text{),}$$

$$- h_2 k_{pom2}(T) \cdot POM_2 \qquad \text{Sediment POM dissolution,}$$

$$- w_2 POM_2 \qquad \text{Sediment POM burial,}$$

where

     h_2 = active sediment layer thickness (m),
  POM_2 = sediment particulate organic matter (mg L^{-1}),
$k_{pom2}(T)$ = sediment POM dissolution rate (d^{-1}),
    w_2 = sediment burial rate (m d^{-1}).

Products of sediment POM dissolution increase amounts of sediment nitrogen, phosphorus, and carbon. The sediment release of these constituents can be specified within NSMI.

3.8 Carbonaceous Biological Oxygen Demand

Carbonaceous Biological Oxygen Demand (CBOD) is included as a state variable in NSMs. The CBOD kinetics described here are identical for both NSMI and NSMII. CBOD, also called ultimate CBOD or CBODU, is modeled. Biological oxygen demand (BOD) is often measured (expressed as O_2) and reported in water quality reports (Wool et al. 2006). The BOD consists of CBOD and nitrogenous biochemical oxygen demand (NBOD)

(Figure 5). CBOD is the concentration of organic material and reflects the oxygen demand exerted on the water column through oxidation of organic carbon. NBOD is a result of biochemical oxidation of organics by nitrogenous bacteria using oxygen. The CBOD is usually exerted first because of the time lag in the growth of the nitrifying bacteria. Therefore, total five day BOD (BOD5) is often equal to five-day CBOD (CBOD5).

Figure 5. A typical oxygen demand curve (Thomann and Mueller 1987).
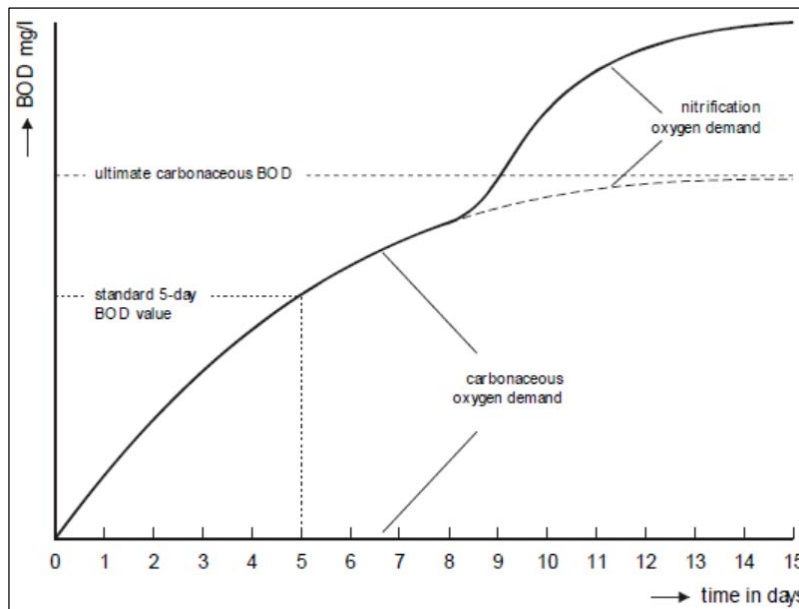
In NSMs, water column CBOD can be modeled up to ten groups because of the different decay rates of each group. This feature allows the user to have the input of data that more accurately characterizes various CBOD sources and their effects on DO. The algal contribution to CBOD is not included in the model. The CBOD is only subject to first-order oxidation loss and additional removal due to sedimentation, scour and flocculation, which do not exert an oxygen demand as described in QUAL2E (Brown and Barnwell 1987). However, the modeling of CBOD is an intercalated part of DO modeling and the CBOD oxidation stops if the water becomes anaerobic.

The internal source and sink equation for water column CBOD can be written as

$$\frac{dCBOD_i}{dt} = -\frac{DO}{K_{sOxbodi} + DO} k_{bodi}(T) \cdot CBOD_i \quad \text{CBOD oxidation,} \tag{3.39}$$

$$-k_{sbodi}(T) \cdot CBOD_i \qquad \text{CBOD net sedimentation,}$$

where

$CBOD_i$ = carbonaceous biochemical oxygen demand (mg-O$_2$ L^{-1}),

$k_{bodi}(T)$ = CBOD oxidation rate (d^{-1}),

$k_{sbodi}(T)$ = CBOD sedimentation rate (m d^{-1}),

$K_{sOxbodi}$ = half saturation oxygen attenuation constant for CBOD oxidation (mg-O$_2$ L^{-1}).

The subscript "*i*" in the above equation is used to represent a specific CBOD group. CBOD forms modeled in NSMs are always the ultimate CBODs. CBOD input to the model from boundary conditions or point sources must also be ultimate CBODs. However, CBOD is often determined by standard methods that measure the oxygen consumption of a filtered sample during laboratory incubation and within a defined period of time. A much-used water quality constituent is CBOD5 (mg-O$_2$ L^{-1}), which represents the amount of oxygen that is consumed when a sample is stored for five days in a dark environment at 20°C. The ratio between CBOD5 and CBOD depends on the decay rate of the organic material. CBOD5 measurements must be converted to CBOD based on individual CBOD decay rates.

$$CBOD_i = \frac{CBOD5}{1 - e^{-5 \cdot k_{bodi}}}, \qquad (3.40)$$

where

$CBOD5$ = 5-day carbonaceous biochemical oxygen demand (mg-O$_2$ L^{-1}),

k_{bodi} = CBOD oxidation rate at 20°C (d^{-1}).

The CBOD5 to CBOD conversion factor will vary depending on the source of the CBOD. Typical CBOD / CBOD5 is 1.2 for raw wastewater and 1.6 for primary / secondary wastewater (Thomann and Muller 1987). Direct comparisons between CBOD5 measurement and the model output cannot be made using computed CBOD. Thus it is necessary to convert computed CBOD into CBOD5 or CBOD5 into CBOD. CBOD5 is computed as the sum of the contributions from dissolved organic matter represented by CBOD and dissolved organic carbon.

$$CBOD5 = \sum CBOD_i \left(1 - e^{-5 k_{bodi}(20)}\right) + r_{oc} DOC \left(1 - e^{-5 \cdot k_{doc}(20)}\right), \qquad (3.41)$$

where

DOC = dissolved organic carbon (mg-C L^{-1}),
r_{oc} = O$_2$: C ratio for carbon oxidation (mg-O$_2$ mg-C^{-1}),
$k_{doc(T)}$ = DOC oxidation rate (d^{-1}).

The CBOD5 shown above reflects only the oxidation of dissolved organic carbon and should be used when compared with a filtered laboratory CBOD5 measurement. If CBOD5 measurements are tainted by algal respiration and the decay of algal carbon, a correction must be made to the computed CBOD so that a valid comparison to observed measurement may be made.

3.9 Carbon Species

Carbon has a fundamental role in water quality processes, which cannot be represented by CBOD alone (Connolly and Coffin 1995, Chapra 1999). NSMI models a carbon cycle with three state variables. They are particulate organic carbon (POC), dissolved organic carbon (DOC), and dissolved inorganic carbon (DIC). POC represents non-living particulate detrital carbon. The POC levels are a function of productivity in the surface water. The DOC is simply that portion of TOC that is dissolved in water compared to that portion of organic carbon in suspension. Furthermore, DOC forms complexes with toxic chemicals and trace metals, creating water-soluble complexes. The dynamics of these chemicals is intimately connected with the generation, transport, and fate of organic carbon. Modeling contaminant sorption processes is not possible without an estimate of the particulate and dissolved fractions of organic carbon. Concentrations of POC and DOC are required in contaminant transport modeling studies (Tye et al. 1996). Finally, organic carbon and other dissolved and particulate matter can affect light penetration in aquatic ecosystems. Organic carbon's behavior, reactivity, and fate in aquatic systems strongly depend on whether that substance is present in the dissolved or particulate phases. Algal contribution is the only source of POC in the water column. Algal mortality is fractioned between POC and DOC.

Inorganic carbon species in NSMI include carbon dioxide (CO$_2$), bicarbonate (HCO$_3^-$), and carbonate (CO$_3^{2-}$). The sum of these species is called DIC. Bicarbonate is usually the most important DIC species in natural waters since it is the dominant species between pH 6.35 and 10.33.

$$DIC = [\text{H}_2\text{CO}_3^*] + [\text{HCO}_3^-] + [\text{CO}_3^{2-}], \qquad (3.42)$$

where

DIC = dissolved inorganic carbon (mol L^{-1}),
$H2CO3^*$ = sum of dissolved CO_2 and carbonic acid (mol L^{-1}),
HCO_3^- = bicarbonate ion (mol L^{-1}),
CO_3^{2-} = carbonate ion (mol L^{-1}).

DIC does not include solid-phase calcium carbonate. The rate of DIC change is proportional to the net primary production. Similar to other nutrients, DIC is produced by decomposition and is assimilated by plants; it also is respired by aquatic plants. Additional sources and sinks of DIC are via exchange with the atmosphere and via the oxidation of organic carbon material (i.e. DOC, CBOD). Water column DIC is tracked in units of mole or mol L^{-1}. A mole mass of DIC is equal to 12 gram (g), 1 mol L^{-1} = 12000 mg-C L^{-1}. Simulating DIC is necessary for calculating pH as a derived variable. The internal source (+) and sink (-) equations for water column POC, DOC, and DIC are given as follows.

3.9.1 State variables

Particulate Organic Carbon (POC):

$$\frac{\partial POC}{\partial t} = F_{pocp} k_{dp}(T) \cdot r_{ca} A_p \qquad \text{Algal mortality (A}_\text{p}\text{-->POC),} \qquad (3.43)$$

$$- k_{poc}(T) \cdot POC \qquad \text{POC hydrolysis (POC-->DOC),}$$

$$- \frac{v_{soc}}{h} POC \qquad \text{POC settling (POC-->Bed),}$$

$$+ \frac{1}{h} F_{pocb} k_{db}(T) \cdot r_{cb} A_b F_b F_w \qquad \text{Benthic algal mortality (A}_\text{b}\text{-->POC),}$$

where

POC = particulate organic carbon (mg-C L^{-1}),
F_{pocp} = fraction of algal mortality into POC (0–1.0),
r_{ca} = algal C : Chla ratio (mg-C μg-Chla^{-1}),
r_{cb} = benthic algae C : D ratio (mg-C mg-D^{-1}),
v_{soc} = POC settling velocity (m d^{-1}),
$k_{poc}(T)$ = POC hydrolysis rate (d^{-1}),
F_{pocb} = fraction of benthic algal mortality into POC (0–1.0).

Dissolved Organic Carbon (DOC):

$$\frac{\partial DOC}{\partial t} = \left(1 - F_{pocp}\right)k_{dp}(T) \cdot r_{ca}A_p \qquad \text{Algal mortality (A}_p\text{-->DOC),} \qquad (3.44)$$

$$+ k_{poc}(T) \cdot POC \qquad \text{POC hydrolysis (POC-->DOC),}$$

$$+ k_{pom}(T) \cdot f_{com}POM \qquad \text{POM dissolution (POM-->DOC),}$$

$$- \frac{DO}{K_{sOxmc} + DO}k_{doc}(T) \cdot DOC \qquad \text{DOC oxidation,}$$

$$- \frac{5 \times 12}{4 \times 14}\left(1 - \frac{DO}{K_{sOxdn} + DO}\right)k_{dnit}(T) \cdot NO3 \qquad \text{DOC consumed by denitrification,}$$

$$+ \frac{1}{h}\left(1 - F_{pocb}\right)k_{db}(T) \cdot r_{cb}A_bF_bF_w \qquad \text{Benthic algal mortality (A}_b\text{-->DOC),}$$

where

K_{sOxmc} = half saturation oxygen attenuation constant for DOC oxidation rate (mg-O$_2$ L^{-1}),

f_{com} = fraction of carbon in organic matter (mg-C mg-D^{-1}).

Dissolved Inorganic Carbon (DIC):

$$12 \cdot 10^3 \frac{\partial DIC}{\partial t} = \qquad\qquad\qquad\qquad\qquad\qquad\qquad (3.45)$$

$$+ 12k_{ac}(T)\left(10^{-3}k_H(T)p_{CO_2} - 10^3 F_{co2}DIC\right) \quad \text{Atmospheric CO}_2 \text{ reaeration (Atm<-->DIC),}$$

$$+ \frac{DO}{K_{sOxmc} + DO}k_{doc}(T) \cdot DOC \qquad \text{DOC mineralization (DOC-->DIC),}$$

$$+ k_{rp}(T) \cdot r_{ca}A_p \qquad \text{Algal respiration (A}_p\text{-->DIC),}$$

$$- \mu_p r_{ca}A_p \qquad \text{Algal photosynthesis (DIC-->A}_p\text{),}$$

$$+ \frac{1}{h}k_{rb}(T) \cdot r_{cb}A_bF_b \qquad \text{Benthic algae respiration (A}_b\text{-->DIC),}$$

$$- \frac{1}{h}\mu_b r_{cb}A_bF_b \qquad \text{Benthic algae photosynthesis (DIC-->A}_b\text{),}$$

$$+\frac{1}{r_{oc}}\sum\frac{DO}{K_{sOxbodi}+DO}k_{bodi}(T)\cdot CBOD_i \qquad \text{CBOD oxidation (CBOD-->DIC),}$$

$$+\frac{1}{h}\frac{SOD(T)}{r_{oc}} \qquad\qquad\qquad \text{Sediment release (Bed-->DIC),}$$

where

$k_{ac}(T)$ = CO_2 reaeration rate (d^{-1}),
$k_H(T)$ = Henry's Law constant (mol L^{-1} atm^{-1}),
p_{CO2} = partial pressure of CO_2 in the atmosphere (ppm),
F_{CO2} = fraction of total inorganic carbon in CO_2 (0–1.0).

3.9.2 CO_2 reaeration

Atmospheric reaeration of CO_2 refers to the transfer of CO_2 across the air–water interface. The CO_2 reaeration proceeds proportional to the difference of the CO_2 saturation and the actual dissolved CO_2. Atmospheric reaeration may cause a CO_2 flux either way, to the atmosphere or to the water. The CO_2 saturation is primarily a function of the partial atmospheric CO_2 pressure (P_{CO2}) and the water temperature. P_{CO2} in the atmosphere can be referenced from Figure 6. The gaseous and aqueous phase CO_2 values are related by Henrys Law. The value of Henry's Law constant (K_H) is a function of water temperature (Edmond and Gieskes 1970)

$$log_{10}K_H(T) = \frac{2385.73}{T_{wk}} + 0.0152642\,T_{wk} - 14.0184, \qquad (3.46)$$

where

T_{wk} = water temperature in Kelvin.

Figure 6. Concentration of CO₂ in the atmosphere as recorded at
Mauna Loa Observatory, Hawaii (NOAA-ESRL).
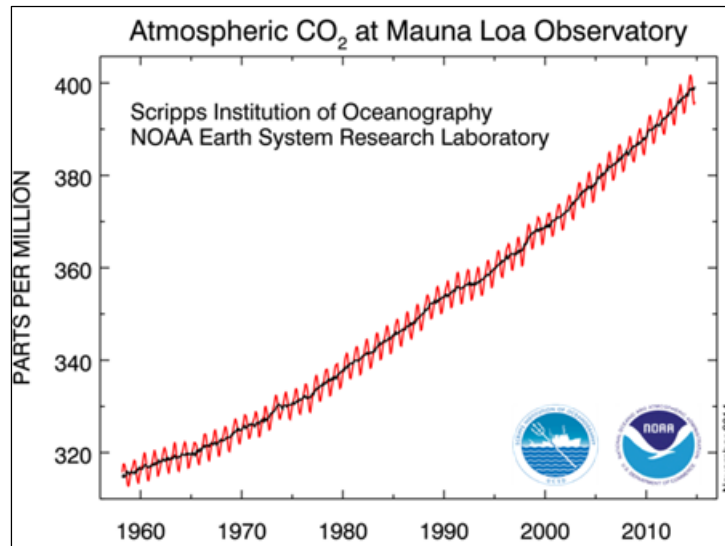
The CO_2 reaeration rate can be derived from the temperature-corrected oxygen reaeration rate using the following relationship.

$$k_{ac}(T) = \left(\frac{MW_{O2}}{MW_{CO2}}\right)^{0.25} k_a(T) ,$$

(3.47)

where

$k_a(T)$ = oxygen reaeration rate (d⁻¹),
MW_{O2} = molecular weight of O_2 (= 32 g mol⁻¹).
MW_{CO2} = molecular weight of CO_2 (= 44 g mol⁻¹).

3.9.3 Derived variables

The total organic carbon (TOC) is the gross amount of organic matter found in natural water. Measured TOC includes particulate (colloidal), dissolved organic carbon forms, CBOD, and algal biomass. Modeled TOC is computed as

$$TOC = DOC + POC + \frac{\sum CBOD_i}{r_{oc}} + r_{ca} A_p .$$

(3.48a)

Total Suspended Solids (TSS) includes all of the inorganic suspended solids fractions and all organic matter, which includes algae and particulate organic matter. Modeled TSS is computed as

$$TSS = \sum m_n + \frac{POC}{f_{com}} + r_{da} A_p .$$
(3.48b)

If POC is turned off and POM is modeled in NSMI, TOC and TSS are computed as

$$TOC = DOC + f_{com} POM + \frac{\sum CBOD_i}{r_{oc}} + r_{ca} A_p ,$$
(3.48c)

$$TSS = \sum m_n + POM + r_{da} A_p ,$$
(3.48d)

where

    TOC = total organic carbon (mg-C L^{-1}),
    TSS = total suspended solids (mg L^{-1}).

Turbidity is an indicator of the amount of suspended solids and related constituents within a water body. Floating algae are often a major component of turbidity. It is possible to develop relationship to predict the turbidity. The relationship between TSS and turbidity is usually considered to be linear on a natural logarithmic scale (Packman et al. 1999). Shown below is a generic relationship between TSS and turbidity in Nephelometric Turbidity Units (NTU). This relationship can be used to estimate the turbidity from computed TSS.

$$\ln(Turbidity) = A \ln(TSS) + B ,$$
(3.49)

where

    A, B = site specific parameters for turbidity.

3.10 Dissolved Oxygen

Dissolved oxygen (DO) is one of the most important variables in water quality modeling. DO concentration is generally viewed as an indicator of the overall well-being of water bodies and their associated ecosystems. An

adequate DO concentration is a basic requirement for a healthy ecosystem. When the DO concentration becomes too low, plants and animals may become impaired and eventually die. The relationship between the growth and death of aquatic plants and the DO rate is a particularly important one. Algal photosynthesis is the source of DO. Algal growth produces DO from photosynthesis. Atmospheric reaeration may be another source of DO, if the water column oxygen is less than DO saturation. The sinks of DO include algal respiration, nitrification, oxidation of organic materials (in particular, DOC, CBOD), SOD, and atmospheric reaeration when DO saturation is exceeded. When anaerobic conditions occur, decay of organic materials slows considerably. Organic decay rates are dependent on the amount of DO present in the water column.

The internal source (+) and sink (-) equation for water column DO can be written as

$$\frac{dDO}{dt} = k_a(T)(DO_s - DO) \qquad \text{Atmospheric O}_2 \text{ reaeration (Atm<-->O}_2\text{)},\qquad (3.50)$$

$$+\left(\frac{138}{106} - \frac{32}{106}F_1\right)\mu_p r_{oc} r_{ca} A_p \qquad \text{Algal photosynthesis (A}_p\text{--> O}_2\text{)},$$

$$-k_{rp}(T)\cdot r_{oc} r_{ca} A_p \qquad \text{Algal respiration (O}_2\text{-->A}_p\text{)},$$

$$-k_{nit}(T)\cdot r_{on} NH4 \qquad \text{Nitrification (O}_2\text{-->Nitrification)},$$

$$-\frac{DO}{K_{sOxmc} + DO} k_{doc}(T)\cdot r_{oc} DOC \qquad \text{DOC oxidation (O}_2\text{-->DOC)},$$

$$-\sum \frac{DO}{K_{sOxbodi} + DO} k_{bodi}(T)\cdot CBOD_i \qquad \text{CBOD oxidation (O}_2\text{-->CBOD)},$$

$$+\frac{1}{h}\left(\frac{138}{106} - \frac{32}{106}F_2\right)\mu_b r_{oc} r_{cb}(T)\cdot A_b F_b \qquad \text{Benthic algae photosynthesis (A}_b\text{--> O}_2\text{)},$$

$$-\frac{1}{h}k_{rb}(T)\cdot r_{oc} r_{cb} A_b F_b \qquad \text{Benthic algae respiration (O}_2\text{-->A}_b\text{)},$$

$$-\frac{DO}{K_{sSOD} + DO}\frac{SOD(T)}{h} \qquad \text{Sediment oxygen demand (SOD)},$$

where

DO = dissolved oxygen (mg-O$_2$ L^{-1}),

DO_s = dissolved oxygen saturation (mg-O_2 L^{-1}),

r_{on} = O_2 : N ratio for nitrification (mg-O_2 mg-N^{-1}),

$SOD(T)$ = sediment oxygen demand (g-O_2 m^{-2} d^{-1}),

K_{sSOD} = half saturation oxygen attenuation constant for SOD (mg-O_2 L^{-1}).

Because of the importance of DO in aquatic systems, it is imperative to include all processes that exert an oxygen demand. If CBOD and DOC are included in the model, care must be taken to ensure that they are properly accounted for. CBOD, DOC, POC or POM are often used to estimate the quantity of organic matter in natural waters. CBOD is typically specified as allochthonous inputs, and the forms of autochthonous organic matter are kept track of in the organic carbon pools (DOC, POC). "Double counting" of organic matter effect on the DO when CBOD and organic carbon should not be included in the model simulation.

3.10.1 Dissolved oxygen saturation

A variety of methods have been developed to estimate the DO saturation (DO_s) (Bowie et al. 1985). DO_s is computed here as a function of water temperature (APHA 1992).

$$DO_s = \exp\left(\begin{array}{l} -139.34410 \\ +\dfrac{1.575701 \cdot 10^5}{T_{wk}} - \dfrac{6.642308 \cdot 10^7}{T_{wk}^{\,2}} + \dfrac{1.243800 \cdot 10^{10}}{T_{wk}^{\,3}} - \dfrac{8.621949 \cdot 10^{11}}{T_{wk}^{\,4}} \end{array}\right) \quad (3.51)$$

Figure 7 shows a fitted curve to the above DO saturation, $DO_{s,}$ as a function of temperature.

The effect of atmospheric pressure on DO_s is corrected based on the following equation (APHA 1992)

$$DO_s = DO_s p_{atm} \frac{\left(1 - \dfrac{p_{wv}}{p_{atm}}\right)(1 - \alpha \cdot p_{atm})}{(1 - p_{wv})(1 - \alpha)}, \quad (3.52)$$

where

p_{atm} = atmospheric pressure (atm),

p_{wv} = partial pressure of water vapor (atm),

α = correction coefficient.

Figure 7. Fitting a curve of the DO saturation as a function of water temperature.
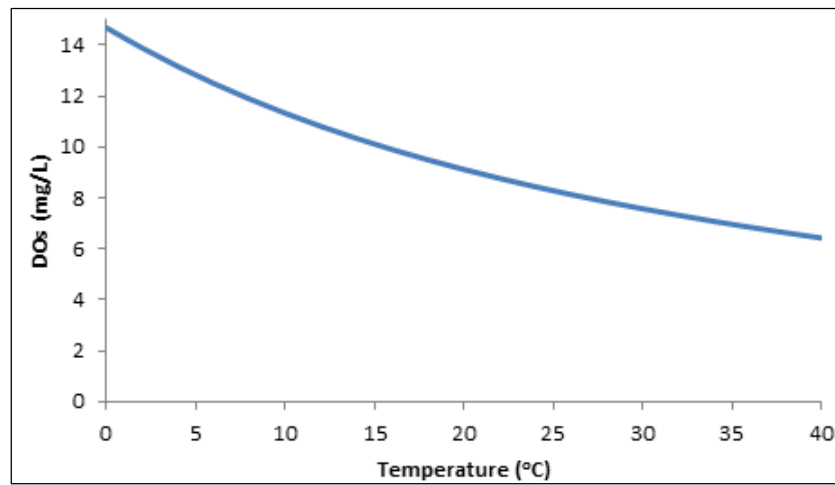
The partial pressure of water vapor (p_{wv}) and correction coefficient (α) are computed as

$$p_{wv} = \exp\left[11.8571 - \frac{3840.70}{T_k} - \frac{216961}{T_k^2}\right],$$ (3.53)

$$\alpha = 0.000975 - 1.426 \cdot 10^{-5}\,T + 6.436 \cdot 10^{-8}\,T^2\,.$$ (3.54)

3.10.2 Oxygen reaeration

Oxygen reaeration refers to the transfer of oxygen across the air–water interface. At concentrations lower than the DO saturation, oxygen is transferred from the air to the water. If the concentration becomes higher than the DO saturation, oxygen will be transferred to the air. This transfer is affected by the difference in DO concentrations between the air and water and by the turbulence in the film of water adjacent to the surface. The turbulence in that thin film may be caused by wind shear or shear produced by water currents. Overall, turbulence controls the rate of oxygen transfer. In streams, the reaeration rate coefficient is a function of the average water velocity, depth, wind, and temperature. The oxygen reaeration rate is estimated as a function of both flow hydraulics and wind velocity.

$$k_a(T) = \frac{k_{aw}(T)}{h} + k_{ah}(T),$$ (3.55)

where

$k_{aw}(T)$ = wind oxygen reaeration velocity (m d^{-1}),
$k_{ah}(T)$ = hydraulic oxygen reaeration rate (d^{-1}).

Numerous formulations have been developed to estimate the rate of oxygen reaeration derived by hydraulic effects. These formulations are often empirical, but most have a deterministic background. Except for a user-defined input, the following six formulas are included to compute the hydraulic derived oxygen reaeration rate (k_{ah}) (Table 4). Note that these formulations are applicable for riverine systems. The computed reaeration rate from these equations is referenced to 20 ºC. It is adjusted for local water temperature using Arrhenius Equation.

Table 4. Equations for computing oxygen reaeration rate on the basis of hydraulic characteristics.

Option	Formulation*	Applicability	Reference
1	$k_{ah} = 3.93 u^{0.5}/h^{1.5}$	natural streams (h = 0.3 – 9)	O'Connor and Dobbins (1958)
2	$k_{ah} = 5.32 u^{0.67}/h^{1.85}$, h < 0.61 $k_{ah} = 5.026 u/h^{1.67}$, otherwise	natural streams (h = 0 – 3.3)	Owens et al. (1964) Churchill et al. (1962)
3	$k_{ah} = 517(u \cdot sl)^{0.524} Q^{-0.242}$, Q < 0.556 m³/s $k_{ah} = 596(u \cdot sl)^{0.528} Q^{-0.136}$, Q > 0.556 m³/s	pool and riffle streams	Melching and Flores (1999)
4	$k_{ah} = 88(u \cdot sl)^{0.313} h^{-0.353}$, Q < 0.556 m³/s $k_{ah} = 142(u \cdot sl)^{0.333} h^{-0.66} B_t^{-0.243}$, Q > 0.556 m³/s	channel control streams	Melching and Flores (1999)
5	$k_{ah} = 31183 u \cdot sl$, Q < 0.425 m³/s $k_{ah} = 15308 u \cdot sl$, Q ≥ 0.425 m³/s	natural streams and rivers	Tsivoglou and Neal (1976)
6	$k_{ah} = 2.16(1 + 9F_d^{0.25}) \dfrac{u_*}{h}$ $F_d = \dfrac{u}{\sqrt{gA_c/B_t}}$, $u_* = \sqrt{gR_h sl}$	natural streams and rivers	Thackston and Dawson (2001)

* u = water velocity (m s^{-1}).

h = water depth (m).

s_l = channel slope.

B_t = top width of the channel (m).

R_h = channel hydraulic radius (m).

A_c = channel cross-sectional area (m²).

Three options are available to incorporate wind effects on the oxygen reaeration: (1) user defined, (2) Banks-Herrera formula (Banks and Herrera 1977), and (3) Wanninkhof formula (Wanninkhof et al. 1991).

Banks and Herrera (Banks and Herrera 1977):

$$k_{aw}(T) = 0.728U_{w10}^{0.5} - 0.317U_{w10} + 0.0372U_{w10}^2 \quad , \qquad (3.56a)$$

Wanninkhof (Wanninkhof et al. 1991):

$$k_{aw}(T) = 0.0986U_{w10}^{1.64}, \qquad (3.56b)$$

where

$k_{aw}(T)$ = wind oxygen reaeration velocity (m d^{-1}),
u_{w10} = wind speed measured 10 meters above the water surface (m s^{-1}).

Wind speed, usually measured at meteorological stations, is also a required data for simulating water temperature.

3.10.3 Sediment oxygen demand and sediment–water fluxes

The SOD is the rate of oxygen consumption exerted by the benthic sediments. The areal fluxes from the benthic sediment can be substantial as oxygen sinks to the overlying water. The SOD involves the degradation and mixing processes in the benthic sediments. This parameter represents the sediment oxygen demand as measured in the field. The SOD is expressed as a zero-order reaction and is a user specified input. A default value of 0.5 g-O$_2$ m^{-2} d^{-1} is recommended for the natural SOD, a value of 1.5 g-O$_2$ m^{-2} d^{-1} for the total oxygen demand (Manivanan 2008). The SOD rates are adjusted according to the local depth and temperature. Table 5 provides some reported in-situ SOD values in rivers and streams. Note that these values may be not applicable for current studies.

Table 5. Reported in-situ values of SOD in some rivers and streams.

SOD (g-O_2 m^2 d^{-1})	Environment	Experimental conditions	References
2.0 – 33	Four Eastern U.S. rivers downstream of paper mill discharge	In-situ respirometer, light, stirred, dark, 22 - 27°C	NCASI (1978)
0.9 – 14.1	Four Eastern U.S. rivers downstream of paper mill discharge	In-situ open-ended tunnel respirometer, light, stirred, dark, 22 - 27°C	NCASI (1978)
0.1 – 1.4	Eastern U.S. rivers downstream of paper mill discharge	In-situ respirometer, stirred, dark, 9 - 16°C, $\theta = 1.08$	NCASI (1979)
0.27 – 9.8	Northern Illinois rivers (89 stations)	In-situ respirometer, stirred, 1 - 3 hrs dark, 5 - 31°C	Butts and Evans (1978)
0.1 – 5.3	Six stations in eastern Michigan rivers	In-situ respirometer, stirred, 15 - 27 hr dark, 19 - 25° C, $\theta = 1.08$	Chiaro and Burke (1980)
1.1 – 12.8	New Jersey rivers (10 stations)	In-situ respirometer, dark, 30 min - 8 hr, stirred	Hunter et al. (1973)
0.3 – 1.4	Swedish rivers	In-situ respirometer, light, stirred, 0 - 10°C	Edberg and Hofsten (1973)
4.6 - 44	Streams	Oxygen mass balance	James (1974)

User-specified sediment–water fluxes include NH4, NO3 and inorganic phosphorous. Such release occurs as a result of a gradient in nutrient concentration between the overlying water and the nutrient in the pore water of the benthic sediment. The impact of sediment nutrient release can be significant. The model assumes that positive fluxes are from sediment to water and that negative fluxes are from water to sediment. Fluxes of NH4 and inorganic phosphorous are most often from sediment to water and are positive quantities. Sediment–water flux of NO3 is defined through the sediment denitrification velocity. NO3 commonly passes in both directions across the sediment–water interface and may be positive or negative.

3.11 Pathogen

A single group of pathogens is included as a state variable in NSMs. The pathogen kinetics described here are identical for NSMI and NSMII. Although there are a variety of indicators and direct enumeration of pathogens, primary emphasis in water quality has been placed in the past on the coliform group of bacteria. The principal waterborne pathogens of concern include *V. cholera*, *Salmonellae*, and the *Shigella* species (Thomann and Mueller 1987). In the model, the concentration of

pathogens in the water column is represented by the CFU, which is a measure of viable bacterial numbers.

The pathogen kinetics were adapted from QUAL2K (Chapra et al. 2008). Pathogens are subject to loss by death, sunlight decay, and settling. The death of pathogens in the absence of sunlight is considered to be first order. The depth-averaged effect of sunlight on decay rate is a function of surface solar radiation and light attenuation coefficient. Pathogen settling losses depend on how many organisms are attached to particles.

The internal source and sink equation for water column pathogen (*PX*) can be written as

$$\frac{dPX}{dt} = -k_{dx}(T) \cdot PX \qquad \text{Pathogen death,} \qquad (3.57)$$

$$-\alpha_{px} \frac{I_0}{\lambda \cdot h} \left(1 - e^{-\lambda \cdot h}\right) PX \qquad \text{Pathogen decay by sunlight,}$$

$$-\frac{v_x}{h} PX \qquad \text{Pathogen net settling,}$$

where

$$
\begin{aligned}
PX &= \text{pathogen ((cfu (100 mL)}^{-1}), \\
k_{dx}(T) &= \text{pathogen death rate (d}^{-1}), \\
\alpha_{px} &= \text{light efficiency factor for pathogen decay,} \\
v_x &= \text{pathogen net settling velocity (m d}^{-1}).
\end{aligned}
$$

Note that net settling loss rate, v_i, can be negative, zero, or positive, depending on the degree of resuspension because benthic sediment may be a significant sources of pathogens.

3.12 Alkalinity

Alkalinity (*Alk*) is included as a state variable in NSMs. The alkalinity kinetics described here are identical for both NSMI and NSMII. Alkalinity is the measurement of the buffering capacity of a solution. It measures the ability of the solution to neutralize acids and bases. In the natural environment, the main ions that neutralize H^+ are HCO_3^- and CO_3^{2-}. In most waters, alkalinity and hardness have similar values because HCO_3^- and CO_3^{2-} are usually derived from C_aCO_3 or $MgCO_3$. Therefore, alkalinity is typically

reported by the laboratory in units of $CaCO_3$ equivalent (mg-$CaCO_3$ L^{-1}). Alkalinity should be measured on filtered samples to eliminate any potential contribution from suspended $CaCO3$ and specified in units of mg L^{-1} of $CaCO_3$. This means that the solution has numerically the same alkalinity as a solution in which the same weight of $CaCO_3$ per liter has been dissolved. A mole mass of $CaCO_3$ is equal to 2 equivalent (eq), and 1 eq L^{-1} = 50000 mg-$CaCO_3$ L^{-1}. Computationally, the variable *Alk* has units of 1 eq L^{-1}.

Alkalinity is affected by all the processes that yield or consume H^+ or OH^-. Algae and benthic algae can affect alkalinity through the photosynthesis and respiration processes. Algal photosynthesis takes up nitrogen as either NH4 or NO3 and inorganic phosphorous. The uptake of NH4 removes positive ions from solution, causing a decrease of alkalinity. The uptake of NO3 removes negative ions from solution, causing an increase of alkalinity. Similarly, the uptake of inorganic P removes negative ions from solution, causing an increase of alkalinity. Algal respiration releases NH4 and inorganic P. The release of NH4 adds positive ions to the water, causing an increase of alkalinity. The release of inorganic P adds negative ions to the water, causing a decrease of alkalinity. Nitrification utilizes NH4 and creates NO3. Hence, because a positive ion is taken up and a negative ion is created, the alkalinity decreases. Denitrification utilizes NO3 and creates nitrogen gas. Hence, the alkalinity increases because a negative ion is taken up and a neutral compound is created.

The internal source and sink equation for water column *Alk* can be written as

$$\frac{\mathrm{d}Alk}{\mathrm{d}t} = r_{alkden}\left(1 - \frac{DO}{K_{sOxdn} + DO}\right)k_{dnit}(T)\cdot NO3 \qquad \text{Alk increased by denitrification,} \qquad (3.58)$$

$$-r_{alkn}\frac{DO}{K_{sOxna}+DO}\frac{NH4}{K_{sNh4}+NH4}k_{nit}(T)\cdot NH4 \qquad \text{Alk decreased by nitrification,}$$

$$+\left(r_{alkaai}F_1 - r_{alkani}(1-F_1)\right)\mu_p A_p \qquad \text{Alk decreased by algal growth,}$$

$$+r_{alkaai}k_{rp}(T)\cdot A_p \qquad \text{Alk increased by algal respiration,}$$

$$-\frac{1}{h}\left(r_{alkba}F_2 - r_{alkbn}(1-F_2)\right)\mu_b A_b F_b \qquad \text{Alk decreased by benthic algae growth,}$$

$$+\frac{1}{h}r_{alkba}k_{rb}(T)\cdot A_b F_b \qquad \text{Alk increased by benthic algae respiration,}$$

where

Alk = alkalinity (eq L^{-1}),

r_{alkaa} = ratio translating algal growth into Alk if NH4 is the N source (eq μg-Chla^{-1}),

r_{alkan} = ratio translating algal growth into Alk if NO3 is the N source (eq μg-Chla^{-1}),

r_{alkn} = ratio translating NH4 nitrification into Alk (eq mg-N^{-1}),

r_{alkden} = ratio translating NO3 denitrification into Alk (eq mg-N^{-1}),

r_{alkba} = ratio translating benthic algae growth into Alk if NH4 is the N source (eq mg-D^{-1}),

r_{alkbn} = ratio translating benthic algae growth into Alk if NO3 is the N source (eq mg-D^{-1}).

Note the units of alkalinity are based on eq L^{-1} or mol L^{-1} for convenience. The numerical factors used in the above equation are computed from the unit conversion between the native mass units used in state variables (algae, benthic algae, NH4, and NO3) and the unit employed for alkalinity.

$$r_{alkaa} = r_{ca} \times \frac{14 \text{ eqH}^+}{106 \text{ moleC}} \times \frac{\text{moleC}}{12 \text{ gC}} \frac{g}{10^3 \text{mg}} = \frac{0.011}{10^{-3}} r_{ca}, \qquad (3.59a)$$

$$r_{alkan} = r_{ca} \left(\frac{\text{mgC}}{\text{mgA}} \right) \times \frac{18 \text{ eqH}^+}{106 \text{ moleC}} \times \frac{\text{moleC}}{12 \text{ gC}} \frac{g}{10^3 \text{mg}} = \frac{0.01415}{10^{-3}} r_{ca}, \quad (3.59b)$$

$$r_{alkn} = \frac{2 \text{ eqH}^+}{\text{moleN}} \frac{\text{moleN}}{14 \text{ gN}} \frac{g}{10^3 \text{mg}} = \frac{0.143}{10^{-3}}, \qquad (3.59c)$$

$$r_{alkden} = \frac{4 \text{ eqH}^+}{\text{moleN}} \frac{\text{moleN}}{14 \text{ gN}} \frac{g}{10^3 \text{mg}} = \frac{0.286}{10^{-3}}, \qquad (3.59d)$$

$$r_{alkba} = r_{cb} \times \frac{14 \text{ eqH}^+}{106 \text{ moleC}} \times \frac{\text{moleC}}{12 \text{ gC}} \frac{g}{10^3 \text{mg}} = \frac{0.011}{10^{-3}} r_{cb}, \qquad (3.59e)$$

$$r_{alkbn} = r_{cb} \times \frac{18 \text{ eqH}^+}{106 \text{ moleC}} \times \frac{\text{moleC}}{12 \text{ gC}} \frac{g}{10^3 \text{mg}} = \frac{0.01415}{10^{-3}} r_{cb}. \qquad (3.59f)$$

The constituents of alkalinity commonly found are HCO_3^-, CO_3^{2-}, and OH^-. HCO_3^- in surface waters at neutral pH is typically greater than 95% of the total alkalinity. Alkalinity usually is defined as

$$Alk = [\text{HCO}_3^-] + 2[\text{CO}_3^{2-}] + [\text{OH}^-] - [\text{H}^+]. \qquad (3.60a)$$

DIC is the sum of the inorganic carbon species in water, including dissolved carbon dioxide (CO_2) and carbonic acid (H_2CO_3), bicarbonate anion (HCO_3^-), and carbonate anion (CO_3^{2-}) based on equation 3.32. Therefore, alkalinity can be computed as

$$Alk = DIC + [\text{OH}^-] - [\text{H}^+], \qquad (3.60b)$$

where

$$H^+ = \text{hydronium ion (mol L}^{-1}),$$
$$OH^- = \text{hydroxyl ion (mol L}^{-1}).$$

3.13 pH

The pH is computed identically in both NSMI and NSMII. DIC and alkalinity are necessary state variables needed to compute pH. This section describes the calculation of pH in the water column. The pH is a very important factor in aquatic environments because certain chemical processes can take place only when water contains a certain pH level. The pH of water determines the solubility and biological availability of chemical constituents such as nutrients (phosphorus, nitrogen, and carbon) and heavy metals (lead, copper, cadmium, etc.). pH affects the ionization and hydrolysis of organic chemicals which potentially has effects on chemical fate and the degree of toxicity.

The pH is a measure of how acidic or basic water is. The range varies from 0 to 14, with 7 being neutral. A pH of less than 7 indicates acidity whereas a pH greater than 7 indicates a base. In most water bodies, pH levels are controlled by total inorganic carbon (C_T) and alkalinity. The relationship of pH and the ratio of *Alk* to C_T (*Alk*/C_T) is illustrated in Figure 8.

Figure 8. Relationship of pH and Alk/C$_T$
(Di Toro 1976).
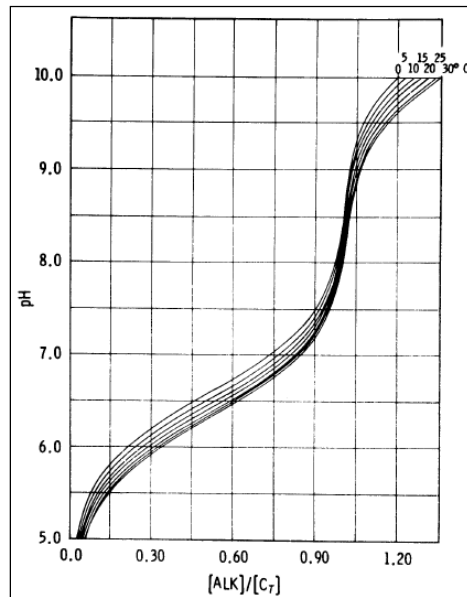
The pH algorithms were adapted from QUAL2K (Chapra et al. 2008). The following equilibrium, mass balance, and electro-neutrality equations define a freshwater that is dominated by inorganic carbon species (Stumm and Morgan 1996).

$$H_2CO_3^* \Leftrightarrow HCO_3^- + H^+, \tag{3.61a}$$

$$HCO_3^- \Leftrightarrow CO_3^{2-} + H^+. \tag{3.61b}$$
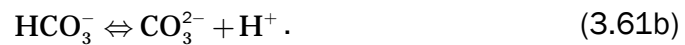
These equilibrium equations are quantified by the dissociation constants as follows:

$$K_1 = \frac{[HCO_3^-][H^+]}{[H_2CO_3^*]}, \tag{3.62}$$

$$K_2 = \frac{[CO_3^{2-}][H^+]}{[HCO_3^-]}. \tag{3.63}$$

The dissociation of water obeys the following equilibrium condition.

$$K_w = [H^+][OH^-], \tag{3.64}$$

where

K_1 = first acidity constant (mol L^{-1}),
K_2 = second acidity constant (mol L^{-1}),
K_w = ion product of water (mol L^{-1})^2.

The K_1, K_2, and K_w values for freshwater are a function of the water temperature. Their values can be computed based on the formulations provided by Plummer and Busenberg (1982) for K_1 and K_2 and by Harned and Hamer (1933) for K_w.

$$\log_{10} K_1 = -356.3094 - 0.06091964 T_{wk} + \frac{21834.37}{T_{wk}} + 126.8339 \log_{10} T_{wk} - \frac{1,684,915}{T_{wk}^2}, \quad (3.65)$$

$$\log_{10} K_2 = -107.8871 - 0.03252849 T_{wk} + \frac{5151.79}{T_{wk}} + 38.92561 \log_{10} T_{wk} - \frac{563,713.9}{T_{wk}^2}, \quad (3.66)$$

$$\log_{10} K_w = -\frac{4787.3}{T_{wk}} - 7.1321 \log_{10} T_{wk} - 0.010365 T_{wk} + 22.80. \quad (3.67)$$

The individual species in the carbonate buffer system are each extremely reactive, so much so that a direct mass balance formulation results in equations that are nonlinear and numerically badly behaved (Di Toro 1976). An efficient solution can be derived by combining equations 3.62, 3.63, and 3.64 to define the following variables

$$\alpha_0 = \frac{[H^+]^2}{[H^+]^2 + K_1[H^+] + K_1 K_2}, \quad (3.68)$$

$$\alpha_1 = \frac{K_1[H^+]}{[H^+]^2 + K_1[H^+] + K_1 K_2}, \quad (3.69)$$

$$\alpha_2 = \frac{K_1 K_2}{[H^+]^2 + K_1[H^+] + K_1 K_2}. \quad (3.70)$$

Equations 3.68, 3.69, and 3.70 can then be substituted into Equation 3.59 to yield

$$\text{Alk} = (\alpha_1 + 2\alpha_2) DIC + \frac{K_w}{[H^+]} - [H^+]. \quad (3.71)$$

Thus, solving for pH is reduced to determining the [H$^+$] from the above equation. The above non-linear equation for [H$^+$], alkalinity, and the carbonate-bicarbonate equilibrium system must be solved simultaneously. Once the unknown [H$^+$] is solved from the above nonlinear equation 3.71, the negative logarithm of [H$^+$] is pH

$$pH = -\log_{10}[H^+].$$ (3.72)

Equation 3.71 is solved for [H$^+$] using two numerical solutions given by Chapra et al. (2008): (1) Newton-Raphson and (2) Bisection. The Newton-Raphson method uses the slope (tangent) of the function at the current iterative solution to find the solution in the next iteration. The bisection method is an incremental search solution where the sub-interval for the next iteration is selected by dividing the current interval in half. For many problems, Newton-Raphson converges quicker than Bisection. However, the Newton-Raphson method is not guaranteed to find a solution.

3.14 NSMI Parameters

This section describes the input parameters associated with NSMI. The user has a number of options in specifying the input parameters. All water quality parameters may be applied uniformly throughout the model domain or may be varied spatially by user-specified water quality regions. Table 6 provides a summary of NSMI input parameters or coefficients. The ratios of C, N, P, and Chla fractions in algae and benthic algae are defined by specifying their relative stoichiometry weight to dry weight biomass (100 mg-D). Temperature-dependent coefficients are specified at 20 ^{o}C. This table will be repeated for each water quality region, allow the user to define the different values for input parameters.

Table 6. NSMI parameters and rate coefficients with default values.

Symbol	Definition	Units	Default Value	Reference Range	Temperature Correction	
		Global				
λ_0	Background light attenuation	m^{-1}	0.02	0.02 - 6.59[e]		
λ_s	Light attenuation by inorganic suspended solids	L mg^{-1} m^{-1}	0.052[a]	0.019 - 0.37[e]		
λ_m	Light attenuation by organic matter	L mg^{-1} m^{-1}	0.174[a]	0.008 - 0.174[e]		
λ_1	Linear light attenuation by algae	m^{-1} (µg-Chla L^{-1})$^{-1}$	0.0088[a]	0.009 - 0.031[e]		

Symbol	Definition	Units	Default Value	Reference Range	Temperature Correction	
λ_2	Nonlinear light attenuation by algae	m^{-1} (µg-Chla L^{-1})$^{-2/3}$	0.054[a]	n/a		
f_{com}	Fraction of carbon in organic matter	mg-C mg-D^{-1}	0.4	0 – 1.0		
k_{dpo4n}	Partition coefficient of inorganic P	L kg^{-1}	0	0 - 200[c] 1000 - 16000[h]		
$k_{ah}(T)$	Hydraulic O$_2$ reaeration rate	d^{-1}	1.0	0.4 - 1.5[h] 4.0 - 10[h]	Yes	1.024[b]
$k_{aw}(T)$	Wind O$_2$ reaeration velocity	m d^{-1}	0	n/a	Yes	1.024
SOD	Sediment oxygen demand	g-O$_2$ m^{-2} d^{-1}	0.2	0.2 - 4.0[c] 0.1 - 10[h]	Yes	1.060[b]
K_{sSOD}	Half saturation oxygen attenuation constant for SOD	mg-O$_2$ L^{-1}	1.0	n/a		
Algae						
AW_d	Algal dry weight stoichiometry	mg-D	100[a]	65 - 130[e]		
AW_c	Algal carbon stoichiometry	mg-C	40[a]	25 - 60[e]		
AW_n	Algal nitrogen stoichiometry	mg-N	7.2[a]	4 - 20[e]		
AW_p	Algal phosphorus stoichiometry	mg-P	1.0[a]	n/a		
AW_a	Algal Chla stoichiometry	µg-Chla	1000[a]	400 - 3500[e]		
$\mu_{mxp}(T)$	Maximum algal growth rate	d^{-1}	1.0	1.0 - 3.0[b] 0.1 - 0.5[c] 0.5 - 3.0[e] 1.0 - 2.0[h]	Yes	1.047[b]
$k_{rp}(T)$	Algal respiration rate	d^{-1}	0.2	0.05 - 0.5[b] 0.02 - 0.8[e]	Yes	1.047[b]
$k_{dp}(T)$	Algal mortality rate	d^{-1}	0.15	0.02 - 0.3[b] 0 - 0.5[e] 0.2 – 8.0[f]	Yes	1.047[b]
v_{sa}	Algal settling velocity	m d^{-1}	0.15	0.15 - 1.8[b] 0 - 1.0[e] 0 - 13.6[j]		
K_L	Light limiting constant for algal growth	W m^{-2}	10	3.7 - 20[b] 14 - 44[e]		
K_{sN}	Half-saturation N limiting constant for algal growth	mg-N L^{-1}	0.04	0.01 - 0.3[b] 0.005 - 0.05[e] 0.002 - 4.34[j]		
K_{sP}	Half-saturation P limiting constant for algal growth	mg-P L^{-1}	0.0012	0.001 - 0.05[b] 0.01 - 0.06[e] 0.001 - 1.52[j]		

Symbol	Definition	Units	Default Value	Reference Range	Temperature Correction	
P_N	NH4 preference factor for algal growth	Unitless	0.5	0 - 1.0		
Benthic algae						
BW_d	Benthic algae dry weight stoichiometry	mg-D	100[a]	65 - 130[e]		
BW_c	Benthic algae carbon stoichiometry	mg-C	40[a]	25 - 60[e]		
BW_n	Benthic algae nitrogen stoichiometry	mg-N	7.2[a]	4 - 20[e]		
BW_p	Benthic algae phosphorus stoichiometry	mg-P	1.0[a]	n/a		
BW_a	Benthic algae Chla stoichiometry	µg-Chla	3500	400 - 3500[e]		
$\mu_{mxb}(T)$	Maximum benthic algae growth rate	d⁻¹	0.4	0.3 - 2.25[b]	Yes	1.047[b]
$k_{rb}(T)$	Benthic algae base respiration rate	d⁻¹	0.2	0.01 - 0.8[b]	Yes	1.06[b]
$k_{db}(T)$	Benthic algae mortality rate	d⁻¹	0.3	0 - 0.8[b]	Yes	1.047[b]
K_{Lb}	Light limiting constant for benthic algae growth	W m⁻²	10	1.7 - 20[b] 14 - 44[e]		
K_{sNb}	Half-saturation N limiting constant for benthic algae	mg-N L⁻¹	0.25	0.01 - 0.766[b] 0.01 - 0.75[e] 0.001 - 0.02[h]		
K_{sPb}	Half-saturation P limiting constant for benthic algae growth	mg-P L⁻¹	0.125	0.01 - 0.08[b] 0.005 - 0.175[e]		
K_{Sb}	Half-saturation density constant for benthic algae growth	g-D m⁻²	10	10 – 30[b]		
P_{Nb}	NH4 preference factor for benthic algae growth	Unitless	0.5	0 - 1.0		
F_{pocb}	Fraction of bethic algae l mortality into POC	Unitless	0.9	0 - 1.0		
F_w	Fraction of benthic algae mortality into water column	Unitless	0.9	0 - 1.0		
F_b	Fraction of bottom area available for benthic algae growth	Unitless	0.9	0 - 1.0		
Nitrogen cycle						
$k_{nit}(T)$	Nitrification rate	d⁻¹	0.1	0.1 - 2.0[b] 0.09 – 0.13[c] 0.01 - 10[e] 0.025 - 6.0[f]	Yes	1.083[b]

Symbol	Definition	Units	Default Value	Reference Range	Temperature Correction	
$k_{on}(T)$	Decay rate of organic N to NH4	d[-1]	0.1	0.02 - 0.4[b] 0.001 - 1.0[e]	Yes	1.047[b]
v_{son}	Organic N settling velocity	m d^{-1}	0.01	0 - 2.0[c] 0 - 0.1[e]		
$k_{dnit}(T)$	Denitrification rate	d[-1]	0.002	0.002 - 2.0[e]	Yes	1.045
K_{sOxdn}	Half-saturation oxygen inhibition constant for denitrification	mg-O_2 L^{-1}	0.1[f]	n/a		
$v_{no3}(T)$	Sediment denitrification velocity	m d^{-1}	0	0 - 1.0[e]	Yes	1.08
r_{nh4}	Sediment release rate of NH4	g-N m^{-2} d^{-1}	0	n/a	Yes	1.074[b]
Phosphorus cycle						
$k_{op}(T)$	Decay rate of organic P to DIP	d[-1]	0.1	0.01 - 0.7[b] 0.001 - 1.0[e]	Yes	1.047[b]
v_{sop}	Organic P settling velocity	m d^{-1}	0.01	0 - 2.0[c] 0 - 0.1[e]		
v_{sp}	Solids settling velocity	m d^{-1}	0.1	0 - 2.0[c] 0 - 30[e]		
r_{po4}	Benthic sediment release rate of DIP	g-P m^{-2} d^{-1}	0	0.001 – 0.15[j]	Yes	1.074[b]
Carbon cycle						
F_{pocp}	Fraction of algal mortality into POC	Unitless	0.9	0 - 1.0		
v_{soc}	POC settling velocity	m d^{-1}	0.01	0 – 2.0[c]		
$k_{poc}(T)$	POC hydrolysis rate	d[-1]	0.005	0.001 - 0.2[c]	Yes	1.047[c]
$k_{doc}(T)$	DOC oxidation rate	d[-1]	0.01	0.01 - 0.2[c]	Yes	1.047[c]
K_{sOxmc}	Half-saturation oxygen attenuation for DOC oxidation	mg-O_2 L^{-1}	1.0	n/a		
F_{co2}	Fraction of DIC in CO_2	Unitless	0.2	0 - 1.0		
p_{CO2}	Partial pressure of CO_2	ppm	383[a]	n/a		
Particulate organic matter						
v_{som}	POM settling velocity	m d^{-1}	0.1	0.05 - 1.0[j]		
$k_{pom}(T)$	POM dissolution rate	d[-1]	0.005	0.001 - 0.11[j]	Yes	1.047[c]
$k_{pom2}(T)$	Sediment POM dissolution rate	d[-1]	0.005	0.001 - 0.2[c]	Yes	1.047[c]
h_2	Active sediment layer thickness	m	0.01	0.001 - 1.0		
w_2	Sediment burial rate	cm yr^{-1}	0.25	n/a		
Carbonaceous biochemical oxygen demand						
$k_{bodi}(T)$	CBOD oxidation rate	d[-1]	0.12	0.02 - 3.4[b]	Yes	1.047[b]

Symbol	Definition	Units	Default Value	Reference Range	Temperature Correction	
$K_{sOxbodi}$	Half-saturation oxygen attenuation for CBOD oxidation	mg-O_2 L^{-1}	0.5[c]	n/a		
$k_{sbodi}(T)$	CBOD sedimentation rate	d^{-1}	0	-0.36 - 0.36[b]	Yes	1.024[b]
Pathogen						
$k_{dx}(T)$	Pathogen death rate	d^{-1}	0.8[a]	n/a	Yes	1.07[a]
α_{px}	Light efficiency factor for pathogen decay	Unitless	1.0[a]	n/a		
v_x	Pathogen settling velocity	m d^{-1}	1.0[a]	n/a		

[*] Subscript i represent a specific CBOD group.

[a] Chapara et al. (2008).

[b] Brown and Barnwell (1987).

[c] Wool et al. (2006).

[d] Brown (2002).

[e] Flynn et al. (2015).

[f] Bowie et al. (1985).

[g] Thomann and Muller (1987).

[h] Thomann and Fitzpatrick (1982).

i. Schnoor (1996).

[j] EL (1995b).

Literature ranges in the above table are taken from published values and from other water quality models. It should be noted that the suggested range values are based on a limited literature review. Most of them are model calibration parameters from real world applications. Parameters should be selected from a range of feasible values, tested in the model, and then adjusted until a satisfactory agreement between predicted and observed variables is obtained. It is also common practice to use model parameters that are determined from other studies.

3.15 NSMI Outputs

This section describes the model outputs associated with NSMI. The output data includes the concentrations of water quality state variables and intermediate variables computed in the NSMI. Table 2 lists the water quality state variables modeled in NSMI.

3.15.1 Derived variables

In order to compare model results with monitoring data, derived water quality constituents are computed directly from the state variables. Table 7 lists the fourteen (14) derived variables computed in NSMI.

Table 7. Derived water quality variables computed in NSMI.

Variable	Definition	Units
A_{pd}	Algale (dry weight)	mg-D L^{-1}
$Chlb$	Benthic chlorophyll-a	mg-Chla m^{-2}
DIN	Dissolved inorganic nitrogen	mg-N L^{-1}
TON	Total organic nitrogen	mg-N L^{-1}
TKN	Total kjeldahl nitrogen	mg-N L^{-1}
TN	Total nitrogen	mg-N L^{-1}
DIP	Dissolved inorganic phosphorus	mg-P L^{-1}
TOP	Total organic phosphorus	mg-P L^{-1}
TP	Total phosphorus	mg-P L^{-1}
TOC	Total organic carbon	mg-C L^{-1}
$CBOD5$	5-day carbonaceous biochemical oxygen demand	mg-O_2 L^{-1}
λ	Light attenuation coefficient	m^{-1}
k_a	Oxygen reaeration rate	d^{-1}
pH	pH	-

3.15.2 Pathway fluxes

Pathway fluxes are important for analyzing individual processes in water quality analysis or they can also be used for debugging the model. Table 8 summarizes a list of pathway fluxes and additional variables that can be reported in NSMI model outputs.

Table 8. Pathway fluxes and additional variables computed in NSMI.

Name	Definition	Units
	Algae	
A_p growth	Algal growth	µg-Chla/L/d
A_p respiration	Algal respiration	µg-Chla/L/d
A_p mortality	Algal mortality	µg-Chla/L/d
A_p settling	Algal settling	µg-Chla/L/d
FL	Algal growth light limit factor	Unitless
FN	Algal growth N limit factor	Unitless

Name	Definition	Units
FP	Algal growth P limit factor	Unitless
Benthic algae		
A_b growth	Benthic algae growth	mg-D/L/d
A_b respiration	Benthic algae respiration	mg-D/L/d
A_b mortality	Benthic algae mortality	mg-D/L/d
FL_b	Benthic algae growth light limit factor	Unitless
FN_b	Benthic algae growth N limit factor	Unitless
FP_b	Benthic algae growth P limit factor	Unitless
FS_b	Benthic algae growth space limit factor	Unitless
Nitrogen cycle		
A_p-->OrgN	Algal mortality into organic N	mg-N/L/d
OrgN-->Bed	Organic N settling	mg-N/L/d
OrgN-->NH4	Organic N decay into NH4	mg-N/L/d
A_p-->NH4	Algal respiration into NH4	mg-N/L/d
NH4-->A_p	Algal uptake from NH4	mg-N/L/d
NH4-->NO3	NH4 nitrification	mg-N/L/d
Bed<-->NH4	Sediment release of NH4	mg-N/L/d
NO3-->A_p	Algal uptake from NO3	mg-N/L/d
NO3 denitrification	NO3 denitrification	mg-N/L/d
NO3<-->Bed	Sdiment NO3 denitrification	mg-N/L/d
A_b-->OrgN	Benthic algae mortality into organic N	mg-N/L/d
A_b-->NH4	Benthic algae respiration into NH4	mg-N/L/d
NH4-->A_b	Benthic algae uptake from NH4	mg-N/L/d
NO3-->A_b	Benthic algae uptake from NO3	mg-N/L/d
Phosphorous cycle		
A_p-->OrgP	Algal mortality into organic P	mg-P/L/d
OrgP-->Bed	Organic P settling	mg-P/L/d
OrgP-->DIP	Organic P decay into DIP	mg-P/L/d
A_p-->DIP	Algal respiration into DIP	mg-P/L/d
DIP-->A_p	Algal uptake from DIP	mg-P/L/d
TIP-->Bed	TIP net settling	mg-P/L/d
Bed<-->DIP	Sediment release of DIP	mg-P/L/d
A_b-->OrgP	Benthic algae mortality into organic P	mg-P/L/d
A_b-->DIP	Benthic algae respiration into DIP	mg-P/L/d
DIP-->A_b	Benthic algae uptake from DIP	mg-P/L/d

Name	Definition	Units
Carbon Cycle		
A_p-->POC	Algal mortality into POC	mg-C/L/d
A_p-->DOC	Algal mortality into DOC	mg-C/L/d
POC-->Bed	POC settling	mg-C/L/d
POC-->DOC	POC hydrolysis	mg-C/L/d
POM-->DOC	POM dissolution	mg-C/L/d
A_b-->POC	Benthic algae mortality into POC	mg-C/L/d
A_b-->DOC	Benthic algae mortality into DOC	mg-C/L/d
DOC-->Denitrification	DOC consumed by denitrification	mg-C/L/d
DOC-->DIC	DOC oxidation	mg-C/L/d
CBOD-->DIC	CBOD oxidation	mg-C/L/d
Atm<-->DIC	Atmospheric CO_2 reaeration	mol/L/d
DIC-->A_p	Algal uptake from DIC	mol/L/d
Bed<-->DIC	Sediment release of DIC	mol/L/d
A_b-->DIC	Benthic algae respiration into DIC	mol/L/d
DIC-->A_b	Benthic algae uptake from DIC	mol/L/d
Particulate organic matter		
A_p-->POM	Algal mortality into POM	mg-D/L/d
POM-->Bed	POM settling	mg-D/L/d
POM dissolution	POM dissolution	mg-D/L/d
A_b-->POM	Benthic algae mortality into POM	mg-D/L/d
POM_2 dissolution	Sediment POM dissolution	mg-D/L/d
POM deposition	POM deposition	mg-D/L/d
POM_2 burial	Sediment POM burial	mg-D/L/d
CBOD i		
CBOD i oxidation	CBOD oxidation	mg-O_2/L/d
CBOD i sedimentation	CBOD net sedimentation	mg-O_2/L/d
Dissolved oxygen		
Atm<-->O_2	Atmospheric O_2 reaeration	mg-O_2/L/d
DO_s	Dissolved oxygen saturation	mg-O_2/L
A_p-->O_2	O_2 produced by algal photosynthesis	mg-O_2/L/d
O_2-->A_p	O_2 consumed by algal respiration	mg-O_2/L/d
O_2-->Nitrification	O_2 consumed by nitrification	mg-O_2/L/d
O_2-->DOC	O_2 consumed by DOC oxidation	mg-O_2/L/d
O_2-->CBOD	O_2 consumed by CBOD oxidation	mg-O_2/L/d
A_b-->O_2	O_2 produced by benthic algae photosynthesis	mg-O_2/L/d

Name	Definition	Units
$O_2 \text{-->} A_b$	O_2 consumed by benthic algae respiration	mg-O_2/L/d
SOD	Sediment oxygen demand	mg-O_2/L/d
Pathogen		
PX death	Pathogen death	cfu/100mL/d
PX decay	Pathogen decay by sunlight	cfu/100mL/d
PX settling	Pathogen settling	cfu/100mL/d
Alklinity		
$A_p \text{-->} Alk$	Alk increased by algal respiration	mg-C_aCO_3/L/d
$Alk \text{-->} A_p$	Alk decreased by algal growth	mg-C_aCO_3/L/d
$Alk \text{-->} Nitrification$	Alk decreased by nitrification	mg-C_aCO_3/L/d
$Denitrification \text{-->} Alk$	Alk increased by denitrification	mg-C_aCO_3/L/d
$A_b \text{-->} Alk$	Alk increased by benthic algae respiration	mg-C_aCO_3/L/d
$Alk \text{-->} A_b$	Alk decreased by benthic algae growth	mg-C_aCO_3/L/d

4   Nutrient Simulation Module II (NSMII)

4.1   Overview

The NSMII was designed to conduct an advanced water quality simulation. An expansion of the water column state variables in NSMII includes twenty-four water quality state variables. Included in NSMII are multiple algal groups, split of organic nitrogen and phosphorous into dissolved and particulate species, carbon cycle, pH, and benthic sediment diagenesis module. In addition, NSMII models algae, nutrient cycles, and DO dynamics in more detail than NSMI. NSMII also allows for a more detailed parameterization of nitrogen, phosphorous, and carbon cycles from organic to inorganic species. The process formulations for organic matter (C, N, P) decomposition, nitrification, and oxidation have been improved in NSMII. The algorithms and formulations incorporated into NSMII were adopted in part from four surface water quality models: QUAL2K (Chapra et al. 2008), WASP (Wool et al. 2006), CE-QUAL-W2 (Cole and Wells 2008), and CE-QUAL-ICM (Cerco and Cole 1993, Cerco et al. 2004). CE-QUAL-W2 (W2) is a 2-D longitudinal/vertical hydrodynamic and water quality model for rivers and lakes. The water quality and hydrodynamic routines are directly coupled in W2. Water quality constituents include suspended solids, coliforms, total dissolved solids, dissolved organic matter, particulate organic matter, algae, phosphorous, ammonia, nitrate, DO, CBOD, inorganic carbon, alkalinity, pH, iron, and zero-order and first-order benthic sediments. CE-QUAL-ICM (ICM) is a dynamic water quality model that can be applied to most water bodies in one, two, or three dimensions. The ICM can model more than 30 state variables, including physical properties; multiple forms of algae, carbon, nitrogen, phosphorus, and silica; and DO, two size classes of zooplankton, two benthos compartments, submerged aquatic vegetation, epiphytes, and benthic algae. The NSMII shares many algorithms and formulations with these models.

Figure 9 provides an overview of the NSMII representation of water quality state variables and major processes involved in the water column. Algae may be either floating (phytoplankton) or attached to the bed such as periphyton. Floating algae are subject to sinking while periphyton are subject to substrate limitations. Diatoms are distinguished from other algae in that they need silicate to grow. Organic matter has a fundamental role in water quality processes, which cannot be identified by single lumped organic nitrogen, phosphorus and carbon state variables alone

(Connolly and Coffin 1995, Shanahan et al. 1998, Chapra 1999). Compared to NSMI, NSMII includes dissolved, refractory, and labile particulate organic species. Labile and refractory organic matter distinctions are based upon relative decay rates of the organics. A labile fraction describes organic materials that decay on a time scale of days to weeks while a refractory fraction accounts for decay processes lasting months to a year. Note that the NSMII splits dissolved organic carbon, particulate organic carbon, nitrogen, and phosphorus into labile and refractory fractions but represents dissolved organic nitrogen and phosphorus as homogenous components. Water quality kinetics for CBOD, pathogen, and alkalinity are modeled in NSMII as for NSMI.

Figure 9. Water quality state variables and major processes modeled in NSMII.
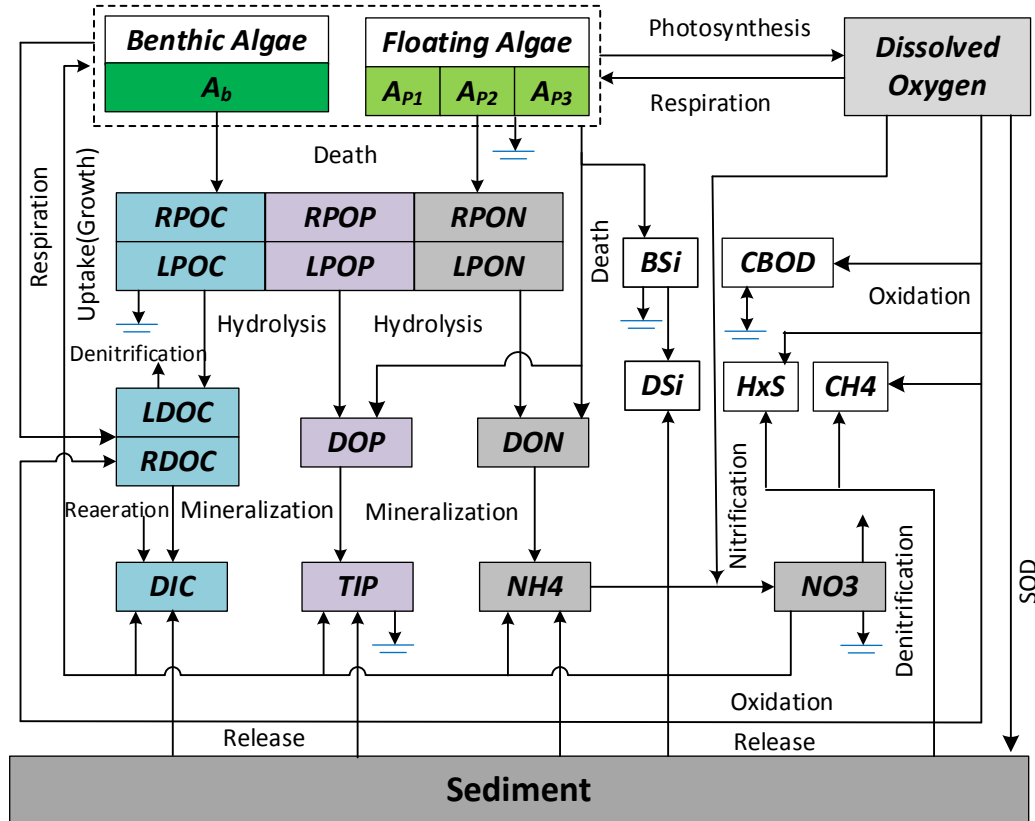
In NSMII, hydrolysis of particulate organic nutrient pools (N, P, C) into dissolved organic form is simulated as a first-order, temperature-dependent process. Mineralization processes account for bacterially mediated oxidation of dissolved organic matter. Mineralization of the organic nutrient pools back to inorganic nutrients (i.e. NH4, DIP, DIC) and is simulated as a first-order, temperature-dependent process. Nitrification and denitrification influence the dissolved inorganic nitrogen (DIN) fraction.

These processes are represented as first-order, oxygen-dependent reactions. The attenuation factor of the kinetic rate due to low oxygen is computed using the half-saturation function. Similar to NSMI, NSMII uses a single settling rate of organic matter and does not include resuspension. Both modules rely on the concept of net settling. This net settling velocity represents the long-term difference between settling and resuspension.

Table 9. Water quality state variables modeled in NSMII.

Variable	Definition	Units	Option
A_{pi}	Algae (Phytoplankton)	µg-Chla L^{-1}	1-3
A_b	Benthic algae	g-D m^{-2}	On/Off
NO3	Nitrate	mg-N L^{-1}	On
NH4	Ammonium	mg-N L^{-1}	On
DON	Dissolved organic nitrogen	mg-N L^{-1}	On
LPON	Labile particulate organic nitrogen	mg-N L^{-1}	On
RPON	Refractory particulate organic nitrogen	mg-N L^{-1}	On
TIP	Total inorganic phosphorus	mg-P L^{-1}	On
DOP	Dissolved organic phosphorus	mg-P L^{-1}	On
LPOP	Labile particulate organic phosphorus	mg-P L^{-1}	On
RPOP	Refractory particulate organic phosphorus	mg-P L^{-1}	On
DIC	Dissolved inorganic carbon	mol L^{-1}	On
LDOC	Labile dissolved organic carbon	mg-C L^{-1}	On
RDOC	Refractory dissolved organic carbon	mg-C L^{-1}	On
LPOC	Labile particulate organic carbon	mg-C L^{-1}	On
RPOC	Refractory particulate organic carbon	mg-C L^{-1}	On
$CBOD_i$	Carbonaceous biochemical oxygen demand	mg-O$_2$ L^{-1}	0-10
CH4	Methane	mg-O$_2$ L^{-1}	On/Off
HxS	Total dissolved sulfides	mg-O$_2$ L^{-1}	On/Off
DO	Dissolved oxygen	mg-O$_2$ L^{-1}	On
BSi	Particulate biogenic silica	mg-Si L^{-1}	On/Off
DSi	Dissolved silica	mg-Si L^{-1}	On/Off
PX	Pathogen	cfu (100 mL)$^{-1}$	On/Off
Alk	Alkalinity	mg-CaCO$_3$ L^{-1}	On/Off

In NSMII, hydrolysis of particulate organic nutrient pools (N, P, C) into dissolved organic form is simulated as a first-order, temperature-dependent process. Mineralization processes account for bacterially mediated oxidation of dissolved organic matter. Mineralization of the

organic nutrient pools back to inorganic nutrients (i.e. NH4, DIP, DIC) is simulated as a first-order, temperature-dependent process. Nitrification and denitrification influence the dissolved inorganic nitrogen (DIN) fraction. These processes are represented as first-order, oxygen-dependent reactions. The attenuation factor of the kinetic rate due to low oxygen is computed using the half-saturation function. Similar to NSMI, NSMII uses a single settling rate of organic matter and does not include resuspension. Both modules rely on the concept of net settling. This net settling velocity represents the long-term difference between settling and resuspension.

Table 9 lists the NSMII's water quality state variables and the symbols. The NSMII allows the user to turn on/off the following state variables: benthic algae, CBOD, silica, methane, sulfide, alkalinity and pathogen. When a state variable is bypassed, the user does not have to provide any input parameters. The concentration of inorganic suspended soilds is a required input for computing partitioning of inorganic P. Alkalinity and DIC are necessary state variables active for computing pH. Two options are available for determining SOD and benthic sediment releases. The first option employs user-specified fluxes. The second option is to couple the water quality kinetics with the benthic sediment diagenesis module, as described in the next chapter. The sediment diagenesis module internally computes the sediment–water fluxes based on deposition of organic particles and other factors.

4.2 Algae

The NSMII can model up to three algae species groups based on dominant functions as diatoms, green algae, blue-greens, etc. Algae may include microscopic phytoplankton and free-floating water weeds or certain types of plants. For example, most freshwater phytoplankton are made up of green algae and cyanobacteria, also known as blue-green algae. Marine phytoplankton are mainly composed of microalgae and diatoms, though other algae and cyanobacteria can be present. Diatoms differ from other species, in part because of their dependency on dissolved silica for growth. The use of multiple groups within NSMII allows for a more detailed representation of the algae dynamics of the system, such as representations of phytoplankton species. Proper group aggregation can provide insight into potential problems associated with modeled algal biomass magnitudes and timing of blooms (Baird 2010).

Algal biomass with each group is modeled as an independent state variable with different nutrient and chlorophyll-a contents, attenuation coefficient, growth rate, respiration rate, and mortality rate. The basic kinetics affecting algal growth and death are identical for the three groups with a distinction in the assigned growth kinetic constants for each group. Algal involvement in the nutrient cycles is explained in the following sections.

4.2.1 Stoichiometric ratios

The stoichiometric ratios associated with algal biomass, carbon, nitrogen, phosphorous, carbon and oxygen must be prescribed in NSMII. Table 10 summarizes stoichiometric ratios internally computed in NSMII.

Table 10. Stoichiometric ratios of algae and oxygen internally computed in NSMII.

Symbol	Definition	Unit	Formulation[a]
r_{nai}	algal N : Chla ratio	mg-N µg-Chla^{-1}	$r_{nai} = AW_n / AW_a$
r_{pai}	algal P : Chla ratio	mg-P µg-Chla^{-1}	$r_{pai} = AW_p / AW_a$
r_{cdi}	algal C : D ratio	mg-C mg-D^{-1}	$r_{cdi} = AW_c / AW_d$
r_{cai}	algal C : Chla ratio	mg-C µg-Chla^{-1}	$r_{cai} = AW_c / AW_a$
r_{dai}	algal D : Chla ratio	mg-D µg-Chla^{-1}	$r_{dai} = AW_d / AW_a$
r_{siai}	algal Si : Chla ratio	mg-Si µg-Chla^{-1}	$r_{siai} = AW_{si} / AW_a$
r_{oc}	O$_2$: C ratio for carbon oxidation	g-O$_2$ g-C^{-1}	$r_{oc} = 32/12$
r_{on}	O$_2$: N ratio for nitrification	g-O$_2$ g-N^{-1}	$r_{on} = 2 \cdot 32/14$

a The symbols are defined in Table 20. Subscript *i* represents a specific algal group.

4.2.2 Algal kinetics

Algae are modeled with NSMII as is done previously with NSMI. The NSMII allows the specification of up to three algal groups. These groups may be defined based on their functions. Each group is governed by the same kinetic equation. Distinctions between the groups are represented by using different parameter values. A variable stoichiometry with respect to each algal group is allowed. Algal sources (+) and sinks (-) include photosynthesis or growth, respiration, mortality, and settling. Attenuation factor due to low oxygen for algal respiration is computed using the half-saturation function. For each algae group, internal source (+) and sink (-) equation of algae biomass can be written as

$$\frac{dA_{pi}}{dt} = \mu_{pi}(T) \cdot A_{pi} \qquad \text{Algal growth,} \qquad (4.1)$$

$$- F_{Oxpi} k_{rpi}(T) \cdot A_{pi} \qquad \text{Algal respiration,}$$

$$- k_{dpi}(T) \cdot A_{pi} \qquad \text{Algal mortality,}$$

$$- \frac{v_{sai}}{h} A_{pi} \qquad \text{Algal settling,}$$

where

A_{pi} = algae (µg-Chla L^{-1}),
$\mu_{pi}(T)$ = growth rate of algal group i [d^{-1}],
$k_{rpi}(T)$ = respiration rate of algal group i (d^{-1}),
$k_{dpi}(T)$ = death rate of algal group i (d^{-1}),
v_{sai} = settling velocity of algal group i (m d^{-1}),
F_{Oxpi} = oxygen attenuation factor for algal respiration (0–1.0).

The subscript "*i*" in the above equation is used to represent a specific algal group.

Attenuation factor due to low oxygen for algal respiration is computed using the half-saturation function

$$F_{Oxpi} = DO \big/ \left(K_{sOxpi} + DO \right), \qquad (4.2)$$

where

K_{sOxpi} = half-saturation oxygen attenuation constant for algal respiration (mg-O$_2$ L^{-1}).

Total algal biomass expressed as chlorophyll-a and dry weight can be computed as

$$Chla = \sum_{1}^{3} A_{pi}, \qquad (4.3a)$$

$$A_{pd} = \sum_{1}^{3} r_{dai} A_{pi}, \qquad (4.3b)$$

where

$Chla$ = chlorophyll-a (µg-Chla L^{-1}),
r_{dai} = algal D : Chla ratio (mg-D µg- Chla^{-1}),
A_{pd} = algae (dry weight) (mg-D L^{-1}).

4.2.3 Algal growth rate

Algal growth is dependent upon temperature, light, and nutrient levels, which modify the maximum growth rate to ambient conditions (Kiffney and Bull 2000, Weckstrom and Korhola 2001, Cascallar et al. 2003). The algal growth rate is a complicated function of the species of algae present and their differing reactions to solar radiation, temperature, and the balance between nutrient availability and algae requirements. Temperature, nutrient, and light impacts on algal growth are simulated using a multiplicative formulation. For each algal group, its growth rate is determined by the maximum potential growth rate multiplied by the minimum value due to limitation by temperature; light; nitrogen; phosphorous; and, when diatoms are considered, silica

$$\mu_{pi}(T) = \mu_{mxpi} FT_{pi} FN_{pi} FL_{pi},$$ (4.4)

where

μ_{mxpi} = maximum growth rate of algal group i (d^{-1}),
FT_{pi} = temperature limiting factor of algal group I,
FN_{pi} = nutrient limiting factor of algal group i (0 - 1.0),
FL_{pi} = light limiting factor of algal group i (0 -1.0).

Note that nutrient limitation and harmonic mean options in NSMI are not included in NSMII; the multiplicative formulation is likely to provide a realistic representation of growth limitation.

4.2.3.1 *Temperature limitation*

Arrhenius Equation or theta temperature function is used in NSMI for adjusting essentially all kinetic rates. This correction function does not account for algae growth at the temperature optimums. In NSMII, the growth rates of algal groups are controlled with temperature optimums that maximize growth at a certain temperature and decrease growth above and below this temperature. In this manner, growth of winter, summer, and fall

algal groups can peak at different times of the year or within different temperature ranges. Algal production increases as a function of temperature until an optimum temperature is reached. Above the optimum, production declines until a temperature lethal to the organism is attained (Figure 10). This function is similar to a Gaussian probability curve and different from the Arrhenius Equation used in NSMI. The temperature correction algorithms for algal growth in NSMII were adapted from ICM. The temperature correction function is given by

$$FT_{pi} = e^{-kt_{p1i}(T_w - T_{opi})^2} \quad Tw \leq Topi, \tag{4.5a}$$

$$FT_{pi} = e^{-kt_{p2i}(T_{opi} - T_w)^2} \quad Tw > Topi, \tag{4.5b}$$

where

T_{Opi} = optimal temperature for algal growth (^{0}C),
kt_{p1i} = effect of temperature below T_{0p} on algal growth (^{0}C^{-2}),
kt_{p2i} = effect of temperature above T_{0p} on algal growth (^{0}C^{-2}).

Figure 10. Dependence of algal growth on temperature.
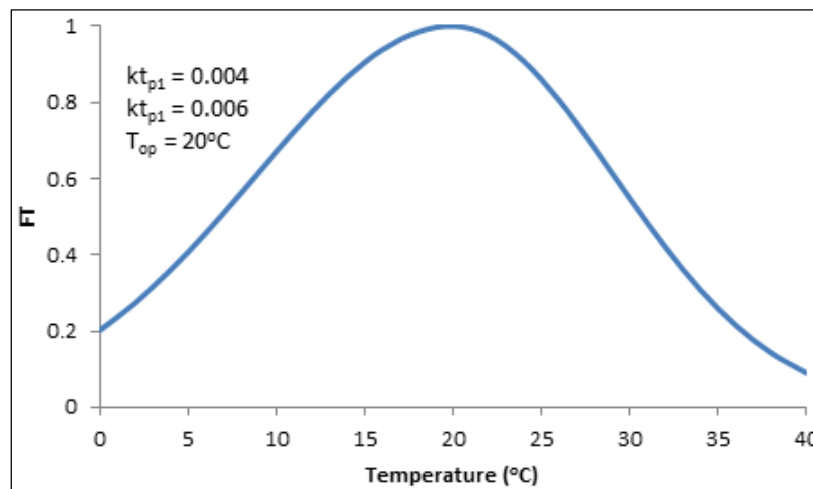
4.2.3.2 Light limitation

Sunlight is the most limiting factor for algal growth, followed by nitrogen and phosphorus limitations. For the effect of light on the algal growth rate, it is assumed that light attenuation through the water follows the Beer-Lambert law. There are three different models for quantifying the effects of light limitation of algal growth: half-saturation function (Baly 1935),

Smith's function (Smith 1936), and Steele's function (Steele 1962). These functions have been described in NSMI.

Half-saturation function:

$$FL_{pi} = \frac{1}{\lambda \cdot h} \ln \left(\frac{K_{Li} + I_0}{K_{Li} + I_0 \cdot e^{-\lambda \cdot h}} \right),$$ (4.6)

Smith's function:

$$FL_{pi} = \frac{1}{\lambda \cdot h} \ln \left(\frac{\frac{I_0}{K_{Li}} + \sqrt{1 + \left(\frac{I_0}{K_{Li}} \right)^2}}{\frac{I_0}{K_{Li}} e^{-\lambda \cdot h} + \sqrt{1 + \left(\frac{I_0}{K_{Li}} e^{-\lambda \cdot h} \right)^2}} \right),$$ (4.7)

Steele's function:

$$FL_{pi} = \frac{2.718}{\lambda \cdot h} \left[e^{-\left(\frac{I_0}{K_{Li}} \right) e^{-\lambda \cdot h}} - e^{-\left(\frac{I_0}{K_{Li}} \right)} \right],$$ (4.8)

where

λ = light attenuation coefficient (m^{-1}),
K_{Li} = light limiting constant for algal growth (W m^{-2}).

4.2.3.3   Nutrient limitation

Varying nutrient levels on the growth rate of algae must be evaluated. Algae require at least some critical nutrients to stimulate the growth of the population. As the nutrient level is increased, growth commences. However, as nutrient levels continue to increase, the effect on the growth rate of algae is reduced. The nutrient limiting factor for each algal group is expressed as

$$FN_{pi} = \min \left[\frac{(NH4 + NO3)}{K_{sNpi} + (NH4 + NO3)}, \frac{DIP}{K_{sPpi} + DIP} \right],$$ (4.9a)

where

$NH4$ = ammonium (mg-N L^{-1}),
$NO3$ = nitrate (mg-N L^{-1}),
DIP = dissolved inorganic phosphorus (mg-P L^{-1}),
K_{sNpi} = half-saturation N limiting constant for algal growth (mg-N L^{-1}),
K_{sPpi} = half-saturation P limiting constant for algal growth (mg-P L^{-1}).

When diatoms are modeled, silica limitation should be included as a component of nutrient limiting factors. The other groups of algae do not require silica for their growth, and therefore silica is not considered as a limiting nutrient. For the diatom species, the silica limitation function is similar to that for nitrogen and phosphorus in the sense that growth rates are reduced owing to the presence of low silica. The nutrient limiting factor with silica limitation is expressed as

$$FN_{pi} = \min\left[\frac{(NH4+NO3)}{K_{sNpi}+(NH4+NO3)}, \frac{DIP}{K_{sPpi}+DIP}, \frac{DSi}{K_{sPSipi}+DSi}\right], \quad (4.9b)$$

where

DSi = dissolved silica (mg-Si L^{-1}),
K_{sSipi} = half-saturation Si limiting constant for algal growth (mg-Si L^{-1}).

4.2.4 Nitrogen uptake preference

Nitrogen and phosphorus are essential to algae for assimilation of proteins and enzymes. Algae reduce the concentration of nutrients in the water by consuming NH4, NO3, and inorganic phosphorous. The uptake of dissolved silica is species dependent. With the exception of diatoms, the other groups of algae do not require silica for their growth. Through assimilation, these nutrients are transformed into organic materials that serve as a food source. A portion of the organic matter that is not used for food decomposes, which further affects the oxygen and nutrient levels in the water bodies. Although algae take up uses both NH4 and NO3, their preference for the former has been demonstrated for physiological reasons (Walsh and Dugdale 1972). Algae and other microorganisms prefer NH4 above NO3. Stanley and Hobbie (1981) observed that the uptake of NH4 by river plankton was three times as high as the NO3 uptake, although the NH4 concentration was only

half of the NO3 concentration. This means the turnover rate of the NH4 was six times higher than the turnover rate of NO3.

The algal preference factor for NH4 defines the relative preference of algae for NH4 and NO3. A preference fraction of algal uptake from NH4 as a nitrogen source is expressed as

$$P_{Npi} = \frac{NH4 \cdot NO3}{(k_{snxpi} + NH4)(k_{snxpi} + NO3)} + \frac{NH4 \cdot k_{snxpi}}{(NH4 + NO3)(k_{snxpi} + NO3)}, \quad (4.10)$$

where

k_{snxpi} = half saturation NH4 preference constant for algal uptake (mg-N L^{-1}),

P_{Npi} = preference fraction of algal N uptake from NH4 (0–1.0).

4.2.5 Algal mortality and settling

Algal mortality can occur as a response to unfavorable environmental conditions. Phytoplankton under stress may suffer greatly increased mortality due to autolysis and parasitism (Harris 1986). Stressful changes include nutrient depletion, unfavorable temperature, and damage by light (LeCren and Lowe-McConnell 1980). A fraction of algal mortality is assumed to go to refractory organic matter; a small fraction goes to labile organic matter.

Phytoplankton that settle to the bottom (that are not linked to benthic algae) are considered to become sediment organic matter. The settling algae can be a significant source of nutrients to the sediments and also contribute an important role in the sediment oxygen demand. Reported algal settling rates typically range from 0.1 to 5 m d^{-1} (Bienfang et al. 1982, Riebesell 1989, Waite et al. 1992). In some instances however, the settling velocity is zero or negative. The algal settling rate used in NSMII represents the net effect of all physiological and behavioral processes that result in the downward transport of algae. Actual settling in natural waters is a complex phenomenon, affected by vertical turbulence, density gradients, and the physiological state of the different species of algae. Settling velocities for each algal group are specified as input parameters.

4.2.6 Light attenuation coefficient

The same formulation included in NSMI is used for calculating the light attenuation coefficient (λ). The light attenuation coefficient in the water column is the sum of background attenuation (λ_0), attenuation due to inorganic material (λ_s), organic matter (λ_m), linear and nonlinear chlorophyll-*a* (λ_1, λ_2)

$$\lambda = \lambda_0 + \lambda_s \sum m_n + \lambda_m POM + \lambda_1 Chla + \lambda_2 \left(Chla\right)^{2/3} , \qquad (4.11)$$

where

λ_0 = background light attenuation (m^{-1}),
λ_s = light attenuation by inorganic suspended solids (L mg^{-1} m^{-1}),
λ_m = light attenuation by organic matter (L mg^{-1} m^{-1}),
λ_1 = linear light attenuation by algae (m^{-1} (µg-Chla L^{-1})$^{-1}$),
λ_2 = nonlinear light attenuation by algae (m^{-1} (µg-Chla L^{-1})$^{-2/3}$),
POM = particulate organic matter (mg-D L^{-1}),
m_n = concentration of inorganic suspended solid "n" (mg L^{-1}).

4.3 Benthic Algae

Benthic algae are included in NSMII as an optional state variable. Benthic algae are computed on an areal base of benthic sediment and quantified as biomass per unit bottom area. Benthic algae are modeled in NSMII as for benthic algae in NSMI, except for the temperature limiting factor. The growth of benthic algae consumes nutrients and produces oxygen. Benthic algae also die and recycle as dissolved and particulate organic matter, adding to the aquatic carbon and nutrient pools.

4.3.1 Stoichiometric ratios

Table 11 summarizes the stoichiometric ratios related to benthic algae in NSMII. Benthic algae nitrogen, phosphorus, and carbon can be converted to dry weight biomass or any of the other units.

Table 11. Stoichiometric ratios of benthic algae internally computed in NSMII.

Symbol	Definition	Unit	Formulation*
r_{nb}	benthic algae N : D ratio	mg-N mg-D^{-1}	$r_{nb} = BW_n / BW_d$
r_{pb}	benthic algae P : D ratio	mg-P mg-D^{-1}	$r_{pb} = BW_p / BW_d$
r_{cb}	benthic algae C : D ratio	mg-C mg-D^{-1}	$r_{cb} = BW_c / BW_d$
r_{ab}	benthic Chla : D ratio	µg-Chla mg-D^{-1}	$r_{ab} = BW_a / BW_d$

* The symbols are defined in Table 21.

4.3.2 Benthic algae kinetics

Benthic algae are computed in terms of density per unit bottom area as dry weight biomass (g-D m^{-2}). The mass balance equation for benthic algae biomass due to the growth, respiration, and death can be written as

$$\frac{dA_b}{dt} = \mu_b(T) \cdot A_b \qquad \text{Benthic algae growth,} \qquad (4.12)$$

$$- F_{oxb} k_{rb}(T) \cdot A_b \qquad \text{Benthic algae respiration,}$$

$$- k_{db}(T) \cdot A_b \qquad \text{Benthic algae mortality,}$$

where

$$A_b = \text{benthic algal biomass (g-D m}^{-2}\text{),}$$
$$\mu_b(T) = \text{benthic algal growth rate (d}^{-1}\text{),}$$
$$k_{rb}(T) = \text{benthic algal base respiration rate (d}^{-1}\text{),}$$
$$k_{db}(T) = \text{benthic algal mortality rate (d}^{-1}\text{),}$$
$$F_{Oxb} = \text{oxygen attenuation factor for benthic algal respiration (0–1.0).}$$

Attenuation factor due to low oxygen for benthic algae respiration is computed using the half-saturation function

$$F_{Oxb} = DO / (K_{sOxb} + DO), \qquad (4.13)$$

where

$$K_{sOxb} = \text{half-saturation oxygen attenuation coefficient for benthic algae respiration (mg-O}_2 \text{ L}^{-1}\text{).}$$

Benthic algal biomass can be converted into chlorophyll-*a* using the following equation

$$Chlb = r_{ab} A_b,$$ (4.14)

where

r_{ab} = benthic Chla : D ratio (µg-Chla mg-D^{-1}).
$Chlb$ = benthic chlorophyll-*a* (mg-Chla m^{-2}).

4.3.3 Benthic algae growth rate

The benthic algae kinetic rate is computed in NSMII as is done previously with NSMI, with the exception that the temperature limiting factor is computed differently. The benthic algae growth rate is a function of temperature, nutrients, and light, all based on the maximum rate. Unlike algae, bottom light rather than average water column light is used in the computation of benthic algae growth

$$\mu_b(T) = \mu_{mxb} FT_b FL_b FN_b FS_b,$$ (4.15)

where

μ_{mxb} = maximum benthic algae growth rate (d^{-1}),
FT_b = temperature effect factor on benthic algal growth,
FN_b = nutrient limiting factor for benthic algal growth (0–1.0),
FL_b = light limiting factor for benthic algal growth (0–1.0),
FS_b = space density limiting factor for benthic algae growth (0–1.0).

4.3.3.1 *Temperature limitation*

The theta function is used in NSMI for calculating the temperature limiting factor. The effect of temperature on benthic algal growth rate is simulated as for floating algae using a Gaussian temperature function

$$FT_b = e^{-kt_{b1}(T_w - T_{ob})^2} \quad \text{Tw} \le \text{Tob,}$$ (4.16a)

$$FT_b = e^{-kt_{b2}(T_{ob} - T_w)^2} \quad \text{Tw} > \text{Tob,}$$ (4.16b)

where

T_{0b} = optimal temperature for benthic algal growth (^{0}C),
kt_{b1} = effect of temperature below T_{0b} on benthic algal growth (^{0}C^{-2}),
kt_{b2} = effect of temperature above T_{0b} on benthic algal growth (^{0}C^{-2}).

4.3.3.2 *Light limitation*

Three alternative formulations are included for calculating the benthic algae light limiting factor. These formulations have been described in NSMI.

Half-saturation function:

$$FL_b = \frac{I_0 \cdot e^{-\lambda \cdot h}}{K_{Lb} + I_0 \cdot e^{-\lambda \cdot h}}, \tag{4.17}$$

Smith's function:

$$FL_b = \frac{I_0 \cdot e^{-\lambda \cdot h}}{\sqrt{K_{Lb}^2 + \left(I_0 \cdot e^{-\lambda \cdot h}\right)^2}}, \tag{4.18}$$

Steele's function:

$$FL_b = \frac{I_0 \cdot e^{-\lambda \cdot h}}{K_{Lb}} e^{\left(1 - \frac{I_0 \cdot e^{-\lambda \cdot h}}{K_{Lb}}\right)}, \tag{4.19}$$

where

K_{Lb} = light limiting constants for benthic algae growth (W m^{-2}).

4.3.3.3 *Nutrient limitation*

The nitrogen and phosphorous limiting factor for benthic algae growth is expressed using a half-saturation function.

$$FN_b = \min\left[\frac{(NH4 + NO3)}{K_{sNb} + (NH4 + NO3)}, \frac{DIP}{K_{sPb} + DIP}\right], \tag{4.20}$$

where

K_{sNb} = half-saturation N limiting constant for benthic algae growth (mg-N L^{-1}),

K_{sPb} = half-saturation P limiting constant for benthic algae growth (mg-P L^{-1}).

4.3.3.4   Space limitation

The following equation is used to attenuate the growth of benthic algae by bottom space

$$FS_b = 1 - \frac{A_b}{K_{Sb} + A_b} \ , \qquad (4.21)$$

where

K_{Sb} = half-saturation density constant for benthic algae growth (g-D m^{-2}).

4.3.4 Nitrogen uptake preference

The nitrogen uptake rates for bottom algae depend on both available NH$_4$ and nitrate. The preference fraction of benthic algae nitrogen uptake from NH$_4$ as a nitrogen source is expressed as

$$P_{Nb} = \frac{NH4 \cdot NO3}{(k_{snxb} + NH4)(k_{snxb} + NO3)} + \frac{NH4 \cdot k_{snxb}}{(NH4 + NO3)(k_{snxb} + NO3)}, \quad (4.22)$$

where

k_{snxb} = half saturation NH4 for benthic algae uptake (mg-N L^{-1}),

P_{Nb} = NH4 preference factor for benthic algae growth (0–1.0).

Mortality of benthic algae contributes to the concentration of particulate organic matter in the sediments. The contribution of benthic algae to sediment particulate organic matter is defined as a fraction of the mortality rate.

4.4 Nitrogen Species

The nitrogen species commonly found in surface water are NO3, NO2, NH4, DON, and PON (Meybeck 1982). The concentration of dissolved organic nitrogen (DON) frequently exceeds that of DIN, including NO3, NO2 and NH4. The DON pool in natural waters is not inert and can be an important sink and source for the nitrogen cycle (Berman and Bronk 2003). Compared to NSMI, DON is included as a state variable. Nonliving particulate organic nitrogen is represented with two state variables as refractory and labile particulate organic nitrogen (RPON and LPON). Figure 11 shows an overview of the NSMII representation of nitrogen species and a simplified nitrogen cycle involved in the water column. Five nitrogen state variables are included in NSMII: RPON, LPON, DON, NH4, and NO3.

Figure 11. Water column nitrogen species and major processes modeled in NSMII.
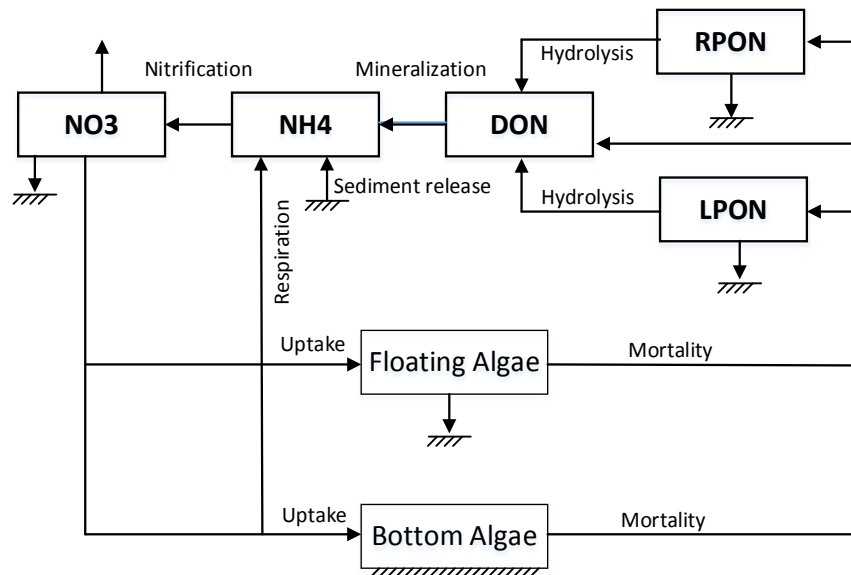
Particulate organic nitrogen, whether refractory or labile, decomposes to DON through hydrolysis. The DON mineralizes to NH4, which is subsequently nitrified to NO2 and NO3 via a reaction in which DO is consumed. The primary internal source of inorganic nitrogen is from organic nitrogen as it transforms into NH4. Nitrification is an aerobic reaction; therefore, the reaction decreases as DO concentrations decrease below a certain value. Thus, the nitrification reaction is dependent on DO concentrations and on water temperature. The denitrification of NO3 to nitrogen gas is an anaerobic reaction that varies with temperature. The primary sink of the inorganic nitrogen forms the algal uptake. NH4 and

NO3 are used during algal growth; however, the preferred form is NH4. The rate at which each is taken up is a function of its concentration relative to the available dissolved inorganic nitrogen (NH4 plus NO3). During algal respiration and death, a fraction of the algal cellular nitrogen is returned to the inorganic pool in the form of NH4. The remaining fraction is recycled to the dissolved and particulate organic nitrogen pools. The benthic algae are linked to the nitrogen cycle via the processes of growth, respiration, and death, as shown in Figure 11.

The nitrification rate is computed using Michaelis-Menten kinetics (Michaelis and Menten 1913) with respect to both DO and NH4. The first function attenuates nitrification due to low DO concentration. The second function takes account of the effect of NH4 concentration on nitrification. Denitrification is included for the water column and benthic sediments. Sediment–water fluxes of NH4 and NO3 are either a source of, or sink for, these nutrients in the water column. If the sediment diagenesis module is included (see Chapter 5), sediment–water fluxes of NH4 and NO3 are explicitly computed, otherwise inorganic nitrogen released from the sediment bed is specified by the user. Table 12 presents the pathway terms (sources and sinks) for the nitrogen state variables included in NSMII.

Table 12. Major pathways for nitrogen state variables in NSMII.

State Variables	Internal Sources (+)	Internal Sinks (-)
RPON	Algal mortality (A_p-->RPON)	Hydrolysis (RPON-->DON) Settling (RPON-->Bed)
LPON	Algal mortality (A_p-->LPON)	Hydrolysis (LPON-->DON) Settling (LPON-->Bed)
DON	Hydrolysis of LPON and RPON (RPON-->DON, LPON-->DON) Algal mortality (A_p-->DON)	Mineralization (DON-->NH4)
NH4	Algal respiration (A_p-->NH4) Mineralization (DON-->NH4) Sediment release (Bed<-->NH4)	Algal uptake (NH4-->A_p) Nitrification (NH4-->NO3)
NO3	Nitrification (NH4-->NO3)	Algal uptake (NO3-->A_p) Denitrification (NO3-->N2) Sediment denitrification (NO3<-->Bed)

The sum of each of source (+) and sink (-) terms in the appropriate column above table can then be used to compute the net rate for each nitrogen state variable. The internal source and sink equations for

nitrogen state variables (RPON, LPON, DON, NH4, NO3) in the water column are given below.

4.4.1 State variables

Refractory Particulate Organic Nitrogen (RPON):

$$\frac{\partial RPON}{\partial t} = F_{rponp} \sum_{i}^{3} k_{dpi}(T) \cdot r_{nai} A_{pi} \quad \text{Algal mortality } (A_p\text{-->RPON)}, \qquad (4.23)$$

$$- k_{rpon}(T) \cdot RPON \qquad\qquad \text{RPON hydrolysis (RPON-->DON)},$$

$$- \frac{v_{sr}}{h} RPON \qquad\qquad\qquad \text{RPON settling (RPON-->Bed)},$$

$$+ \frac{1}{h} F_{rponb} k_{db}(T) \cdot r_{nb} A_b F_b F_w \qquad \text{Benthic algae mortality } (A_b\text{-->RPON)},$$

where

$$RPON = \text{refractory particulate organic nitrogen (mg-N L}^{-1}\text{)},$$
$$F_{rponp} = \text{fraction of benthic algae mortality into RPON (0–1.0)},$$
$$k_{rpon}(T) = \text{hydrolysis rate of RPON (d}^{-1}\text{)},$$
$$v_{sr} = \text{refractory organic particulate (C,N,P) settling velocity (m d}^{-1}\text{)},$$
$$F_{rponb} = \text{fraction of benthic algal mortality into RPON (0–1.0)},$$
$$F_w = \text{fraction of benthic algae mortality into the water column (0–1.0)},$$
$$F_b = \text{fraction of bottom area available for benthic algae growth (0–1.0)}.$$

Labile Particulate Organic Nitrogen (LPON):

$$\frac{\partial LPON}{\partial t} = F_{lponp} \sum_{i}^{3} k_{dpi}(T) \cdot r_{nai} A_{pi} \quad \text{Algal mortality } (A_p\text{-->LPON)}, \qquad (4.24)$$

$$- k_{lpon}(T) \cdot LPON \qquad\qquad \text{LPON hydrolysis (LPON-->DON)},$$

$$- \frac{v_{sl}}{h} LPON \qquad\qquad\qquad \text{LPON settling (LPON-->Bed)},$$

$$+ \frac{1}{h} F_{lponb} k_{db}(T) \cdot r_{nb} A_b F_b F_w \qquad \text{Benthic algae mortality } (A_b\text{-->LPON)},$$

where

$LPON$ = labile particulate organic nitrogen (mg-N L^{-1}),
F_{lponp} = fraction of algal mortality into LPON (0–1.0),
$k_{lpon}(T)$ = hydrolysis rate of LPON (d^{-1}),
v_{sl} = labile organic particulate (C,N,P) settling velocity (m d^{-1}),
F_{lponb} = fraction of benthic algal mortality into LPON (0–1.0).

Dissolved Organic Nitrogen (DON):

$$\frac{\partial DON}{\partial t} = k_{rpon}(T) \cdot RPON \qquad \text{RPON hydrolysis (RPON-->DON),} \qquad (4.25)$$

$$+ k_{lpon}(T) \cdot LPON \qquad \text{LPON hydrolysis (LPON-->DON),}$$

$$- \frac{DO}{K_{sOxmn} + DO} k_{don}(T) \cdot DON \qquad \text{DON mineralization (DON-->NH4),}$$

$$+ \left(1 - F_{rponp} - F_{lponp}\right)\sum_{i}^{3} k_{dpi}(T) \cdot r_{nai} A_{pi} \qquad \text{Algal mortality (A}_\text{p}\text{-->DON),}$$

$$+ \frac{1}{h}\left(1 - F_{rponb} - F_{lponb}\right)k_{db}(T) \cdot r_{nb} A_b F_b F_w \qquad \text{Benthic algae mortality (A}_\text{b}\text{-->DON),}$$

where

DON = dissolved organic nitrogen (mg-N L^{-1}),
$k_{don}(T)$ = mineralization rate of DON (d^{-1}),
K_{sOxmn} = half-saturation oxygen attenuation constant for DON, mineralization (mg-O$_2$ L^{-1}).

Ammonium (NH4):

$$\frac{\partial NH4}{\partial t} = \frac{DO}{K_{sOxmn} + DO} k_{don}(T) \cdot DON \qquad \text{DON mineralization (DON-->NH4),} \qquad (4.26)$$

$$- \frac{DO}{K_{sOxna} + DO} \frac{NH4}{K_{sNh4} + NH4} k_{nit}(T) \cdot NH4 \qquad \text{NH4 nitrification (NH4-->NO3),}$$

$$+ \sum_{i}^{3} F_{Oxpi} k_{rpi}(T) \cdot r_{nai} A_{pi} \qquad \text{Algal respiration (A}_\text{p}\text{-->NH4),}$$

$$- \sum_{i}^{3} P_{Npi} \mu_{pi}(T) \cdot r_{nai} A_{pi} \qquad \text{Algal uptake (NH4-->A}_\text{p}\text{),}$$

$$+\frac{1}{h}F_{Oxb}k_{rb}(T)\cdot r_{nb}A_bF_b \qquad\qquad \text{Benthic algae respiration (A}_b\text{-->NH4),}$$

$$-\frac{1}{h}p_{Nb}\mu_b(T)\cdot r_{nb}A_bF_b \qquad\qquad \text{Benthic algae uptake (NH4-->A}_b\text{),}$$

$$+\frac{1}{h}r_{hn4} \qquad\qquad\qquad\qquad\qquad \text{Sediment release (Bed<-->NH4),}$$

where

$k_{nit}(T)$ = nitrification rate (d^{-1}),
r_{nh4} = sediment release rate of NH4 (g-N m^{-2} d^{-1}),
K_{sOxna} = half-saturation oxygen attenuation constant for nitrification (mg-O$_2$ L^{-1}).

Nitrate (NO3):

$$\frac{\partial NO3}{\partial t} = \frac{DO}{K_{sOxna}+DO}\frac{NH4}{K_{sNh4}+NH4}k_{nit}(T)\cdot NH4 \quad \text{NH4 nitrification (NH4-->NO3),} \qquad (4.27)$$

$$-\left(1-\frac{DO}{K_{sOxdn}+DO}\right)k_{dnit}(T)\cdot NO3 \qquad \begin{array}{l}\text{NO3 denitrification (NO3--}\\ \text{>Loss),}\end{array}$$

$$-\sum_{i}^{3}(1-P_{Npi})\mu_{pi}(T)\cdot r_{nai}A_{pi} \qquad\qquad \text{Algal uptake (NO3-->A}_p\text{),}$$

$$-\frac{1}{h}(1-P_{Nb})\mu_b(T)\cdot r_{nb}A_bF_b \qquad\qquad \begin{array}{l}\text{Benthic algae uptake from NO3}\\ \text{(NO3-->A}_b\text{),}\end{array}$$

$$-\frac{v_{no3}}{h}NO3 \qquad\qquad\qquad\qquad\qquad \begin{array}{l}\text{Sediment denitrification (NO3<--}\\ \text{>Bed),}\end{array}$$

where

$k_{dnit}(T)$ = denitrification rate (d^{-1}),
K_{sOxdn} = half-saturation oxygen inhibition constant for denitrification (mg-O$_2$ L^{-1}),
v_{no3} = sediment denitrification velocity (m d^{-1}).

4.4.2 Derived variables

Derived variables related to nitrogen species are computed as

$$DIN = NH4 + NO3 , \tag{4.28a}$$

$$TON = DON + LPON + RPON + \sum_{i}^{3} r_{nai} A_{pi} , \tag{4.28b}$$

$$TKN = NH4 + TON , \tag{4.28c}$$

$$TN = NO3 + TKN , \tag{4.28d}$$

where

DIN = dissolved inorganic nitrogen (mg-N L^{-1}),
TON = total organic nitrogen (mg-N L^{-1}),
TKN = total Kjeldahl nitrogen (mg-N L^{-1}),
TN = total nitrogen (mg-N L^{-1}).

4.5 Phosphorus Species

Phosphorus is found as soluble organic compounds, such as DNA and RNA (collectively known as Dissolved Organic Phosphorus—DOP), and in a number of insoluble (particulate) forms. Similar to the nitrogen cycle, DOP is included in NSMII as a state variable. Particulate organic phosphorus is represented with two state variables: as refractory and as labile particulate organic phosphorus (RPOP and LPOP). Similar to NSMI, TIP is included as a single state variable. The TIP accounts for both the dissolved inorganic phosphorous (DIP) and the particulate inorganic phosphorous (PIP). Figure 12 shows an overview of the NSMII representation of phosphorous species and a simplified phosphorous cycle involved in the water column. Four phosphorus state variables are included in NSMII: RPOP, LPOP, DOP, and TIP.

Figure 12. Water column phosphorus species and major processes modeled in NSMII.
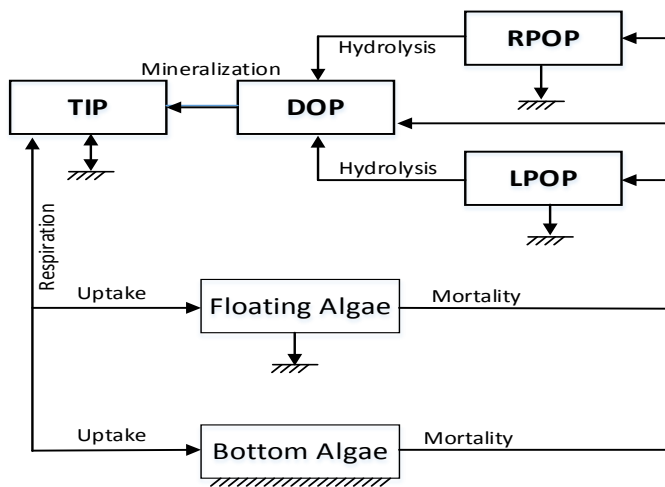
The particulate and dissolved forms of organic phosphorus decompose through the same reaction pathways as nitrogen with the particulate fractions settling to the sediment. The dissolved form of organic phosphorus further decomposes through mineralization into the inorganic form of phosphorus. Additionally, phosphorus is generally much less mobile than nitrogen, being strongly adsorbed to sediment and organic matter. Inorganic phosphorus is lost through its utilization by algae as a nutrient essential for growth and is supplied from or lost to the sediment through sediment fluxes. Inorganic phosphorous is partitioned between the dissolved phase and that part adsorbed on solids. Sorption of inorganic phosphorous on suspended solids is modeled in NSMII. At equilibrium, the distribution of inorganic phosphorus between solids and water is determined by a linear equilibrium partitioning isotherm. In the sediment bed, if the optional sediment diagenesis module is included (see Chapter 5), sediment–water flux of inorganic phosphorus is internally computed; otherwise inorganic phosphorus released from the sediment bed is a user-specified input. Most plants, algae, and bacteria are capable of rapid uptake of phosphorous, especially in the form of orthophosphate, even when it is present at low concentrations. DIP is assumed to be in a completely available form for uptake. A fraction of the phosphorus released during algal respiration is in the inorganic form. The benthic algae are linked to the phosphorus cycle via the processes of growth, respiration, and death, as shown in Figure 12. Table 13 presents the pathway terms (sources and sinks) for the phosphorus state variables included in NSMII.

Table 13. Major pathways for phosphorus state variables in NSMII.

State Variables	Internal Sources (+)	Internal Sinks (-)
RPOP	Algal mortality (Ap-->RPOP)	Hydrolysis (RPOP-->DOP) Settling (RPOP-->Bed)
LPOP	Algal mortality (Ap-->LPOP)	Hydrolysis (LPOP-->DOP) Settling (LPOP-->Bed)
DOP	Hydrolysis of LPOP and RPOP (RPOP-->DOP, LPOP-->DOP) Algal mortality (Ap-->DOP)	Mineralization (DOP-->DIP)
TIP	Mineralization (DOP-->DIP) Algal respiration (Ap-->DIP) Sediment release (Bed<-->DIP)	Algal uptake (DIP-->Ap) Algal uptake (DIP-->Ap)

The sum of each of source (+) and sink (-) terms in the appropriate column of Table 13 can then be used to compute the net rate for each phosphorous state variable. The internal source and sink equations for phosphorus state variables (RPOP, LPOP, DOP, TIP) in the water column are given below.

4.5.1　State variables

Refractory Particulate Organic Phosphorus (RPOP):

$$\frac{\partial RPOP}{\partial t} = F_{rpopp} \sum_{i}^{3} k_{dpi}(T) \cdot r_{pai} A_{pi} \qquad \text{Algal mortality (Ap-->RPOP),} \qquad (4.29)$$

$$-k_{rpop}(T) \cdot RPOP \qquad \text{RPOP hydrolysis (RPOP-->DOP),}$$

$$-\frac{v_{sr}}{h} RPOP \qquad \text{RPOP settling (RPOP-->Bed),}$$

$$+\frac{1}{h} F_{rpopb} k_{db}(T) \cdot r_{pb} A_b F_b F_w \qquad \text{Benthic algae mortality (Ab-->RPOP),}$$

where

$RPOP$ = refractory particulate organic phosphorous (mg-P L^{-1}),
F_{rpopp} = fraction of algal mortality into RPOP (0–1.0),
$k_{rpop}(T)$ = RPOP hydrolysis rate (d^{-1}),
F_{rpopb} = fraction of benthic algal mortality into RPOP (0–1.0).

Labile Particulate Organic Phosphorus (LPOP):

$$\frac{\partial LPOP}{\partial t} = F_{lpopp} \sum_i^3 k_{dpi}(T) \cdot r_{pai} A_{pi} \qquad \text{Algal mortality } (A_p\text{-->LPOP}), \qquad (4.30)$$

$$- k_{lpop}(T) \cdot LPOP \qquad\qquad\qquad \text{LPOP hydrolysis (LPOP-->DOP)},$$

$$- \frac{v_{sl}}{h} LPOP \qquad\qquad\qquad\qquad \text{LPOP settling (LPOP-->Bed)},$$

$$+ F_{lpopb} k_{db}(T) \frac{1}{h} r_{pb} A_b F_b F_w \qquad \text{Benthic algae mortality } (A_b\text{-->LPOP}),$$

where

$LPOP$ = labile particulate organic phosphorous (mg-P L^{-1}),
F_{lpopp} = fraction of algal mortality into LPOP (0–1.0),
$k_{lpop}(T)$ = LPOP hydrolysis rate (d^{-1}),
F_{lpopb} = fraction of benthic algal mortality into LPOP (0–1.0).

Dissolved Organic Phosphorus (DOP):

$$\frac{\partial DOP}{\partial t} = k_{rpop}(T) \cdot RPOP \qquad\qquad \text{RPOP hydrolysis (RPOP-->DOP)}, \qquad (4.31)$$

$$+ k_{lpop}(T) \cdot LPOP \qquad\qquad\qquad \text{LPOP hydrolysis (LPOP-->DOP)},$$

$$- \frac{DO}{K_{sOxmp} + DO} k_{dop}(T) \cdot DOP \qquad \text{DOP mineralization (DOP-->DIP)},$$

$$+ \left(1 - F_{rpopp} - F_{lpopp}\right) \sum_i^3 k_{dpi}(T) \cdot r_{pai} A_{pi} \qquad \text{Algal mortality } (A_p\text{-->DOP}),$$

$$+ \frac{1}{h}\left(1 - F_{rpopb} - F_{lpopb}\right) k_{db}(T) \cdot r_{pb} A_b F_b F_w \qquad \text{Benthic algae mortality } (A_b\text{-->DOP}),$$

where

DOP = dissolved organic phosphorous (mg-P L^{-1}),
$k_{dop}(T)$ = DOP mineralization rate (d^{-1}),
K_{sOxmp} = half-saturation oxygen attenuation constant for DOP mineralization (mg-O$_2$ L^{-1}).

Total Inorganic Phosphorus (TIP):

$$\frac{\partial TIP}{\partial t} = \frac{DO}{K_{sOxmp} + DO} k_{dop}(T) \cdot DOP \quad \text{DOP mineralization (DOP-->DIP),} \quad (4.32)$$

$$-\frac{v_{sp}}{h} f_{pp} TIP \qquad\qquad\qquad \text{TIP settling (TIP-->Bed),}$$

$$-\frac{v_{sp}}{h} f_{pp} TIP \qquad\qquad\qquad \text{Algal respiration (A}_p\text{-->DIP),}$$

$$-\sum_{i}^{3} \mu_{pi}(T) \cdot r_{pai} A_{pi} \qquad\qquad \text{Algal uptake (DIP-->A}_p\text{),}$$

$$+\frac{1}{h} F_{Oxb} k_{rb}(T) \cdot r_{pb} A_b F_b \qquad \text{Benthic algae respiration (A}_b\text{-->DIP),}$$

$$-\frac{1}{h} \mu_b(T) \cdot r_{pb} A_b F_b \qquad\qquad \text{Benthic algae uptake (DIP-->A}_b\text{),}$$

$$+\frac{1}{h} r_{po4} \qquad\qquad\qquad\qquad \text{Sediment release (Bed<-->DIP),}$$

where

TIP = total inorganic phosphorous (mg-P L^{-1}),
r_{po4} = sediment release rate of DIP (g-P m^{-2} d^{-1}),
f_{dp}, f_{pp} = dissolved and particulate fractions of inorganic P (0–1.0).

The particulate and dissolved fractions of inorganic phosphorus are internally computed using the equilibrium partitioning method

$$f_{dp} = \frac{1}{1 + 10^{-6} \sum k_{po4n} m_n} = 1 - f_{pp}, \qquad (4.33)$$

where

k_{dpo4n} = partition coefficient of inorganic P for solid "n" (L kg^{-1}).

4.5.2 Derived variables

The derived variables related to phosphorus species are computed as

$$DIP = f_{dp} TIP, \qquad\qquad (4.34a)$$

$$TOP = DOP + LPOP + RPOP + \sum_{i}^{3} r_{pa}(T) A_{pi}, \qquad (4.34b)$$

$$TP = TIP + TOP, \qquad (4.34c)$$

where

DIP = dissolved inorganic phosphorus (mg-P L^{-1}),
TOP = total organic phosphorus (mg-P L^{-1}),
TP = total phosphorus (mg-P L^{-1}).

4.6 Carbon Species

NSMII models a detailed carbon cycle. The organic carbon is represented by four state variables: as refractory and labile dissolved organic carbon (RDOC and LDOC) and as refractory and labile particulate organic carbon (RPOC and LPOC). The splitting of dissolved organic carbon into labile and refractory, reflects obvious differences in carbon derived from internal versus external sources (Tillman et al. 2004). Dissolved organic carbon in surface water is usually composed of minor amounts of biodegradable plant, phytoplankton, bacterial residues, and major amounts of biological refractory residues. Highly reactive dissolved organic material, such as carbonaceous inputs associated with sewage treatment plants or combined sewer outfalls that decay on a time scale of days to a week or two, is classified as LDOC. Dissolved organic carbon will be oxidized into CO_2 and methane. The particulate and dissolved forms of carbon decompose through the same reaction pathways as phosphorus and nitrogen with the particulate fractions settling to the sediment. Oxidation of dissolved organic carbon is aerobic and, therefore, reduced at low DO concentrations. Under low DO conditions, the denitrification reaction consumes organic carbon. The rate of DIC change is proportional to the net primary production from each of the algal groups, and it is lost via plant photosynthesis. Additional sources and sinks of DIC are via exchange with the atmosphere, via the oxidation of organic carbon material, (i.e. RDOC, LDOC, CBOD) and denitrification. The benthic algae are linked to the carbon cycle via the processes of growth, respiration, and death. Figure 13 shows an overview of the NSMII representation of carbon species and a simplified carbon cycle involved in the water column.

Figure 13. Water column carbon species and major processes modeled in NSMII.
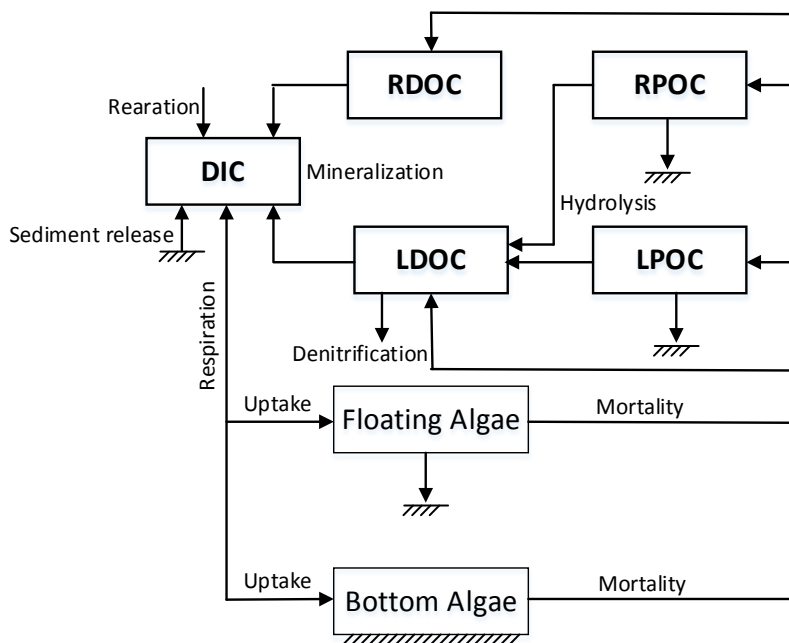
Five carbon state variables are included in NSMII: RPOC, LPOC, RDOC, LDOC, and DIC. Table 14 presents the pathway terms (sources and sinks) for the carbon state variables included in NSMII.

Table 14. Major pathways for carbon state variables in NSMII.

State Variables	Internal Sources (+)	Internal Sinks (-)
RPOC	Algal mortality (A_p-->RPOC)	Hydrolysis (RPOC-->LDOC) Settling (RPOC-->Bed)
LPOC	Algal mortality (A_p-->LPOC)	Hydrolysis (LPOC-->LDOC) Settling (LPOC-->Bed)
RDOC	Algal mortality (A_p-->RDOC)	Mineralization (RDOC-->DIC)
LDOC	Algal mortality (A_p-->LDOC) Hydrolysis of RPOC and LPOC (RPOC-->LDOC, LPOC-->LDOC)	Mineralization (LDOC-->DIC) Denitrification
DIC	Atmospheric rearation (Atm<-->DIC) Mineralization (RDOC-->DIC, LDOC-->DIC) Algal respiration (A_p-->DIC) Sediment release (Bed-->DIC) Denitrification (Denitrification-->DIC) CBOD oxidation (CBOD-->DIC)	Algal photosynthesis (DIC-->A_p)

The sum of each source (+) and sink (-) terms in the appropriate column above table can then be used to compute the net rate for each carbon state

variable. The internal source and sink equations for carbon cycle state variables (RPOC, LPOC, RDOC, LDOC, DIC) in the water column are given below.

4.6.1 State variables

Refractory Particulate Organic Carbon (RPOC):

$$\frac{\partial RPOC}{\partial t} = F_{rpocp} \sum_i^3 k_{dpi}(T) \cdot r_{cai} A_{pi} \qquad \text{Algal mortality (A}_p\text{--}>\text{RPOC),} \qquad (4.36)$$

$$- k_{rpoc}(T) \cdot RPOC \qquad\qquad \text{RPOC hydrolysis (RPOP--}>\text{LDOC),}$$

$$- \frac{v_{sr}}{h} RPOC \qquad\qquad \text{RPOC settling (RPOC--}>\text{Bed),}$$

$$+ \frac{1}{h} F_{rpocb} k_{db}(T) \cdot r_{cb} A_b F_b F_w \qquad \text{Benthic algae mortality (A}_b\text{--}>\text{RPOC),}$$

where

$\quad RPOC$ = refractory particulate organic carbon (mg-C L^{-1}),
$\quad F_{rpocp}$ = fraction of algal mortality into RPOC (0–1.0),
$\quad k_{rpoc}(T)$ = RPOC hydrolysis rate (d^{-1}),
$\quad F_{rpocb}$ = fraction of benthic algal mortality into RPOC (0–1.0).

Labile Particulate Organic Carbon (LPOC):

$$\frac{\partial LPOC}{\partial t} = F_{lpocp} \sum_i^3 k_{dpi}(T) \cdot r_{cai} A_{pi} \qquad \text{Algal mortality (A}_p\text{--}>\text{LPOC),} \qquad (4.37)$$

$$- k_{lpoc}(T) \cdot LPOC \qquad\qquad \text{LPOC hydrolysis (LPOP--}>\text{LDOC),}$$

$$- \frac{v_{sl}}{h} LPOC \qquad\qquad \text{LPOC settling (LPOC--}>\text{Bed),}$$

$$+ \frac{1}{h} F_{lpocb} k_{db}(T) \cdot r_{cb} A_b F_b F_w \qquad \text{Benthic algae mortality (A}_b\text{--}>\text{LPOC),}$$

where

$\quad LPOC$ = labile particulate organic carbon (mg-C L^{-1}),

F_{lpocp} = fraction of benthic algal mortality into LPOC (0–1.0),
$k_{lpoc}(T)$ = LPOC hydrolysis rate (d^{-1}),
F_{lpocb} = fraction of benthic algal mortality into LPOC (0–1.0).

Refractory Dissolved Organic Carbon (RDOC):

$$\frac{\partial RDOC}{\partial t} = F_{rdocp} \sum_{i}^{3} k_{dpi}(T) \cdot r_{cai} A_{pi} \qquad \text{Algal mortality (A}_p\text{-->RDOC),} \qquad (4.38)$$

$$-\frac{DO}{K_{sOxmc} + DO} k_{rdoc}(T) \cdot RDOC \qquad \text{RDOC mineralization (RDOC-->DIC),}$$

$$+\frac{1}{h} F_{rdocb} k_{db}(T) \cdot r_{cb} A_b F_b F_w \qquad \text{POM dissolution (POM-->RDOC),}$$

where

$RDOC$ = refractory dissolved organic carbon (mg-C L^{-1}),
F_{rdocp} = fraction of algal mortality into RDOC (0–1.0),
$k_{rdoc}(T)$ = mineralization rate of RDOC (d^{-1}),
F_{rdocb} = fraction of benthic algal mortality into RDOC (0–1.0),
K_{sOxmc} = half-saturation oxygen attenuation constant for DOC mineralization (mg-O$_2$ L^{-1}).

Labile Dissolved Organic Carbon (LDOC):

$$\frac{\partial LDOC}{\partial t} = k_{rpoc}(T) \cdot RPOC \qquad \text{RPOC hydrolysis (RPOC-->LDOC),} \qquad (4.39)$$

$$+ k_{lpoc}(T) \cdot LPOC \qquad \text{LPOC hydrolysis (LPOC-->LDOC),}$$

$$-\frac{DO}{K_{sOxmp} + DO} k_{ldoc}(T) \cdot LDOC \qquad \text{LDOC mineralization (LDOC-->DIC),}$$

$$-\frac{5 \times 12}{4 \times 14}\left(1 - \frac{DO}{K_{sOxdn} + DO}\right) k_{dnit}(T) \cdot NO3 \qquad \text{LDOC consumed by denitrification,}$$

$$+\left(1 - F_{rpocp} - F_{lpocp} - F_{rdocp}\right) \sum_{i}^{3} k_{dpi}(T) \cdot r_{cai} A_{pi} \qquad \text{Algal mortality (A}_p\text{-->LDOC),}$$

$$+\frac{1}{h}\left(1 - F_{rpocb} - F_{lpocb} - F_{rdocb}\right) k_{db}(T) \cdot r_{cb} A_b F_b F_w \qquad \text{Benthic algal mortality (A}_b\text{-->LDOC),}$$

where

$LDOC$ = labile dissolved organic carbon (mg-C L^{-1}),
$k_{ldoc}(T)$ = LDOC mineralization rate (d^{-1}).

Dissolved Inorganic Carbon (DIC):

$$12 \cdot 10^3 \frac{\partial DIC}{\partial t} = \tag{4.40}$$

$$+12 k_{ac}(T) \left(10^{-3} k_H(T) p_{CO_2} - 10^3 F_{co2} DIC \right) \quad \text{Atmospheric CO}_2 \text{ reaeration (Atm<-->DIC),}$$

$$+ \frac{DO}{K_{sOxmp} + DO} k_{rdoc}(T) \cdot RDOC \quad \text{RDOC mineralization (RDOC-->DIC),}$$

$$+ \frac{DO}{K_{sOxmp} + DO} k_{ldoc}(T) \cdot LDOC \quad \text{LDOC mineralization (LDOC-->DIC),}$$

$$+ \sum_i^3 F_{Oxpi} k_{rpi}(T) \cdot r_{cai} A_{pi} \quad \text{Algal respiration (A}_p\text{-->DIC),}$$

$$- \sum_i^3 \mu_{pi}(T) \cdot r_{cai} A_{pi} \quad \text{Algal photosynthesis (DIC-->A}_p\text{),}$$

$$+ \frac{1}{h} F_{Oxb} k_{rb}(T) \cdot r_{cb} A_b F_b \quad \text{Benthic algae respiration (A}_b\text{-->DIC),}$$

$$- \frac{1}{h} \mu_b(T) \cdot r_{cb} A_b F_b \quad \text{Benthic algae photosynthesis (DIC-->A}_b\text{),}$$

$$+ \frac{1}{r_{oc}} \sum \frac{DO}{K_{sOxbodi} + DO} k_{bodi}(T) \cdot CBOD_i \quad \text{CBOD oxidation (CBOD-->DIC),}$$

$$+ \frac{12}{64} \frac{DO}{K_{sOch4} + DO} k_{ch4}(T) \cdot CH4 \quad \text{CH4 oxidation (CH4-->DIC),}$$

$$+ \frac{1}{h} \frac{SOD(T)}{r_{oc}} \quad \text{Sediment release (Bed-->DIC),}$$

where

DIC = dissolved inorganic carbon (mol L^{-1}),
$k_{ac}(T)$ = CO$_2$ reaeration rate (d^{-1}),
$k_H(T)$ = Henry's Law constant (mol L^{-1} atm^{-1}),

p_{CO2} = partial pressure of CO_2 in the atmosphere (ppm),

F_{CO2} = fraction of CO_2 in total inorganic carbon (0–1.0).

4.6.2 Derived variables

Particulate organic matter is a derived variable in NSMII. Suspended particulate, colloidal, dissolved organic matter, and the amount of carbon in algal biomass are part of the TOC. TSS includes all the inorganic suspended solids fractions and all organic matter. Derived carbon variables are computed as

$$DOC = LDOC + RDOC, \tag{4.41a}$$

$$POC = LPOC + RPOC, \tag{4.41b}$$

$$POM = \frac{POC}{f_{com}}, \tag{4.41c}$$

$$TOC = DOC + POC + \frac{\sum CBOD_i}{r_{oc}} + \sum_i^3 r_{cai} A_{pi}, \tag{4.41d}$$

$$TSS = \sum m_n + POM + r_{da} A_p, \tag{4.41e}$$

where

f_{com} = fraction of carbon in organic matter (mg-C mg-D^{-1}),

DOC = dissolved organic carbon (mg-C L^{-1}),

POC = particulate organic carbon (mg-C L^{-1}),

POM = particulate organic matter (mg-D L^{-1}),

TOC = total organic carbon (mg-C L^{-1}),

TSS = total suspended solids (mg-C L^{-1}).

4.7 Methane and Sulfides

Methane and sulfides are two major by-products of decomposing organic matter in the sediment of aquatic ecosystems. Both constituents are modeled in the sediment diagenesis module. Therefore, water column methane (CH4) and total dissolved sulfides (HxS) are included as state variables in NSMII. Both state variables are modeled as dissolved forms with units of mg-O_2 L^{-1}. Dissolved sulfides can exist as hydrogen sulfide (H_2S), bisulfide ion (HS$^-$), and S^{2-}. Negligible amounts (less than 0.5%) of

dissolved sulfide exist as S^{-2} for the pH range of most streams and lakes; the distribution between HS^- and H_2S varies with pH, with high pH favoring HS^- and low pH favoring H_2S (APHA 1992). Sulfides exist as H_2S and half HS^- at a pH of 7.0. Their internal sources and sinks include bed sediment release, oxidation, and volatilization (atmospheric reaeration) (Figure 14). Table 15 presents the pathway terms (sources and sinks) for methane and sulfides included in NSMII.

Figure 14. Water column methane and sulfides processes modeled in NSMII.
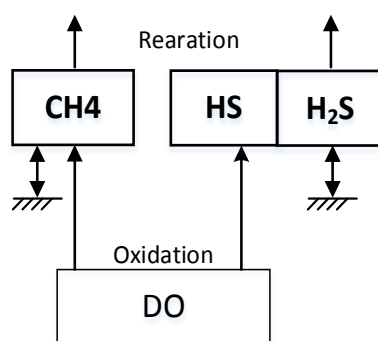
Table 15. Major pathways for methane and sulfides in NSMII.

State Variables	Internal Sources (+)	Internal Sinks (-)
CH4	Atmospheric rearation (CH4-->Atm)	Oxidation (CH4-->DIC) Sediment release (Bed<-->CH4)
H_2S	Atmospheric rearation (H_2S-->Atm)	Oxidation Sediment release (Bed<-->H_2S)

The concentrations of CH4 and H_2S in the atmosphere are low (assuming saturation values in the atmosphere of 0 mg/L for both gases). The reaeration rate equations for CH4 and H_2S are identical with the reaeration of DO. The reaeration coefficients for CH4 and H_2S are scaled relative to oxygen reaeration using the following expressions

$$k_{ach4} = k_a \left(\frac{MW_{O2}}{MW_{CH4}} \right)^{0.25} = 1.188 \cdot k_a, \qquad (4.42a)$$

$$k_{ah2s} = k_a \left(\frac{MW_{O2}}{MW_{H_2S}} \right)^{0.25} = 0.984 \cdot k_a, \qquad (4.42b)$$

where

$k_{ach4}(T)$ = CH4 reaeration rate (d^{-1}),
$k_{ah2s}(T)$ = H2S reaeration rate (d^{-1}),
$k_a(T)$ = oxygen reaeration rate (d^{-1}),
MW_{CH4} = molecular weights of CH4 (=16.04) (g mol^{-1}),
MW_{H2S} = molecular weights of H2S (=34.08) (g mol^{-1}).

4.7.1 Methane

Bacteria oxidize methane with DO or sulfite (SO4). The oxidation with sulfite has not been extensively investigated and is therefore not considered here. The bacterium oxidizes methane to CO2 within the water column (Hanson and Hanson 1996), which can be described as

$$CH4 + 2O_2 \rightarrow CO_2 + 2H_2O.$$
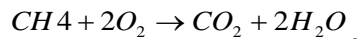
This process requires 5.33 g-O2 g-C^{-1}. In NSMII, methane oxidation is simulated as a temperature dependent first-order decay process. The rate is computed according to a half-saturation function with regard to both the availability of methane and DO.

The only source (+) of CH4 in the water column is sediment release. The sink (-) terms include atmospheric rearation and oxidation given in Table 15. The internal source and sink equation for water column CH4 can be written as

$$\frac{\partial CH4}{\partial t} = -k_{ach4}(T) \cdot CH4 \qquad \text{Atmospheric CH4 rearation (Atm<-->CH4),} \qquad (4.43)$$

$$-\frac{DO}{K_{sOch4} + DO} k_{ch4}(T) \cdot CH4 \qquad \text{CH4 oxidation (CH4-->DIC),}$$

$$+\frac{r_{ch4}}{h} \qquad \text{Sediment release (Bed-->CH4),}$$

where

$CH4$ = methane (mg-O2 L^{-1}),
$k_{ch4}(T)$ = CH4 oxidation rate (d^{-1}),
K_{sOch4} = half saturation oxygen attenuation constant for CH4 oxidation (mg-O2 L^{-1}),
r_{ch4} = sediment release rate of CH4 (g-O2 m^{-2} d^{-1}).

4.7.2 Total dissolved sulfides

Hydrogen sulfide (H_2S) and bisulfide ion (HS^-) together constitute total dissolved sulfides (HxS), which is included as a state variable in NSMII. The distribution between H_2S and HS^- varies with pH, with high pH favoring HS^-, and low pH favoring H_2S (APHA 1992). H_2S is a highly volatile dissolved gas that oxidizes very slowly (Chen and Morris 1972). The major loss of H_2S is through volatilization from the water. HS^- is removed primarily by its oxidation. There is also general agreement that sulfur bacteria play an important role in sulfide oxidation in natural and waste waters. These influencing factors help to explain why the first-order sulfide oxidation rates reported vary between 0.26 and about 55.0 day^{-1} (Millero 1986). The oxidation rate of sulfide is strongly dependent on pH. For an increase in pH from about 6.0 to 8.0, there is an eight-fold increase in the oxidation rate (Chen and Morris 1972). Millero (1986) attributes this to the shift in sulfide concentration from predominantly nonreactive H_2S to predominantly reactive HS^- with increasing pH. This reasoning suggests that HS^- concentration should be used in the sulfide oxidation rate equation.

The oxidation of dissolved sulfide is modelled as a temperature-dependent first-order process with regard to both HS^- and DO. Oxidation of sulfide can produce sulfur (S), thiosulfate ($S_2O_3^{-2}$), sulfite (SO_3^{-2}), or sulfate (SO_4^{-2}). O'Brien and Birkner (1977) indicated that most experiments observed SO_3^{-2}, $S_2O_3^{-2}$, and SO_4^{-2} as oxidation products of sulfide. They proposed a hypothetical reaction

$$4 HS^- + \frac{6}{5}O_2 \rightarrow S_2O_3^{2-} + SO_3^{2-} + SO_4^{2-} + 2H^+ + H_2O.$$
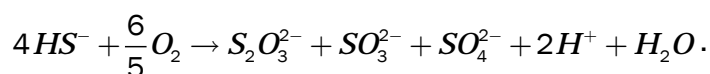
This reaction requires 1.38 mg-O_2 L^{-1} per 1.0 mg-S^{2-} L^{-1}, or 1.33 mg-O_2 L^{-1} per 1.0 mg-HS^{-1} L^{-1} (O'Brien and Birkner 1977). NSMII however, does not consider the precipitation of sulfide.

The only source (+) of HxS in the water column is generated by sulfate reduction or sediment release. The sink (-) terms include atmospheric rearation and oxidation given in Table 15. The internal source and sink equation for water column HxS can be can be written as

$$\frac{\partial HxS}{\partial t} = -k_{ah2s}(T) \cdot H_2 S \qquad \text{Atmospheric H}_2\text{S rearation (Atm<-->H}_2\text{S),} \qquad (4.44)$$

$$-\frac{DO}{K_{sOhs} + DO} k_{hs}(T) \cdot HS \qquad \text{HS oxidation,}$$

$$+\frac{r_{h2s}}{h} \qquad \text{Sediment release (Bed-->H}_2\text{S),}$$

where

HxS = total dissolved sulfides (mg-O$_2$ L^{-1}),
K_{sOhs} = half saturation oxygen attenuation constant for HS oxidation (mg-O$_2$ L^{-1}),
$k_{hs}(T)$ = HS oxidation rate (L mg-O$_2$$^{-1}$ d^{-1}),
r_{h2s} = sediment release rate of H$_2$S (g-O$_2$ m^{-2} d^{-1}).

The dissolved fractions of H$_2$S and HS$^-$ are computed from the HxS concentration and the pH. Their fractions are given in Standard Methods (APHA 1992).

$$f_{h2s} = \frac{-8.3813\,pH^3 + 135.898\,pH^2 - 742.31\,pH + 1461.46}{100}, \; 5 \le \text{pH} < 7, \; (4.45a)$$

$$f_{h2s} = \frac{-8.25406\,pH^3 + 213.821\,pH^2 - 1852.79\,pH + 5374.11}{100}, \; 7 \le \text{pH} \le 9, \qquad (4.45b)$$

where

f_{h2s} = H$_2$S fraction of HxS (0 − 1.0).

The fraction of HxS as HS$^-$ is then computed as (1 - f_{h2s}). If pH is less than 5 or greater than 9 (pH < 5 or pH > 9), f_{h2s} is set to 1.0 and 0, respectively. The concentrations of the relevant sulfide species (H$_2$S and HS$^-$) are computed as

$$H_2 S = f_{h2s} HxS, \qquad (4.46a)$$

$$HS = \left(1 - f_{h2s}\right) HxS, \qquad (4.46b)$$

where

H_2S = dissolved hydrogen sulfide (mg-O$_2$ L^{-1}),

HS = dissolved bisulfide ion (mg-O_2 L^{-1}).

4.8 Dissolved Oxygen

Figure 15 provides an overview of the NSMII representation of DO source and sink processes. Additional processes for DO kinetics are also considered in NSMII. The total consumption of oxygen is the sum of RDOC, LDOC, CBOD, CH4, and HS oxidation reactions. These oxidation processes are limited by the concentration of DO. SOD is the quantity of oxygen transferred from the water column to the benthic sediment that is necessary to satisfy the oxygen requirements of bacteria as they decompose previously deposited organic matter. If the sediment diagenesis module is activated (see Chapter 5), SOD is internally computed in NSMII; otherwise, SOD is a user input parameter. Because oxygen moves from water to sediments, sediment oxygen consumption is represented as a negative quantity.

Figure 15. DO source and sink processes modeled in NSMII.

Eight water quality state variables are involved in the DO mass balance: algae, benthic algae, NH4, LDOC, RDOC, CBOD, CH4, and HxS. Table 16 summarizes the major processes and mechanisms affecting the DO in the water column. The sum of each source (+) and sink (-) terms in the appropriate column below table can then be used to compute the net rate for water column DO.

Table 16. Source and sink processes affecting dissolved oxygen in NSMII.

State Variables	Internal Sources (+)	Internal Sinks (-)
DO	Atmospheric rearation	
A_p	Algal photosynthesis (A_p-->DO)	Algae respiration (DO-->A_b)
A_b	Benthic algae photosynthesis (A_b-->DO)	Benthic algal respiration (DO-->A_p)
$NH4$	-	Do-->nitrification
$LDOC$	-	Oxidation (DO-->LDOC)
$RDOC$	-	Oxidation (DO-->RDOC)

CBOD	-	Oxidation (DO-->CBOD)
CH4	-	Oxidation (DO-->CH4)
HS	-	Oxidation (DO-->HS)
DO	-	SOD

The internal source and sink equation for water column DO can be written as

$$\frac{dDO}{dt} = k_a(T)(DO_s - DO)$$

Atmospheric O$_2$ reaeration   (Atm<-->O$_2$),   (4.47)

$$-\frac{DO}{K_{sOxna} + DO}k_{nit}(T) \cdot r_{on}NH4$$

Nitrification (O$_2$-->Nitrification),

$$-\frac{DO}{K_{sOxmc} + DO}k_{rdoc}(T) \cdot r_{oc}RDOC$$

RDOC oxidation (O$_2$-->RDOC),

$$-\frac{DO}{K_{sOxmc} + DO}k_{ldoc}(T) \cdot r_{oc}LDOC$$

LDOC oxidation (O$_2$-->LDOC),

$$-\sum\frac{DO}{K_{sOxbodi} + DO}k_{bodi}(T) \cdot CBOD_i$$

CBOD oxidation (O$_2$-->CBOD),

$$-\frac{DO}{K_{sOch4} + DO}k_{ch4}(T) \cdot CH4$$

CH4 oxidation (O$_2$-->CH4),

$$-\frac{DO}{K_{sOhs} + DO}k_{hs}(T) \cdot HS$$

HS oxidation (O$_2$-->HS),

$$-\frac{DO}{K_{sSOD} + DO}\frac{SOD(T)}{h}$$

Sediment oxygen demand (SOD),

$$+\sum_i^3\left(P_{Npi} + \frac{138}{106}(1 - P_{Npi})\right)\mu_{pi}(T) \cdot r_{oc}r_{cai}A_{pi}$$

Algal photosynthesis (A$_p$--> O$_2$),

$$-\sum_i^3 F_{Oxpi}k_{rpi}(T) \cdot r_{oc}r_{cai}A_{pi}$$

Algal respiration (O$_2$-->A$_p$),

$$+\frac{1}{h}\left(P_{Nb} + \frac{138}{106}(1 - P_{Nb})\right)\mu_b(T) \cdot r_{oc}r_{cb}A_bF_b$$

Benthic algae photosynthesis (A$_b$--> O$_2$),

$$-\frac{1}{h}F_{Oxb}k_{rb}(T) \cdot r_{oc}r_{cb}A_bF_b$$

Benthic algae respiration (O$_2$-->A$_b$),

where

DO_s = dissolved oxygen saturation (mg-O_2 L^{-1}),

K_{sSOD} = half saturation oxygen attenuation constant for SOD (mg-O_2 L^{-1}).

4.8.1 Dissolved oxygen saturation

The effect of salinity on the DO saturation in surface water is included in NSMII. DO_s is computed as a function of salinity and temperature via the following equation (APHA 1992)

$$DO_s = DO_s \cdot \exp\left[-Salt\left(1.7674 \cdot 10^{-2} - \frac{1.0754 \cdot 10^1}{T_{wk}} + \frac{2.1407 \cdot 10^3}{T_{wk}^2}\right)\right], \quad (4.48)$$

where

$Salt$ = salinity (ppt).

Salinity is the total of all non-carbonate salts dissolved in water, usually expressed in parts per thousand (ppt). Salinity is an important measurement in seawater or in estuaries where freshwater from rivers and streams mixes with salty ocean water. Because most anions in seawater or brackish water are chloride ions, salinity can be estimated from chloride concentration below

$$Salt = 0.03 + 0.0018066 \cdot Cl, \quad (4.49)$$

where

Cl = chloride concentration (mg-Cl L^{-1}).

Vice versa, water column chloride concentration can be computed from known salinity. While salinity and chloride are proportional in seawater, the above equation is not accurate in freshwater (MDNR 2009).

4.8.2 Oxygen reaeration

Depending on whether the water is undersaturated or oversaturated, the DO is gained or lost via atmospheric reaeration. The oxygen reaeration rate is dependent on either the flow, the wind speed, or both. In NSMII the oxygen reaeration rate is estimated as a function of both flow hydraulics

and wind velocity as in NSMI. Three options are available to incorporate wind effects on the oxygen reaeration: (1) user defined, (2) Banks-Herrera formula (Banks and Herrera 1977), and (3) Wanninkhof formula (Wanninkhof et al. 1991). The six oxygen reaeration options are included in NSMII and listed in Table 4.

4.9   Silica Species

Silica is an important nutrient for some algae such as diatoms, because of this, the Silica cycle is included in NSMII. Two silica forms are considered: particulate biogenic silica (BSi) and dissolved silica (DSi). DSi is also called available silica and can be used as a nutrient during algal growth (primarily for diatoms). DSi is produced by the dissolution of BSi and can interact with the sediment through silica fluxes. Silica is used by only diatoms, so uptake by algae depends on the presence of diatoms. If the optional sediment diagenesis module is included (see Chapter 5), sediment–water flux of silica is internally computed; otherwise, silica released from the sediment bed is specified. Particulate or unavailable biogenic silica is produced from diatom mortality. BSi dissolutes into DSi or settles to the sediment from the water column. Dissolution is a chemical–physical process proceeding in an undersaturated solution. The dissolution of the BSi can also be understood as the desorption from organic matter, which is proportional to its concentration and the difference between the saturation and actual DSi concentrations. Once silica is used by the algal group during photosynthesis, it is lost from the system. Figure 16 shows an overview of the NSMII representation of silica species and a simplified silica cycle involved in the water column. Table 17 presents the pathway terms (sources and sinks) for silica state variables included in NSMII.

Figure 16. Silica species and major processes modeled in NSMII.

Table 17. Major pathways for silica state variables in NSMII.

State Variables	Internal Sources (+)	Internal Sinks (-)
BSi	Algal mortality (A$_p$-->BSi)	Dissolution (BSi-->DSi) Settling (BSi-->Bed)
DSi	Algal mortality (A$_p$-->DSi) Dissolution (BSi-->DSi) Algal respiration (A$_p$-->DSi) Sediment release (Bed<-->DSi)	Algal uptake (DSi-->A$_p$)

Note that the silica cycle is modeled in NSMII if the diatom species are included. Diatoms are conventionally assigned as one of the algal groups. The potential also exists to have multiple diatom groups, or groups of mixed algae composed of diatoms and other groups. The sum of each of source (+) and sink (-) terms can then be used to compute the net rate for each silica state variable. The source and sink equations for silica state variables (BSi and DSi) in the water column are given below.

Particulate Biogenic Silica (BSi):

$$\frac{\partial BSi}{\partial t} = F_{bsi} \sum_{i}^{3} k_{dpi}(T) \cdot r_{siai} A_{pi} \qquad \text{Algal mortality (A}_p\text{-->BSi),} \qquad (4.50)$$

$$- k_{bsi}(T) \frac{BSi}{K_{sSi} + BSi}\left(Si_s - DSi\right) \qquad \text{BSi dissolution (BSi-->DSi),}$$

$$- \frac{v_{bsi}}{h} BSi \qquad \text{BSi settling (BSi-->Bed),}$$

where

BSi = particulate biogenic silica (mg-Si L^{-1}),
F_{bsi} = fraction of algal mortality into BSi (0–1.0),
r_{siai} = algal Si : Chla ratio (mg-Si/µg-Chla),
v_{bsi} = BSi settling velocity (m d^{-1}),
$k_{bsi}(T)$ = BSi dissolution rate (d^{-1}),
K_{sSi} = half saturation Si constant for dissolution (mg-Si L^{-1}),
Si_s = Si saturation (mg-Si L^{-1}).

Dissolved Silica (DSi):

$$\frac{\partial DSi}{\partial t} = \left(1 - F_{bsi}\right)\sum_{i}^{3} k_{dpi}(T) \cdot r_{siai} A_{pi} \quad \text{Algal mortality (A}_\text{p}\text{-->DSi)}, \tag{4.51}$$

$$+ k_{bsi}(T)\frac{BSi}{K_{sSi} + BSi}\left(Si_s - DSi\right) \quad \text{BSi dissolution (BSi-->DSi)},$$

$$+ \sum_{i}^{3} F_{Oxpi} k_{rpi}(T) \cdot r_{siai} A_{pi} \quad \text{Algal respiration (A}_\text{p}\text{-->DSi)},$$

$$- \sum_{i}^{3} \mu_{pi}(T) \cdot r_{siai} A_{pi} \quad \text{Algal uptake (DSi-->A}_\text{p}\text{)},$$

$$+ \frac{1}{h} r_{si} \quad \text{Sediment release (Bed<-->DSi)},$$

where

r_{si} = sediment release rate of DSi (g-Si m^{-2} d^{-1}).

4.10 Alkalinity

Alkalinity is modeled in NSMII as is done previously with NSMI except for considering multiple algae groups in the water column. The major processes and mechanisms affecting the alkalinity in the water column are summarized in Table 18. The ratios used in the following alkalinity equation have been defined and described in NSMI.

Table 18. Reaction processes affecting alkalinity in NSMII.

Reaction Process	Utilize	Create	Source/Sink
Algae and benthic algae growth	NH4	-	Sink (-)
	NO3	-	Source (+)
Algae and benthic algae respiration	-	NH4	Source (+)
NH$_4$ nitrification	NH4	NO3	Sink (-)
NO$_3$ denitrification	NO3	N$_2$	Source (+)

The change of water column alkalinity (*Alk*) with respect to time due to source (+) and sink (-) mechanisms listed in Table 18 can be written as

$$\frac{dAlk}{dt} = r_{alkden}\left(1 - \frac{DO}{K_{sOxdn} + DO}\right)k_{dnit}(T) \cdot NO3 \qquad \text{Alk increased by denitrification,} \qquad (4.52)$$

$$-r_{alkn}\frac{DO}{K_{sOxna} + DO}\frac{NH4}{K_{sNh4} + NH4}k_{nit}(T) \cdot NH4 \qquad \text{Alk decreased by nitrification,}$$

$$-\sum\left(r_{alkaai}P_{Npi} - r_{alkani}(1 - P_{Npi})\right)\mu_{pi}(T) \cdot A_{pi} \qquad \text{Alk decreased by algal growth,}$$

$$+\sum r_{alkaai}F_{Oxpi}k_{rpi}(T) \cdot A_{pi} \qquad \text{Alk increased by algal respiration,}$$

$$-\frac{1}{h}\left(r_{alkba}P_{Nb} - r_{alkbn}(1 - P_{Nb})\right)\mu_{b}(T) \cdot A_{b}F_{b} \qquad \text{Alk decreased by benthic algae growth,}$$

$$+\frac{1}{h}r_{alkba}F_{Oxb}k_{rb}(T) \cdot A_{b}F_{b} \qquad \text{Alk increased by benthic algae respiration,}$$

where

Alk = alkalinity (eq L^{-1}),
r_{alkaai} = ratio translating algal growth into Alk if NH$_4$ is the N source (eq µg-Chla^{-1}),
r_{alkani} = ratio translating algal growth into Alk if NO$_3$ is the N source (eq µg-Chla^{-1}),
r_{alkn} = ratio translating NH$_4$ nitrification into Alk (eq mg-N^{-1}),
r_{alkden} = ratio translating NO$_3$ denitrification into Alk (eq mg-N^{-1}),
r_{alkbai} = ratio translating benthic algae growth into Alk if NH$_4$ is the N source (eq mg-D^{-1}),
r_{alkbni} = ratio translating benthic algae growth into Alk if NO$_3$ is the N source (eq mg-D^{-1}).

The subscript "i" in equation 4.52 represents a specific algal group.

4.11 NSMII Parameters

This section describes the input parameters associated with NSMII. The user-defined input parameters consist of eight groups. Most of the temperature-dependent rate coefficients are specified at 20 ℃. Besides algae and benthic algae growth rates, the temperature-dependent reaction rates in NSMII are adjusted according to a modified Arrhenius Equation. As previously stated in NSMI, the default values and suggested ranges of NSMII parameters are provided for initial model development. Most of them are calibration parameters. All parameter tables will be repeated for

each water quality region, allow the user to define the different values for input parameters.

4.11.1 Global parameters

Table 19 below provides a summary of NSMII global parameters (or coefficients) and default values.

Table 19. NSMII global parameters and coefficients with default values.

Symbol	Definition	Unit	Default Value	Reference Range
v_{sp}	Solids settling velocity	m d^{-1}	0.1	0 - 30[c]
v_{sr}	Refractory organic matter settling velocity	m d^{-1}	0.01	0 - 2.0[b]
v_{sl}	Labile organic matter settling velocity	m d^{-1}	0.01	0 - 2.0[b]
λ_0	Background light attenuation	m^{-1}	0.02	0.02 - 6.59[c]
λ_s	Light attenuation by inorganic suspended solids	L mg^{-1} m^{-1}	0.052[a]	0.019 - 0.37[c]
λ_m	Light attenuation by organic matter	L mg^{-1} m^{-1}	0.174[a]	0.008 - 0.174[c]
λ_1	Linear light attenuation by algae	m^{-1} (μg-Chla L^{-1})$^{-1}$	0.0088[a]	0.0088 - 0.031[d]
λ_2	Nonlinear light attenuation by algae	m^{-1} (μg-Chla L^{-1})$^{2/3}$	0.054[a]	n/a
f_{com}	Fraction of carbon in organic matter	mg-C mg-D^{-1}	0.01	0 – 1.0
k_{dpo4n}	Partition coefficient of inorganic P for solid "n"	L kg^{-1}	0	0 - 80000[d]

a. Chapara et al. (2008).

b. Wool et al. (2006).

c. Flynn et al. (2015).

d. Derived from Table 6.

4.11.2 Algae parameters

Table 20 below summarizes a list of NSMII algae parameters (or coefficients) and default values. It is important to know the type of algae to define the algal growth, respiration, mortality rates, and other coefficients accurately. A variable stoichiometry with respect to each algal group is allowed. The ratios of C, N, P, Si, and Chla fractions in algae are defined by specifying their relative stoichiometry weight to dry weight biomass (100 mg-D). The mortality rates of algae are converted into three pools: dissolved, particulate, and other organic material. Two fractions of these pools are defined by the user while the third fraction is internally computed.

Table 20. NSMII algae parameters and rate coefficients with default values.

Symbol*	Definition	Unit	Default Value	Reference Range	Temperature Correction	
AW_{di}	Algal dry weight stoichiometry	mg-D	100[a]	65 - 130[c]		
AW_{ci}	Algal carbon stoichiometry	mg-C	40[a]	25 - 60[c]		
AW_{ni}	Algal nitrogen stoichiometry	mg-N	7.2[a]	4 - 20[c]		
AW_{pi}	Algal phosphorus stoichiometry	mg-P	1.0[a]	n/a		
AW_{ai}	Algal Chla stoichiometry	µg-Chla	1000[a]	400 - 3500[c]		
AW_{si}	Algal silica stoichiometry	mg-Si	18[a]	n/a		
$k_{rpi}(T)$	Algal respiration rate	d^{-1}	0.2	0.02 - 0.8[c]	Yes	1.08
$k_{dpi}(T)$	Algal death rate	d^{-1}	0.15	0 - 0.5[c]	Yes	1.07
v_{sai}	Algal settling velocity	m d^{-1}	0.15	0 - 1.8[e]		
k_{snxpi}	Half saturation NH4 concentration for algal uptake	mg-N L^{-1}	0.02	0.005 - 0.03[c]		
K_{sOxpi}	Half-saturation oxygen attenuation constant for algal respiration	mg-O_2 L^{-1}	0.5	n/a		
K_{sNpi}	Half-saturation N limiting constant for algal growth	mg-N L^{-1}	0.04	0.005 - 0.3[f]		
K_{sPpi}	Half-saturation P limiting constant for algal growth	mg-P L^{-1}	0.0012	0.001 - 0.06[f]		
K_{Li}	Light limiting constant for algal growth	W m^{-2}	10	3.7 - 44[f]		
μ_{mxpi}	Maximum algal growth rate	d^{-1}	1.0	0.1 - 3.0[f]		
T_{opi}	Optimal temperature for algal growth	^0C	25[e]	n/a		
kt_{p1i}	Effect of temperature below T_{0p} on algal growth	$^0C^{-2}$	0.003[e]	n/a		
kt_{p2i}	Effect of temperature above T_{0p} on algal growth	$^0C^{-2}$	0.01[e]	n/a		

* Subscript i represents a specific algal group.

a. Chapara et al. (2008).

b. Brown and Barnwell (1987).

c. Flynn et al. (2015).

d. Tillman et al. (2004).

e. Cerco et al. (2004).

f. Derived from Table 6.

4.11.3   Benthic algae parameters

Table 21 below summarizes a list of NSMII benthic algae parameters (or coefficients) and their associated default values. The ratios of C, N, P, and Chla fractions in benthic algae are defined by specifying their relative stoichiometry weight to dry weight biomass (100 mg-D).

Table 21. NSMII benthic algae parameters and rate coefficients with default values.

Symbol	Definition	Unit	Default Value	Reference Range	Temperature Correction	
BW_d	Benthic algae dry weight stoichiometry	mg-D	100[a]	65 - 130[c]		
BW_c	Benthic algae carbon stoichiometry	mg-C	40[a]	25 - 60[c]		
BW_n	Benthic algae nitrogen stoichiometry	mg-N	7.2[a]	4 - 20[c]		
BW_p	Benthic algae phosphorus stoichiometry	mg-P	1.0[a]	n/a		
BW_a	Benthic Chla stoichiometry	µg-Chla	5000[a]	400 - 3500[c]		
$k_{rb}(T)$	Benthic algal base respiration rate	d^{-1}	0.2	0.01 - 0.8[b]	Yes	1.047[b]
$k_{db}(T)$	Benthic algae death rate	d^{-1}	0.3	0 - 0.8[b]	Yes	1.047[b]
K_{Lb}	Light limiting constant for benthic algae growth	W m^{-2}	10	1.7 – 44[e]		
K_{sOxb}	Half-saturation oxygen attenuation constant for benthic algae respiration	mg-O_2 L^{-1}	1.0	n/a		
μ_{mxb}	Maximum benthic algal growth rate	d^{-1}	0.4	0.3 - 2.25[b]		
T_{ob}	Optimal temperature for benthic algal growth	^{0}C	25[d]	n/a		
kt_{b1}	Effect of temperature below T_{0p} on benthic algal growth	^{0}C^{-2}	0.003[d]	n/a		
kt_{b2}	Effect of temperature above T_{0p} on benthic algal growth	^{0}C^{-2}	0.01[d]	n/a		
K_{Sb}	Half-saturation density constant for benthic algae growth	mg-D m^{-2}	10	10 - 30[b]		
F_b	Fraction of bottom area available for benthic algae growth	unitless	0.9	0 - 1.0		
F_w	Fraction of benthic algae mortality into water column	unitless	0.9	0 - 1.0		
F_{rponb}	Fraction of benthic algae mortality into RPON	unitless	0.8	0 - 1.0		
F_{lponb}	Fraction of benthic algae mortality into LPON	unitless	0.1	0 - 1.0		
k_{snxb}	Half saturation NH4 concentration for benthic algae uptake	mg-N L^{-1}	0.02	0.005 - 0.3[c]		
K_{sNb}	Half-saturation N limiting constant of benthic algae growth	mg-N L^{-1}	0.25	0.01 - 0.766[b]		
F_{rpopb}	Fraction of benthic algae mortality into RPOP	unitless	0.8	0 - 1.0		
F_{lpopb}	Fraction of benthic algae mortality into LPOP	unitless	0.1	0 - 1.0		
K_{sPb}	Half-saturation P limiting constant of benthic algae growth	mg-P L^{-1}	0.125	0.005 - 0.175[c]		
F_{rpocb}	Fraction of benthic algae mortality into RPOC	unitless	0.8	0 - 1.0		
F_{lpocb}	Fraction of benthic algae mortality into LPOC	unitless	0.1	0 - 1.0		
F_{rdocb}	Fraction of benthic algae mortality into RDOC	unitless	0.05	0 - 1.0		

a. Chapara et al. (2008).

b. Brown (2002).

c. Flynn et al. (2015).

d. Cerco et al. (2004).

e. Derived from Table 6.

4.11.4 Nitrogen cycle parameters

Table 22 below summarizes a list of NSMII nitrogen cycle parameters (or coefficients) with their associated default values.

Table 22. NSMII nitrogen cycle parameters and rate coefficients with default values.

Symbol	Definition	Units	Default Value	Reference Range	Temperature Correction	
F_{rponp}	Fraction of algal mortality into RPON	unitless	0.8	0 - 1.0		
F_{lponp}	Fraction of algal mortality into LPON	unitless	0.15	0 - 1.0		
$k_{rpon}(T)$	RPON hydrolysis rate	d^{-1}	0.001[b]	0.007 – 0.01	Yes	1.08
$k_{lpon}(T)$	LPON hydrolysis rate	d^{-1}	0.08[b]	0.05 – 0.07[d]	Yes	1.08
$k_{don}(T)$	DON mineralization rate	d^{-1}	0.018[b]	0.0025 - 0.025[c]	Yes	1.08
$k_{nit}(T)$	Nitrification rate	d^{-1}	0.1	0.01 - 10[a]	Yes	1.083
$k_{dnit}(T)$	Denitrification rate	d^{-1}	0.002	0.002 - 2.0[a]	Yes	1.045
v_{no3}	Sediment denitrification velocity	m d^{-1}	0	0 - 1.0[a]	Yes	1.08
K_{sOxmn}	Half-saturation oxygen attenuation constant for for DON mineralization	mg-O$_2$ L^{-1}	0.5	n/a		
K_{sOxna}	Half-saturation oxygen attenuation constant for nitrification	mg-O$_2$ L^{-1}	2.0[c]	n/a		
K_{sOxdn}	Half-saturation oxygen inhibition constant for denitrification	mg-O$_2$ L^{-1}	0.1[c]	n/a		
r_{nh4}	Sediment release rate of NH4	g-N m^{-2} d^{-1}	0	n/a	Yes	1.074[b]

a. Flynn et al. (2015).

b. Cerco et al. (2004).

c. Wool et al. (2006).

d. HydroQual (2004).

4.11.5 Phosphorus cycle parameters

Table 23 below summarizes a list of NSMII phosphorus cycle parameters (or coefficients) with their associated default values.

4.11.6 Carbon cycle parameters

Table 24 below summarizes a list of NSMII carbon cycle parameters (or coefficients) with their associated default values.

Table 23. NSMII phosphorus cycle parameters and rate coefficients with default values.

Symbol	Definition	Units	Default Value	Reference Range	Temperature Correction	
F_{rpopp}	Fraction of algal mortality into RPOP	unitless	0.8	0 - 1.0		
F_{lpopp}	Fraction of algal mortality into LPOP	unitless	0.15	0 - 1.0		
$k_{rpop}(T)$	RPOP hydrolysis rate	d-1	0.001[a]	0.007 – 0.01[d]	Yes	1.08
$k_{lpop}(T)$	LPOP hydrolysis rate	d-1	0.1[a]	0.085 – 0.1[d]	Yes	1.08
$k_{dop}(T)$	DOP mineralization rate	d-1	0.22[b]	0.01 – 0.2[d]	Yes	1.08
K_{sOxmp}	Half-saturation oxygen attenuation constant for DOP mineralization	mg-O L-1	1.0	n/a		
r_{po4}	Sediment release rate of DIP	g-P m-2 d-1	0	n/a	Yes	1.074[b]

a. Cerco et al. (2004).

b. Wool et al. (2006).

c. Thomann and Pitzpatrick (1982).

d. HydroQual (2004).

Table 24. NSMII carbon cycle parameters and rate coefficients with default values.

Symbol	Definition	Units	Default Value	Reference Range	Temperature Correction	
F_{rpocp}	Fraction of algal mortality into RPOC	unitless	0.8	0 - 1.0		
F_{lpocp}	Fraction of algal mortality into LPOC	unitless	0.1	0 - 1.0		
F_{rdocp}	Fraction of algal mortality into RDOC	unitless	0.05	0 - 1.0		
F_{co2}	Fraction of CO_2 in total inorganic carbon	unitless	0.2	0 - 1.0		
p_{CO2}	Partial pressure of CO_2	ppm	383[a]	n/a		
$k_{rpoc}(T)$	RPOC hydrolysis rate	d-1	0.0025[b]	0.007 – 0.01[c]	Yes	1.08
$k_{lpoc}(T)$	LPOC hydrolysis rate	d-1	0.075[b]	0.007 – 0.1[c]	Yes	1.08
$k_{rdoc}(T)$	RDOC mineralization rate	d-1	0.0025[b]	0.008 – 0.01[c]	Yes	1.08
$k_{ldoc}(T)$	LDOC mineralization rate	d-1	0.05[b]	0.1 – 0.15[c]	Yes	1.047
K_{sOxmc}	Half-saturation oxygen attenuation for DOC mineralization	mg-O_2 L-1	1.0	n/a		

a. Chapara et al. (2008).

b. Tillman et al. (2004).

c. HydroQual (2004).

4.11.7 CBOD parameters

Table 25 below summarizes a list of NSMII CBOD parameters (or coefficients) with their associated default values.

Table 25. NSMII CBOD parameters and rate coefficients with default values.

Symbol*	Definition	Units	Default Value	Reference Range	Temperature Correction	
k_{bodi}	CBOD oxidation rate	d^{-1}	0.12	0.02 - 3.4[a]	Yes	1.047
$K_{sOxbodi}$	Half-saturation oxygen attenuation for CBOD oxidation	mg-O$_2$ L^{-1}	0.5[b]	n/a		
k_{sbodi}	CBOD sedimentation rate	d^{-1}	0	-0.36 - 0.36[a]	Yes	1.024

* Subscript i represents a specific CBOD group.

a. Brown and Barnwell (1987).

b. Wool et al. (2006).

4.11.8   Methane and sulfide parameters

Table 26 below summarizes a list of NSMII methane and sulfide parameters (or coefficients) with their associated default values.

Table 26. NSMII methane and sulfide parameters and rate coefficients with default values.

Symbol	Definition	Units	Default Value	Reference Range	Temperature Correction	
k_{ch4}	CH4 oxidation rate	d^{-1}	0.1	n/a	Yes	1.079
K_{sOch4}	Half saturation oxygen attenuation constant for CH4 oxidation	mg-O$_2$ L^{-1}	1.0	n/a		
r_{ch4}	Sediment release rate of CH4	g-O$_2$ m^{-2} d^{-1}	0	n/a	Yes	1.079
k_{hs}	HS oxidation rate	d^{-1}	25[a]	0.15 – 0.5[b]	Yes	1.08
K_{sOhs}	Half saturation oxygen attenuation constant for HS oxidation	mg-O$_2$ L^{-1}	0.5[a] 0.2[b]	n/a		
r_{h2s}	Sediment release rate of H$_2$S	g-O$_2$ m^{-2} d^{-1}	0	n/a	Yes	1.079

a. Dortch et al. (1992).

b. HydroQual (2004).

4.11.9   Dissolved oxygen parameters

Table 27 below summarizes a list of NSMII DO parameters (or coefficients) with their associated default values.

Table 27. NSMII DO parameters and rate coefficients with default values.

Symbol	Definition	Units	Default Value	Reference Range	Temperature Correction	
$k_{ah}(T)$	Hydraulic oxygen reaeration rate	d^{-1}	1	0 - 100	Yes	1.024
$k_{aw}(T)$	Wind oxygen reaeration velocity	m d^{-1}	0	n/a	Yes	1.024
$SOD(T)$	Sediment oxygen demand	g-O$_2$ m^{-2} d^{-1}	0.2	0.05 - 10[a]	Yes	1.060
K_{sSOD}	Half saturation oxygen attenuation constant for SOD	mg-O$_2$ L^{-1}	1	n/a		

a. Thomann and Muller (1987).

4.11.10 Silica cycle parameters

Table 28 below summarizes a list of NSMII silica cycle parameters (or coefficients) with their associated default values.

Table 28. NSMII silica cycle parameters and rate coefficients with default values.

Symbol*	Definition	Units	Default Value	Reference Range	Temperature Correction	
F_{bsi}	Fraction of algal mortality into BSi	unitless	0.9	0 - 1.0		
K_{sSipi}	Half-saturation Si constant for algal growth	mg-Si L^{-1}	0.03[b]	0.02 - 0.08[d]		
K_{sSi}	Half-saturation Si constant for dissolution	mg-Si L^{-1}	50000	n/a		
v_{bsi}	BSi settling velocity	m d^{-1}	0.25[b]	0.5 – 1.0[e]		
$k_{bsi}(T)$	BSi dissolution rate	d^{-1}	0.03[b]	0.1 – 0.25[e]	Yes	1.08
Si_s	Silica saturation	mg-Si L^{-1}	n/a	n/a		
r_{si}	Sediment release rate of DSi	g-Si m^{-2} d^{-1}	0	n/a	Yes	1.074

* Subscript i represents an algal group as diatom.

[a] Cole and Wells (2008).

[b] Tillman et al. (2004).

[c] Di Toro (2001).

[d] Thomann and Muller (1987).

[e]. HydroQual (2004).

4.11.11 Pathogen parameters

Table 29 below summarizes a list of NSMII pathogen parameters (or coefficients) with their associated default values.

Table 29. NSMII pathogen parameters and rate coefficients with default values.

Symbol	Definition	Units	Default Value	Reference Range	Temperature Correction	
$k_{dx}(T)$	Pathogen death rate	d^{-1}	0.8[a]	n/a	Yes	1.07[a]
α_{px}	Light efficiency factor for pathogen decay	unitless	1.0[a]	n/a		
v_x	Pathogen settling velocity	m d^{-1}	1.0[a]	n/a		

a Chapara et al. (2008).

4.12 NSMII Outputs

This section describes the model outputs associated with NSMII. The model output data includes the water quality state varaibles, derived

variables, and intermediate variables computed in NSMII. Table 19 lists the water quality state variables modeled in NSMII.

4.12.1 Derived variables

Nineteen derived water quality variables are computed in NSMII and are listed in Table 30.

Table 30. Derived water quality variables computed in NSMII.

Variable	Definition	Units
A_{pd}	Algae (dry weight)	mg-D L^{-1}
$Chla$	Chlorophyll-a	µg-Chla L^{-1}
$Chlb$	Benthic chlorophyll-a	mg-Chla m^{-2}
DIN	Dissolved inorganic nitrogen	mg-N L^{-1}
TON	Total organic nitrogen	mg-N L^{-1}
TKN	Total kjeldahl nitrogen	mg-N L^{-1}
TN	Total nitrogen	mg-N L^{-1}
DIP	Dissolved inorganic phosphorus	mg-P L^{-1}
TOP	Total organic phosphorus	mg-P L^{-1}
TP	Total phosphorus	mg-P L^{-1}
DOC	Dissolved organic carbon	mg-C L^{-1}
POC	Particulate organic carbon	mg-C L^{-1}
POM	Particulate organic matter	mg-D L^{-1}
TOC	Total organic carbon	mg-C L^{-1}
$CBOD_5$	5-day carbonaceous biochemical oxygen demand	mg-O$_2$ L^{-1}
H_2S	Dissolved hydrogen sulfide	mg-O$_2$ L^{-1}
λ	Light attenuation coefficient	m^{-1}
k_a	Oxygen reaeration rate	d^{-1}
pH	pH	-

CBOD5 is computed as the sum of the contributions from dissolved organic matter represented by CBOD and labile anf refractory dissolved organic carbon

$$
\begin{aligned}
CBOD5 = &\sum CBOD_i \left(1 - e^{-5 k_{bodi}(20)}\right) \\
&+ r_{oc} LDOC \left(1 - e^{-5 \cdot k_{ldoc}(20)}\right) + r_{oc} RDOC \left(1 - e^{-5 \cdot k_{rdoc}(20)}\right)
\end{aligned}
\tag{4.56}
$$

4.12.2   Pathway fluxes

Table 31 provides a summary of pathway fluxes and additional variables that can be reported in NSMII model outputs.

Table 31. Pathway fluxes and additional variables computed in NSMII.

Name	Definition	Units
Algae i		
A_p growth	Algal growth	µg-Chla/L/d
A_p respiration	Algal respiration	µg-Chla/L/d
A_p mortality	Algal mortality	µg-Chla/L/d
A_p settling	Algal settling	µg-Chla/L/d
FL	Algal growth light limit factor	Unitless
FN	Algal growth N limit factor	Unitless
FP	Algal growth P limit factor	Unitless
FT	Algal growth temperature limit factor	Unitless
Benthic algae		
A_b growth	Benthic algae growth	mg-D/L/d
A_b respiration	Benthic algae respiration	mg-D/L/d
A_b mortality	Benthic algae mortality	mg-D/L/d
FL_b	Benthic algae growth light limit factor	Unitless
FN_b	Benthic algae growth N limit factor	Unitless
FP_b	Benthic algae growth P limit factor	Unitless
FT_b	Benthic algal growth temperature limit factor	Unitless
FS_b	Benthic algae growth space limit factor	Unitless
Nitrogen cycle		
A_p-->RPON	Algal mortality into RPON	mg-N/L/d
RPON-->DON	RPON hydrolysis	mg-N/L/d
RPON-->Bed	RPON settling	mg-N/L/d
A_p-->LPON	Algal mortality into LPON	mg-N/L/d
LPON-->DON	LPON hydrolysis	mg-N/L/d
LPON-->Bed	LPON settling	mg-N/L/d
A_p-->DON	Algal mortality into DON	mg-N/L/d
DON-->NH4	DON mineraliztion	mg-N/L/d
A_p-->NH4	Algal respiration into NH4	mg-N/L/d
NH4-->A_p	Algal uptake from NH4	mg-N/L/d
Bed<-->NH4	Sediment release of NH4	mg-N/L/d
NH4-->NO3	NH4 nitrification	mg-N/L/d

Name	Definition	Units
NO3 denitrification	NO3 denitrification	mg-N/L/d
NO3<-->Bed	Sediment denitrification	mg-N/L/d
NO3-->A_p	Algal uptake from NO3	mg-N/L/d
A_b-->RPON	Benthic algae mortality into RPON	mg-N/L/d
A_b-->LPON	Benthic algae mortality into LPON	mg-N/L/d
A_b-->DON	Benthic algae mortality into DON	mg-N/L/d
A_b-->NH4	Benthic algae respiration into NH4	mg-N/L/d
NH4-->A_b	Benthic algae uptake from NH4	mg-N/L/d
NO3-->A_b	Benthic algae uptake from NO3	mg-N/L/d
	Phosphorous cycle	
A_p-->RPOP	Algal mortality into RPOP	mg-P/L/d
RPOP-->DOP	RPOP hydrolysis	mg-P/L/d
RPOP-->Bed	RPOP settling	mg-P/L/d
A_p-->LPOP	Algal mortality into LPOP	mg-P/L/d
LPOP-->DOP	LPOP hydrolysis	mg-P/L/d
LPOP-->Bed	LPOP settling	mg-P/L/d
A_p-->DOP	Algal mortality into DOP	mg-P/L/d
DOP-->DIP	DOP mineraliztion	mg-P/L/d
A_p-->DIP	Algae respiration into DIP	mg-P/L/d
DIP-->A_p	Algal uptake from DIP	mg-P/L/d
TIP-->Bed	TIP settling	mg-P/L/d
Bed<-->DIP	Sediment release of DIP	mg-P/L/d
A_b-->RPOP	Benthic algae mortality into RPOP	mg-P/L/d
A_b-->LPOP	Benthic algae mortality into LPOP	mg-P/L/d
A_b-->DOP	Benthic algae mortality into DOP	mg-P/L/d
A_b-->DIP	Benthic algae respiration into DIP	mg-P/L/d
DIP-->A_b	Benthic algae uptake from DIP	mg-P/L/d
	Carbon cycle	
A_p-->RPOC	Algal mortality into RPOC	mg-C/L/d
RPOC-->LDOC	RPOC hydrolysis	mg-C/L/d
RPOC-->Bed	RPOC settling	mg-C/L/d
A_p-->LPOC	Algal mortality into LPOC	mg-C/L/d
LPOC-->LDOC	LPOC hydrolysis	mg-C/L/d
LPOC-->Bed	LPOC settling	mg-C/L/d
A_p-->RDOC	Algal mortality into RDOC	mg-C/L/d
A_p-->LDOC	Algal mortality into LDOC	mg-C/L/d

Name	Definition	Units
RDOC-->DIC	RDOC mineraliztion	mg-C/L/d
LDOC-->DIC	LDOC mineraliztion	mg-C/L/d
CBOD-->DIC	CBOD oxidation	mg-C/L/d
LDOC-->Denitrification	LDOC consumed by denitrification	mg-C/L/d
Atm<-->DIC	Atmospheric CO_2 reaeration	mol/L/d
A_p-->DIC	Algal respiration into DIC	mol/L/d
DIC-->A_p	Algal uptake from DIC	mol/L/d
Bed<-->DIC	Sediment release of DIC	mol/L/d
A_b-->RPOC	Benthic algae mortality into RPOC	mg-C/L/d
A_b-->LPOC	Benthic algae mortality into LPOC	mg-C/L/d
A_b-->RDOC	Benthic algae mortality into RDOC	mg-C/L/d
A_b-->LDOC	Benthic algae mortality into LDOC	mg-C/L/d
A_b-->DIC	Benthic algae respiration into DIC	mol/L/d
DIC-->A_b	Benthic algae uptake from DIC	mol/L/d
CBOD i		
CBOD i oxidation	CBOD oxidation	mg-O_2/L/d
CBOD i sedimentation	CBOD sedimentation	mg-O_2/L/d
Methane and sulfides		
CH4-->Atm	Atmospheric CH4 reaeration	mg-O_2/L/d
Bed<-->CH4	Sediment release of CH4	mg-O_2/L/d
CH4-->DIC	CH4 oxidation	mg-C/L/d
H_2S-->Atm	Atmospheric H_2S reaeration	mg-O_2/L/d
Bed<-->H_2S	Sediment release of H_2S	mg-O_2/L/d
Dissolved oxygen		
Atm<-->O_2	Atmospheric O_2 reaeration	mg-O_2/L/d
A_p--> O_2	O_2 produced by algal photosynthesis	mg-O_2/L/d
O_2-->A_p	O_2 consumed by algal respiration	mg-O_2/L/d
O_2-->RDOC	O_2 consumed by RDOC oxidation	mg-O_2/L/d
O_2-->LDOC	O_2 consumed by LDOC oxidation	mg-O_2/L/d
O_2-->CBOD	O_2 consumed by CBOD oxidation	mg-O_2/L/d
O_2-->CH4	O_2 consumed by CH4 oxidation	mg-O_2/L/d
O_2-->HS	O_2 consumed by H_2S oxidation	mg-O_2/L/d
O_2-->Nitrification	O_2 consumed by nitrification rate	mg-O_2/L/d
DO_s	O_2 saturation	mg-O_2/L
O_2-->Bed	Sediment oxygen demand	mg-O_2/L/d
A_b-->O_2	O_2 produced by benthic algae photosynthesis	mg-O_2/L/d

Name	Definition	Units
O_2-->A_b	O_2 consumed by benthic algae respiration	mg-O_2/L/d
Silica cycle		
A_p-->BSi	Algal mortality into BSi	mg-Si/L/d
BSi-->Bed	BSi settling	mg-Si/L/d
BSi-->DSi	BSi dissolution	mg-Si/L/d
A_p-->DSi	Algal mortality into DSi	mg-Si/L/d
A_p-->DSi	Algal respiration into DSi	mg-Si/L/d
DSi-->A_p	Algal uptake from DSi	mg-Si/L/d
Bed<-->DSi	Sediment release of DSi	mg-Si/L/d
Pathogen		
PX death	Pathogen death	cfu/100mL/d
PX decay	Pathogen decay by sunlight	cfu/100mL/d
PX settling	Pathogen settling	cfu/100mL/d
Alklinity		
A_p-->Alk	Alk increased by algae respiration	mg-C_aCO_3/L/d
Alk-->A_p	Alk decreased by algal growth	mg-C_aCO_3/L/d
Alk-->Nitrification	Alk decreased by nitrification	mg-C_aCO_3/L/d
Denitrification-->Alk	Alk increased by denitrification	mg-C_aCO_3/L/d
A_b-->Alk	Alk increased by benthic algae respiration	mg-C_aCO_3/L/d
Alk-->A_b	Alk decreased by benthic algae growth	mg-C_aCO_3/L/d

5 Benthic Sediment Diagenesis Module

5.1 Overview

Sediments process, store, and release carbon and nutrients. The benthic sediments are not just depositories for the material from the water column, but the flux of constituents from the sediments into the water column, and vice versa. Therefore, benthic sediments are an important part of controlling the composition of the water quality. Both NSMI and NSMII, as described in previous chapters, have the capability of specifying rather than predicting SOD and sediment nutrient releases. The use of a zero-order rate or constant source term in water quality modeling has a major limitation. The models do not provide for a mechanistic link between sediment organic matter and its conversion into oxygen demand and nutrient release (Martin and Wool 2012). An overview of the benthic sediment diagenesis processes is illustrated in Figure 17.

Figure 17. Diagram of the benthic sediment diagenesis processes.

The basis of sediment diagenesis models was laid out by Berner (1980) and further developed by authors such as by Di Toro and Fitzpatrick (1993). Di Toro (2001) provides a comprehensive analysis of dynamic sediment-water flux models. The sediment diagenesis model has been successfully integrated into several water quality models, including CE-QUAL-ICM (Cerco and Cole 1993, Cerco et al. 2004), QUAL2K (Chapra et al. 2008) and WASP (Martin and Wool 2012). To have a full sediment diagenesis model capability, a benthic sediment diagenesis module was coupled with NSMII's water column kinetics. This module was developed based on the algorithms and formulations presented by Di Toro (2001), it

is henceforth referred to as NSMII-SedFlux. NSMII-SedFlux is used to track the effects of organic matter decomposition and to dynamically compute the SOD and fluxes of key solutes (e.g., nitrogen, phosphorus, methane, sulfide, silica, oxygen) from the pore waters to the water column. Sediment-water fluxes computed in NSMII-SedFlux are supplied to appropriate water quality mass-balance equations.

The basic framework of the NSMII-SedFlux used here consists of two well-mixed sediment layers: a thin upper layer (layer 1) and a thicker active layer on the order of 10 cm (layer 2). The upper layer (layer 1), in contact with the water column, may be oxic or anoxic depending on the DO concentration. The lower layer (layer 2) is always anoxic. The upper layer depth is at its maximum when only a small fraction of the active sediment thickness (~ 0.1 cm) is present. The NSMII-SedFlux models four basic processes: (1) algae and particulate organic matter (POC, PON, POP) delivery to benthic sediments from the water column; (2) diagenesis of the sediment particulate organic matter in the second layer that produces dissolved chemicals; (3) production, diffusion, and burial of sediment dissolved chemicals; and (4) sediment–water exchanges of dissolved chemicals. Figure 18 provides an overview of the model representation of state variables and the major processes modeled in NSMII-SedFlux. Sediment diagenesis (mineralization) reactions only occur in the second layer.

The heterogeneous nature of the sediment organic matter is recognized and typically accommodated by adopting a multi-G approach. The basis of the multi-G assumption came from laboratory experiments that showed organic matter decay could be approximated as a function of different pools (Berner 1980). Three "G classes," labile, refractory, and inert, are included. Labile, refractory, and inert distinctions are based upon the timescales of oxidation or decomposition. The G1 class has a half-life of 20 days. The G2 class has a half-life of one year. The G3 class undergoes no significant decay before burial into deep, inactive sediments (Di Toro 2001).

The sediment diagenesis module focuses on four components of organic matter: carbon, nitrogen, phosphorous, and silica. This results in an additional 27 sediment diagenesis state variables. Table 32 lists the sediment diagenesis state variables and their associated symbols. Each one is associated with the benthic sediments. The units of these variables are depicted as grams per sediment layer volume basis, or mg L^{-1}. The silica state variables are included in the sediment diagenesis module only if the

water column silica is activated within the model. Methane, sulfate, and sulfide are tracked in units of oxygen equivalents (mg-O_2 L^{-1}) to easily balance the model's computations. The sediment diagenesis computational time step is set equal to the water quality model time step.

Figure 18. State variables and major processes modeled in NSMII-SedFlux.

Table 32. Sediment diagenesis state variables.

Variable	Layer	Definition	Units
$NH4_1$	1	Sediment ammonium	mg-N L^{-1}
$NO3_1$	1	Sediment nitrate	mg-N L^{-1}
$CH4_1$	1	Sediment methane	mg-O_2 L^{-1}
TH_2S_1	1	Sediment total hydrogen sulfide	mg-O_2 L^{-1}
$SO4_1$	1	Sediment sulfate	mg-O_2 L^{-1}
DIC_1	1	Sediment dissolved inorganic carbon	mg-C L^{-1}
TIP_1	1	Sediment total inorganic phosphorous	mg-P L^{-1}
DSi_1	1	Sediment dissolved silica	mg-Si L^{-1}
$NH4_2$	2	Sediment ammonium	mg-N L^{-1}
$NO3_2$	2	Sediment nitrate	mg-N L^{-1}
$CH4_2$	2	Sediment methane	mg-O_2 L^{-1}
TH_2S_2	2	Sediment total sulfide	mg-O_2 L^{-1}

Variable	Layer	Definition	Units
$SO4_2$	2	Sediment sulfate	mg-O_2 L^{-1}
DIC_2	2	Sediment dissolved inorganic carbon	mg-C L^{-1}
TIP_2	2	Sediment total inorganic phosphorous	mg-P L^{-1}
DSi_2	2	Sediment dissolved silica	mg-Si L^{-1}
$POC_{Gi,2}$	2	Sediment particulate organic carbon (G1 – G3)	mg-C L^{-1}
$PON_{Gi,2}$	2	Sediment particulate organic nitrogen (G1 – G3)	mg-N L^{-1}
$POP_{Gi,2}$	2	Sediment particulate organic phosphorous (G1 – G3)	mg-P L^{-1}
BSi_2	2	Sediment particulate biogenic silica	mg-Si L^{-1}
ST	2	Sediment benthic stress	d

The NSMII-SedFlux offers two options for the numerical solutions of mass balance equations of sediment diagenesis state variables: (1) steady-state and (2) unsteady-state. The first option does not require initial conditions for state variables. However, the initial conditions are required for the second option. The initial conditions are specified separately for the sediment segments, and differ from those for the water column. In NSMII-SedFlux, initial conditions are only required for sediment diagenesis state variables in layer 2. The steady-state solution is typically used as an initial condition for time-dependent, unsteady-state simulations. Some caution should be exercised using this approach, particularly for phosphorus. As indicated by Di Toro (2001), a steady-state model cannot be used to successfully predict the range of phosphorus fluxes from the sediments, particularly under anoxic water column conditions. As a result, the steady-state option for computing initial conditions of diagenesis segments should not be used where the initial DO concentrations in the overlying water column are near zero.

In general, the quasi-dynamic approach is used to refine the initial conditions and the model is run for a period of a year or more with reasonably repeating water column conditions. The predicted concentrations in sediment diagenesis segments at the end of that period are used to refine and replace the specified initial conditions. This process is repeated until the resulting predictions approach a quasi-steady state condition (Di Toro 2001).

5.2   Water Column Depositional Fluxes

Sedimentation of solids and entrapment of water in the pore spaces are two major fluxes of materials across the sediment-water interface. As

organic matter settle to the bottom, they are converted to organic sediment. Settling phytoplankton are assumed to contribute to sediment organic matter. Due to the negligible thickness of the first layer, deposition of particulates from the water column is directly delivered to the anaerobic sediments. Once deposition in the sediments occurs, water column state variables are required to convert into the benthic sediment's state variables that are listed in Table 32. If the benthic algae are included in NSMII, the effect of benthic algae mortality is taken into account in computing sediment diagenesis flux. Three classes of organic sediment are modeled in NSMII-SedFlux: labile (G1), refractory (G2), and inert (G3). Labile particulates from the water column are transferred directly into the sediment G1 class. Refractory particulates from the water column need to be split among G1, G2 and G3 classes upon entering the sediments based upon user-supplied fractions. The depositional fluxes of algae are first converted into PON, POP, and POC based on stoichiometric ratios and then split into three organic sediment G classes.

In NSMII-SedFlux, the depositional fluxes of organic matter are computed using the water column concentrations and specified settling rates and given below.

Sediment Particulate Organic Carbon (POC):

$$J_{POC,G1} = \sum_{i}^{3} F_{AP1} v_{sai} r_{cai} A_{pi} + v_{sl} LPOC + F_{RPOC1} v_{sr} RPOC + \left(1 - F_w\right) F_{AB1} r_{cb} A_b , \quad (5.1a)$$

$$J_{POC,G2} = \sum_{i}^{3} F_{AP2} v_{sai} r_{cai} A_{pi} + F_{RPOC2} v_{sr} RPOC + \left(1 - F_w\right) F_{AB2} r_{cb} A_b , \quad (5.1b)$$

$$J_{POC,G3} = \sum_{i}^{3} \left(1 - F_{AP1} - F_{AP2}\right) v_{sai} r_{cai} A_{pi} + \left(1 - F_{RPOC1} - F_{RPOC2}\right) v_{sr} RPOC \\ + \left(1 - F_w\right)\left(1 - F_{AB1} - F_{AB2}\right) r_{cb} A_b \quad , \quad (5.1c)$$

where

F_{AP1} = fraction of algae deposit to sediment G1 (0–1.0),
F_{AP2} = fraction of algae deposit to sediment G2 (0–1.0),
F_{AB1} = fraction of dead benthic algae to sediment G1 (0–1.0),
F_{AB2} = fraction of dead benthic algae to sediment G2 (0–1.0),
$J_{POC,G1}$ = total deposition to sediment POC G1 (g-C m^{-2} d^{-1}),

$J_{POC,G2}$ = total deposition to sediment POC G2 (g-C m^{-2} d^{-1}),
F_{RPOC1} = fraction of RPOC deposit to sediment POC G1 (0–1.0),
F_{RPOC2} = fraction of RPOC deposit to sediment POC G2 (0–1.0),
$J_{POC,G3}$ = total deposition to sediment POC G3 (g-C m^{-2} d^{-1}).

Sediment Particulate Organic Nitrogen (PON):

$$J_{PON,G1} = \sum_i^3 F_{AP1} v_{sai} r_{nai} A_{pi} + v_{sl} LPON + F_{RPON1} v_{sr} RPON + (1 - F_w) F_{AB1} r_{nb} A_b, \quad (5.2a)$$

$$J_{PON,G2} = \sum_i^3 F_{AP2} v_{sai} r_{nai} A_{pi} + F_{RPON2} v_{sr} RPON + (1 - F_w) F_{AB2} r_{nb} A_b, \quad (5.2b)$$

$$J_{PON,G3} = \sum_i^3 (1 - F_{AP1} - F_{AP2}) v_{sai} r_{nai} A_{pi} + (1 - F_{RPON1} - F_{RPON2}) v_{sr} RPON \\ + (1 - F_w)(1 - F_{AB1} - F_{AB2}) r_{nb} A_b \quad (5.2c)$$

where

$J_{PON,G1}$ = total deposition to sediment PON G1 (g-N m^{-2} d^{-1}),
$J_{PON,G2}$ = total deposition to sediment PON G2 (g-N m^{-2} d^{-1}),
F_{RPON1} = fraction of RPON deposit to sediment PON G1 (0–1.0),
F_{RPON2} = fraction of RPON deposit to sediment PON G2 (0–1.0),
$J_{PON,G3}$ = total deposition to sediment PON G3 (g-N m^{-2} d^{-1}).

Sediment Particulate Organic Phosphorus (POP):

$$J_{POP,G1} = \sum_i^3 F_{AP1} v_{sai} r_{pai} A_{pi} + v_{sl} LPOP + F_{RPOP1} v_{sr} RPOP + (1 - F_w) F_{AB1} r_{pb} A_b, \quad (5.3a)$$

$$J_{POP,G2} = \sum_i^3 F_{AP2} v_{sai} r_{pai} A_{pi} + F_{RPOP2} v_{sr} RPOP + (1 - F_w) F_{AB2} r_{pb} A_b, \quad (5.3b)$$

$$J_{POP,G3} = \sum_i^3 (1 - F_{AP1} - F_{AP2}) v_{sai} r_{pai} A_{pi} + (1 - F_{RPOP1} - F_{RPOP2}) v_{sr} RPOP \\ + (1 - F_w)(1 - F_{AB1} - F_{AB2}) r_{pb} A_b \quad (5.3c)$$

where

$J_{POP,G1}$ = total depositional flux to sediment POP G1 (g-P m^{-2} d^{-1}),
$J_{POP,G2}$ = total depositional flux to sediment POP G2 (g-P m^{-2} d^{-1}),
F_{RPOP1} = fraction of RPOP deposit to sediment POP G1 (0–1.0),
F_{RPOP2} = fraction of RPOP deposit to sediment POP G2 (0–1.0),
$J_{POP,G3}$ = total organic P deposit to sediment POP G3 (g-P m^{-2} d^{-1}).

Sediment Particulate Biogenic Silica (BSi):

$$J_{BSi} = \sum_{i}^{3} v_{sai} r_{siai} A_{pi} + v_{bsi} BSi,$$ (5.4)

where

J_{BSi} = total deposition to sediment BSi (g-Si m^{-2} d^{-1}).

5.3 Sediment Organic Matter

Once algae and particulate organic matter deposited on the bottom, sediment particulate organic matter is assumed to be located exclusively in the second layer of sediment. The sediment diagenesis is simulated by partitioning deposited organic matter into three reactivity classes. The diagenesis processes are assumed to follow first-order kinetics. The end products of diagenesis or decay of sediment organic matter include ammonium, methane, sulfide, inorganic phosphorus, and silica. These constituents can undergo additional biological, chemical, and physical processing and reactions in sediments. Burial of sediment organic matter is included in the sediment diagenesis module. Although the sediment layer is assumed not to move vertically, its position relative to the sediment–water interface changes as additional material is deposited on the bed. Thus, deposition of solids from the water column results in older sediments moving further from the sediment-water interface. For all state variables, burial is solved as a function of the user input burial rate. Magnitude of the burial rate is influenced by the depositional flux of solids from the water column. In NSMII-SedFlux, the mass balance equations are solved for each form of particulate organic matter (N, P and C) and for each G class (1-3) are analogous.

5.3.1 Sediment particulate organic carbon

Sediment POC is a component of the particulate organic matter that settles from the water column into the second layer. Three state variables are used to represent three reactivity classes (G1 to G3). The mass balance equation of each G class (i) of the sediment POC diagenesis can be written as

$$h_2 \frac{dPOC_{Gi,2}}{dt} = J_{POC,Gi} \qquad \text{Organic carbon settling to sediment POC,} \qquad (5.5)$$

$$-h_2 K_{POC,Gi}(T) \cdot POC_{Gi,2} \qquad \text{Sediment POC diagenesis } (POC_2 \text{-->} CH4_2),$$

$$-w_2 POC_{Gi,2} \qquad \text{Sediment POC burial,}$$

where

h_2 = sediment layer thickness (m),
$POC_{Gi,2}$ = sediment POC (G1 to G3) (mg-C L^{-1}), (i = 1 to 3),
$K_{POC,Gi}(T)$ = sediment POC (G1 to G3) diagenesis rate (d^{-1}),
w_2 = sediment burial rate (m d^{-1}).

As there is no decay or byproduct, $K_{POC,G3}(T)$ is set as zero. Equation 5.5 is solved using an implicit integration scheme for sediment POC (G1 to G3) at the present time step $(t + \Delta t)$.

$$\frac{POC_{Gi,2}^{t+\Delta t} - POC_{Gi,2}^{t}}{\Delta t} = \frac{J_{POC,Gi}^{t}}{h_2} - K_{POC,Gi}(T) POC_{Gi,2}^{t+\Delta t} - \frac{w_2}{h_2} POC_{Gi,2}^{t+\Delta t}, \qquad (5.6)$$

Steady-state solution:

$$POC_{Gi,2}^{t+\Delta t} = \frac{\dfrac{J_{POC,Gi}^{t}}{h_2}}{K_{POC,Gi}(T) + \dfrac{w_2}{h_2}}, \qquad (5.7)$$

Unsteady-state solution:

$$POC_{Gi,2}^{t+\Delta t} = \frac{\dfrac{J_{POC,Gi}^{t}}{h_2}\Delta t + POC_{Gi,2}^{t}}{1 + K_{POC,Gi}(T)\Delta t + \dfrac{w_2}{h_2}\Delta t}, \tag{5.8}$$

Once the concentrations of sediment particulate organic carbon are known, as described above, sediment diagenesis fluxes for carbon reactions and transfers at the present time step $(t + \Delta t)$ are computed below:

$$J_{C,G1}^{t+\Delta t} = K_{POC,G1}(T)h_2 POC_{G1,2}^{t+\Delta t}, \tag{5.9a}$$

$$J_{C,G2}^{t+\Delta t} = K_{POC,G2}(T)h_2 POC_{G2,2}^{t+\Delta t}, \tag{5.9b}$$

$$J_C^{t+\Delta t} = J_{C,G1}^{t+\Delta t} + J_{C,G2}^{t+\Delta t}, \tag{5.9c}$$

where

$J_{C,G1}$ = sediment POC G1 diagenesis flux (g-C m^{-2} d^{-1}),
$J_{C,G2}$ = sediment POC G2 diagenesis flux (g-C m^{-2} d^{-1}),
J_C = sediment POC diagenesis flux (g-C m^{-2} d^{-1}).

5.3.2 Sediment particulate organic nitrogen

The mass balance equation of each G class (i) of the sediment PON diagenesis is developed in a similar manner to POC for computing the diagenesis flux of nitrogen, J_N.

$$h_2 \frac{dPON_{Gi,2}}{dt} = J_{PON,Gi} \qquad \text{Organic N settling to sediment PON,} \tag{5.10}$$

$$-h_2 K_{PON,Gi}(T)\cdot PON_{Gi,2} \qquad \text{Sediment PON diagenesis (PON}_2\text{-->NH4}_2),$$

$$-w_2 PON_{Gi,2} \qquad \text{Sediment PON burial,}$$

where

$PON_{Gi,2}$ = sediment PON (G1 to G3) (g-N m^{-3}),
$K_{PON,Gi}(T)$ = sediment PON (G1 to G3) diagenesis rate (d^{-1}).

Equation 5.10 is solved algebraically for three G-class sediment PON at the present time step $(t + \Delta t)$ as follows

Steady-state solution:

$$PON_{Gi,2}^{t+\Delta t} = \frac{\dfrac{J_{PON,Gi}^{t}}{h_2}}{K_{PON,Gi}(T) + \dfrac{w_2}{h_2}}, \tag{5.11}$$

Unsteady-state solution:

$$PON_{Gi,2}^{t+\Delta t} = \frac{\dfrac{J_{PON,Gi}^{t}}{h_2}\Delta t + PON_{Gi,2}^{t}}{1 + K_{PON,Gi}(T)\Delta t + \dfrac{w_2}{h_2}\Delta t}, \tag{5.12}$$

Total sediment diagenesis fluxes for nitrogen reactions and transfers at the present time step $(t + \Delta t)$ are computed below

$$J_{N,G1}^{t+\Delta t} = K_{PON,G1}(T)h_2 PON_{G1,2}^{t+\Delta t}, \tag{5.13a}$$

$$J_{N,G2}^{t+\Delta t} = K_{PON,G2}(T)h_2 PON_{G2,2}^{t+\Delta t}, \tag{5.13b}$$

$$J_N^{t+\Delta t} = J_{N,G1}^{t+\Delta t} + J_{N,G2}^{t+\Delta t}, \tag{5.13c}$$

where

$J_{N,G1}$ = sediment PON G1 diagenesis flux (g-N m^{-2} d^{-1}),
$J_{N,G2}$ = sediment PON G2 diagenesis flux (g-N m^{-2} d^{-1}),
J_N = sediment PON diagenesis flux (g-N m^{-2} d^{-1}).

5.3.3 Sediment particulate organic phosphorus

The mass balance equation of each G class (i) of the sediment POP diagenesis is developed in a similar manner to POC and PON for computing the diagenesis flux of phosphorus, J_P.

$$h_2 \frac{dPOP_{Gi,2}}{dt} = J_{POP,Gi}$$ Organic P settling to sediment POP,   (5.14)

$$-h_2 K_{POP,Gi}(T) \cdot POP_{Gi,2}$$ Sediment POP diagenesis (POP$_2$-->DIP$_2$),

$$-w_2 POP_{Gi,2}$$ Sediment POP burial,

where

$POP_{Gi,2}$ = sediment POP (G1 to G3) (g-P m^{-3}),
$K_{POP,Gi}(T)$ = sediment POP (G1 to G3) diagenesis rate (d^{-1}).

Equation 5.14 is solved algebraically for three G-class sediment POP at the present time step $(t + \Delta t)$ as follows

Steady-state solution:

$$POP_{Gi,2}^{t+\Delta t} = \frac{\dfrac{J_{POP,Gi}^t}{h_2}}{K_{POP,Gi}(T) + \dfrac{w_2}{h_2}}, \tag{5.15}$$

Unsteady-state solution:

$$POP_{Gi,2}^{t+\Delta t} = \frac{\dfrac{J_{POP,Gi}^t}{h_2}\Delta t + POP_{Gi,2}^t}{1 + K_{POP,Gi}(T)\Delta t + \dfrac{w_2}{h_2}\Delta t}, \tag{5.16}$$

Total sediment diagenesis fluxes for phosphorus reactions and transfers at the present time step $(t + \Delta t)$ are computed below

$$J_{P,G1}^{t+\Delta t} = K_{POP,G1}(T) h_2 POP_{G1,2}^{t+\Delta t}, \tag{5.17a}$$

$$J_{P,G2}^{t+\Delta t} = K_{POP,G2}(T) h_2 POP_{G2,2}^{t+\Delta t}, \tag{5.17b}$$

$$J_P^{t+\Delta t} = J_{P,G1}^{t+\Delta t} + J_{P,G2}^{t+\Delta t}, \tag{5.17c}$$

where

$J_{P,G1}$ = sediment POP G1 diagenesis flux (g-P m^{-2} d^{-1}),
$J_{P,G2}$ = sediment POP G2 diagenesis flux (g-P m^{-2} d^{-1}),

J_P = sediment POP diagenesis flux (g-P m^{-2} d^{-1}).

5.3.4 Sediment particulate biogenic silica

Silica associated with diatoms and deposited from the water column is represented as particulate biogenic silica (BSi) and is modeled in layer 2. Sediment biogenic silica can then undergo either deep burial or dissolution to dissolved silica. Production of dissolved silica in sediments occurs via a different mechanism than the diagenesis used for carbon, nitrogen and phosphorous. It results from the dissolution of sediment particulate biogenic silica. The dissolution releases silica to the pore water (Hurd 1973, Di Toro 2001). The kinetics of biogenic silica dissolution is computed using Michaelis-Menton expression (Conley and Kilham 1989). The mass balance equation of the sediment BSi can be written as

$$h_2 \frac{dBSi_2}{dt} = J_{BSi}$$ Organic silica settling to sediment BSi, (5.18)

$$-h_2 k_{bsi2}(T) \frac{BSi_2}{K_{sSi} + BSi_2} \left(Si_s - f_{dsi2} Si_2\right)$$ Sediment BSi dissolution (BSi$_2$-->DSi$_2$),

$$-w_2 BSi_2$$ Sediment BSi burial,

where

$\quad BSi_2$ = sediment BSi (mg-Si L^{-1}),
$\quad K_{sSi}$ = half saturation Si constant for BSi dissolution (mg-Si L^{-1}),
$\quad k_{bsi2}(T)$ = sediment BSi dissolution rate (d^{-1}),
$\quad Si_s$ = Si saturation (mg-Si L^{-1}).

Equation 5.18 can be solved for the sediment BSi. Unsteady state solution at the present time step $(t + \Delta t)$ is derived from an explicit scheme due to a nonlinear relationship.

Steady-state solution:

$$BSi_2^{t+\Delta t} = \frac{-b + \sqrt{b^2 - 4 w_2 K_{sSi} J_{BSi}^t}}{2 w_2}, \quad b = J_{BSi}^t + w_2 K_{sSi} - h_2 k_{bsi2}(T)\left(Si_s - f_{dsi2} Si_2^t\right)$$

, (5.19)

Unsteady-state solution:

$$BSi_2^{t+\Delta t} = BSi_2^t + \frac{\Delta t}{h_2}\left[J_{BSi}^t - w_2 BSi_2^t - h_2 k_{bsi2}(T)\frac{BSi_2^t}{K_{sSi} + BSi_2^t}\left(Si_s - f_{dsi2}Si_2^t\right)\right], \quad (5.20)$$

Biogenic silica dissolution rate at the present time step $(t + \Delta t)$ is computed using the following equation

$$J_{Si}^{t+\Delta t} = h_2 k_{bsi2}(T)\frac{BSi_2^{t+\Delta t}}{K_{sSi} + BSi_2^{t+\Delta t}}\left(Si_{sat} - f_{dsi2}Si_2^t\right), \quad (5.21)$$

where

J_{Si} = sediment BSi dissolution rate (g-Si m^{-2} d^{-1}).

5.4 Sediment Reaction Constants and Coefficients

Sediment inorganic state variables in the two layers are subject to a number of reactions and mass transfer. This section describes the sediment reaction processes and their rates internally computed in NSMII-SedFlux. These constants are necessary for solving the mass balances of sediment inorganic state variables.

5.4.1 Temperature dependent coefficients

Most of sediment diagenesis reaction rates are temperature dependent and must be corrected according to the temperature correction function described earlier in Chapter 2. The following coefficients must be corrected with a modified temperature correction equation

$$v_{nh4,1}(T) = v_{nh4,1}(20)\theta^{\frac{T-20}{2}}, \quad (5.22a)$$

$$v_{no3,1}(T) = v_{no3,1}(20)\theta^{\frac{T-20}{2}}, \quad (5.22b)$$

$$v_{ch4,1}(T) = v_{ch4,1}(20)\theta^{\frac{T-20}{2}}, \quad (5.22c)$$

$$v_{h2s,d}(T) = v_{h2s,d}(20)\theta^{\frac{T-20}{2}}, \quad (5.22d)$$

$$V_{h2s,p}(T) = V_{h2s,p}(20)\theta^{\frac{T-20}{2}}, \qquad (5.22e)$$

where

$v_{nh4,1}(T)$ = sediment layer 1 nitrification transfer velocity at local temperature (m d^{-1}),

$v_{nh4,1}(20)$ = sediment layer 1 nitrification transfer velocity at 20°C (m d^{-1}),

$v_{no3,1}(T)$ = sediment layer 1 denitrification transfer velocity at local temperature (m d^{-1}),

$v_{no3,1}(20)$ = sediment layer 1 denitrification transfer velocity at 20°C (m d^{-1}),

$v_{nh4,1}(T)$ = sediment layer 1 CH4 oxidation transfer velocity at local temperature (m d^{-1}),

$v_{nh4,1}(20)$ = sediment layer 1 CH4 oxidation transfer velocity at 20°C (m d^{-1}),

$v_{h2s,d}(T)$ = sediment layer 1 H$_2$S dissolved oxidation transfer velocity at local temperature (m d^{-1}),

$v_{h2s,p}(T)$ = sediment layer 1 H$_2$S particulate oxidation transfer velocity at local temperature (m d^{-1}),

$v_{h2s,d}(20)$ = sediment layer 1 H$_2$S dissolved oxidation transfer velocity at 20°C (m d^{-1}),

$v_{h2s,p}(20)$ = sediment layer 1 H$_2$S particulate oxidation transfer velocity 1 at 20°C (m d^{-1}).

5.4.2 Sediment equilibrium partitioning fractions

Dissolved constituents, including ammonium, sulfide, inorganic phosphorous, and silica, can sorb to the sediment particles. A linear equilibrium partitioning is assumed at all times between dissolved and adsorbed phases in the two layers. The dissolved (f_d), and particulate (f_p), fractions are computed using the partition coefficients and the concentration of sediment solids in each layer

$$f_{di} = \frac{1}{1 + C_{ssi}k_{di}} = 1 - f_{pi}, \qquad (5.23)$$

where

k_{di} = partition coefficient in sediment layer i (L^{-1} kg),

C_{ssi} = solids concentration in sediment layer i (kg L^{-1}).

5.4.3 Sediment half-saturation oxygen attenuation

Sediment DO is not included as a state variable in the sediment diagenesis module.DO is assumed to be zero in the anaerobic layer (layer 2). Using the overlying water DO concentration as a boundary, a linear decline of DO is assumed from water column the aerobic layer. Therefore, DO in aerobic layer is approximately half of DO in the water column. Oxygen attenuation factors for sediment nitrification and oxidation are computed using the half-saturation function

$$F_{Oxna1} = 0.5 \cdot DO / \left(K_{sOxna1} + 0.5 \cdot DO \right), \tag{5.24a}$$

$$F_{Oxch1} = 0.5 \cdot DO / \left(K_{sOxch} + 0.5 \cdot DO \right), \tag{5.24b}$$

where

K_{sOxna1} = half-saturation oxygen attenuation constant for sediment nitrification (mg-O_2 L^{-1}),

K_{sOxch} = half-saturation oxygen attenuation constant for CH_4 oxidation (mg-O_2 L^{-1}),

F_{Oxna1} = oxygen attenuation factor for sediment nitrification (0–1.0),

F_{Oxch1} = oxygen attenuation factor for sediment CH_4 oxidation (0–1.0).

5.4.4 Sediment-water transfer

The surface mass transfer velocity controls dissolved constituent exchange between the aerobic layer and the overlying water column. The sediment diagenesis module uses the same mass transfer coefficient for all sediment dissolved state variables since differences in the diffusion coefficients are subsumed in the kinetic parameters (Di Toro 2001). The mass transfer velocity between the overlying water and the aerobic layer is defined as

$$K_{L01} = \frac{SOD}{DO}, \tag{5.25}$$

where

K_{L01} = sediment-water mass transfer velocity (m d^{-1}).

5.4.5 Dissolved mass transfer between two layers

The dissolved and particulate phase mixing coefficients between the two layers determine the rate at which chemicals stored in the anaerobic layer are transferred to the aerobic layer and potentially to the overlaying water column. Dissolved phase mixing between layers 1 and 2 is via molecular diffusion, which is enhanced by the mixing activities of the benthic organisms. Benthic organisms cause bio-irrigation and the dispersion of dissolved substances. The overall mass transfer coefficient includes the effects of flow, bio-irrigation, and molecular diffusion. The dissolved mass transfer velocity is estimated through specifying a sediment pore-water diffusion coefficient

$$K_{L12} = \frac{D_d(T)}{0.5h_2},$$
(5.26)

where

K_{L12} = dissolved mass transfer velocity between layers 1 and 2 (m d^{-1}),
$D_d(T)$ = sediment pore-water diffusion coefficient (m d^{-1}).

K_{L12} is used to compute sediment diffusion of NH4, NO3, CH4, H$_2$S, DIC, DIP, and DSi between layers 1 and 2.

5.4.6 Particle mixing transfer between two layers

Particle mixing transfer velocity is used to compute transfer of particulate ammonium, sulfide, phosphorous, and silica between layers 1 and 2. Sediment particle phase mixing is controlled by temperature, carbon input, and oxygen. The particle phase mixing transfer velocity is computed using the apparent particle diffusion coefficient and sediment organic carbon

$$\omega_{12} = \frac{D_p(T)}{0.5h_2} \frac{POC_{G1,2}}{\left(10^3 C_{ss2} POC_r\right)},$$
(5.27)

where

ω_{12} = sediment particle phase mixing transfer velocity due to bioturbation (m d^{-1}),
POC_r = reference POC_{G1} for sediment particle phase mixing (mg-C g^{-1}).

The above formulation assumes that particle mixing is correlated with the amount of labile carbon (e.g., $POC_{G1,2}$) present in the sediment. However, if excess carbon loading creates unfavorable oxygen conditions, the model accumulates a benthic stress (equation 5.28). After the stress has passed, the minimum is carried forward for the rest of the year to simulate the observation that benthic communities do not recover until the following year (Diaz and Rosenberg 1995). Therefore, particle mixing transfer velocity is corrected by modeled benthic stress.

Note that the same formulations for computing K_{L12} and ω_{12} are used in QUAL2K and WASP. However, h_2 is used in original sediment diagenesis models, rather than 0.5h.

5.4.7 Sediment benthic stress

One additional impact, if anoxia occurs for periods of time, the benthic population will be ultimately reduced or eliminated, so that bioturbation is consequently reduced or eliminated. To include this effect, the benthic stress that low DO conditions impose on the population is simulated using a benthic stress defined by Di Toro (2001).

$$\frac{\partial ST}{\partial t} = -k_{st}ST + \frac{K_{sDp}}{K_{sDp} + DO},\tag{5.28}$$

where

$$
\begin{aligned}
ST &= \text{sediment benthic stress (d),}\\
k_{st} &= \text{decay rate for benthic stress (d}^{-1}\text{),}\\
K_{sDp} &= \text{half-saturation oxygen constant for sediment particle mixing}\\
&\quad \text{(mg-O}_2\text{ L}^{-1}\text{).}
\end{aligned}
$$

Equation 5.28 can be solved for the sediment benthic stress

$$ST^{t+\Delta t} = \frac{ST^t + \left(\dfrac{K_{sDp}}{K_{sDp} + DO}\right)\Delta t}{1 + k_{st}\Delta t},\tag{5.29}$$

Particle phase mixing coefficient given in equation 5.27 is modified to

$$\omega_{12} = \omega_{12}\left(1 - k_{st}ST^{t+\Delta t}\right). \tag{5.30}$$

5.4.8 Sediment sulfate penetration

Sulfate reduction removes sulfate and ultimately produces sulfide in the anaerobic layer. Sulfate is also produced in the aerobic layer because of sulfide oxidation. Sulfate reduction and sulfide production are competing processes, and the preference of pathway is dependent solely on the concentration of sulfate causing inhibition. The sediment sulfate concentration decreases with sulfide formation and increases with sulfide consumption. Because sulfate in the anaerobic layer may become limiting to sulfate reduction in low-salinity sediments, the thickness of sulfate penetration is often less than the active sediment layer thickness; therefore, K_{L12} is scaled to sulfate penetration thickness to yield a sulfate specific mass-transfer coefficient, $K_{L12,SO4}$.

Sediment sulfate specific mass-transfer velocity, $K_{L12,SO4}$ and thickness of sulfate penetration, h_{so4}, are given by Di Toro (2001)

$$KL_{12\,SO4} = \frac{D_d(T)}{0.5h_{so4}}, \tag{5.31a}$$

$$h_{so4} = \sqrt{\frac{2D_d(T)\cdot SO4_2 \cdot h_2}{J_{Cc}}}, \tag{5.31b}$$

where

$K_{L12,SO4}$ = sediment sulfate specific mass-transfer velocity (m d^{-1}),
h_{so4} = thickness of sediment sulfate penetration (m),
J_{Cc} = total sediment POC diagenesis flux corrected for denitrification (g-O$_2$ m^{-2} d^{-1}).

5.5 Sediment Inorganic Constituents

The sediment inorganic constituent state variables include ammonium, nitrate, inorganic phosphorus, dissolved silica, methane, sulfide, and hydrogen sulfide. This section describes mass-balance equations of these state variables and their numerical solutions. Each state variable is modeled for two layers: an aerobic layer and an anaerobic layer. The NSMII-SedFlux models biogeochemical reactions, burial, diffusion of

dissolved material between the aerobic sediments and overlying water column and between sediment layers, and the mixing of particulate material between layers. Burial from layer 1 is added to layer 2, whereas burial from layer 2 is considered deep burial out of the modeled system.

Two solutions for each state variable are included in NSMII-SedFlux. One is solved based on steady state conditions. The other is solved based on the unsteady-state conditions. Because the aerobic layer is thinner when compared to the anaerobic layer, it is always assumed that the aerobic layer is under a steady-state when compared to the slower processes that are occurring within the anaerobic layer. The finite difference equations are solved using the same matrix solution provided in this chapter.

5.5.1 Sediment ammonium

Sediment ammonium (NH4) is produced by decomposition of the reactive G1 and G2 classes of PON (PONG1 and PONG2) in layer 2. NH4 may be transferred to layer 1 through porewater diffusion. While in the aerobic layer, NH4 is converted to nitrate via nitrification. The nitrification rate is computed according to Michaelis-Menten kinetics with respect to NH4 and DO. The nitrification rate decreases as the NH4 concentration increases. Similarly, the nitrification reaction decreases with the decreasing DO. Sediment-water transfer of NH4 depends on the concentration gradient between aerobic layer and overlying water. Sediment NH4 may undergo burial due to sedimentation. Sorption of NH4 on sediments is modeled. At equilibrium, the distribution of NH4 between sediments and pore water can be described by the equilibrium partitioning isotherm. So sediment total ammonium (TNH4) is used as a single state variable. The mass balance equations of TNH4 in layers 1 and 2 can be written as

$$h_1 \frac{dTNH4_1}{dt} = -w_2 TNH4_1$$

NH$_4$ burial from layer 1, (5.32a)

$$-F_{Oxna1} \frac{K_{sNH4}}{K_{sNH4} + f_{dn1}TNH4_1} \frac{v_{nh4,1}(T)^2}{K_{L01}} f_{dn1}TNH4_1$$

NH$_4$ nitrification in layer 1 (NH4$_1$-->NO3$_1$),

$$+\omega_{12}\left(f_{pn2}TNH4_2 - f_{pn1}TNH4_1\right)$$

NH$_4$ particulate transfer between layers 1 and 2 (PNH4$_2$<-->PNH4$_1$),

$$+K_{L12}\left(f_{dn2}TNH4_2 - f_{dn1}TNH4_1\right)$$

NH$_4$ dissolved transfer between layers 1 and 2 (NH4$_2$<-->NH4$_1$),

$$-K_{L01}\left(f_{dn1}TNH4_1 - NH4\right)$$

NH4 sediment-water transfer (NH4$_1$<-->NH4),

$$h_2\frac{dTNH4_2}{dt} = J_N$$

Total PON diagenesis flux in layer 2   (5.32b)

$$+\,w_2 TNH4_1$$

NH$_4$ burial from layer 1,

$$-\,w_2 TNH4_2$$

NH$_4$ burial from layer 2,

$$-\,\omega_{12}\left(f_{pn2}TNH4_2 - f_{pn1}TNH4_1\right)$$

NH4 particulate transfer between layers 1 and 2 (PNH4$_2$<-->PNH4$_1$),

$$-\,K_{L12}\left(f_{dn2}TNH4_2 - f_{dn1}TNH4_1\right)$$

NH4 dissolved transfer between layers 1 and 2 (NH4$_2$<-->NH4$_1$),

where

$TNH4_i$ = total ammonium in sediment layer i (mg-N L^{-1}),

K_{sNh4} = half saturation NH$_4$ constant for sediment nitrification (mg-N L^{-1}),

f_{dni}, f_{pni} = dissolved and particulate fractions of NH$_4$ in sediment layer i.

Implicit finite difference forms of above mass balance equations of TNH4 are written as

$$a_{11}TNH4_1^{t+\Delta t} + a_{12}TNH4_2^{t+\Delta t} = b_1, \tag{5.33a}$$

$$a_{21}TNH4_1^{t+\Delta t} + a_{22}TNH4_2^{t+\Delta t} = b_2, \tag{5.33b}$$

Unsteady-state solution:

$$a_{11} = \omega_{12}f_{pn1} + K_{L12}f_{dn1} + w_2 + f_{dn1}F_{Oxna1}\frac{K_{sNH4}}{K_{sNH4} + f_{dn1}TNH4_1}\frac{v_{nh4,1}(T)^2}{K_{L01}} + K_{L01}f_{dn1}, \tag{5.34a}$$

$$a_{12} = -\omega_{12}f_{pn2} - K_{L12}f_{dn2}, \tag{5.34b}$$

$$b_1 = K_{L01}NH4^t, \tag{5.34c}$$

$$a_{21} = -\omega_{12}f_{pn1} - K_{L12}f_{dn1} - w_2, \tag{5.34d}$$

$$a_{22} = \left(\omega_{12} f_{pn2} + K_{L12} f_{dn2} + w_2 \right) + \frac{h_2}{\Delta t}, \tag{5.34e}$$

$$b_2 = J_N^{t+\Delta t} + \frac{h_2}{\Delta t} TNH4_2^t, \tag{5.34f}$$

Steady-state solution:

$$a_{22} = \omega_{12} f_{pn2} + K_{L12} f_{dn2} + w_2, \tag{5.35a}$$

$$b_2 = J_N^{t+\Delta t}, \tag{5.35b}$$

Initial sediment ammonium in sediment layers 1 and 2 need to be converted into total concentration for solving TNH4. Dissolved ammonium in each layer is computed as

$$NH4_i = f_{dni} TNH4_i, \tag{5.36a}$$

$$f_{dni} = \frac{1}{1 + C_{ssi} k_{dnh4i}} = 1 - f_{pni}, \tag{5.36b}$$

where

$NH4_i$ = ammonium in sediment layer i (mg-N L^{-1}) (i = 1, 2).

When oxygen is available, sediment ammonium may be nitrified and then denitrified to nitrogen gas. Nitrification reaction can be represented by

$$NH4^+ + 2O_2 \rightarrow 2H + H_2O + NO_3^-,$$

$2 \cdot 32/14 = 4.57$ g-O$_2$ are required for 1 g-N^{-1} oxidized. The sediment nitrification process consumes oxygen, which is defined as nitrogenous SOD (NSOD)

$$NSOD = F_{Oxna1} \frac{K_{sNH4}}{K_{sNH4} + f_{dn1} TNH4_1} \frac{v_{nh4,1}(T)^2}{K_{L01}} f_{dn1} r_{on} TNH4_1, \tag{5.37}$$

where

r_{on} = O$_2$: N ratio for nitrification (g-O$_2$ g-N^{-1}).

5.5.2 Sediment nitrate

The only source term for sediment nitrate is nitrification in the aerobic layer. Sediment nitrate (NO3) is produced by the nitrification of ammonium in the aerobic layer and can be reduced to gaseous nitrogen through denitrification in either layer. Sediment denitrification is simulated for both layers. The mass balance equations of NO3 in layers 1 and 2 can be written as

$$h_1 \frac{dNO3_1}{dt} = -\frac{v_{no3,1}(T)^2}{K_{L01}} NO3_1$$ NO3 denitrification in layer 1,   (5.38a)

$$F_{Oxna1} \frac{K_{sNH4}}{K_{sNH4} + f_{dn1}TNH4_1} \frac{v_{nh4,1}(T)^2}{K_{L01}} f_{dn1}TNH4_1$$ NH4 nitrification in layer 1 (NH4$_1$-->NO3$_1$),

$$+ K_{L12}(NO3_2 - NO3_1)$$ NO3 transfer between layers 1 and 2   (NO3$_2$<-->NO3$_1$),

$$- K_{L01}(NO3_1 - NO3)$$ NO3 sediment-water transfer (NO3<-->NO3$_1$),

$$h_2 \frac{dNO3_2}{dt} = -v_{no3,2}(T) \cdot NO3_2$$ NO3 denitrification in layer 2,   (5.38b)

$$- K_{L12}(NO3_2 - NO3_1)$$ NO3 transfer between layers 1 and 2 (NO3$_2$<-->NO3$_1$),

where

$NO3_i$ = nitrate in sediment layer i (mg-N L^{-1}).

Implicit finite difference forms of the above mass balance equations of NO3 are written as

$$a_{11} NO3_1^{t+\Delta t} + a_{12} NO3_2^{t+\Delta t} = b_1,$$ (5.39a)

$$a_{21} NO3_1^{t+\Delta t} + a_{22} NO3_2^{t+\Delta t} = b_2,$$ (5.39b)

Unsteady-state solution:

$$a_{11} = K_{L12} + \frac{v_{no3,1}(T)^2}{K_{L01}} + K_{L01}, \tag{5.40a}$$

$$a_{12} = -K_{L12}, \tag{5.40b}$$

$$b_1 = F_{Oxna1} \frac{K_{sNH4}}{K_{sNH4} + f_{dn1} TNH4_1^t} \frac{v_{nh4,1}(T)^2}{K_{L01}} f_{dn1} TNH4_1^{t+\Delta t} + K_{L01} NO3^t, \tag{5.40c}$$

$$a_{21} = -K_{L12}, \tag{5.40d}$$

$$a_{22} = \left(K_{L12} + v_{no3,2}(T)\right) + \frac{h_2}{\Delta t}, \tag{5.40e}$$

$$b_2 = \frac{h_2}{\Delta t} NO3_2^t, \tag{5.40f}$$

Steady-state solution:

$$a_{22} = K_{L12} + v_{no3,2}(T), \tag{5.41a}$$

$$b_2 = 0, \tag{5.41b}$$

Movement of nitrate between water and sediments is strongly influenced by the concentration of nitrate in the water column. When nitrate is abundant in the water column, nitrate usually diffuses from overlying water into the sediments where it is denitrified to gaseous form. Sediment is a net sink for nitrate in the overlying water in this case. When nitrate is absent from the water column, small quantities of nitrate may diffuse from sediment interstitial water into the overlying water.

5.5.3 Sediment methane

Sediment carbon diagenesis in the anaerobic layer produces either hydrogen sulfide (H_2S) or methane ($CH4$) (Di Toro 2001). In fresh water sediments, the organic carbon decomposes to yield methane. In salt water, hydrogen sulfide is produced by the diagenesis through reduction of sulfate. The process of sulfate reduction is very important; sulfate is a major

constituent of salt water (28 mM). Sediment carbon diagenesis produces methane and hydrogen sulfide via the following reactions (Di Toro 2001).

$$2CH_2O \rightarrow CH4 + CO_2 \text{,}$$

$$2CH_2O + H_2SO_4 \rightarrow 2CO_2 + H_2S + 2H_2O \text{,}$$

where CH$_2$O is a simplified representation of sediment organic matter. One gram of organic matter would yield 0.5 g of methane or 0.5 g of hydrogen sulfide in the anaerobic sediments. However, some of the sediment organic carbon does not decompose. Sediment organic carbon is first used by denitrification (Di Toro 2001)

$$5CH_2O + 4H^+ + 4NO_3^- \rightarrow 5CO_2 + 2N_2 + 7H_2O \text{.}$$

The sediment carbon diagenesis flux consumed during denitrification, $J_{C,dn}$, is computed as

$$J_{C,dn}^{t+\Delta t} = r_{oc} \frac{5*12}{4*14}\left[\frac{v_{no3,1}(T)^2}{K_{L01}} NO3_1^{t+\Delta t} + v_{no3,2}(T)\, NO3_2^{t+\Delta t} \right]. \qquad (5.42)$$

Any remaining carbon is processed by sulfate reduction, after which methanogenesis occurs. Remaining sediment carbon flux become

$$J_{Cc}^{t+\Delta t} = r_{oc} J_C^{t+\Delta t} - J_{C,dn}^{t+\Delta t}. \qquad (5.43)$$

Methane dissolves and often increases rapidly in concentration until saturation in the sediments of fresh water bodies. The methane saturation is primarily a function of water pressure (depth) and water temperature although salinity will affect the saturation, too. Di Toro (2001) provides the following methane saturation equation

$$CH4_s = 100\left(1 + \frac{h}{10}\right)1.024^{20-T} \text{,} \qquad (5.44)$$

where

$CH4_s$ = methane saturation (mg-O$_2$ L^{-1}),
   h = overlying water depth (m).

After interstitial waters become saturated with respect to methane, methane may then be stored and removed as gas bubbles (Rudd and Taylor 1980). The loss of methane as bubbles is an important sink. Two options are included in NSMII-SedFlux for computing sediment methane and its oxygen demand: (1) numerical solutions and (2) analytical solutions. If the methane saturation is exceeded, the numerical solution is not appropriate because the CSOD becomes constant and hits a ceiling (Chapra 1997).

5.5.3.1 Numerical solution

The mass balance equations of sediment methane (CH4) in layers 1 and 2 can be written as

$$h_1 \frac{dCH4_1}{dt} = -F_{Oxch1} \frac{v_{ch4,1}(T)^2}{K_{L01}} CH4_1 \qquad \text{CH4 oxidation in layer 1 (CSOD}_{CH4}), \qquad (5.45a)$$

$$+ K_{L12}(CH4_2 - CH4_1) \qquad \text{CH4 transfer between layers 1 and 2} \\ (CH4_2 \text{<-->} CH4_1),$$

$$- K_{L01}(CH4_1 - CH4) \qquad \text{CH4 sediment-water transfer (}J_{CH4(d)}),$$

$$h_2 \frac{dCH4_2}{dt} = J_{C,CH4} \qquad \text{Total POC diagenesis into CH4 in layer 2,} \qquad (5.45b)$$

$$- K_{L12}(CH4_2 - CH4_1) \qquad \text{CH4 transfer between layers 1 and 2} \\ (CH4_2 \text{<-->} CH4_1),$$

where

    $CH4_i$ = methane in sediment layer i (mg-O_2 L^{-1}),
    $J_{C,CH4}$ = total sediment POC diagenesis flux into CH4 (g-O_2 m^{-2} d^{-1}).

Implicit finite difference forms of above mass balance equations of CH4 are written as

$$a_{11} CH4_1^{t+\Delta t} + a_{12} CH4_2^{t+\Delta t} = b_1, \qquad (5.46a)$$

$$a_{21} CH4_1^{t+\Delta t} + a_{22} CH4_2^{t+\Delta t} = b_2. \qquad (5.46b)$$

Unsteady-state solution:

$$a_{11} = K_{L12} + F_{Oxch1} \frac{v_{ch4,1}(T)^2}{K_{L01}} + K_{L01},$$ (5.47a)

$$a_{12} = -K_{L12},$$ (5.47b)

$$b_1 = K_{L01} CH4^t,$$ (5.47c)

$$a_{21} = -K_{L12},$$ (5.47d)

$$a_{22} = K_{L12} + \frac{h_2}{\Delta t},$$ (5.47e)

$$b_2 = J_{C,CH4}^{t+\Delta t} + \frac{h_2}{\Delta t} CH4_2^t,$$ (5.47f)

Steady-state solution:

$$a_{22} = K_{L12},$$ (5.48a)

$$b_2 = J_{C,CH4}^{t+\Delta t}.$$ (5.48b)

If the modeled concentration in layer 2 ($CH4_2$) exceeds the saturation, then the $CH4_2$ is set to saturation ($CH4_s$) and the concentration in layer 1 ($CH4_1$) is recomputed from equations 5.44a,b. It is assumed that super-saturation does not occur and that all methane produced in excess of the saturation is immediately transferred to gas bubbles. This means that all methane produced after the establishment of the saturation is lost to the atmosphere. The gas flux of methane is computed via a mass balance of sediment methane when $CH4_2 > CH4_s$.

$$J_{CH4(g)}^{t+\Delta t} = J_{C,CH4}^{t+\Delta t} - J_{CH4(d)}^{t+\Delta t} - CSOD_{CH4}^{t+\Delta t} - \frac{h_2}{\Delta t}\left(CH4_2^{t+\Delta t} - CH4_2^t\right),$$ (5.49)

If $CH4_2 < CH4_s$, then no gas forms and dissolved methane flux is equal to carbon diagenesis flux.

The dissolved methane produced by carbon diagenesis can either be oxidized by bacteria in the aerobic layer, which then exerts an oxygen

demand on the overlying water, or released as a flux to the water column. Methane consumes oxygen to produce CO_2. If the overlying water oxygen is low, the methane is not completely oxidized. Therefore, methane oxidation is computed according to Michaelis-Menten kinetics with regard to both methane and the oxidizing agent, whereas the oxidation with DO excludes the oxidation with sulfide (Di Toro 2001). The oxygen consumed by oxidation of methane is a part of SOD and expressed as

$$CSOD_{CH4} = F_{Oxch1} \frac{v_{ch4,1}(T)^2}{K_{L01}} CH4_1, \tag{5.50}$$

Where CSOD represents the ultimate amount of biodegradable organic matter oxidized by methane, excluding organic nitrogen.

5.5.3.2 Analytical solution

Di Toro (2001) provided an analytical solution that can be used to determine the SOD consumed by oxidation of methane and steady-state flux of dissolved methane. The oxygen consumed by oxidation of methane is computed as a function of the methane saturation in pore water

$$CSOD_{CH4} = CSOD_{max} \left[1 - \textbf{sech} \left(\frac{v_{ch4}(T)}{K_{L01}} \right) \right], \tag{5.51a}$$

$$CSOD_{max} = min \left(\sqrt{2 K_{L12} CH4_s J_{C,CH4}}, \ J_{C,CH4} \right), \tag{5.51b}$$

where

$CSOD_{max}$ = maximum SOD when all CH4 in layer 1 is oxidized (g-O_2 m^{-2} d^{-1}),
$CSOD_{CH4}$ = SOD generated by CH4 oxidation (g-O_2 m^{-2} d^{-1}).

In this approach, sediment carbon is mineralized to produce methane only. Sediment methane is only computed for layer 1, and its concentration is computed as

$$CH4_1 = \frac{K_{L01}}{v_{ch4}(T)} \sqrt{2 K_{L12} CH4_s J_{C,CH4}} \left[1 - \textbf{sech} \left(\frac{v_{ch4}(T)}{K_{L01}} \right) \right]. \tag{5.52}$$

If the overlying water oxygen is low, the methane that is not completely oxidized can escape the sediment into the overlying water either as aqueous flux or as gas flux. The dissolved methane flux, which contributes to the water column model, is computed using the analytical solution

$$J_{CH4(d)}^{t+\Delta t} = CSOD_{\max}^{t+\Delta t} - CSOD_{CH4}^{t+\Delta t}. \tag{5.53}$$

The loss of sediment methane as bubbles become

$$J_{CH4(g)}^{t+\Delta t} = J_{C,CH4}^{t+\Delta t} - J_{CH4(d)}^{t+\Delta t} - CSOD_{CH4}^{t+\Delta t}. \tag{5.54}$$

5.5.4 Sediment sulfate

Sulfate (SO4) reduction is an important diagenetic process occurring in high-salinity sediments and is the source of sulfide. The sulfide oxidation is a large portion of SOD (Howarth and Jorgensen 1984); and therefore, sediment sulfate is included in NSMII-SedFlux. Sulfate in the water column is not modeled and is computed via a linear regression with salinity. The mass balance equations of sediment SO4 in layers 1 and 2 can be written as

$$h_1 \frac{dSO4_1}{dt} = \tag{5.55a}$$

$$+ \frac{0.5DO}{K_{sH2S}} \frac{v_{h2s,d}^2(T)f_{dh1} + v_{h2s,p}^2(T)f_{ph1}}{K_{L01}} TH_2S_1 \quad \text{H}_2\text{S oxidation in layer 1,}$$

$$+ K_{L12,SO4}(SO4_2 - SO4_1) \qquad\qquad \text{SO4 transfer between layers 1 and 2}$$
$$\text{(SO4}_2\text{<-->SO4}_1\text{),}$$

$$+ K_{L01}(SO4 - SO4_1) \qquad\qquad \text{SO4 sediment-water transfer (SO4}_1\text{<-}$$
$$\text{-> SO4),}$$

$$h_2 \frac{dSO4_4}{dt} = -J_{C,H2S} \qquad\qquad \text{Total POC diagenesis into H}_2\text{S in layer 2,} \qquad (5.55b)$$

$$- K_{L12,SO4}(SO4_2 - SO4_1) \qquad\qquad \text{SO4 transfer between layers 1 and 2}$$
$$\text{(SO4}_2\text{<-->SO4}_1\text{),}$$

where

$SO4_i$ = sulfate in sediment layer i (mg-O_2 L^{-1}) (i = 1, 2),

$J_{C,H2S}$ = total sediment POC diagenesis flux into H_2S (g-O_2 m^{-2} d^{-1}),

$K_{L12,SO4}$ = sediment sulfate specific mass-transfer velocity (m d^{-1}).

Two options are included when calculating sediment total POC diagenesis flux that is reduced by sulfate into sulfide and methane: (1) sulfate penetration thickness and (2) sulfate half-saturation function. The optional use of sulfate as a factor is meant to reflect the possibility that a greater fraction of overall sediment POC diagenesis may be associated with sulfate reduction if sulfate concentrations are higher. If users want to eliminate any dependency of sediment diagenesis on sulfate, set the water column $SO4$ to zero in the model inputs. Using the first approach, the following equations are used to compute the sediment POC diagenesis flux reduced by sulfate

$$J_{C,H2S} = J_{Cc} \frac{h_{so4}}{h_2},$$ (5.56a)

$$J_{CH4} = J_{Cc} \left(1 - \frac{h_{so4}}{h_2} \right),$$ (5.56b)

For mixing zones, sediment POC diagenesis flux is more appropriately computed using this approach. The following half-saturation functions can be used to compute sediment POC diagenesis flux reduced by sulfate

$$J_{C,H2S} = J_{Cc} \frac{SO4_2}{SO4_2 + K_{sSO4}},$$ (5.57a)

$$J_{C,CH4} = J_{Cc} \left(1 - \frac{SO4_2}{SO4_2 + K_{sSO4}} \right),$$ (5.57b)

where

K_{sSO4} = sediment SO4 half-saturation constant (mg-O_2 L^{-1}).

This function has been used in saltwater sediments. Sediment POC diagenesis flux, $J_{C,H2S}$, results in dependencies that are nearly linear when sediment sulfate concentration is much less than K_{sSO4}. Conversely, $J_{C,H2S}$ does not vary with sulfate if sulfate concentration is much greater than K_{sSO4}.

Implicit finite difference forms of above mass balance equations of SO4 are written as

$$a_{11} SO4_1^{t+\Delta t} + a_{12} SO4_2^{t+\Delta t} = b_1 , \qquad (5.58a)$$

$$a_{21} SO4_1^{t+\Delta t} + a_{22} SO4_2^{t+\Delta t} = b_2 . \qquad (5.58b)$$

Unsteady-state solution:

$$a_{11} = -K_{L01} - K_{L12,SO4} , \qquad (5.59a)$$

$$a_{12} = K_{L12,SO4} , \qquad (5.59b)$$

$$b_1 = K_{L01} SO4^t + \frac{0.5\,DO}{K_{sH2S}} \frac{v_{h2s,d}^2(T)\,f_{dh1} + v_{h2s,p}^2(T)\,f_{ph1}}{K_{L01}} TH_2 S_1^t , \qquad (5.59c)$$

$$a_{21} = K_{L12,SO4} , \qquad (5.59d)$$

$$a_{22} = -K_{L12,SO4} + \frac{h_2}{\Delta t} , \qquad (5.59e)$$

$$b_2 = \frac{h_2}{\Delta t} SO4_2^t . \qquad (5.59f)$$

Steady-state solution:

$$a_{22} = -K_{L12,SO4} , \qquad (5.60a)$$

$$b_2 = 0 . \qquad (5.60b)$$

5.5.5 Sediment total hydrogen sulfide

Sulfate reduction produces hydrogen sulfide (H_2S) in the anaerobic layer. A portion of it reacts with the iron to form particulate iron sulfide (FeS) (Morse et al. 1987). The remainder diffuses into the aerobic layer where a portion is oxidized to sulfate, consuming oxygen in the process. In addition, particle mixing can move some of the particulate iron sulfide into the aerobic layer where it can be oxidized to form ferric oxyhydroxide (Fe_2O_3), again consuming oxygen from the water column. The oxidation of both dissolved and particulate hydrogen sulfides are modeled in the

sediment diagenesis module. If the overlying water oxygen is low, then the sulfide that is not completely oxidized in the aerobic layer can diffuse into the overlying water. Hydrogen sulfides in sediments may undergo burial due to the sedimentation. The mass balance equations of sediment total hydrogen sulfide (TH_2S) in layers 1 and 2 can be written as

$$h_1 \frac{dTH_2S_1}{dt} = -w_2TH_2S_1 \qquad \text{TH}_2\text{S burial from layer 1,} \qquad (5.61a)$$

$$-\frac{0.5DO}{K_{sH2S}} \frac{v_{h2s,d}^2(T)f_{dh1} + v_{h2s,p}^2(T)f_{ph1}}{K_{L01}}TH_2S_1 \qquad \text{H}_2\text{S oxidation in layer 1 (CSOD}_{\text{H2S}}\text{),}$$

$$+\omega_{12}\left(f_{ph2}TH_2S_2 - f_{ph1}TH_2S_1\right) \qquad \text{H}_2\text{S particulate transfer between layers 1 and 2 (PH}_2\text{S}_2\text{<-->PH}_2\text{S}_1\text{),}$$

$$+K_{L12,SO4}\left(f_{dh2}TH_2S_2 - f_{dh1}TH_2S_1\right) \qquad \text{H}_2\text{S dissolved transfer between layers 1 and 2 (H}_2\text{S}_2\text{<-->H}_2\text{S}_1\text{),}$$

$$-K_{L01}\left(f_{dh1}TH_2S_1 - H_2S\right) \qquad \text{H}_2\text{S sediment-water transfer (H}_2\text{S}_1\text{<-->H}_2\text{S),}$$

$$h_2 \frac{dTH_2S_2}{dt} = J_{C,H_2S} \qquad \text{Total POC diagenesis into H}_2\text{S in layer 2,} \qquad (5.61b)$$

$$-\omega_{12}\left(f_{ph2}TH_2S_2 - f_{ph1}TH_2S_1\right) \qquad \text{H}_2\text{S particulate transfer between layers 1 and 2 (PH}_2\text{S}_2\text{<-->PH}_2\text{S}_1\text{),}$$

$$-K_{L12,SO4}\left(f_{dh2}TH_2S_2 - f_{dh1}TH_2S_1\right) \qquad \text{H}_2\text{S dissolved transfer between layers 1 and 2 (H}_2\text{S}_2\text{<-->H}_2\text{S}_1\text{),}$$

$$+w_2TH_2S_1 \qquad \text{TH}_2\text{S burial from layer 1,}$$

$$-w_2TH_2S_2 \qquad \text{TH}_2\text{S burial from layer 2,}$$

where

TH_2S_i = total hydrogen sulfide in sediment layer i (mg-O_2 L^{-1}) (i = 1, 2),
K_{sH2S} = H$_2$S oxidation normalization constant (g-O_2 m^{-3}),
f_{dhi}, f_{phi} = dissolved and particulate fractions of H$_2$S in sediment layer i.

Implicit finite difference forms of the above mass balance equations of TH_2S are written as

$$a_{11} TH_2 S_1^{t+\Delta t} + a_{12} TH_2 S_2^{t+\Delta t} = b_1 \;, \tag{5.62a}$$

$$a_{21} TH_2 S_1^{t+\Delta t} + a_{22} TH_2 S_2^{t+\Delta t} = b_2 \;, \tag{5.62b}$$

Unsteady-state solution:

$$a_{11} = \omega_{12} f_{ph1} + K_{L12,SO4} f_{dh1} + w_2 + v_m f_{dh1} + \frac{0.5\, DO}{K_{sH_2 S}} \frac{v_{h2s,d}^2 (T)\, f_{dh1} + v_{h2s,p}^2 (T)\, f_{ph1}}{K_{L01}} , \tag{5.63a}$$

$$a_{12} = -\omega_{12} f_{ph2} - K_{L12,SO4} f_{dh2} \;, \tag{5.63b}$$

$$b_1 = K_{L01} TH_2 S^t \;, \tag{5.63c}$$

$$a_{21} = -\omega_{12} f_{ph1} - K_{L12} f_{dh1} - w_2 , \tag{5.63d}$$

$$a_{22} = \left(\omega_{12} f_{ph2} + K_{L12,SO4} f_{dh2} + w_2 \right) + \frac{h_2}{\Delta t} , \tag{5.63e}$$

$$b_2 = J_{C,H_2 S}^{t+\Delta t} + \frac{h_2}{\Delta t} TH_2 S_2^t . \tag{5.63f}$$

Steady-state solution:

$$a_{22} = \omega_{12} f_{ph2} + K_{L12,SO4} f_{dh2} + w_2 , \tag{5.64a}$$

$$b_2 = J_{C,H_2 S}^{t+\Delta t} . \tag{5.64b}$$

Dissolved hydrogen sulfide in each layer is computed as

$$H_2 S_i = f_{dni} TH_2 S_i , \tag{5.65a}$$

$$f_{dhi} = \frac{1}{1 + C_{ssi} k_{dh2si}} = 1 - f_{phi} . \tag{5.65b}$$

The oxygen consumed by the oxidation of hydrogen sulfide is computed using the following equation

$$CSOD_{H2S} = \frac{0.5\,DO}{K_{sH_2S}} \frac{v^2_{h2s,d}(T)\,f_{dh1} + v^2_{h2s,p}(T)\,f_{ph1}}{K_{L01}} TH_2S_1 \,. \qquad (5.66)$$

5.5.6 Sediment dissolved inorganic carbon

The POC diagenesis in the anaerobic layer and methane oxidation in the aerobic layer produce CO_2. Sediment denitrification also releases CO_2. The mass balance equations of sediment dissolved inorganic carbon (DIC) in layers 1 and 2 can be written as

$$h_1 \frac{dDIC_1}{dt} = \frac{1}{2r_{oc}} F_{Oxch1} \frac{v_{ch4,1}(T)^2}{K_{L01}} CH4_1 \qquad \text{CH4 oxidation in layer 1 (CH4}_1\text{--}>\text{DIC}_1\text{),} \qquad (5.67a)$$

$$+ \frac{5 \times 12}{4 \times 14} \frac{v_{no3,1}(T)^2}{K_{L01}} NO3_1 \qquad \text{Denitrification (Denitrification--}>\text{DIC}_1\text{),}$$

$$+ K_{L12}(DIC_2 - DIC_1) \qquad \text{DIC transfer between layers 1 and 2 (DIC}_2\text{<-->DIC}_1\text{),}$$

$$- K_{L01}(DIC_1 - 12000 \cdot DIC) \qquad \text{DIC sediment-water transfer (DIC}_1\text{<-->DIC),}$$

$$h_2 \frac{dDIC_2}{dt} = \frac{1}{r_{oc}} \left(\frac{1}{2} J_{C,CH4} + J_{C,H2S} \right) \qquad \text{Carbon diagenesis into DIC in layer 2,} \qquad (5.67b)$$

$$+ \frac{5 \times 12}{4 \times 14} v_{no3,2}(T) \cdot NO3_2 \qquad \text{Denitrification (Denitrification--}>\text{DIC}_2\text{),}$$

$$- K_{L12}(DIC_2 - DIC_1) \qquad \text{DIC transfer between layers 1 and 2 (DIC}_2\text{<-->DIC}_1\text{),}$$

where

DIC_i = dissolved inorganic carbon in sediment layer i (mg-C L^{-1}).

Sediment DIC is tracked in units of mg-C L^{-1} for convenience. However, water column DIC is computed using mol L^{-1}, 1 mol L^{-1} = 12000 mg-C L^{-1}. Implicit finite difference forms of above mass balance equations of DIC are written as

$$a_{11} DIC_1^{t+\Delta t} + a_{12} DIC_2^{t+\Delta t} = b_1 \,, \qquad (5.68a)$$

$$a_{21} DIC_1^{t+\Delta t} + a_{22} DIC_2^{t+\Delta t} = b_2.$$ (5.68b)

Unsteady-state solution:

$$a_{11} = K_{L12} + K_{L01},$$ (5.69a)

$$a_{12} = -K_{L12},$$ (5.69b)

$$b_1 = \frac{1}{2r_{oc}} F_{Oxch1} \frac{v_{ch4,1}(T)^2}{K_{L01}} CH4_1^{t+\Delta t} + \frac{5 \times 12}{4 \times 14} \frac{v_{no3,1}(T)^2}{K_{L01}} NO3_1 + 1200 K_{L01} DIC^t,$$ (5.69c)

$$a_{21} = -K_{L12},$$ (5.69d)

$$a_{22} = K_{L12} + \frac{h_2}{\Delta t},$$ (5.69e)

$$b_2 = \frac{1}{r_{oc}} \left(\frac{1}{2} J_{C,CH4}^t + J_{C,H2S}^t \right) + \frac{5 \times 12}{4 \times 14} v_{no3,2}(T) NO3_2 + \frac{h_2}{\Delta t} DIC_2^t.$$ (5.69f)

Steady-state solution:

$$a_{22} = K_{L12},$$ (5.70a)

$$b_2 = 0.$$ (5.70b)

5.5.7 Sediment total inorganic phosphorous

The dissolved and particulate fractions of sediment inorganic phosphorus (TIP) are considered. There are two sources of TIP: (1) Phosphorus produced by decomposition of the reactive G1 and G2 classes of POP (POP$_{G1}$ and POP$_{G2}$) in the anaerobic layer and (2) Phosphorus sorbed onto suspended solids deposited to benthic sediments. Inorganic phosphorus in sediments may undergo burial and flux to the water column. The mass balance equations of TIP in layers 1 and 2 can be written as

$$h_1 \frac{dTIP_1}{dt} = -w_2 TIP_1$$ TIP burial from layer 1,   (5.71a)

$$+ \omega_{12} \left(f_{pp2} TIP_2 - f_{pp1} TIP_1 \right)$$ TIP particulate transfer between layers 1 and 2 (PIP$_2$<-->PIP$_1$),

$+ K_{L12}\left(f_{dp2}TIP_2 - f_{dp1}TIP_1\right)$

TIP dissolved transfer between layers 1 and 2 (DIP_2<-->DIP_1),

$- K_{L01}\left(f_{dp1}TIP_1 - f_{dp}TIP\right)$

DIP sediment-water transfer (DIP_1<-->DIP),

$$h_2 \frac{dTIP_2}{dt} = J_P$$

Total POP diagenesis flux in layer 2,   (5.71b)

$- \omega_{12}\left(f_{pp2}TIP_2 - f_{pp1}TIP_1\right)$

PIP between layers 1 and 2 (PIP_2<-->PIP_1),

$- K_{L12}\left(f_{dp2}TIP_2 - f_{dp1}TIP_1\right)$

DIP transfer between layers 1 and 2 (DIP_2<-->DIP_1),

$+ w_2 TIP_1$

TIP burial from layer 1,

$- w_2 TIP_2$

TIP burial from layer 2,

$+ v_{sp} f_{pp} TIP$

Water column PIP deposition,

where

TIP_i = total inorganic P in sediment layer i (mg-P L^{-1}) (i = 1, 2),
f_{dpi}, f_{ppi} = dissolved and particulate fractions of inorganic P in layer i.

Di Toro (2001) incorporates the effect of oxygen on phosphate flux into his model by making the dissolved fraction of phosphate a function of oxygen in the water column. For the aerobic layer, the partition coefficient of sediment inorganic phosphorous is adjusted based on the DO in the overlying water column and compared with a critical concentration, DO_c. When the oxygen in water increases above a critical threshold, the partition coefficient for inorganic phosphorous is increased by a user-entered factor. As the oxygen goes to zero, the partition coefficient is smoothly reduced to the anaerobic coefficient by using an exponential function

$$k_{dpo41} = k_{dpo42}\left(\Delta k_{PO41}\right), \ DO > DO_c,$$ (5.72a)

$$k_{dpo41} = k_{dpo42}\left(\Delta k_{PO41}\right)^{DO/DO_c}, \ DO \leq DO_c,$$ (5.72b)

where

$\Delta k_{PO4,1}$ = incremental partition coefficient of inorganic P in aerobic layer.

Implicit finite difference forms of above mass balance equations of TIP are written as

$$a_{11} TIP_1^{t+\Delta t} + a_{12} TIP_2^{t+\Delta t} = b_1 \ ,$$ (5.73a)

$$a_{21} TIP_1^{t+\Delta t} + a_{22} TIP_2^{t+\Delta t} = b_2 .$$ (5.73b)

Unsteady-state solution:

$$a_{11} = \omega_{12} f_{pp1} + K_{L12} f_{dp1} + w_2 + K_{L01} f_{dp1} ,$$ (5.74a)

$$a_{12} = -\omega_{12} f_{pp2} - K_{L12} f_{dp2} \ ,$$ (5.74b)

$$b_1 = K_{L01} f_{dp1} TIP^t \ ,$$ (5.74c)

$$a_{21} = -\omega_{12} f_{pp1} - K_{L12} f_{dp1} - w_2 ,$$ (5.74d)

$$a_{22} = \left(\omega_{12} f_{pp2} + K_{L12} f_{dp2} + w_2 \right) + \frac{h_2}{\Delta t} ,$$ (5.74e)

$$b_2 = J_P^{t+\Delta t} + v_s f_{pp} TIP^t + \frac{h_2}{\Delta t} TIP_2^t .$$ (5.74f)

Steady-state solution:

$$a_{22} = \omega_{12} f_{pp2} + K_{L12} f_{dp2} + w_2 ,$$ (5.75a)

$$b_2 = J_P^{t+\Delta t} + v_s f_{pp} TIP^t .$$ (5.75b)

Dissolved inorganic phosphorous (DIP_i) in each layer is computed as

$$DIP_i = f_{dpo4\,i} TIP_i ,$$ (5.76a)

$$f_{dpi} = \frac{1}{1 + C_{ssi}k_{dpo4i}} = 1 - f_{ppi}. \qquad (5.76b)$$

5.5.8 Sediment dissolved silica

Sediment dissolved silica (DSi) will be included in NSMII-SedFlux as a state variable if the silica cycle is simulated for the water column. DSi is produced when biogenic silica breaks down due to dissolution. Silica in sediments may undergo burial and flux to the water column. The mass balance equations of sediment total silica (Si) in layers 1 and 2 can be written as

$$h_1 \frac{dSi_1}{dt} = -w_2 Si_1 \qquad \text{Silica burial from layer 1,} \qquad (5.77a)$$

$$+ \omega_{12}(f_{ps2}Si_2 - f_{ps1}Si_1) \qquad \text{Silica particulate transfer between layers 1 and 2 (PSi}_2\text{<-->PSi}_1\text{),}$$

$$+ K_{L12}(f_{ds2}Si_2 - f_{ds1}Si_1) \qquad \text{Silica dissolved transfer between layers 1 and 2 (DSi}_2\text{<-->DSi}_1\text{),}$$

$$- K_{L01}(f_{ds1}Si_1 - DSi) \qquad \text{Silica sediment-water transfer (DSi}_1\text{<-->DSi),}$$

$$h_2 \frac{dSi_2}{dt} = J_{Si} \qquad \text{BSi dissolution in layer 2,} \qquad (5.77b)$$

$$- \omega_{12}(f_{ps2}Si_2 - f_{ps1}Si_1) \qquad \text{Silica particulate between layers 1 and 2 (PSi}_2\text{<-->PSi}_1\text{),}$$

$$- K_{L12}(f_{ds2}Si_2 - f_{ds1}Si_1) \qquad \text{Silica dissolved between layers 1 and 2 (DSi}_2\text{<-->DSi}_1\text{),}$$

$$+ w_2 Si_1 \qquad \text{Silica burial from layer 1,}$$

$$- w_2 Si_2 \qquad \text{Silica burial from layer 2,}$$

where

Si_i = silica in sediment layer i (mg-Si L^{-1}) (i = 1, 2),

f_{dsii}, f_{psii} = dissolved and particulate fractions of Si in layer i (i = 1, 2).

Similar to inorganic phosphorous, DO affects the sediment-water flux of silica. The sediment partition coefficient of silica in layer 1 is adjusted based on overlying water column DO and compared with a critical concentration, DO_c.

$$k_{dsi1} = k_{dsi2}\left(\Delta k_{si1}\right), \ DO > DO_c, \tag{5.78a}$$

$$k_{dsi1} = k_{dsi2}\left(\Delta k_{si1}\right)^{DO/DO_c}, \ DO \le DO_c, \tag{5.78b}$$

where

Δk_{si1} = incremental partition coefficient of sediment Si in aerobic layer.

Implicit finite difference forms of above mass balance equations of sediment Si are written as

$$a_{11} Si_1^{t+\Delta t} + a_{12} Si_2^{t+\Delta t} = b_1 \ , \tag{5.79a}$$

$$a_{21} Si_1^{t+\Delta t} + a_{22} Si_2^{t+\Delta t} = b_2 . \tag{5.79b}$$

Unsteady-state solution:

$$a_{11} = \omega_{12} f_{psi1} + K_{L12} f_{dsi1} + w_2 + K_{L01} f_{dsi1} \ , \tag{5.80a}$$

$$a_{12} = -\omega_{12} f_{psi2} - K_{L12} f_{dsi2} \ , \tag{5.80b}$$

$$b_1 = \ K_{L01} DSi^t \ , \tag{5.80c}$$

$$a_{21} = -\omega_{12} f_{psi1} - K_{L12} f_{dsi1} - w_2 , \tag{5.80d}$$

$$a_{22} = \omega_{12} f_{psi2} + K_{L12} f_{dsi2} + w_2 + \frac{h_2}{\Delta t} , \tag{5.80e}$$

$$b_2 = J_{si}^{t+\Delta t} + \frac{h_2}{\Delta t} Si_2^t . \tag{5.80f}$$

Steady-state condition:

$$a_{22} = \omega_{12} f_{psi2} + K_{L12} f_{dsi2} + w_2 , \tag{5.81a}$$

$$b_2 = J_{si}^{t+\Delta t}.$$ (5.81b)

Initial sediment dissolved silica in layers 1 and 2 is first converted into total concentration for solving sediment silica. Dissolved silica (*DSi*) in each layer is computed as

$$DSi_i = f_{dsii} Si_i,$$ (5.82a)

$$f_{dsii} = \frac{1}{1 + C_{ssi} k_{dSii}} = 1 - f_{psii},$$ (5.82b)

where

DSi_i = dissolved silica in sediment layer i (mg-Si L^{-1}).

5.6 Sediment-Water Flux

Sediment–water fluxes of the following state variables are computed from the sediment diagenesis module. The flux may be in either direction across the sediment–water interface, depending on the concentration gradient. Positive fluxes are from benthic sediment to the water column. Negative fluxes are from the water column to sediments. These fluxes will be incorporated into the appropriate source and sink equations of water column state variables and substitute user-specified sediment release rates in NSMII.

- Ammonium (NH4)
- Nitrate (NO3)
- Inorganic Phosphorous (TIP)
- Dissolved Inorganic Carbon (DIC)
- Methane (CH4)
- Dissolved Sulfide (HxS)
- Dissolved Silica (DSi)
- Dissolved Oxygen (DO)

5.6.1 Ammonium

The sediment–water flux of NH4 is internally computed as the product of concentration difference between the water column, sediment layer 1, and the mass transfer coefficient when the sediment diagenesis module is activated. The internal source and sink equation for NH₄ in the water

column (equation 4.26) is modified to include the sediment–water flux of NH4 from the sediment diagenesis module

$$
\begin{aligned}
\frac{\partial NH4}{\partial t} = {} & \frac{DO}{K_{Oxmn} + DO} k_{don}(T) DON \\
& - \frac{DO}{K_{Oxna} + DO} \frac{NH4}{K_{sNh4} + NH4} k_{nit}(T) NH4 \\
& + \sum_i^3 F_{Oxpi} k_{rpi}(T) r_{nai} A_{pi} \\
& - \sum_i^3 P_{Npi} \mu_{pi}(T) r_{nai} A_{pi} \\
& + \frac{1}{h} F_{Oxb} k_{rb} r_{nb} A_b F_b \\
& - \frac{1}{h} p_{Nb} \mu_b r_{nb} A_b F_w F_b \\
& + \frac{K_{L01}}{h} \left(f_{dn1} TNH4_1 - NH4 \right)
\end{aligned}
\tag{5.83}
$$

5.6.2 Nitrate

Sediment denitrification is set to zero when the sediment diagenesis module is activated, because denitrification in the sediment layer is tracked within the sediment diagenesis module. The internal source and sink equation for NO3 in the water column (equation 4.27) is modified to account for the sediment flux of NO3 to the overlying water.

$$
\begin{aligned}
\frac{\partial NO3}{\partial t} = {} & \frac{DO}{K_{Oxna} + DO} \frac{NH4}{K_{sNh4} + NH4} k_{nit}(T) NH4 \\
& - \left(1 - \frac{DO}{K_{Oxdn} + DO} \right) k_{dnit}(T) NO3 \\
& - \sum_i^3 (1 - P_{Npi}) \mu_{pi}(T) r_{nai} A_{pi} \\
& - \frac{1}{h} (1 - P_{Nb}) \mu_b r_{nb} A_b F_w F_b \\
& + \frac{K_{L01}}{h} \left(NO3_1 - NO3 \right)
\end{aligned}
\tag{5.84}
$$

5.6.3 Total inorganic phosphorus

The internal source and sink equation for TIP in the water column (equation 4.32) is modified to include the sediment–water flux of DIP from the sediment diagenesis module.

$$
\begin{aligned}
\frac{\partial TIP}{\partial t} = {} & \frac{DO}{K_{Oxmp} + DO} k_{dop}(T) DOP \\
& - \frac{v_{sp}}{h} f_{pp} TIP \\
& + \sum_i^3 F_{Oxpi} k_{rpi}(T) r_{pai} A_{pi} \\
& - \sum_i^3 \mu_{pi}(T) r_{pai} A_{pi} \\
& + \frac{1}{h} F_{Oxb} k_{rb}(T) r_{pb} A_b F_b \\
& - \frac{1}{h} \mu_b(T) r_{pb} A_b F_w F_b \\
& + \frac{K_{L01}}{h} \left(f_{dp1} TIP_1 - f_{dp} TIP \right)
\end{aligned}
\tag{5.85}
$$

5.6.4 Dissolved inorganic carbon

The internal source and sink equation for DIC in the water column (equation 4.40) is modified to include the sediment–water flux of DIC from the sediment diagenesis module.

$$
\begin{aligned}
12 \cdot 10^3 \frac{\partial DIC}{\partial t} = {} & 12 k_{ac}(T) \left(10^{-3} k_H(T) p_{CO_2} - 10^3 F_{co2} DIC \right) \\
& + \frac{DO}{K_{Oxmc} + DO} k_{rdoc}(T) RDOC \\
& + \frac{DO}{K_{Oxmc} + DO} k_{ldoc}(T) LDOC \\
& + \sum_i^3 F_{Oxpi} k_{rpi}(T) r_{cai} A_{pi} \\
& - \sum_i^3 \mu_{pi}(T) r_{cai} A_{pi} \\
& + \frac{1}{h} F_{Oxb} k_{rb}(T) r_{cb} A_b F_b
\end{aligned}
\tag{5.86}
$$

$$-\frac{1}{h}\mu_b r_{cb} A_b F_b$$

$$+\frac{1}{r_{oc}}\sum\frac{DO}{K_{sOxbodi}+DO}k_{bodi}CBOD_i$$

$$+\frac{12}{64}\frac{DO}{K_{sOch4}+DO}k_{ch4}(T)CH4$$

$$+\frac{K_{L01}}{h}\left(DIC_1-12\cdot10^3\,DIC\right)$$

5.6.5 Methane

The internal source and sink equation for dissolved methane in the water column (equation 4.43) is modified to include the sediment–water flux of CH4 from the sediment diagenesis module.

$$\frac{\partial CH4}{\partial t}=-k_{ach4}(T)CH4$$

$$-\frac{DO}{K_{sOch4}+DO}k_{ch4}(T)CH4 \tag{5.87}$$

$$+\frac{K_{L01}}{h}\left(CH4_1-CH4\right)$$

5.6.6 Total dissolved sulfides

The internal source and sink equation for HxS in the water column (equation 4.44) is modified to include the sediment–water flux of H_2S from the sediment diagenesis module.

$$\frac{\partial HxS}{\partial t}=-k_{ah2s}(T)H_2S$$

$$-\frac{DO}{K_{sOhs}+DO}k_{hs}(T)\cdot HS \tag{5.88}$$

$$+\frac{K_{L01}}{h}\left(H_2S_1-H_2S\right)$$

5.6.7 Dissolved silica

The internal source and sink equation for DSi in the water column (equation 4.51) is modified to include the sediment–water flux of DSi from the sediment diagenesis module.

$$\frac{\partial DSi}{\partial t} = \left(1 - F_{bsi}\right) \sum_i^3 k_{dpi}(T) r_{siai} A_{pi}$$

$$+ k_{bsi}(T) \frac{BSi}{K_{sSi} + BSi}\left(Si_s - DSi\right)$$

$$+ \sum_i^3 F_{Oxpi} k_{rpi}(T) r_{siai} A_{pi} \qquad (5.89)$$

$$- \sum_i^3 \mu_{pi}(T) r_{siai} A_{pi}$$

$$+ \frac{K_{L01}}{h}\left(DSi_1 - DSi\right)$$

5.6.8 Dissolved oxygen

When the sediment diagenesis module is activated, SOD becomes a function of specific chemical reactions that follow the decomposition of organic matter. The processes affect SOD are the oxidation of methane, sulfide and the nitrification. *SOD(T)* in the source and sink equation for DO, equation 4.47, will be internally computed instead of user specified.

5.7 Sediment Oxygen Demand and Numerical Solution

5.7.1 Sediment oxygen demand

Within the aerobic layer, the diagenetic products undergo oxidation that consumes diffused oxygen from the water column, thereby exerting SOD on the overlying water column. SOD is computed by summing all processes that consume oxygen, including ammonium, sulfide and methane. Carbonaceous SOD (CSOD) consists of *CSOD_H2S* and *CSOD_CH4*.

$$SOD = CSOD + NSOD = CSOD_{CH4} + CSOD_{H2S} + NSOD. \qquad (5.90)$$

The SOD and the surface transfer rate (K_{L0I}) are computed in NSMII-SedFlux through the following procedure.

1. Compute the diagenesis fluxes at $t + \Delta t$: $J_C^{t+\Delta t}$, $J_N^{t+\Delta t}$, $J_P^{t+\Delta t}$, $J_{BSI}^{t+\Delta t}$.
2. Define an initial estimate of SOD:

$$SOD^i = r_{oc} J_C^{t+\Delta t} + 1.714 J_N^{t+\Delta t} \qquad (5.91)$$

3. Compute K_{L0I} using

$$K_{L01} = \frac{SOD^i}{DO^t} \tag{5.92}$$

4. Compute sediment concentration at $t + \Delta t$ using equation 5.31a, b for NH4, 5.38a, b for NO3, 5.45a, b for CH4, 5.61a, b for H2S.

    The finite difference equations are solved using an implicit numerical scheme for the unknown concentration at $t + \Delta t$ through the following matrix solution.

5. Compute the *CSOD* and *NSOD* using equation 5.49 and 5.65, 5.36 respectively.
6. Compute an updated SOD using the following weighted average.

$$SOD = \frac{SOD^i + CSOD^{t+\Delta t} + NSOD^{t+\Delta t}}{2}. \tag{5.93}$$

7. Check the convergence by calculating an approximate relative error (ε_a)

$$\varepsilon_a = \left| \frac{SOD - SOD^i}{SOD} \right| \times 100\%. \tag{5.94}$$

    If $\varepsilon_a > \varepsilon_s$, a user-specified criterion, then set $SOD^i = SOD$ and return to step 2.

    If $\varepsilon_a \leq \varepsilon_s$ convergence is adequate, then compute the sediment DIC, TIP, and DSi concentrations using equations 5.67a,b; 5.72a,b; and 5.78a,b based on the matrix solutions.

8. Compute the sediment-water fluxes of NH4, NO3, TIP, DIC, CH4, HxS, and DSi.
9. Compute updated source and sink terms for the water column's NH4, NO3, TIP, DIC, CH4, HxS, and DSi by using corresponding rate equations 5.82, 5.83, 5.84, 5.85, 5.86, 5.87 and 5.88.

5.7.2 Matrix solution

The mass balance equations of inorganic substances for layer 1 and layer 2 include two unknown variables. These equations are written in their general forms as

$$a_{11}x_1 + a_{12}x_2 = b_1, \qquad\qquad (5.95a)$$

$$a_{21}x_1 + a_{22}x_2 = b_2. \qquad\qquad (5.95b)$$

The above equations are solved using a matrix solution provided by Chapra and Canale (2006).

$$x_1 = \frac{a_{22}b_1 - a_{12}b_2}{a_{11}a_{22} - a_{12}a_{21}}, \qquad\qquad (5.96a)$$

$$x_2 = \frac{a_{11}b_2 - a_{21}b_1}{a_{11}a_{22} - a_{12}a_{21}}. \qquad\qquad (5.96b)$$

5.8   Sediment Diagenesis Parameters

Table 33 summarizes sediment diagenesis input parameters with their associated default values. These parameters and coefficients are compiled from Di Toro (2001) and Martin and Wool (2012). The first group includes global parameters and the second group includes all parameters associated with layer 1. The third group contains parameters related to the diagenesis in layer 2. POC, PON, or POP in the settled material must be assigned by a fraction to the three reactivity classes (G1 to G3). The temperature dependent coefficients are specified at 20 °C. Di Toro (2001) noted some of sediment diagenesis coefficients frequently required revision. This table will be repeated for each water quality region, allow the user to define the different values for input parameters.

Table 33. Sediment diagenesis parameters and coefficients with default values.

Symbol	Definition	Units	Default Value[a]	Reference Range[c]	Temperature Dependent	
Global Parameters						
h_2	Sediment layer thickness	m	0.01	0.001 – 1.0		
$Dd(T)$	Sediment pore-water diffusion coefficient	$m^2 d^{-1}$	0.0025	0.0005 – 0.005	Yes	1.08
$Dp(T)$	Sediment particle mixing diffusion coefficient	$m^2 d^{-1}$	0.00006	n/a	Yes	1.117
K_{sDp}	Half-saturation oxygen constant for sediment particle phase mixing	$mg\text{-}O_2 L^{-1}$	4.0	n/a		
POC_r	Reference sediment POC for bioturbation	$mg\text{-}C g^{-1}$	0.1	n/a		
$SO4$	Overlaying freshwater SO4	$mg\text{-}O_2 L^{-1}$	9.14[b]	n/a		
ε_{no}	Maximum iterations of numerical solution	unitless	50	n/a		
ε_s	Relative error of numerical solution	unitless	0.001	n/a		
Sediment Layer 1						
DO_c	Critical O2 for incremental sorption	$mg\text{-}O_2 L^{-1}$	2.0	n/a		
Δk_{PO41}	Incremental inorganic P partition coeff.	unitless	20	20 – 300		
Δk_{SI1}	Incremental Si partition coefficient	unitless	20	10 – 100		
$v_{ch4,1}(T)$	CH4 oxidation transfer velocity	$m d^{-1}$	0.7	n/a	Yes	1.079
$v_{h2s,d}(T)$	Dissolved H2S oxidation transfer velocity	$m d^{-1}$	0.2	n/a	Yes	1.079
$v_{h2s,p}(T)$	Particulate H2S oxidation transfer velocity	$m d^{-1}$	0.4	n/a	Yes	1.079
k_{sH2S}	H2S oxidation normalization constant	$mg\text{-}O_2 L^{-1}$	4.0	n/a		
K_{sOxch}	Half-saturation oxygen constant for CH4 oxidation	$mg\text{-}O_2 L^{-1}$	0.1	n/a		
$v_{nh4,1}(T)$	Nitrification transfer velocity	$m d^{-1}$	0.1313	0.13 – 0.2	Yes	1.123
K_{sOxna1}	Half-saturation oxygen constant for nitrification	$mg\text{-}O_2 L^{-1}$	0.37	n/a		
K_{sNh4}	Half-saturation NH4 constant for nitrification	$mg\text{-}N L^{-1}$	0.728	n/a		
$v_{no3,1}(T)$	Denitrification transfer velocity	$m d^{-1}$	0.2	0.2 – 1.25	Yes	1.08
C_{ss1}	Solids concentration	$kg L^{-1}$	0.5	0.2 – 1.2		
Sediment Layer 2						
F_{AP1}	Fraction of algae deposit into sediment G1	unitless	0.6	0 – 1.0		
F_{AP2}	Fraction of algae deposit into sediment G2	unitless	0.2	0 - 1.0		
F_{AB1}	Fraction of dead benthic algae into sediment G1	unitless	0.6	0 – 1.0		
F_{AB2}	Fraction of dead benthic algae into sediment G2	unitless	0.2	0 - 1.0		
F_{RPOC1}	Fraction of RPOC deposit into sediment POC G1	unitless	0.0	0 – 1.0		
F_{RPOC2}	Fraction of RPOC deposit into sediment POC G2	unitless	0.5	0 - 1.0		
F_{RPON1}	Fraction of RPON deposit into sediment PON G1	unitless	0.0	0 – 1.0		

F_{RPON2}	Fraction of RPON deposit into sediment PON G2	unitless	0.6	0 - 1.0		
F_{RPOP1}	Fraction of RPOP deposit into sediment POP G1	unitless	0.0	0 – 1.0		
F_{RPOP2}	Fraction of RPOP deposit into sediment POP G2	unitless	0.5	0 - 1.0		
$K_{POCG1}(T)$	Diagenesis rate of sediment POC G1	d^{-1}	0.035	n/a	Yes	1.1
$K_{POCG2}(T)$	Diagenesis rate of sediment POC G2	d^{-1}	0.0018	n/a	Yes	1.15
$K_{PONG1}(T)$	Diagenesis rate of sediment PON G1	d^{-1}	0.035	n/a	Yes	1.1
$K_{PONG2}(T)$	Diagenesis rate of sediment PON G2	d^{-1}	0.0018	n/a	Yes	1.15
$K_{POPG1}(T)$	Diagenesis rate of sediment POP G1	d^{-1}	0.035	n/a	Yes	1.1
$K_{POPG2}(T)$	Diagenesis rate of sediment POP G2	d^{-1}	0.0018	n/a	Yes	1.15
k_{dnh42}	NH4 partition coefficient	L kg^{-1}	1.0	n/a		
k_{dh2s2}	H$_2$S partition coefficient	L kg^{-1}	100	n/a		
$v_{no3,2}(T)$	Denitrification transfer velocity	m d^{-1}	0.25	n/a	Yes	1.08
k_{dpo42}	Inorganic P partition coefficient	L kg^{-1}	20	20 – 1000		
$k_{bsi2}(T)$	BSi dissolution rate	d^{-1}	0.5	n/a	Yes	1.10
K_{sSi}	Half-saturation Si constant for dissolution	mg-Si L^{-1}	50000	n/a		
k_{dsi2}	Si partition coefficient	L kg^{-1}	100	n/a		
k_{st}	Decay rate of sediment benthic stress	d^{-1}	0.03	n/a		
K_{sSO4}	SO4 half-saturation constant for reduction	mg-O$_2$ L^{-1}	0.0032	n/a		
C_{ss2}	Solids concentration	kg L^{-1}	0.5	0.2 – 1.2		
w_2	Sediment burial rate	cm yr^{-1}	0.25	0.25 – 0.75		

a. Di Toro (2001) and Martin and Wool (2012)

b. Morel and Hering (1993).

c. HydroQual (2004).

5.9   Sediment Diagenesis Outputs

This section describes the model outputs associated with the sediment diagenesis simulation. The NSMII-SedFlux outputs include the concentrations of state variables listed in Table 32. Derived sediment variables and the pathway fluxes can also be reported in model outputs.

5.9.1   Derived variables

Table 34 lists the eight derived variables computed in NSMII-SedFlux.

Table 34. Derived benthic sediment variables computed in sediment diagenesis.

Variable	Layer	Definition	Units
H_2S_1	1	Sediment dissolved hydrogen sulfide	mg-O_2 L^{-1}
DIP_1	1	Sediment dissolved inorganic phosphorous	mg-P L^{-1}
H_2S_2	2	Sediment dissolved hydrogen sulfide	mg-O_2 L^{-1}
DIP_2	2	Sediment dissolved inorganic phosphorous	mg-P L^{-1}
POC_2	2	Sediment particulate organic carbon	mg-C L^{-1}
POM_2	2	Sediment particulate organic matter	mg-D L^{-1}
PON_2	2	Sediment particulate organic nitrogen	mg-N L^{-1}
POP_2	2	Sediment particulate organic phosphorous	mg-P L^{-1}

The sediment concentration of particulate organic matter is the sum of the contribution of the three G classes

$$POC_2 = \sum_{j}^{3} POC_{Gj,2} \,, \tag{5.96a}$$

$$POM_2 = \frac{POC_2}{f_{com}} \,, \tag{5.96b}$$

$$PON_2 = \sum_{j}^{3} PON_{Gj,2} \,, \tag{5.96c}$$

$$POP_2 = \sum_{j}^{3} POP_{Gj,2} \,. \tag{5.96d}$$

5.9.2 Pathway fluxes

Table 35 provides a summary of pathways and additional variables that can be reported in NSMII-SedFlux outputs.

Table 35. Pathway fluxes and additional variables computed in sediment diagenesis.

Name	Definition	Units
Carbon Diagenesis		
$J_{POC,G1}$	Total deposition to sediment POC G1	g-C/m^2/d
$J_{POC,G2}$	Total deposition to sediment POC G2	g-C/m^2/d
$J_{POC,G3}$	Total deposition to sediment POC G3	g-C/m^2/d
POCG1$_2$ diagenesis	Sediment POC G1 diagenesis	g-C/m^2/d
POCG2$_2$ diagenesis	Sediment POC G2 diagenesis	g-C/m^2/d

Name	Definition	Units
$POCG1_2$ burial	Sediment POC G1 burial	$g\text{-}C/m^2/d$
$POCG2_2$ burial	Sediment POC G2 burial	$g\text{-}C/m^2/d$
POC_2 diagenesis	Sediment POC diagenesis	$g\text{-}C/m^2/d$
POC_2 denitrification	Sediment POC consumed by denitrification	$g\text{-}O_2/m^2/d$
$POC_2\text{-->}CH4_2$	Sediment POC diagenesis into CH4	$g\text{-}O_2/m^2/d$
$POC_2\text{-->}H2S_2$	Sediment POC diagenesis into H_2S	$g\text{-}O_2/m^2/d$
$CH4_s$	Saturated methane	$g\text{-}O_2/m^3$
$CH4_1\text{-->}CSOD$	CH4 oxidation from layer 1	$g\text{-}O_2/m^2/d$
$CH4_1\text{<-->}CH4$	CH4 sediment-water transfer	$g\text{-}O_2/m^2/d$
$CH4_2\text{-->}Gas$	CH4 gas loss from layer 2	$g\text{-}O_2/m^2/d$
$SO4_1\text{<-->}SO4$	SO4 sediment-water transfer	$g\text{-}O_2/m^2/d$
$SO4_2\text{<-->}SO4_1$	SO4 dissolved transfer between layers 1 and 2	$g\text{-}O_2/m^2/d$
$H_2S_1\text{-->}CSOD$	H_2S oxidation from layer 1	$g\text{-}O_2/m^2/d$
$H_2S_1\text{<-->}H_2S$	H_2S sediment-water transfer	$g\text{-}O_2/m^2/d$
TH_2S_1 burial	H_2S burial from layer 1	$g\text{-}O_2/m^2/d$
$H_2S_2\text{<-->}H_2S_1$	H_2S dissolved transfer between layers 1 and 2	$g\text{-}O_2/m^2/d$
$PH_2S_2\text{<-->}PH_2S_1$	H_2S particulate transfer between layers 1 and 2	$g\text{-}O_2/m^2/d$
TH_2S_2 burial	H_2S burial from layer 2	$g\text{-}O_2/m^2/d$
$POC_2\text{<-->}DIC_2$	Sediment POC diagenesis into CO_2	$g\text{-}C/m^2/d$
$DIC_1\text{<-->}DIC$	DIC sediment-water flux	$g\text{-}C/m^2/d$
$DIC_2\text{<-->}DIC_1$	DIC transfer between layers 1 and 2	$g\text{-}C/m^2/d$
$NO3_1$ denitrification --$>DIC_1$	DIC produced by denitrification from layer 1	$g\text{-}C/m^2/d$
$NO3_2$ denitrification --$>DIC_2$	DIC produced by denitrification from layer 2	$g\text{-}C/m^2/d$
Nitrogen Diagenesis		
$J_{PON,G1}$	Total deposition to sediment PON G1	$g\text{-}N/m^2/d$
$J_{PON,G2}$	Total deposition to sediment PON G2	$g\text{-}N/m^2/d$
$J_{PON,G3}$	Total deposition to sediment PON G3	$g\text{-}N/m^2/d$
$PONG1_2$ burial	Sediment PON G1 burial	$g\text{-}N/m^2/d$
$PONG2_2$ burial	Sediment PON G2 burial	$g\text{-}N/m^2/d$
$PONG1_2\text{-->}NH4_2$	Sediment PON G1 diagenesis	$g\text{-}N/m^2/d$
$PONG2_2\text{-->}NH4_2$	Sediment PON G2 diagenesis	$g\text{-}N/m^2/d$
PON_2 diagenesis	Sediment PON diagenesis	$g\text{-}N/m^2/d$
$NH4_1\text{<-->}NH4$	NH4 sediment-water transfer	$g\text{-}N/m^2/d$
$TNH4_1\text{-->}TNH4_2$	NH4 buried from layer 1	$g\text{-}N/m^2/d$
$NH4_1\text{-->}NO3_1$	NH4 nitrification in layer 1	$g\text{-}N/m^2/d$
$PNH4_2\text{<-->}PNH4_1$	NH4 particulate transfer between layers 1 and 2	$g\text{-}N/m^2/d$
$NH4_2\text{<-->}NH4_1$	NH4 dissolved transfer between layers 1 and 2	$g\text{-}N/m^2/d$
$TNH4_2$ burial	NH4 burial from layer 2	$g\text{-}N/m^2/d$

Name	Definition	Units
$NO3_1$<-->$NO3$	NO3 sediment-water transfer	g-N/m²/d
$NO3_1$ denitrification	NO3 denitrification in layer 1	g-N/m²/d
$NO3_2$<-->$NO3_1$	NO3 transfer between layers 1 and 2	g-N/m²/d
$NO3_2$ denitrification	NO3 denitrification in layer 2	g-N/m²/d
Phosphorous Diagenesis		
$J_{POP,G1}$	Total deposition to sediment POP G1	g-P/m²/d
$J_{POP,G2}$	Total deposition to sediment POP G2	g-P/m²/d
$J_{POP,G3}$	Total deposition to sediment POP G3	g-P/m²/d
PIP-->PIP_2	PIP deposition to sediment PIP	g-P/m²/d
$POPG1_2$ burial	Sediment POP G1 burial	g-P/m²/d
$POPG2_2$ burial	Sediment POP G2 burial	g-P/m²/d
$POPG1_2$-->DIP_2	Sediment POP G1 diagenesis	g-P/m²/d
$POPG2_2$-->DIP_2	Sediment POP G2 diagenesis	g-P/m²/d
POP_2 diagenesis	Sediment POP diagenesis	g-P/m²/d
DIP_1<-->DIP	DIP sediment-water transfer	g-P/m²/d
TIP_1-->TIP_2	TIP burial from layer 1	g-P/m²/d
PIP_2<-->PIP_1	PIP transfer between layers 1 and 2	g-P/m²/d
DIP_2<-->DIP_1	DIP transfer between layers 1 and 2	g-P/m²/d
TIP_2 burial	TIP burial from layer 2	g-P/m²/d
Silica Diagenesis		
J_{BSi}	Total deposition to sediment BSi	g-Si/m²/d
BSi_2 burial	Sediment BSi burial	g-Si/m²/d
BSi_2 dissolution	Sediment BSi dissolution	g-Si/m²/d
DSi_1<-->DSi	Si dissolved sediment-water transfer	g-Si/m²/d
Si_1-->Si_2	Si burial from layer 1	g-Si/m²/d
PSi_2<-->PSi_1	Si particulate transfer between layers 1 and 2	g-Si/m²/d
DSi_2<-->DSi_1	Si dissolved transfer between layers 1 and 2	g-Si/m²/d
Si_2 burial	Si burial from layer 2	g-Si/m²/d
Additional Variables		
SOD	Sediment oxygen demand	mg-O₂/L/d
ω_{12}	Sediment particle mass transfer velocity	m/d
K_{L12}	Sediment dissolved mass transfer velocity	m/d
K_{L01}	Sediment-water transfer velocity	m/d

6 Integrating Water Quality Modules into Hydrologic Engineering Center-River Analysis System (HEC-RAS)

The water quality modules that have been developed include several DLLs (TEMP, NSMI, and NSMII). These modules have, and will be integrated into a variety of Hydrologic and Hydraulic (H&H) models. H&H models vary considerably in the way they store spatial variables such as flow outputs, the manner they process the transport terms, and solving relevant differential equations. This chapter focuses on a framework for integrating "plug in" water quality modules into 1-D HEC-RAS wherein the HEC-RAS is used to describe the physical processes of advection and dispersion, and when the water quality module is used to quantify speciation, reactions and transformations. The model integration approach and mechanisms we developed here are applicable to other H&H models.

6.1 HEC-RAS

HEC-RAS is an industry standard hydraulic tool that is used worldwide. It is designed to perform 1-D hydraulic simulation for a full network of open channels and a wide variety of hydraulic structures, such as bridges, culverts, spillways, and weirs. The HEC-RAS system contains five components (HEC 2010a): (1) 1-D steady flow water surface profile computations, (2) 1-D unsteady flow simulation, (3) 1D unsteady flow simulation, (4) movable boundary sediment transport computations, and (5) water quality analysis through "plug in" water quality modules. All five components use a common geometric data representation and common geometric and hydraulic computation routines. In HEC-RAS, its graphical user interface (GUI) standardizes many aspects of data entry, facilitates an efficient display of model results, data checking, data conversion, and communication between model subcomponents. The latest HEC-RAS model can be freely accessed and downloaded from the HEC website: *http://www.hec.usace.army.mil*. Water quality modules have been integrated with only a 1-D flow computation engine.

It is useful to first present the fundamental model that will be used to compute the hydraulic information required for simulating water quality. The 1-D unsteady flow component uses a numerical solution derived from the complete equations of gradually varied unsteady flow, commonly

referred to as the Saint Venant equations. The mass and momentum equations that govern the unsteady flow are given as (HEC 2010b):

$$\frac{\partial A}{\partial t} + \frac{\partial Q}{\partial x} - q_l = 0,$$ (6.1a)

$$\frac{\partial A}{\partial t} + \frac{\partial Q}{\partial x} + gA\left(\frac{\partial z}{\partial x} + S_f\right) = 0,$$ (6.1b)

where

Q = volumetric flow rate,
A = channel cross-sectional flow area,
x = distance along channel,
q_l = lateral inflow per unit length of channel,
z = elevation of the water surface,
S_f = friction slope,
g = gravitational acceleration.

To solve the above equations, the required input data include channel network connectivity, cross-section geometry, reach lengths, energy loss coefficients, stream junction information, and hydraulic works data. Cross sections are required at representative locations throughout the reach and at locations where changes in discharge, slope, shape, or roughness occur. Boundary conditions are necessary to define discharge and water depth at the system endpoints, (i.e. upstream and downstream). Lateral inflows can also be prescribed in the model.

The HEC-RAS model solves the mass conservation and momentum conservation equations with an implicit linearized system of equations using Preissman's second-order box scheme (HEC 2010b). The state variables for the numerical scheme are flow and stage, which are computed and stored at each cross section.

6.2 Model Integration

A seamless internal coupling of the 1-D HEC-RAS and "plug in" DLLs is implemented for performing water quality analysis. Figure 19 shows an overview of the model integration. The NSMs and its supporting water quality modules define standard functions and interfaces that allow HEC-RAS to make data calls from each DLL. The DLL obtains water-quality-

specific parameters and hydraulic information from the HEC-RAS GUI and performs the kinetics computation for each state variable. HEC-RAS obtains source and sink terms from the water quality module and performs the transport and mass balance computation for each cell and each state variable. Note that HEC-RAS has the control over the initial and boundary conditions. The DLL returns the state variables, derived variables, and pathways to HEC-RAS for model outputs.

Figure 19. HEC-RAS integrated with "plug in" water quality modules.

6.2.1 Transport of water quality constituents

Contaminant inputs to streams vary in time and space. Inputs can be both point sources, such as sewage outfalls, or more widely distributed, non-point sources. Contaminant may reach the stream network at the surface and via the subsurface. Regardless of the source type, the processes of transport and biogeochemical reactions control the spatial and temporal distributions of constituent concentrations and loads (as the product of discharge and concentration) throughout stream networks. Further, the transport of constituents occurs in several processes simultaneously. The transport of contaminants in surface water is generally described with the advection–dispersion equation, or appropriate modifications. The constituent transport model included in 1-D HEC-RAS is based on an advection and dispersion equation with additional terms to account for inflow boundary and kinetics.

$$\frac{\partial}{\partial t}(VC) = -\frac{\partial}{\partial x}(QC)\Delta x + \frac{\partial}{\partial x}\left(AD_x\frac{\partial C}{\partial x}\right)\Delta x + S_B + S_K,\qquad(6.2)$$

where

V = volume of the water quality cell (m^3),
C = concentration of a constituent (g m^{-3}),
Dx = dispersion coefficient (m^2 s^{-1}),
S_B = total source sink term representing boundary loading rate (g s^{-1}),
S_K = total source sink term representing internal rate (g s^{-1}).

Equation 6.2 describes the transport and fate of constituents in stream networks. The dispersion term, which is the second term on the right side of equation 6.2, often plays a small role in 1-D water quality modeling (Fischer et al. 1979). Two options are available for defining the dispersion coefficient. First, the user can simply specify estimated values. Secondly, the dispersion coefficient is internally computed based on the channel's hydraulics.

The above mass balance relationship is the same regardless of the state variable. This equation requires boundary conditions if there exists a source of mass at a location, the mass being introduced must be accounted for. Source and sink terms of kinetic change occur due to biochemical reactions and sediment–water interactions. These are obtained from the water quality modules (TEMP.dll, NSMI.dll, and NSMII.dll). Water quality modules operate on local variable values (e.g., local temperature, light, and concentration) and return local sink and source terms—they need not be aware of their physical locations. The source and sink terms (S_k) for each of the state variables included in NSMI and NSMII have been discussed in Chapters 3 to 5.

6.2.2 Numerical solution

Differential equation 6.2 must be solved numerically because the analytical solution to the full equation is impossible for most of real world cases. To present a numerical solution, a schematic diagram of a 1-D river system is illustrated in Figure 20. Each element or segment represents a control volume over which the governing equations apply. Heat and mass pass through each segment by advection and diffusion. The model domain defines the spatial limit of model representation.

Figure 20. Schematic diagram of 1-D segmented system.

The coupled advection-dispersion-reaction, equation 6.2, that governs the behavior of constituents in aquatic systems is conceptually split into the reaction part (i.e. sink and source terms) provided by water quality modules and "everything else," to be handled by the hydraulic model. "Everything else" includes transport (advection, dispersion), lateral inflow, and any boundaries. Effectively, the advection – dispersion – reaction equation is solved (time integrated) by the hydraulic model, with the reaction terms that it in turn obtains from the active water quality modules.

Numerical solutions for solving differential equations may be loosely grouped into explicit and implicit methods. In short, explicit methods compute a solution using values of the dependent variable (for example, constituent concentration) from the current time level. Implicit methods use values from both current and future time levels. For reasons of accuracy, efficiency, and stability, the QUICKEST–ULTIMATE explicit numerical scheme has been implemented in HEC-RAS (Leonard 1979, 1991). Using this scheme, equation 6.2 is approximated as

$$V^{n+1}C^{n+1} = V^n C^n + \Delta t \left(Q_{up} C_{up}^* - Q_{dn} C_{dn}^* + D_{dn} A_{dn} \frac{\partial C^*}{\partial x}\bigg|_{dn} - D_{up} A_{up} \frac{\partial C^*}{\partial x}\bigg|_{up} \right) + \Delta t \left(S_B + S_K \right), \quad (6.3)$$

where

C^{n+1} = concentration of a constituent at present time step (g m^{-3}),

C^n = concentration of a constituent at previous time step (g m^{-3}),

C_{up}^* = QUICKEST concentration of a constituent at upstream (g m^{-3}),

$\frac{\partial C^*}{\partial x}\bigg|_{up}$ = QUICKEST derivative of a constituent at upstream (g m^{-4}),

C_{dn}^* = QUICKEST concentration of a constituent at downstream (g m^{-3}),

$\frac{\partial C^*}{\partial x}\bigg|_{dn}$ = QUICKEST derivative of a constituent at downstream (g m^{-4}),

D_{up} = upstream face dispersion coefficient (m^2 s^{-1}),

V^{n+1} = volume of the water quality cell at present time step (m^3),

V^n = volume of the water quality cell at previous time step (m^3),

Q_{up} = upstream face flow (m³ s⁻¹),
A_{up} = upstream face cross section area (m²),
Q_{dn} = downstream face flow (m³ s⁻¹),
A_{dn} = downstream face cross section area (m²).

The transport scheme used is common to all water quality modules. The primary difference in NSMI and NSMII is in the number of state variables. HEC-RAS solves equation 6.3 for each water quality cell and for each state variable selected. Equation 6.3 that governs the behavior of constituents in aquatic systems is conceptually split into the reaction part (i.e. sink and source terms) provided by water quality modules and "everything else," to be handled by the hydraulic model. "Everything else" includes transport (advection, dispersion), lateral inflow, and any boundaries. Effectively, the advection – dispersion - reaction equation is solved (time integrated) by the hydraulic model, with the reaction terms that it in turn obtains from the active water quality modules. During each time step, state variable derivatives are computed for each water quality cell based on the biogeochemical processes (i.e. reaction kinetics) included in NSMs. Hydraulic information required for executing the NSM is passed from the HEC-RAS model. This step provides a partial computation of Σ S in equation 6.3. The effects of lateral and boundary loads are added to the complete computation of the total source and sink term in equation 6.3. Finally, concentrations at time t+Δt in the model domain combined from transport, kinetics, and external loads are solved.

The water quality model's time step is dynamically computed and adjusted so that Courant and Peclet constraints are automatically met. The water quality time step varies throughout a model run. The auto-stepping algorithm estimates the maximum time step to maintain stability. This differs from the hydraulic model where the user may specify the time step. Typical practice in water quality modeling is to select the largest time step possible to minimize computation time while remaining within predefined model stability limits. The selection of the time step within the transport model must satisfy Courant and Peclet constraints

$$C_{us} = u_{us} \frac{\Delta t}{\Delta x} \leq 0.9 , \qquad (6.4a)$$

$$\alpha_{us} = D_{us} \frac{\Delta t}{\Delta x^2} \leq 0.4 , \qquad (6.4b)$$

where

C_{us} = Courant number,
u_{us} = velocity at water quality cell face (m s^{-1}),
α_{us} = local Peclet number,
D_{us} = dispersion coefficient at water quality cell face (m^2 s^{-1}).

The Courant and Peclet numbers are cross section face properties. Both constraints can force a short time step if water quality cells are small. Therefore small water quality cells within the model domain should be avoided. The numerical solution of above equation 6.3 requires initial and boundary conditions for each state variable in water quality modules.

Boundary conditions:

The QUICKEST solution uses a three-point interpolation scheme to estimate concentrations at a face. This requires that the solution scheme know the concentration in the two upstream cells for a positive flow and the two downstream cells for a negative flow. Thus, for each face, four cell numbers are required. For the case of a 1-D stream network shown in Figure 20, water quality boundary conditions are required at the upstream and downstream boundaries. The upstream boundary condition is the constituent concentration at the upstream end of the domain during the period of simulation. The downstream boundary condition is specified as a constant longitudinal gradient of constituent. Where flow enters or leaves the model domain (i.e., crosses the domain boundary) information must be supplied to the model. Lateral boundary conditions can be specified either of two approaches within the model. One approach is to specify the concentrations at the hydraulic boundaries where in which concentrations of state variables are provided. This approach requires that the boundary receives flows from the hydraulic model. Concentrations may be specified at arbitrary intervals. The other approach is to specify the inflow boundary as a load (mass/time) where the inflow enters. The product of flow and concentration is load. This approach does not require a flow from the hydraulic model at the boundary. Some water quality variables are best specified as a concentration at the inflow boundary, such as temperature and dissolved oxygen. Other water quality variables, such as nutrients, may be more conveniently specified as loads.

Initial conditions:

The above differential equations also require starting values or initial conditions at the beginning of the simulation period. These initial conditions may consist of temperature and constituent profile conditions for the modeled domain. Initial conditions of the state variables must be specified in each water quality cell (Figure 20). They are used only to start the model simulation. Initial conditions can be derived from measured data, from other model simulations, or estimated. Initial conditions of the sediment diagenesis state variables can be defined from a steady-state solution included in the sediment diagenesis module. Because the assigned initial concentrations usually do not reflect the actual conditions in the system, model "spin-up" (Thornton and Rosenbloom 2005) is often applied to create quasi-steady-state concentrations and then used for initial conditions.

6.3   Model Inputs and Outputs

To run a water quality module in HEC-RAS, a working hydraulic model must already be in place. Once the hydraulic model has been calibrated, the user can turn on the water quality modules in HEC-RAS. Water quality cells are initially established between cross sections. The user can adjust the water quality cells to avoid model instability and longer simulation times. Note that model results can often be improved with accurate channel geometry, planned model construct based on specific questions to be answered, and a computational cross-section-reach configuration designed to capture hydrodynamic, thermal, and water quality constituent gradients. The HEC-RAS model GUI is responsible for handling data input and output. Input and output data for the HEC-RAS model with water quality modules are managed as shown in Figure 19.

6.3.1   Water quality inputs

Major water quality model inputs include meteorological data, measured boundary input water quality from all inflow sources, initial water quality throughout the modeled reach, and water quality parameters. Complete sets of meteorological and water quality data at the appropriate time intervals are required for all low flow or high flow conditions; these are used for model development and calibration. In addition, accurate measurements of water quality parameters are required to represent controlling conditions for modeled systems. Model calibration requires an

entire set of several types of data. Proper collection of complete modeling data sets is critical to ensure adequate model calibration.

Accurate meteorological data is an essential part of a water quality simulation. These data points provide the basis for coefficients applied in model equations affecting water quality. Hourly meteorological data points are typically required for modeling water quality due to large fluctuations in air temperature and solar radiation. There are often numerous NWS and other nearby meteorological stations that provide this data. Meteorological data influences the water quality processes and should reflect actual conditions near the model domain. In general, meteorological stations that are installed near the water body specifically for modeling purposes tend to produce better results. The following meteorological data is needed for a full energy balance temperature simulation module: atmospheric pressure, air temperature, dew point, humidity, short-wave radiation, cloud cover, and wind speed.

Inflow temperature and water quality information are required to capture diurnal thermal and water quality dynamics for water quality model development and calibration. Adequate temperature and water quality data must be collected at modeled flow boundaries and tributary inflow locations. If more complicated water quality issues must be modeled, a significant amount of data collection may be required for the water quality model calibration.

Local water quality parameters and coefficients used to describe biochemical transformation properties of the model domain are specified by the user. Input parameters for NSMI, NSMII, and NSMII-SedFlux have been discussed in previous chapters.

6.3.2 Water quality outputs

With respect to output, the HEC-RAS model offers a mechanism to include the water quality constituents as defined by the water quality module in its output, along with defining any pathway and diagnostic variables. The primary outputs of a HEC-RAS water quality simulation include concentrations of water column state variables at designated cells and benthic sediment–water quality concentrations at the same locations (if the benthic sediment diagenesis is being activated). In addition, derived water quality variables and pathway fluxes for individual biogeochemical process are available for model outputs. These values are typically

produced as time series and/or tabulated values. Desired output parameters, specific locations, reporting time interval, period of interest, and summary statistics can be defined. The model also produces a binary water quality output file. The restart output file is produced for use as input in subsequent model runs.

7 Summary

The Nutrient Simulation Modules (NSMs) are developed to describe chemical, biological processes, interactions between state variables, and the physical process of sedimentation of state variables. The newly developed NSMs and its supporting water quality modules are written in Fortran for Windows and are packaged as "plug in" DLLs. Each module must be coupled with available H&H models in order to perform water quality analysis from various stressors. It can be implemented as a basic water quality model or as a complex eutrophication model depending on the needs of the user. The NSMI approach for water quality analysis provides more flexibility where each state variable can be turned on and off. This approach allows for the rapid assessments that can be conducted with minimum modeling expertise and limited data input requirements. NSMII is better suited than NSMI for assessing the impact for multiple algae groups and benthic sediment diagenesis effects on water quality. The best way to accurately assess water quality is to use the more advanced models, but only if the data needs of the models can be met and there is sufficient time to run the data.

This report provides mathematical and programming formulations used within the newly developed NSMs and its supporting water quality modules. It describes the basis for the water quality modules and how they are formulated. The scientific basis of the NSMs reflects empirical and theoretical support precedence found within the literature, and in widely used water quality models. The NSMs have been tested and verified with a variety of examples, and compared against other water quality models. The results from the comparison showed that the predictions were similar. Additional validation of the NSMs against observations in aquatic systems is underway.

The variable names in the report correspond to those used in the computer code so that the mathematical formulations and codes can be compared. The computer codes in all modules has been checked for consistency with the formulations described in the report. The modularity forms the basis for the flexibility of all the water quality modules, including the ability to add and modify state variables and processes for future enhancement. The water quality modules have been integrated into HEC-RAS with pre- and post-processer to setup the model, perform the runs, and to present and

analyze the results. This report is primarily intended for use as a technical reference for applying these modules.

Integrating the water quality modules described in the report into HEC-ResSim (Hydrologic Engineering Center-Reservoir System Simulation) and other H&H models is currently planned and will be implemented in the future. As the scope and scale of environmental and ecosystem studies expands, coupled with advances in science and improved understanding, these water quality modules can be continuously enhanced and further developed through revision of water quality formulations and computer codes.

References

Andrews, F. A., and G. M. Rodvey. 1980. Heat exchange between water and tidal flats. *Dtsch. Gewaesserkd. Mitt.* 24(2).

American Public Health Association, Inc. (APHA). 1992. *Standard methods for the examination of water and wastewater*. 18th ed. Washington, DC: American Public Health Association.

Baird, M. E. 2010. Limits to prediction in a size-resolved pelagic ecosystem model. *Journal of Plankton Research* 32(8):1131–46.

Baly, E. C. C. 1935. The Kinetics of photosynthesis. *Proceedings of the Royal Society of London, Series B* 117:218–239.

Banks, R. B., and F. F. Herrera. 1977. Effect of wind and rain on surface reaeration. *Journal of Environmental Engineering Division* 103 (EE3):489–504.

Berman, T., and D. A. Bronk. 2003. Dissolved organic nitrogen: a dynamic participant in aquatic ecosystems. *Aquatic Microbial Ecology* 31:273–305.

Berner R. A. 1980. *Early diagenesis: a theoretical approach*. Princeton University Press, Princeton, NJ.

Bienfang, P. K., P .J. Harrison, and L. M. Quarmby. 1982. Sinking rate response to depletion of nitrate, phosphate, and silicate in four marine diatoms. *Marine Biology* 67:295–302.

Bowie, G. L., B. M. Williams, D. B. Porcella, C. L. Campbell, J. R. Pagenkopf, G. L. Rupp, K. M. Johnson, P. W. H. Chen, and S. A. Gherini. 1985. *Rates, constants and kinetics formulations in surface water quality*. EPA/600/3–85/040. Athens, GA: U.S. Environmental Protection Agency.

Brown, L. C., and T. O. Barnwell. 1987. *The enhanced stream water quality models QUAL2E and QUAL2E-UNCAS*. EPA/600/3-87-007. Athens, GA: U.S. Environmental Protection Agency.

Brown, L. C. 2002. *Addendum to the enhanced stream water quality models QUAL2E and QUAL2E-UNCAS*. EPA/600/3-87-007. Medford, MA: Tufts University.

Butts, T. A., and R. L. Evans. 1978. Sediment oxygen demand studies of selected northeastern Illinois streams. *Illinois State Water Survey Circular* 129. Urbana, IL: State of Illinois, Department of Registration and Education.

Carpenter, S. R., J. J. Cole, J. F. Kitchell, and M. L. Pace. 1998. Impact of dissolved organic carbon, phosphorus, and grazing on phytoplankton biomass and production in experimental lakes. *Limnology and Oceanography* 43:73–80.

Carslaw, H. S., and J. C. Jaeger. 1959. *Conduction of heat in solids*. Oxford, UK: Oxford Press.

Cascallar, L. P., P. Mastranduono, P. Mosto, M. Rheinfeld, J. Santiago, C. Tsoukalis, and S. Wallace. 2003. Periphytic algae as bioindicators of nitrogen inputs in lakes. *Journal of Psycology* 39(1):7–8.

Cerco, C., and T. Cole. 1993. Three-dimensional eutrophication model of Chesapeake Bay. *Journal of Environmental Engineering* 119(6):1006–1025.

Cerco, C. F., M. R. Noel, and S. C. Kim. 2004. *Three-dimensional eutrophication model of Lake Washington, Washington State*. ERDC/EL TR-04-12. Vicksburg, MS: U.S. Army Engineer Research and Development Center.

Chapra, S. C. 1997. *Surface water quality modeling*. New York, NY: McGraw-Hill.

Chapra, S. C. 1999. Organic carbon and surface water quality modeling. *Progress in Environmental Science* 1 (1):49–70.

Chapra S. C., and R. P. Canale. 2006. *Numerical methods for engineers*. 5th Ed. New York, NY: McGraw-Hill.

Chapra, S. C., and G. J. Pelletier, and H. Tao. 2008. *QUAL2K: A modeling framework for simulating river and stream water quality, Version 2.11: Documentation and users manual*. Medford, MA: Tufts University, Civil and Environmental Engineering Department.

Chen, K. Y., and J. C. Morris. 1972. Kinetics of oxidation of aqueous sulfide by O_2. *Environmental Science and Technology* 6(6):529–537.

Chiaro, P. S., and D. A. Burke. 1980. Sediment oxygen demand and nutrient release. *Journal of the Environmental Engineering Division* 106:177–195.

Chow, V. T., D. R. Maidment, and L. W. Mays. 1988. *Applied hydrology*. New York, NY: McGraw-Hill.

Churchill, M. A., H. L. Elmore, and R. A. Buckingham. 1962. The prediction of stream reaeration rates. *Journal of the Sanitary Engineering Division* 88(4):1–46.

Cole, T. M., and S. A. Wells. 2008. *CE-QUAL-W–2: A two-dimensional, laterally averaged, hydrodynamic and water quality model, Version 3.6*. Instruction Report EL-08-1. Vicksburg, MS: U.S. Army Engineering and Research Development Center.

Conley D. J., and S. S. Kilham. 1989. Differences in silica content between marine and freshwater diatoms. *Limnology and Oceanography* 34:205–13.

Connolly, J. P., and R. B. Coffin. 1995. Model of carbon cycling in planktonic food webs. *Journal of Environmental Engineering* 121(10):682–690.

Correll, D. L. 1998. The role of phosphorus in the eutrophication of receiving waters: A review. *Journal of Environmental Quality* 27:261–267.

Deas, M. L. and C. L. Lowney. 2000. *Water temperature modeling review*. Central Vally, CA.

Diaz, R. J. and R. Rosenberg. 1995. Marine benthic hypoxia: a review of its ecological effects and the behavioral responses of benthic macrofauna. *Oceanography and Marine Biology, An Annual Review* 33:245-303.

Di Toro, D. M. 1976. Combining chemical equilibrium and phytoplankton models—A general methodology. *Modeling Biochemical Processes in Aquatic Ecosystems*, ed. R. P. Canale, 224–243. Ann Arbor, MI: Ann Arbor Science.

Di Toro, D. M. 2001. *Sediment flux modeling.* New York, NY: Wiley-Interscience.

Di Toro, D. M., and J. F. Fitzpatrick. 1993. *Chesapeake Bay sediment flux model.* Contract Report EL-93-2. Vicksburg, MS: U.S. Army Corps of Engineers, Waterways Experiment Station.

Dortch, M. S., D. H. Tillman, and B. W. Bunch. 1992. *Modeling water quality of reservoir tailwaters.* Technical Report W-92-1. Vicksburg, MS: U.S. Army Corps of Engineers, Waterways Experiment Station.

Edberg, N., and B. V. Hofsten. 1973. Oxygen uptake of bottom sediments studied in situ and in the laboratory. *Water Research* 7:1285–1294.

Edinger, J. E., D. K. Brady, and J. C. Geyer. 1974. *Heat exchange and transport in the environment.* Report No. 14, Electrical Power Research. Institution Publication, EA-74-049-00-3, Palo Alto, CA.

Edmond, J. M., and T. M. Gieskes. 1970. On the calculation of the degree of saturation of sea water with respect to calcium carbonate under in situ conditions. *Geochimica et Cosmochimica Acta* 34:1261–1291.

Ekholm, P., K. Kallio, S. Salo, O. P. Pietilainen, S. Rekolainen, Y. Laine, and M. Joukola. 2000. Relationship between catchment characteristics and nutrient concentrations in an agricultural river system. *Water Research* 34:3709–3716.

Environmental Laboratory (EL). 1995a. *CE-QUAL-RIV1: A dynamic, one-dimensional (longitudinal) water quality model for streams user's manual.* Vicksburg, MS: Army Corps of Engineers, Waterways Experiment Station.

Environmental Laboratory (EL). 1995b. *CE-QUAL-R1: A numerical one-dimensional model of reservoir water quality user's manual.* Vicksburg, MS: Army Corps of Engineers, Waterways Experiment Station.

Field, S. D., and S. W. Effler. 1982. Photosynthesis-light mathematical formulations. *Journal of Environmental Engineering* 108:199–203.

Finlay, J. C., S. Khandwala, and M. E. Power. 2002. Spatial scales of carbon flow in a river food web. *Ecology* 83(7):1845–1859.

Fischer, H. B., E. J. List, R. C. Y. Koh, J. Imberger, and N. H. Brooks. 1979. *Mixing in inland and coastal waters.* New York: Academic Press. 484.

Flynn, K. F., M. W. Suplee, S. C. Chapra, and H. Tao. 2015. Model-Based nitrogen and phosphorus (nutrient) criteria for large temperate rivers: 1. Model development and application. *Journal of the American Water Resources Association* 51(2):421–446.

Geiger, R. 1965. *The climate near the ground.* Cambridge, MA: Harvard University Press.

Hanson, R. S., and T. E. Hanson. 1996. Methanotrophic bacteria. *Microbiology and Molecular Biology Reviews* 60(2):439-471 1.

Harned, H. S., and W. J. Hamer. 1933. The ionization constant of water. *Journal of American Chemistry Society* 51:21–94.

Harris, G. P. 1986. *Phytoplankton ecology: structure, function, and fluctuation.* London, UK: Chapman and Hall.

Hutchinson, G. E. 1957. *A treatise on limnology, Vol. 1, physics and chemistry.* New York, NY: John Wiley and Sons.

Hydrologic Engineering Center (HEC). 2010a. *HEC-RAS: River analysis system user's reference manual version 4.1.* Davis, CA: Hydrologic Engineering Center. U.S. Corps of Engineers.

Hydrologic Engineering Center (HEC). 2010b. *HEC-RAS: River analysis system hydraulic reference manual version 4.1.* Davis, CA: Hydrologic Engineering Center, U.S. Corps of Engineers.

HydroQual. 2004. *User's Guide for RCA (Release 3.0).* Mahwah, NJ 07430.

House, W. A., F. A. Denison, and P. D. Armitage. 1995. Comparison of the uptake of inorganic phosphorus to a suspended and stream bed sediment. *Water Research* 29:767–779.

Howarth, R. W. and B. B. Jorgensen. 1984. Formation of S labelled elemental sulfur and pyrite in coastal marine sediments during short term SO_4^{-2} reduction measurements. *Geochimica et Cosmochimica Acta* 48:1807–1818.

Hunter, J. V., M. A. Hartnett, and A. P. Cryan. 1973. *A study of the factors determining the oxygen uptake of benthal stream deposits.* Department of Environmental Sciences, Rutgers University, Project B-022-N.U. Office of Water Resources Research, Department of the Interior.

Hurd, D. C. 1973. Interactions of biogenic opal, sediment and seawater in the central equatorial Pacific. *Geochimica et Cosmochimica* 37:2257–2282.

Jobson, H. E. 1977. Bed conduction computation for thermal models. *Journal of the Hydraulics Division (ASCE).* 103(10):1213–1217.

James, A. 1974. The measurement of benthal respiration. *Water Research* 8:955–959.

Kiffney, P. M, and J. P. Bull. 2000. Factors controlling periphyton accrual during summer in headwater streams of southwestern British Columbia, Canada. *Journal of Freshwater Ecology* 15(3):339–351.

Kusuda, T., T. Futawatari, and K. Oishi. 1994. Simulation of nitrification and denitrification processes in a tidal river. *Water Science and Technology* 30(2):43–52.

Le Cren, E.P., and R. H. Lowe-McConnell. 1980. *The functioning of freshwater ecosystems.* Cambridge MA: Cambridge University Press, 588 pp.

Leonard, B. P. 1979. A stable and accurate convection modeling procedure based on quadratic upstream interpolation. *Computer Methods in Applied Mechanics and Engineering* 19:59–98.

Leonard, B. P. 1991. The ULTIMATE conservative difference scheme applied to unsteady one-dimensional advection. *Computer Methods in Applied Mechanics and Engineering* 88:17–74.

Likens, G. E., and N. M. Johnson. 1969. Measurements and analysis of the annual heat budget for sediments of two Wisconsin lakes. *Limnology and Oceanography* 14(1):115–135.

Manivanan, R. 2008. *Water quality modeling rivers, streams and estuaries*, New Delhi, India.

Michaelis, L., and M. L. Menten. 1913. Kinetik der Invertinwirkung. *Biochem Zeitung* 49 (1913):333–369.

Martin, J. L., and T. A. Wool. 2012. *WASP sediment diagenesis routines: Model theory and user's guide.* U.S. Environmental Protection Agency, Washington, DC. 20460.

Melching, C. S., and H. E. Flores. 1999. Reaeration equations from U.S. Geological Survey database. *Journal of Environmental Engineering* 125(5):407–414.

Meybeck, M. 1982. Carbon, nitrogen, and phosphorus transport by world rivers. *American Journal of Science* 282:401–450.

Millero, F. J. 1986. The thermodynamics and kinetics of the hydrogen sulfide system in natural waters. *Marine Chemistry* 18:121–147.

Missouri Department of Natural Resources (MDNR). 2009. Chapter 3: stream discharge. in introductory level volunteer water quality monitoring training notebook. Retrieved from http://www.dnr.mo.gov/env/wpp/vmqmp/level1-ch3.pdf.

Morel, F. M. M., and J. G. Hering. 1993. *Principles and applications of aquatic chemistry.* New York: John Wiley & Sons, Inc.

Morse, J. W., F. J. Millero, J. C. Cornwall, and D. Rickard. 1987, The chemistry of the hydrogen sulfide and iron sulfide systems in natural waters, *Earth-Science Review* 24(1): 1–42.

Nakshabandi, G. A., and H. Kohnke. 1965. Thermal conductivity and diffusivity of soils as related to moisture tension and other physical properties. *Agricultural Meteorology* 2(4):271–27.

National Council for Air and Stream Improvement, Inc (NCASI). 1978. Interfacial velocity effects on the measurement of sediment oxygen demand. *NCASI Technical Bulletin* No. 317. NY.

National Council for Air and Stream Improvement, Inc (NCASI). 1979. Further studies of sediment oxygen demand measurement and its variability. *NCASI Technical Bulletin* No. 321. NY.

National Oceanic and Atmospheric Administration – Earth system research laboratory (NOAA/ESRL): http://www.esrl.noaa.gov/gmd/ccgg/trends/.

O'Brien, D. J., and F. B. Birkner. 1977. Kinetics of oxygenation of reduced sulfur species in aqueous solution. *Environmental Science and Technology* 11(12):1114–1120.

O'Connor, D. J., and W. E. Dobbins. 1958. Mechanism of reaeration in natural streams. *Transactions of the American Society of Civil Engineers* 123:641–684.

Owens, M., R. W. Edwards, and J. W. Gibbs. 1964. Some reaeration studies in streams. *International Journal of Air and Water Pollution* 8:469–486.

Packman, J. J., K. J. Comings, and D. B. Booth. 1999. Using turbidity to determine total suspended solids in urbanizing streams in the Puget lowlands. *Confronting Uncertainty: Managing Change in Water Resources and the Environment, Canadian Water Resources Association annual meeting*, Vancouver, BC. 158–165.

Park, R. A., and J. S. Clough. 2010. *AQUATOX (Release 3) Modeling environmental fate and ecological effects in aquatic ecosystems.* Volume 2: Technical Documentation. U.S. Environmental Protection Agency, Office of Science and Technology, Washington, DC.

Pauer, J. J., and M. T. Auer. 2000. Nitrification in the water column and sediment of a hypereutrophic lake and adjoining river system. *Water Research* 34(4):1247–1254.

Platt, T., K. H. Mann, and R. E. Ulanowicz. 1981. *Mathematical models in biological oceanography, UNESCO monographs on oceanographic methodology.* Paris: UNESCO Press.

Plummer, L. N., and E. Busenberg. 1982. The solubilities of calcite, aragonite and vaterite in CO2-H2O solutions between 0 and 90 ºC, and an evaluation of the aqueous model for the system $CaCO_3$–CO_2–H_2O. *Geochimica et Cosmochimica Acta* 46:1011–1040.

Redfield, A. C. 1958. The biological control of chemical factors in the environment. *American Scientist* 46:205–222.

Riebesell, U. 1989. Comparison of sinking and sedimentation rate measurements in a diatom winter/spring bloom. *Marine Ecology Progress Series* 54:109–119.

Rudd, J. W., and C. D. Taylor. 1980. Methane cycling in aquatic environments. ed. M.R. Droop and H.W. Jannasch*, Advanced Aquatic Microbiology* 2:77–150.

Schnoor, J. L. 1996. *Environmental modeling: Fate and transport of pollutants in water, air, and soil.* New York: John Wiley and Sons.

Shanahan, P., M. Henze, L. Koncsos, W. Rauch, P. Reichert, L. Somlyódy, and P. Vanrolleghem. 1998. River water quality modeling: II. Problems of the art. *Water Science and Technology* 38(11):245–252.

Smith, E. L. 1936. Photosynthesis in relation to light and carbon dioxide. *Proceedings of the National Academy of Sciences of the United States of America* 22:504–511.

Stanley, D. W., and J. E. Hobbie. 1981. Nitrogen recycling in a North Carolina coastal river. *Limnology and Oceanography* 26:30–42.

Steele, J. H. 1962. Environmental control of photosynthesis in the Sea. *Limnology and Oceanography* 7:137–150.

Stevenson, R. J. 1996. Algal ecology in freshwater benthic habitats. In *Algal ecology. freshwater benthic ecosystems.* ed. R. J. Stevenson, M. L. Bothwell, and R. L. Lowe. San Diego: Academic Press 3–30.

Stumm, W., and J. J. Morgan. 1996. *Aquatic chemistry*, 3rd Ed. New York: Wiley-Interscience.

Tate, C. M., R. E. Broshears, and D. M. McKnight. 1995. Phosphate dynamics in an acidic mountain stream: interactions involving algal uptake, sorption by iron oxide and photoreduction. *Limnology and Oceanography* 40(5):938.

Thackston, E. L., and J. W. Dawson, III. 2001. Recalibration of a reaeration equation. *Journal of Environmental Engineering* 127(4):317–320.

Thomann, R. V., and J. A. Mueller. 1987. *Principles of surfacewater quality modelling and control.* New York: Harper and Row.

Thomann, R. V., and J. J. Fitzpatrick. 1982. *Calibration and verification of a mathematical model of the eutrophication of the Potomac estuary.* Prepared for Department of Environmental Services, Government of the District of Columbia, Washington, D.C.

Thornton, P.E. and N.A. Rosenbloom, 2005. Ecosystem model spin-up: Estimating steady state conditions in a coupled terrestrial carbon and nitrogen cycle model. *Ecological Modelling* 189:25–48.

Tillman, D. H., C. R. Cerco, M. R. Noel, J. L. Martin, and J. Hamrick. 2004. *Three-dimensional eutrophication model of the lower St. Johns River, Florida.* ERDC/EL TR-04-13, Vicksburg, MS: U.S. Army Engineer Research and Development Center.

Tsivoglou, E. C., and L. A. Neal. 1976. Tracer measurement of reaeration. Predicting the reaeration capacity of inland streams. *Journal of the Water Pollution Control Federation* 48(12):2669–2689.

Tye, R., R. Jepsen, and W. Lick. 1996. Effects of colloids, flocculation, particle size, and organic matter on the adsorption of hexachlorobenzene to sediments. *Environmental Toxicology and Chemistry* 15(5):643–651.

Waite, A. M., P. A. Thompson, and P. J. Harrison. 1992. Does energy control the sinking rate of marine diatoms? *Limnology and Oceanography* 37:468–477.

Walsh, J. J., and R. C. Dugdale. 1972. Nutrient submodels and simulation models of phytoplankton production in the sea. In *Nutrients in Natural Waters*, ed. Allen, H.E. and J.R. Kramer. New York: John Wiley and Sons, 171–191.

Wanninkhof, R., I. R. Ledwell, and I. Crusius. 1991. Gas transfer velocities on lakes measured with sulfur hexafluoride. *Symposium Volume of the Second International Conference on Gas Transfer at Water Surfaces,* ed. S.C. Wilhelms and I.S. Gulliver. Minneapolis, MN.

Water Resources Engineers Inc. 1967. *Prediction of thermal distribution in streams and reservoirs*, report to California Department of Fish and Game, Walnut Creek, CA.

Weckström, J., and A. Korhola. 2001. Patterns in the distribution, composition and diversity of diatom assemblages in relation to ecoclimatic factors in Arctic Lapland. *Journal of Biogeography,* 28:31–45.

Wool, T. A., R. B. Ambrose, J. L. Martin, and E. A. Comer. 2006. *Water quality analysis simulation program (WASP), Version 6, User's Manual.* U.S. Environmental Protection Agency, Athens, GA.

Appendix A: Definition of Mathematical Symbols used in the TEMP

Symbol	Definition	Units
A_s	surface area of the water column	m^2
a	user defined coefficient on order of 10^{-6}	unitless
b	user defined coefficient on order of 10^{-6}	unitless
c	user defined coefficient on order of one	unitless
C_p	specific heat capacity of air at constant pressure	J kg^{-1} °C^{-1}
C_{pw}	specific heat capacity of water	J kg^{-1} °C^{-1}
C_L	percent sky covered with clouds	unitless
C_{ps}	specific heat capacity of benthic sediments	J kg^{-1} °C^{-1}
e_s	saturated vapor pressure at water temperature	mb
e_a	vapor pressure of overlying air	mb
$f(u_w)$	wind function	m s^{-1}
g	acceleration of gravity (= 9.806)	m s^{-2}
h_2	sediment layer thickness	m
h_r	local hour angle	rad
K_h/K_w	diffusivity ratio	unitless
K_T	overall heat exchange coefficient	W m^{-2} °C^{-1}
$k(T)$	kinetic rate at local temperature	d^{-1}
$k(20)$	measured kinetic rate at 20°C	d^{-1}
L	latent heat of vaporization	J kg^{-1}
P	atmospheric pressure	mb
q_{net}	net heat flux	W m^{-2}
q_{sw}	short-wave solar radiation flux	W m^{-2}
q_{atm}	atmospheric (downwelling) longwave radiation flux	W m^{-2}
q_b	back (upwelling) longwave radiation flux	W m^{-2}
q_h	sensible heat flux	W m^{-2}
q_l	latent heat flux	W m^{-2}
q_{sed}	sediment-water heat flux	W m^{-2}
q_0	extraterrestrial radiation	W m^{-2}
Q_0	solar constant (= 1360)	W m^{-2}
R_s	reflectivity of the water surface	unitless

Symbol	Definition	Units
R_i	Richardson number	unitless
r	normalized radius of the earth's orbit	unitless
t	time	d
T_w	water temperature in Celsius	^{o}C
T_{wk}	water temperature in Kelvin	^{o}K
T_a	air temperature in Celsius	^{o}C
T_{ak}	air temperature in Kelvin	^{o}K
T_{sed}	sediment temperature	^{o}C
T_d	dew point temperature	^{o}C
T_{eq}	equilibrium temperature	^{o}C
u_w	wind speed measured at a fixed height	m s^{-1}
u_{w2}	wind speed measured at 2 m	m s^{-1}
u_{w7}	wind speed measured at 7 m	m s^{-1}
V	volume of the water column cell	m^3
z	station height	m
z_0	wind roughness height	m
Greek		
α_s	sediment thermal diffusivity	m^2 d^{-1}
α_t	atmospheric attenuation	unitless
σ	Stefan-Boltzman constant	W m^{-2} ^{0}K^{-1}
δ	declination of the sun	rad
ϕ	latitude of the site	rad
θ	temperature correction coefficient	unitless
ρ_{air}	density of moist air at air temperature	kg m^{-3}
ρ_{sat}	density of saturated air at water temperature	kg m^{-3}
ρ_s	density of sediments	kg m^{-3}
ρ_w	density of water	kg m^{-3}

Appendix B: Definition of Mathematical Symbols used in NSMI

Symbol	Definition	Units
A	site specific parameter for turbidity	unitless
A_p	algae (phytoplankton)	µg-Chla L^{-1}
A_{pd}	algae (dry weight)	mg-D L^{-1}
A_b	benthic algae biomass	g-D m^{-2}
A_c	cross-sectional area	m^2
Alk	alkalinity	eq L^{-1}
AW_d	algal dry weight stoichiometry	mg-D
AW_c	algal carbon stoichiometry	mg-C
AW_n	algal nitrogen stoichiometry	mg-N
AW_p	algal phosphorus stoichiometry	mg-P
AW_a	algal Chla stoichiometry	µg-Chla
B	site specific parameter for turbidity	unitless
BW_d	benthic algae dry weight stoichiometry	mg-D
BW_c	benthic algae carbon stoichiometry	mg-C
BW_n	benthic algae nitrogen stoichiometry	mg-N
BW_p	benthic algae phosphorus stoichiometry	mg-P
BW_a	benthic Chla stoichiometry	µg-Chla
B_t	top width of the channel	m
$CBOD_i$	carbonaceous biochemical oxygen demand	mg-O_2 L^{-1}
$CBOD5$	5-day carbonaceous biochemical oxygen demand	mg-O_2 L^{-1}
$CBODU$	ultimate carbonaceous biochemical oxygen demand	mg-O_2 L^{-1}
$Chlb$	benthic chlorophyll-a	mg-Chla m^{-2}
DIN	dissolved inorganic nitrogen	mg-N L^{-1}
DIP	dissolved inorganic phosphorus	mg-P L^{-1}
DO	dissolved oxygen	mg-O_2 L^{-1}
DO_s	dissolved oxygen saturation	mg-O_2 L^{-1}
DIC	dissolved inorganic carbon	mol L^{-1}
DOC	dissolved organic carbon	mg-C L^{-1}
f_{com}	fraction of carbon in organic matter	mg-C mg-D^{-1}
f_{dp}	dissolved fraction of inorganic P	unitless

Symbol	Definition	Units
f_{pp}	particulate fraction of inorganic P	unitless
F_{CO2}	fraction of CO_2 in total inorganic carbon	unitless
F_1	preference fraction of algal uptake from NH_4	unitless
F_2	preference fraction of benthic algae uptake from NH_4	unitless
F_{pocp}	fraction of algal mortality into POC	unitless
F_{pocb}	fraction of benthic algal mortality into POC	unitless
F_w	fraction of benthic algae mortality into the water column	unitless
F_b	fraction of bottom area available for benthic algae growth	unitless
FL	light limiting factor for algal growth	unitless
FN	N limiting factor for algal growth	unitless
FP	P limiting factor for algal growth	unitless
FL_b	light limiting factor for benthic algae growth	unitless
FN_b	N limiting factor for benthic algae growth	unitless
FP_b	P limiting factor for benthic algae growth	unitless
FS_b	bottom area density limiting factor for benthic algae growth	unitless
FL_z	light attenuation factor for algal growth at depth z	unitless
I_z	PAR intensity at a depth z below the water surface	W m^{-2}
I_0	surface light intensity	W m^{-2}
h	water depth	m
h_2	sediment layer thickness	m
$k_a(T)$	oxygen reaeration rate	d^{-1}
$k_{ah}(T)$	hydraulic oxygen reaeration velocity	m d^{-1}
$k_{aw}(T)$	wind oxygen reaeration velocity	m d^{-1}
$k_{ac}(T)$	CO_2 reaeration rate	d^{-1}
$k_{bodi}(T)$	CBOD oxidation rate	d^{-1}
$k_{sbodi}(T)$	CBOD sedimentation rate	d^{-1}
$k_{rp}(T)$	algal respiration rate	d^{-1}
$k_{dnit}(T)$	denitrification rate	d^{-1}
$k_{dp}(T)$	algal mortality rate	d^{-1}
$k_{rb}(T)$	benthic algae base respiration rate	d^{-1}
$k_{db}(T)$	benthic algae mortality rate	d^{-1}

Symbol	Definition	Units
k_{dpo4n}	partition coefficient of inorganic P for solid "n"	L kg^{-1}
$k_{pom}(T)$	POM dissolution rate	d^{-1}
$k_{pom2}(T)$	sediment POM dissolution rate	d^{-1}
$k_{poc}(T)$	POC hydrolysis rate	d^{-1}
$k_{doc}(T)$	DOC oxidation rate	d^{-1}
$k_{nit}(T)$	nitrification rate	d^{-1}
$k_{on}(T)$	decay rate of organic N to NH$_4$	d^{-1}
$k_{op}(T)$	decay rate of organic P to DIP	d^{-1}
$k_{dx}(T)$	pathogen death rate	d^{-1}
$K_{sOxbodi}$	half saturation oxygen attenuation constant for CBOD oxidation	mg-O$_2$ L^{-1}
K_{sOxdn}	half-saturation oxygen inhibition constant for denitrification	mg-O$_2$ L^{-1}
K_{sOxmc}	half saturation oxygen attenuation constant for the DOC oxidation	mg-O$_2$ L^{-1}
$k_H(T)$	Henry's Law constant	mol L^{-1} atm^{-1}
K_{NR}	oxygen inhibition factor for nitrification	mg-O$_2$ L^{-1}
K_L	light limiting constant for algal growth	W m^{-2}
K_{sN}	half-saturation N limiting constant for algal growth	mg-N L^{-1}
K_{sP}	half-saturation P limiting constant for algal growth	mg-P L^{-1}
K_{Lb}	light limiting constant for benthic algae growth	W m^{-2}
K_{sNb}	half-saturation N limiting constant for benthic algae	mg-N L^{-1}
K_{sPb}	half-saturation P limiting constant for benthic algae growth	mg-P L^{-1}
K_{sSOD}	half saturation oxygen attenuation constant for SOD	mg-O$_2$ L^{-1}
K_{Sb}	half-saturation density constant for benthic algae growth	g-D m^{-2}
K_1	first acidity constant	mol L^{-1}
K_2	second acidity constant	mol L^{-1}
K_w	ion product of water	(mol L^{-1})^2
m_n	inorganic suspended solid "n"	mg L^{-1}
MW_{O2}	molecular weight of O$_2$	g mol^{-1}
MW_{CO2}	molecular weight of CO$_2$	g mol^{-1}
$NH4$	ammonium	mg-N L^{-1}
$NO3$	nitrate	mg-N L^{-1}

Symbol	Definition	Units
$OrgN$	organic nitrogen	mg-N L^{-1}
$OrgP$	organic phosphorous	mg-P L^{-1}
p_{atm}	atmospheric pressure	atm
p_{wv}	partial pressure of water vapor	atm
P_N	NH$_4$ preference factor for algal growth	unitless
P_{Nb}	NH$_4$ preference factor for benthic algae growth	unitless
POC	particulate organic carbon	mg-C L^{-1}
POM	particulate organic matter	mg-D L^{-1}
POM_2	sediment particulate organic matter	mg-D L^{-1}
PX	pathogen	cfu (100 mL)$^{-1}$
p_{CO2}	partial pressure of CO$_2$ in the atmosphere	ppm
q_{sw}	short-wave solar radiation	W m^{-2}
r_{na}	algal N : Chla ratio	mg-N µg-Chla^{-1}
r_{pa}	algal P : Chla ratio	mg-P µg-Chla^{-1}
r_{ca}	algal C : Chla ratio	mg-C µg-Chla^{-1}
r_{cd}	algal C : D ratio	mg-C mg-D^{-1}
r_{da}	algal D : Chla ratio	mg-D µg- Chla^{-1}
r_{oc}	O$_2$: C ratio for oxidation	mg-O$_2$ mg-C^{-1}
r_{on}	O$_2$: N ratio for nitrification	mg-O$_2$ mg-N^{-1}
r_{nb}	benthic algae N : D ratio	mg-N mg-D^{-1}
r_{pb}	benthic algae P : D ratio	mg-P mg-D^{-1}
r_{cb}	benthic algae C : D ratio	mg-C mg-D^{-1}
r_{ab}	benthic Chla: D ratio	µg-Chla mg-D^{-1}
r_{po4}	sediment release rate of DIP	g-P m^{-2} d^{-1}
r_{nh4}	sediment release rate of NH$_4$	g-N m^{-2} d^{-1}
r_{alkaa}	ratio translating algal growth into Alk if NH$_4$ is the N source	eq µg-Chla^{-1}
r_{alkan}	ratio translating algal growth into Alk if NO$_3$ is the N source	eq µg-Chla^{-1}
r_{alkn}	ratio translating NH$_4$ nitrification into Alk	eq mg-N^{-1}
r_{alkden}	ratio translating NO$_3$ denitrification into Alk	eq mg-N^{-1}
r_{alkba}	ratio translating benthic algae growth into Alk if NH$_4$ is the N source	eq mg-D^{-1}
r_{alkbn}	ratio translating benthic algae growth into Alk if NO$_3$ is the N source	eq mg-D^{-1}

Symbol	Definition	Units
R_h	channel hydraulic radius	m
sl	channel slope	unitless
$SOD(T)$	sediment oxygen demand	g-O_2 m^{-2} d^{-1}
T_{wk}	water temperature in Kelvin	^{o}K
TIP	total inorganic phosphorous	mg-P L^{-1}
TON	total organic nitrogen	mg-N L^{-1}
TKN	total Kjeldahl nitrogen	mg-N L^{-1}
TN	total nitrogen	mg-N L^{-1}
TOP	total organic phosphorus	mg-P L^{-1}
TP	total phosphorus	mg-P L^{-1}
TOC	total organic carbon	mg-C L^{-1}
TSS	Total suspended solids	mg L^{-1}
u	water velocity	m s^{-1}
v_{son}	organic N settling velocity	m d^{-1}
v_{sop}	organic P settling velocity	m d^{-1}
v_{soc}	POC settling velocity	m d^{-1}
v_{som}	POM settling velocity	m d^{-1}
v_{sa}	algal settling velocity	m d^{-1}
v_{sp}	solids settling velocity	m d^{-1}
v_{no3}	sediment denitrification transfer velocity	m d^{-1}
v_x	pathogen settling velocity	m d^{-1}
z	depth from the water surface	m
CO_3^{2-}	carbonate ion	mol L^{-1}
H^+	hydronium ion	mol L^{-1}
H_2CO_3*	sum of dissolved carbon dioxide and carbonic acid	mol L^{-1}
HCO_3^-	bicarbonate ion	mol L^{-1}
OH^-	hydroxyl ion	mol L^{-1}
Greek		
α	correction coefficient	Unitless
α_{px}	light efficiency factor for pathogen decay	Unitless
$\mu_{mxp}(T)$	maximum algal growth rate	d^{-1}
μ_p	algal growth rate	d^{-1}
$\mu_{mxb}(T)$	maximum benthic algae growth rate	d^{-1}

Symbol	Definition	Units
μ_b	growth rate for benthic algae	d^{-1}
λ	light attenuation coefficient	m^{-1}
λ_0	background light attenuation	m^{-1}
λ_s	light attenuation by inorganic suspended solids	L mg^{-1} m^{-1}
λ_m	light attenuation by organic matter	L mg^{-1} m^{-1}
λ_1	linear light attenuation by algae	m^{-1} (µg-Chla L^{-1})$^{-1}$
λ_2	nonlinear light attenuation by algae	m^{-1} (µg-Chla L^{-1})$^{-2/3}$
w_2	sediment burial rate	m d^{-1}

Appendix C: Definition of Mathematical Symbols used in NSMII

Symbol	Definition	Units
A_{pd}	algae (dry weight)	mg-D L^{-1}
A_{pi}	algae (phytoplankton)	µg-Chla L^{-1}
A_b	benthic algae	g-D m^{-2}
Alk	alkalinity	mg-CaCO$_3$ L^{-1}
AW_{di}	algal dry weight stoichiometry	mg-D
AW_{ci}	algal carbon stoichiometry	mg-C
AW_{ni}	algal nitrogen stoichiometry	mg-N
AW_{pi}	algal phosphorus stoichiometry	mg-P
AW_{ai}	algal Chla stoichiometry	µg-Chla
AW_{si}	algal silica stoichiometry	mg-Si
BSi	particulate biogenic silica	mg-Si
BW_d	benthic algae dry weight stoichiometry	mg-D
BW_c	benthic algae carbon stoichiometry	mg-C
BW_n	benthic algae nitrogen stoichiometry	mg-N
BW_p	benthic algae phosphorus stoichiometry	mg-P
BW_a	benthic Chla stoichiometry	µg-Chla
$CBOD_i$	carbonaceous biochemical oxygen demand	mg-O$_2$ L^{-1}
$CBOD5$	5-day carbonaceous biochemical oxygen demand	mg-O$_2$ L^{-1}
$CH4$	dissolved methane	mg-O$_2$ L^{-1}
$Chla$	chlorophyll-a	µg-Chla L^{-1}
$Chlb$	benthic chlorophyll-a	mg-Chla L^{-2}
Cl	chloride	mg L^{-1}
DIN	dissolved inorganic nitrogen	mg-N L^{-1}
DIP	dissolved inorganic phosphorus	mg-P L^{-1}
DO	dissolved oxygen	mg-O$_2$ L^{-1}
DO_s	dissolved oxygen saturation	mg-O$_2$ L^{-1}
DOC	dissolved organic carbon	mg-C L^{-1}
DON	dissolved organic nitrogen	mg-N L^{-1}
DOP	dissolved organic phosphorus	mg-P L^{-1}
DIC	dissolved inorganic carbon	mol L^{-1}

Symbol	Definition	Units
DSi	dissolved silica	mg-Si
f_{com}	fraction of carbon in organic matter	mg-C mg-D^{-1}
f_{pp}	particulate fraction of inorganic P	unitless
F_{rponp}	fraction of algal mortality into RPON	unitless
F_{lponp}	fraction of algal mortality into LPON	unitless
F_{rpopp}	fraction of algal mortality into RPOP	unitless
F_{lpopp}	fraction of algal mortality into LPOP	unitless
F_{rpocp}	fraction of algal mortality into RPOC	unitless
F_{lpocp}	fraction of algal mortality into LPOC	unitless
F_{rdocp}	fraction of algal mortality into RDOC	unitless
F_{co2}	fraction of CO_2 in total inorganic carbon	unitless
F_{bsi}	fraction of algal mortality into BSi	unitless
F_{rponb}	fraction of benthic algae mortality into RPON	unitless
F_{lponb}	fraction of benthic algae mortality into LPON	unitless
F_{rpopb}	fraction of benthic algae mortality into RPOP	unitless
F_{lpopb}	fraction of benthic algae mortality into LPOP	unitless
F_{rpocb}	fraction of benthic algae mortality into RPOC	unitless
F_{lpocb}	fraction of benthic algae mortality into LPOC	unitless
F_{rdocb}	fraction of benthic algae mortality into RDOC	unitless
F_w	fraction of benthic algae mortality into the water column	unitless
F_b	fraction of bottom area available for benthic algae growth	unitless
FL_{pi}	light limiting factor for algal growth	unitless
FN_{pi}	algal nutrient limiting factor	unitless
FT_{pi}	effect of temperature on algal growth	unitless
F_{Oxpi}	oxygen attenuation for algal respiration	unitless
F_{Oxb}	oxygen attenuation for benthic algal respiration	unitless
FL_b	light limiting factor for benthic algae growth	unitless
FN_b	nutrient limiting factor for benthic algae growth	unitless
FT_b	temperature effect factor on benthic algal growth	unitless
FS_b	bottom area density limiting factor for benthic algae growth	unitless
FL_z	light limiting factor for algal growth at depth z	unitless
I_z	PAR intensity at a depth z below the water surface	W m^{-2}

Symbol	Definition	Units
I_0	surface light intensity	W m^{-2}
h	water depth	m
HxS	total dissolved sulfides	mg-O$_2$ L^{-1}
H_2S	dissolved hydrogen sulfide	mg-O$_2$ L^{-1}
HS	bisulfide ion	mg-O$_2$ L^{-1}
$k_{bodi}(T)$	CBOD oxidation rate	d^{-1}
$k_{sbodi}(T)$	CBOD sedimentation rate	d^{-1}
$k_{rpi}(T)$	algal respiration rate	d^{-1}
$k_{dpi}(T)$	algal mortality rate	d^{-1}
$k_{rb}(T)$	benthic algae base respiration rate	d^{-1}
$k_{db}(T)$	benthic algae mortality rate	d^{-1}
k_{dpo4n}	partition coefficient of inorganic P for solid "n"	L kg^{-1}
kt_{p1i}	effect of temperature below T_{0p} on algal growth	^{0}C^{-2}
kt_{p2i}	effect of temperature above T_{0p} on algal growth	^{0}C^{-2}
kt_{b1}	effect of temperature below T_{0p} on benthic algal growth	^{0}C^{-2}
kt_{b2}	effect of temperature above T_{0p} on benthic algal growth	^{0}C^{-2}
$k_a(T)$	oxygen reaeration rate	d^{-1}
$k_{rpon}(T)$	hydrolysis rate of RPON	d^{-1}
$k_{lpon}(T)$	hydrolysis rate of LPON	d^{-1}
$k_{don}(T)$	mineralization rate of DON	d^{-1}
$k_{hs}(T)$	HS oxidation rate	L mg-O$_2^{-1}$ d^{-1}
$k_{ah2s}(T)$	H$_2$S reaeration rate	d^{-1}
$k_{bsi}(T)$	BSi dissolution rate	d^{-1}
$k_{nit}(T)$	nitrification rate	d^{-1}
$k_{dnit}(T)$	denitrification rate	d^{-1}
$k_{ah}(T)$	hydraulic derived oxygen reaeration rate	d^{-1}
$k_{aw}(T)$	wind derived oxygen reaeration rate	m d^{-1}
$k_{rpop}(T)$	RPOP hydrolysis rate	d^{-1}
$k_{lpop}(T)$	LPOP hydrolysis rate	d^{-1}
$k_{dop}(T)$	DOP mineralization rate	d^{-1}
$k_{rpoc}(T)$	RPOC hydrolysis rate	d^{-1}
$k_{lpoc}(T)$	LPOC hydrolysis rate	d^{-1}
$k_{pom}(T)$	POM decay rate	d^{-1}

Symbol	Definition	Units
$k_{rdoc}(T)$	RDOC mineralization rate	d^{-1}
$k_{ldoc}(T)$	LDOC mineralization rate	d^{-1}
$K_H(T)$	Henry's Law constant	mol L^{-1} atm^{-1}
$k_{ac}(T)$	CO_2 reaeration coefficient	d^{-1}
kt_{b1}	effect of temperature below T_{0b} on benthic algal growth	$^0C^{-2}$
kt_{b2}	effect of temperature above T_{0b} on benthic algal growth	$^0C^{-2}$
K_{Li}	light limiting constant for algal growth	W m^{-2}
K_{snxpi}	half-saturation NH_4 preference constant for algal uptake	mg-N L^{-1}
K_{sOxpi}	half-saturation oxygen attenuation constant for algal respiration	mg-O_2 L^{-1}
K_{sNpi}	half-saturation N limiting constant for algal growth	mg-N L^{-1}
K_{sPpi}	half-saturation P limiting constant for algal growth	mg-P L^{-1}
K_{sSipi}	Half-saturation Si limiting constant for algal growth	mg-Si L^{-1}
K_{sSi}	Half-saturation Si constant for dissolution	mg-Si L^{-1}
K_{sOxmn}	half-saturation oxygen attenuation constant for DON mineralization	mg-O_2 L^{-1}
K_{sOxna}	half-saturation oxygen attenuation constant for nitrification	mg-O_2 L^{-1}
K_{sOxdn}	half-saturation oxygen attenuation constant for denitrification	mg-O_2 L^{-1}
K_{sOxmp}	half-saturation oxygen attenuation constant for DOP mineralization	mg-O_2 L^{-1}
K_{sOxmc}	half-saturation oxygen attenuation constant for DOC mineralization	mg-O_2 L^{-1}
K_{sSOD}	half saturation oxygen attenuation constant for SOD	mg-O_2 L^{-1}
K_{Lb}	light limiting constant for benthic algae growth	W m^{-2}
K_{sOxb}	half-saturation oxygen attenuation coefficient for benthic algae respiration	mg-O_2 L^{-1}
K_{snxb}	half-saturation NH_4 preference constant for benthic algae uptake	mg-N L^{-1}
K_{sNb}	half-saturation N limiting constant for benthic algae growth	mg-N L^{-1}
K_{sPb}	half-saturation P limiting constant for benthic algae growth	mg-P L^{-1}
K_{Sb}	half-saturation density constant for benthic algae growth	g-D m^{-2}
K_{sOhs}	half saturation oxygen attenuation constant for HS oxidation	mg-O_2 L^{-1}
$LPON$	labile particulate organic nitrogen	mg-N L^{-1}

Symbol	Definition	Units
$LPOP$	labile particulate organic phosphorus	mg-P L^{-1}
$LPOC$	labile particulate organic carbon	mg-C L^{-1}
$LDOC$	labile dissolved organic carbon	mg-C L^{-1}
m_n	inorganic suspended solid "n"	mg L^{-1}
$NH4$	ammonium	mg-N L^{-1}
$NO3$	nitrate	mg-N L^{-1}
P_{Npi}	preference fraction of algal uptake from NH4	unitless
P_{Nb}	NH$_4$ preference factor for benthic algae growth	unitless
p_{CO2}	partial pressure of CO$_2$ in the atmosphere	ppm
POC	particulate organic carbon	mg-C L^{-1}
POM	particulate organic matter	mg-D L^{-1}
PX	pathogen	cfu (100 mL)$^{-1}$
$RPON$	refractory particulate organic nitrogen	mg-N L^{-1}
$RPOP$	refractory particulate organic phosphorus	mg-P L^{-1}
$RPOC$	refractory particulate organic carbon	mg-C L^{-1}
$RDOC$	refractory dissolved organic carbon	mg-C L^{-1}
r_{dai}	algal D : Chla ratio	mg-D^{-1} µg- Chla^{-1}
r_{nai}	algal N : Chla ratio	mg-N µg-Chla^{-1}
r_{pai}	algal P : Chla ratio	mg-P µg-Chla^{-1}
r_{cai}	algal C : Chla ratio	mg-C µg-Chla^{-1}
r_{cdi}	algal C : D ratio	mg-C mg-D^{-1}
r_{siai}	algal Si : Chla ratio	mg-Si µg-Chla^{-1}
r_{oc}	O$_2$: C ratio for oxidation	mg-O$_2$ mg-C^{-1}
r_{on}	O$_2$: N ratio for nitrification	mg-O$_2$ mg-N^{-1}
r_{nb}	benthic algae N : D ratio	mg-N mg-D^{-1}
r_{pb}	benthic algae P : D ratio	mg-P mg-D^{-1}
r_{cb}	benthic algae C : D ratio	mg-C mg-D^{-1}
r_{ab}	benthic Chla : D ratio	µg-Chla mg-D^{-1}
r_{ccai}	algal mol-C : Chla ratio	mol-C µg-Chla^{-1}
r_{ccb}	benthic algae mol-C : D ratio	mol-C mg-D^{-1}
r_{alkaai}	ratio translating algal growth into Alk if NH$_4$ is the N source	eq µg-Chla^{-1}
r_{alkani}	ratio translating algal growth into Alk y if NO$_3$ is the N source	eq µg-Chla^{-1}

Symbol	Definition	Units
r_{alkn}	ratio translating NH_4 nitrification into Alk	eq mg-N^{-1}
r_{alkden}	ratio translating NO_3 denitrification into Alk	eq mg-N^{-1}
r_{alkba}	ratio translating benthic algae growth into Alk if NH_4 is the N source	eq mg-D^{-1}
r_{alkbn}	ratio translating benthic algae growth into Alk if NO_3 is the N source	eq mg-D^{-1}
r_{po4}	sediment release rate of DIP	g-P m^{-2} d^{-1}
r_{nh4}	sediment release rate of NH_4	g-N m^{-2} d^{-1}
r_{si}	sediment release rate of DSi	g-Si m^{-2} d^{-1}
r_{h2s}	sediment release rate of H_2S	g-O_2 m^{-2} d^{-1}
Si_s	Si saturation	mg-Si L^{-1}
$Salt$	salinity	ppt
$SOD(T)$	sediment oxygen demand	g-O_2 m^{-2} d^{-1}
T_{wk}	water temperature in Kelvin	°K
T_{opi}	optimal temperature for algal growth	°C
T_{ob}	optimal temperature for benthic algal growth	°C
TIP	total inorganic phosphorous	mg-P L^{-1}
TON	total organic nitrogen	mg-N L^{-1}
TKN	total Kjeldahl nitrogen	mg-N L^{-1}
TN	total nitrogen	mg-N L^{-1}
TOP	total organic phosphorus	mg-P L^{-1}
TP	total phosphorus	mg-P L^{-1}
TOC	total organic carbon	mg-C L^{-1}
TSS	total suspended solids	mg L^{-1}
u_{w10}	wind speed measured at 10 m above the water surface	m s^{-1}
v_{sai}	algal settling velocity	m d^{-1}
v_{spi}	solids settling velocity	m d^{-1}
v_{sr}	refractory particulate organic matter settling velocity	m d^{-1}
v_{sl}	labile particulate organic matter settling velocity	m d^{-1}
v_{bsi}	BSi settling velocity	m d^{-1}
v_{no3}	sediment denitrification transfer velocity	m d^{-1}
Greek		
μ_{mxpi}	maximum algal growth rate	d^{-1}
$\mu_{pi}(T)$	algal growth rate	d^{-1}

Symbol	Definition	Units
μ_{mxb}	maximum benthic algae growth rate	d^{-1}
μ_b	growth rate for benthic algae	d^{-1}
λ	light attenuation coefficient	m^{-1}
λ_0	background light attenuation	m^{-1}
λ_s	light attenuation by suspended solids	$L\ mg^{-1}\ m^{-1}$
λ_m	light attenuation by organic matter	$L\ mg^{-1}\ m^{-1}$
λ_1	linear light attenuation by algae	$m^{-1}\ (\mu g\text{-}Chla\ L^{-1})^{-1}$
λ_2	nonlinear light attenuation by algae	$m^{-1}\ (\mu g\text{-}Chla\ L^{-1})^{-2/3}$

Appendix D: Definition of Mathematical Symbols used in the Sediment Diagenesis Module

Symbol	Definition	Units
a_{11}	matrix coefficient	unitless
a_{12}	matrix coefficient	unitless
a_{21}	matrix coefficient	unitless
a_{22}	matrix coefficient	unitless
b_1	matrix coefficient	unitless
b_2	matrix coefficient	unitless
BSi	particulate biogenic silica	mg-Si L^{-1}
BSi_2	sediment particulate biogenic silica	mg-Si L^{-1}
C_{ssi}	solids concentration in sediment layer i	kg L^{-1}
$CH4_i$	methane in sediment layer i	mg-O$_2$ L^{-1}
$CH4_s$	methane saturation	mg-O$_2$ L^{-1}
$CSOD$	carbonaceous SOD	g-O$_2$ m^{-2} d^{-1}
$CSOD_{max}$	maximum CSOD	g-O$_2$ m^{-2} d^{-1}
$CSOD_{CH4}$	SOD generated by CH4 oxidation	g-O$_2$ m^{-2} d^{-1}
DIC_i	dissolved inorganic carbon in sediment layer i	M-C L^{-1}
DIP_i	dissolved inorganic P in sediment layer i	mg-P L^{-1}
DSi_i	dissolved silica in sediment layer i	mg-Si L^{-1}
DO_c	critical oxygen for incremental inorganic P partition	mg-O$_2$ L^{-1}
$Dd(T)$	sediment pore-water diffusion coefficient	m^2 d^{-1}
$Dp(T)$	sediment particle phase mixing diffusion coefficient	m^2 d^{-1}
f_{com}	fraction of carbon in organic matter	mg-C mg-D^{-1}
f_{dpi}	dissolved fraction of inorganic P in sediment layer i	unitless
f_{ppi}	particulate fraction of inorganic P in sediment layer i	unitless
f_{dhi}	dissolved fraction of H$_2$S in sediment layer i	unitless
f_{phi}	particulate fraction of H$_2$S in sediment layer i	unitless
f_{dsii}	dissolved fraction of Si in sediment layer i	unitless
f_{psii}	particulate fraction of Si in sediment layer i	unitless
F_{Oxna1}	oxygen attenuation factor for sediment nitrification	unitless
F_{Oxch1}	oxygen attenuation factor for sediment CH$_4$ oxidation	unitless

Symbol	Definition	Units
F_{RPON1}	fraction of RPON deposit to sediment PON G1	unitless
F_{RPON2}	fraction of RPON deposit to sediment PON G2	unitless
F_{RPOP1}	fraction of RPOP deposit to sediment POP G1	unitless
F_{RPOP2}	fraction of RPOP deposit to sediment POP G2	unitless
F_{RPOC1}	fraction of RPOC deposit to sediment POC G1	unitless
F_{RPOC2}	fraction of RPOC deposit to sediment POC G2	unitless
F_{AP1}	fraction of algae deposit to sediment G1	unitless
F_{AP2}	fraction of algae deposit to sediment G2	unitless
F_{AB1}	fraction of dead benthic algae to sediment G1	unitless
F_{AB2}	fraction of dead benthic algae to sediment G2	unitless
h	overlying water depth	m
h_2	sediment layer thickness	m
h_{so4}	thickness of sediment SO4 penetration	m
H_2S_i	dissolved hydrogen sulfide in sediment layer i	mg-O_2 L^{-1}
J_{BSi}	total deposition to sediment BSi	g-Si m^{-2} d^{-1}
$J_{POC,G1}$	total deposition to sediment POC G1	g-C m^{-2} d^{-1}
$J_{POC,G2}$	total deposition to sediment POC G2	g-C m^{-2} d^{-1}
$J_{POC,G3}$	total deposition to sediment POC G3	g-C m^{-2} d^{-1}
$J_{PON,G1}$	total deposition to sediment PON G1	g-N m^{-2} d^{-1}
$J_{PON,G2}$	total deposition to sediment PON G2	g-N m^{-2} d^{-1}
$J_{PON,G3}$	total deposition to sediment PON G3	g-N m^{-2} d^{-1}
$J_{POP,G1}$	total deposition to sediment POP G1	g-P m^{-2} d^{-1}
$J_{POP,G2}$	total deposition to sediment POP G2	g-P m^{-2} d^{-1}
$J_{POP,G3}$	total deposition to sediment POP G3	g-P m^{-2} d^{-1}
$J_{C,G1}$	sediment POC G1 diagenesis flux	g-C m^{-2} d^{-1}
$J_{C,G2}$	sediment POC G2 diagenesis flux	g-C m^{-2} d^{-1}
J_C	sediment POC diagenesis flux	g-C m^{-2} d^{-1}
J_{Cc}	total sediment POC diagenesis flux corrected for denitrification	g-O m^{-2} d^{-1}
$J_{C,CH4}$	sediment POC diagenesis into CH$_4$	g-O_2 m^{-2} d^{-1}
$J_{C,H2S}$	sediment POC diagenesis into H$_2$S	g-O_2 m^{-2} d^{-1}
$J_{N,G1}$	sediment PON G1 diagenesis flux	g-N m^{-2} d^{-1}
$J_{N,G2}$	sediment PON G2 diagenesis flux	g-N m^{-2} d^{-1}
J_N	sediment PON diagenesis flux	g-N m^{-2} d^{-1}

Symbol	Definition	Units
$J_{P,G1}$	sediment POP G1 diagenesis flux	g-P m^{-2} d^{-1}
$J_{P,G2}$	sediment POP G2 diagenesis flux	g-P m^{-2} d^{-1}
J_P	sediment POP diagenesis flux	g-P m^{-2} d^{-1}
J_{Si}	sediment BSi dissolution	g-Si m^{-2} d^{-1}
$k_{bsi2}(T)$	sediment BSi dissolution rate	d^{-1}
k_{dnh4i}	partition coefficient of NH$_4$ in sediment layer i	L kg^{-1}
k_{dh2si}	partition coefficient of H$_2$S in sediment layer i	L kg^{-1}
k_{dpo4i}	partition coefficient of inorganic P in sediment layer i	L kg^{-1}
k_{dsii}	partition coefficient of Si in sediment layer i	L kg^{-1}
k_{di}	partition coefficient in sediment layer i	L kg^{-1}
k_{st}	decay rate for benthic stress	d^{-1}
K_{L01}	sediment-water mass transfer velocity	m d^{-1}
K_{L12}	dissolved mass transfer velocity between sediment layers	m d^{-1}
$K_{L12,SO4}$	sediment sulfate specific mass-transfer velocity	m d^{-1}
K_{sOxch}	half-saturation oxygen constant for sediment CH$_4$ oxidation	mg-O$_2$ L^{-1}
K_{sOxna1}	half-saturation oxygen constant for sediment nitrification	mg-O$_2$ L^{-1}
K_{sNh4}	half-saturation NH$_4$ constant for sediment nitrification	mg-N L^{-1}
K_{sOxpm}	half-saturation oxygen constant for sediment particle phase mixing	mg-O$_2$ L^{-1}
$K_{PONG1}(T)$	sediment PON G1 diagenesis rate	d^{-1}
$K_{PONG2}(T)$	sediment PON G2 diagenesis rate	d^{-1}
$K_{POPG1}(T)$	sediment POP G1 diagenesis rate	d^{-1}
$K_{POPG2}(T)$	sediment POP G2 diagenesis rate	d^{-1}
$K_{POCG1}(T)$	sediment POC G1 diagenesis rate	d^{-1}
$K_{POCG2}(T)$	sediment POC G2 diagenesis rate	d^{-1}
K_{sDp}	half-saturation oxygen constant for sediment particle mixing	mg-O$_2$ L^{-1}
K_{sSi}	half-saturation Si constant for dissolution	mg-Si L^{-1}
K_{sSO4}	SO4 half-saturation constant for SO4 reduction	g-O$_2$ m^{-3}
k_{Sh2s}	H$_2$S oxidation normalization constant	g-O$_2$ m^{-3}
$NO3_i$	nitrate in sediment layer i	mg-N L^{-1}
$NH4_i$	ammonium in sediment layer i	mg-N L^{-1}
$NSOD$	nitrogenous SOD	g-O$_2$ m^{-2} d^{-1}
POM_2	sediment particulate organic matter	mg-D L^{-1}
$POC_{Gi,2}$	sediment particulate organic carbon Gi	mg-C L^{-1}

Symbol	Definition	Units
POC_2	sediment total particulate organic carbon	mg-C L^{-1}
POC_r	reference POC_{G1} for sediment particle phase mixing	mg-C g^{-1}
$PON_{Gi,2}$	sediment particulate organic nitrogen Gi	mg-N L^{-1}
PON_2	sediment total particulate organic nitrogen	mg-N L^{-1}
$POP_{Gi,2}$	sediment particulate organic phosphorous Gi	mg-P L^{-1}
POP_2	sediment total particulate organic phosphorous	mg-P L^{-1}
r_{on}	O_2 : N ratio for nitrification	g-O_2 g-N^{-1}
$SO4$	freshwater sulfate	mg-O_2 L^{-1}
Si_i	total silica in sediment layer i	mg-Si L^{-1}
Si_s	Si saturation	mg-Si L^{-1}
$SO4_i$	sulfate in sediment layer i	mg-O_2 L^{-1}
ST	sediment benthic stress	d
TH_2S_i	total sulfide in sediment layer i	mg-O_2 L^{-1}
$TNH4_i$	total ammonium in sediment layer i	mg-N L^{-1}
TIP_i	total inorganic phosphorous in sediment layer i	mg-P L^{-1}
$v_{nh4,1}(20)$	sediment layer 1 nitrification transfer velocity at 20°C	m d^{-1}
$v_{nh4,1}(T)$	sediment layer 1 nitrification transfer velocity	m d^{-1}
$v_{no3,1}(20)$	sediment layer 1 denitrification transfer velocity at 20°C	m d^{-1}
$v_{no3,1}(T)$	sediment layer 1 denitrification transfer velocity	m d^{-1}
$v_{ch4,1}(20)$	sediment layer 1 CH4 oxidation transfer velocity at 20°C	m d^{-1}
$v_{ch4,1}(T)$	sediment layer 1 CH4 oxidation transfer velocity	m d^{-1}
$v_{h2s,d}(20)$	sediment layer 1 H_2S dissolved oxidation transfer velocity at 20°C	m d^{-1}
$v_{h2s,d}(T)$	sediment layer 1 H_2S dissolved oxidation transfer velocity	m d^{-1}
$v_{h2s,p}(20)$	sediment layer 1 H_2S particulate oxidation transfer velocity at 20°C	m d^{-1}
$v_{h2s,p}(T)$	sediment layer 1 H_2S particulate oxidation transfer velocity	m d^{-1}
$v_{no3,2}(20)$	sediment layer 2 denitrification transfer velocity at 20°C	m d^{-1}
$v_{no3,2}(T)$	sediment layer 2 denitrification transfer velocity	m d^{-1}
w_2	sediment burial rate	m d^{-1}
ω_{12}	sediment particle phase mixing transfer velocity due to bioturbation	m d^{-1}
Δk_{PO41}	incremental partition coefficient of sediment inorganic P	unitless
Δk_{Si1}	incremental partition coefficient of sediment Si	unitless

REPORT DOCUMENTATION PAGE

Form Approved
OMB No. 0704-0188

1. REPORT DATE *(DD-MM-YYYY)*	2. REPORT TYPE	3. DATES COVERED *(From - To)*
February 2016	Final report	

4. TITLE AND SUBTITLE

Aquatic Nutrient Simulation Modules (NSMs) Developed for Hydrologic and Hydraulic Models

5a. CONTRACT NUMBER

5b. GRANT NUMBER

5c. PROGRAM ELEMENT NUMBER

6. AUTHOR(S)

Zhonglong Zhang and Billy E. Johnson

5d. PROJECT NUMBER

5e. TASK NUMBER

5f. WORK UNIT NUMBER

7. PERFORMING ORGANIZATION NAME(S) AND ADDRESS(ES)

U.S. Army Engineer Research and Development Center
Environmental Laboratory
3909 Halls Ferry Road, Vicksburg, MS 39180-6199

8. PERFORMING ORGANIZATION REPORT NUMBER

ERDC/EL TR-16-1

9. SPONSORING / MONITORING AGENCY NAME(S) AND ADDRESS(ES)

Headquarters, U.S. Army Corps of Engineers
Washington, DC 20314-1000

10. SPONSOR/MONITOR'S ACRONYM(S)

11. SPONSOR/MONITOR'S REPORT NUMBER(S)

12. DISTRIBUTION / AVAILABILITY STATEMENT

Approved for public release; distribution unlimited.

13. SUPPLEMENTARY NOTES

14. ABSTRACT

This report offers details regarding the theory and mathematical formulations used within the newly developed nutrient simulation modules (NSMs) and its supporting water quality modules. The NSMs model the aquatic ecosystem by computing the changing concentrations of water quality constituents in a unit volume of water. The NSMs includes two kinetics: NSMI, NSMII. The levels of NSMs are determined by the number of interacting state variables involved in water quality simulation and the degree of their interactions. NSMI models algae and benthic algae biomass, simple nitrogen and phosphorus cycles, organic carbon, carbonaceous biochemical oxygen demand, dissolved oxygen and pathogen using 16 state variables. Water quality state variables may be individually activated or deactivated. Using 24 state variables, NSMII models multiple algal groups, benthic algae, nitrogen, phosphorus, and carbon cycles, carbonaceous biochemical oxygen demand, dissolved oxygen, and pathogen. Additionally, an optional benthic sediment diagenesis module was developed for coupling with NSMII's water column kinetics. Sediment–water fluxes of dissolved oxygen and nutrients are internally computed in the sediment diagenesis module. The NSMs and its supporting water quality modules are written in Fortran for Windows and are packaged as "plug in" dynamic linked libraries. Each module must be coupled with hydrologic or hydraulic models to perform water quality analysis.

15. SUBJECT TERMS

NSMI	Nutrient Simulation Modules (NSMs)	Water Quality Knetics
NSMII	Hydrologic and Hydraulic Models	HEC-RAS
	Water Quality Models	Hydrologic and hydraulic (H&H) models

16. SECURITY CLASSIFICATION OF:			17. LIMITATION OF ABSTRACT	18. NUMBER OF PAGES	19a. NAME OF RESPONSIBLE PERSON
a. REPORT	b. ABSTRACT	c. THIS PAGE			19b. TELEPHONE NUMBER *(include area code)*
UNCLASSIFIED	UNCLASSIFIED	UNCLASSIFIED		229	

Standard Form 298 (Rev. 8-98)
Prescribed by ANSI Std. 239.18